ASSOCIATION OF BIOTECHNOLOGY AND PHARMACY

KNOWLEDGE IS POWER

www.abap.co.in

Association of Biotechnology and Pharmacy
(Regn. No. 28 OF 2007)

The Association of Biotechnology and Pharmacy (ABAP) was established for promoting the science of Biotechnology and Pharmacy. The objective of the Association is to advance and disseminate the knowledge and information in the areas of Biotechnology and Pharmacy by organising annual scientific meetings, seminars and symposia.

Members

The persons involved in research, teaching and work can become members of Association by paying membership fees to Association.

The members of the Association are allowed to write the title MABAP (Member of the Association of Biotechnology and Pharmacy) with their names.

Fellows

Every year, the Association will award Fellowships to the limited number of members of the   Association with a distinguished academic and scientific career to be as Fellows of the Association during annual convention. The fellows can write the title FABAP (Fellow of the Association of Biotechnology and Pharmacy) with their names.

Membership details

(Membership and Journal)		India	SAARC	Others
Individuals	– 1 year `	Rs. 600	Rs. 1000	$100
LifeMember		Rs. 4000	Rs. 6000	$500
Institutions	– 1 year	Rs. 1500	Rs. 2000	$200
(Journal only)	Life member	Rs.10000	Rs.12000	$1200

Individuals can pay in two instalments, however the membership certificate will be issued on payment of full amount. All the members and Fellows will receive a copy of the journal free.

Association of Biotechnology and Pharmacy
(Regn. No. 28 OF 2007)
#5-69-64; 6/19, Brodipet
Guntur – 522 002, Andhra Pradesh, India

Current Trends in Biotechnology and Pharmacy

Volume 18(4A)	CONTENTS	November (Supplement) 2024

Research Papers

Integrated Analysis of Non-Small Cell Lung Cancer Through Competing Endogenous RNA Network and Its Implications in Immune Evasion Regulation

Ranjini, and Dr. H. Jemmy Christy*

Department of Bioinformatics, Sathyabama Institute of Science and Technology, Chennai
*Corresponding author: jemmychristy.bioinfo@sathyabama.ac.in

Abstract

Lung cancer is a complex disease integrated with diverse histological and molecular types that have clinical relevance. Non-small cell lung cancer (NSCLC), comprised of adenocarcinoma (LUAD), squamous cell carcinoma (LUSC), and large cell carcinoma (LCC), accounts for the majority of lung cancers. This study harnesses the recent surge in biomarker identification, exploring the promising potential of the competing endogenous RNA (ceRNA) network in deciphering the intricate interplay among lncRNA-miRNA-mRNA components, providing insights into the tumorigenesis of NSCLC. Datasets encompassing differentially expressed mRNA, miRNAs, and lncRNAs were curated from the Gene Expression Omnibus (GEO), Differentially Expressed miRNAs in human Cancers (dbDEMC), and The Cancer Genome Atlas (TCGA) databases. miRNAs were selected with respect to their established roles in immune regulation, pathways, and the tumor microenvironment (TME), and an integrative analysis was performed, based on which a comprehensive ceRNA regulatory network was constructed using Cytoscape software with 26 lncRNAs, 13 miRNAs, and 143 target genes. Gene Ontology (GO)-based functional enrichment analysis focusing specifically on immune system processes uncovered genes in pathways associated with immune cell differentiation, cytokine signaling, the immune response to cancer, and so on, positioning them as potential key biomarkers within the tumor microenvironment. Furthermore, a novel lncRNA, ALAL1, supported by a lone study, was known to bind with the SART3 gene in NSCLC. Simultaneously, another study also established a connection between the SART3 gene and miR-34a. Leveraging these individual interactions, this study revealed a previously unexplored link between ALAL1, SART3, and miR-34a. This plausible ceRNA interaction is suggested to potentially exert a regulatory influence on the progression of NSCLC cells. These computationally inferred interactions, though promising, necessitate rigorous clinical validation. However, the identified biomarkers lay the groundwork for subsequent research, offering valuable insights that can guide future investigations in the realm of NSCLC.

Keywords: NSCLC, ceRNA Network, ALAL-1, Biomarkers, Network Biology

Introduction

Non-small cell lung cancer (NSCLC) presents a formidable challenge due to the diverse patient groups with varying smoking histories. There are only a few cases of NSCLC associated with genetic aberrations in non-smokers.Understanding these profiles opens up new avenues for personalized treatment strategies and for improving diagnostics in non-smoker patientswith NSCLC (1-2).

Investigations into the interplay between NSCLC and the immune system have revealed significant impacts on clinical outcomes. Qinet al. detail on mechanisms like MHC-I (major histocompatibility complex Class I) alterations, tumor-infiltrating cytotoxic T cells (CTLs) affected by Treg (regulatory T cells) recruitment, and the TCR (T cell receptor) complex altered by tumor-

Current Trends in Biotechnology and Pharmacy
Vol. 18 (Supplementry Issue 4A) 1 - 17, November 2024, ISSN 0973-8916 (Print), 2230-7303 (Online)
10.5530/ctbp.2024.4s.1

2

associated myeloid cells, suppressing antigen-specific T cell responses.These mechanisms contributed to hindering immune recognition and creating an immunosuppressive environment in the tumor (3).Recent studies have identified that, active immune escape mechanisms exist even in pre-invasive lesions progressing to NSCLC histotypes, including reduced cytolytic CD8+ T cells and Natural Killer (NK) cells, increased PD-1expressing CD8+ T cells, andHLA loss of heterozygosity (LOH) associated with increased PD-L1 expression. These mechanismspotentially influence the progression to LUAD and LUSC. Furthermore, intra-tumor immunological heterogeneity, which ischaracterized by complex immune landscapes, is found to be increased in aggressive stages (4).

The intricacies of the RNA world surpass initial molecular biology assumptions, challenge conventional beliefs, and reveal its role in specific regulatory processes with functional significance (5). Key RNA molecules, including long non-coding RNA (lncRNA), microRNA (miRNA), and messenger RNA (mRNA), emerge as crucial players in gene expression regulation, and aberrations in these RNA molecules are implicated in various cancer-related pathways (6). An intriguing facet lies in the ability of lncRNAsto act as miRNA sponges. By competitively binding to miRNAs, lncRNAs can regulate intracellular miRNA activity, which in turn influences the respective mRNA expression (7). This dynamic interaction extends to complex competing endogenous RNA (ceRNA) mechanisms, facilitating cross-talk among diverse RNA types, including lncRNA, miRNA, mRNA, and others. By analyzingceRNA networks, researchers are exploring the potential to identify novel biomarkers for early cancer detection and intervention, including NSCLC.

Dysregulation of these networks contributes to disease onset and impacts various biological mechanisms associated with tumorigenesis, with the expression profiles of ceRNA elements varying across diverse cancer subtypes (8-9). For example, in breast cancer (BC), MALAT1 acts as an oncogene through the miR-561-3p/TOP2A axis, leading to increased proliferation and malignancy (10). Conversely, in glioma, MALAT1 functions as a tumor suppressorby downregulating mir-155, which in turn inhibits FBXW7, reducing tumorigenicity (11). In NSCLC, MALAT1 plays a dual role as a predictive marker for metastasis and a potential therapeutic target(12).

Dysregulated ceRNA networks in NSCLC have been linked to promoting cell proliferation, survival, invasion, and metastasis. For instance, upregulated lncRNAs like ADAMTS9-AS2 and H19 disrupt the miRNA-mediated pathways, driving cell proliferation and survival (13). They are also implicated in driving metastasis via the axes like lncRNA LEF1-AS1/miR-489/SOX4 pathway (14) and inducing therapy resistance through anti-apoptotic gene expressionand signaling pathway alterations such as the NF-kB pathways, exemplified by lncRNA ATP2B1/miR-222-5p/TAB2 and lncRNA HUWE1/miR-222-5p/TAB1 (15). The seceRNA components, involving lncRNAs, miRNAs and mRNAs, couldbe a promising avenue for discovering biomarkers, facilitating the early diagnosis of lung cancer. Moreover, studies suggest the need for effective strategies aimed at overcoming the challenges related to drug resistance in malignant diseases.The lncRNA and miRNA interactions, acting as ceRNA elements, could emerge as one of these strategiesby understanding the mechanisms that drives therapy resistance in these diseases, thereby, improving treatment, including for NSCLC (16-17)

This study investigates the intricate interplay of lncRNA-miRNA-mRNA components in NSCLC tumorigenesis. By identifying potential biomarkers and analyzing the ceRNA network, we aim togain valuable clinical insights. Specifically, the miRNAswere selected for their significant impact on immune regulation and, generally,

the tumor microenvironment (TME). An integrative analysis was then undertaken, serving as the foundation for the construction of a comprehensive competing endogenous RNA (ceRNA) regulatory network. Furthermore, gene ontology (GO) analysis specifically focused on immune system processes revealed a prominent enrichment of genes associated with the complex TMEand its impact on various immune responses in NSCLC.

Materials and Methods
Data Screening for mRNA, miRNA, and lncRNA Expression Profile

In this study, the data for mRNA expression profiles were acquired from the Gene Expression Omnibus (GEO) database, a public repository of gene expression data (http://www.ncbi.nlm.nih.gov/geo/). The chosen dataset was GSE19804, undertaken on the GPL570 platform; Affymetrix Human Genome U133 Plus 2.0 Array. It focused on female, non-smoker NSCLC patients from Taiwan. The miRNA expression profiles necessary for understanding potential mRNA interactions were obtained from thedatabase of Differentially Expressed MiRNAs in human Cancers (dbDEMC); (https://www.biosino.org/dbDEMC/index). The search involved the retrieval of experiment ID EXP00710, comprising a sample case of NSCLC patients, analyzed using a microarray platform. For lncRNA expression profile data, The Cancer Genome Atlas (TCGA) database, a comprehensive resource providing genomic and clinical data from cancer patients; (https://portal.gdc.cancer.gov/), was used. The retrieval process involved parameters related to sample characteristics and experimental methods. A flowchart of this study was drawn to explain the analytical process (Figure 1).
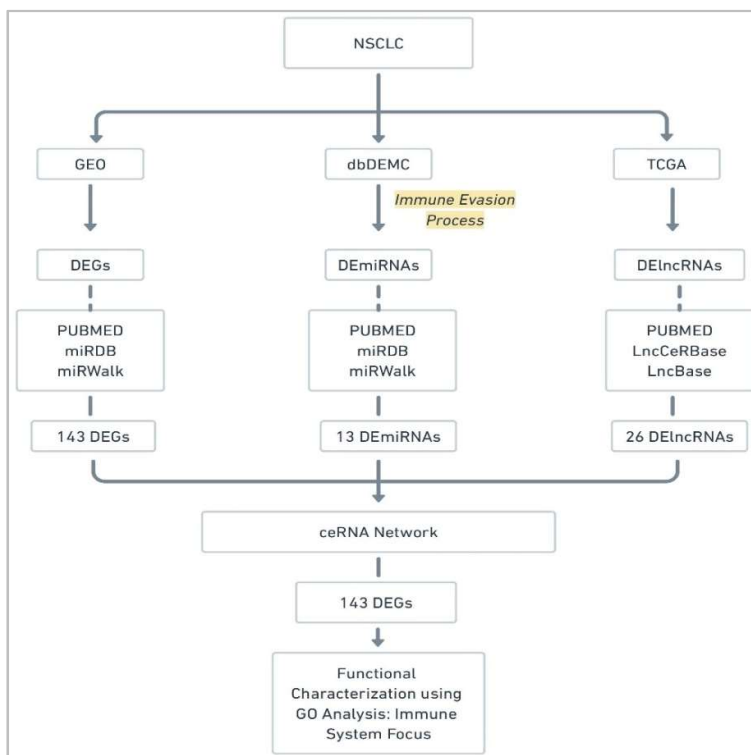
Figure 1: Overall Workflow of the study

Christy et al

Current Trends in Biotechnology and Pharmacy
Vol. 18 (Supplementry Issue 4A) 1 - 17, November 2024, ISSN 0973-8916 (Print), 2230-7303 (Online)
10.5530/ctbp.2024.4s.1

4

Differential Expression Analysis

To identify the differentially expressed genes (DEGs) between tumor samples and normal samples (normal: 60, tumor: 60), we employed the GEO2R tool, a specialized analysis tool integrated within the GEO database, designed for the comparison of gene expression profiles in different experimental conditions (https://www.ncbi.nlm.nih.gov/geo/geo2r/). The samples were appropriately grouped and subjected to GEO2R, utilizing the Benjamini Hochberg method, also known as the False Discovery Rate (FDR) method, for p-value correction. It is a statistical technique used to control the rate of false positives in multiple hypothesis testing, with a significance cut-off of 0.05.

Literature Mining for DEmiRNAs and DElncRNAs

We conducted a thorough literature study to identify differentially expressed miRNAs (DEmiRNAs) and differentially expressed lncRNAs (DElncRNAs), that aligned with our research objectives. The original DEmiRNAs dataset was refined, and those with established roles in immune regulation and the tumor microenvironment were prioritized. For DElncRNAs, the analysis targeted candidates with potential binding affinity to the previously identified miRNAs, specifically those crucial to NSCLC and, more broadly, lung cancer.

Construction of ceRNA-Interaction Network

To identify key components for the ceRNA network, we employed a combined approach involving database mining and literature studies. For miRNA-mRNA interactions, we conducted a predictive analysis using the databases miRWalk v2.0 (http://mirwalk.umm.uni-heidelberg.de/) and miRDB v6.0 (https://mirdb.org/). For lncRNA-miRNA interactions, screening was conducted using LncCeRBase v1.0 (http://www.insect-genome.com/LncCeRBase/front/) and the DIANA-LncBase v3.0 database (https://diana.e-ce.uth.gr/lncbasev3). Analogous interactions in other cancer types were also extrapolated in this study, focusing on their specific interactions.

An in-depth analysis of interactions among the selected lncRNA-miRNA-mRNA components was conducted, and the final ceRNA network was then constructed and visualized using the Cytoscape v3.10.0 software (https://cytoscape.org). Cytoscape is an open-source software platform designed for visualizing and analyzing complex networks, including biological networks. While Cytoscape offers a range of network layout algorithms, we opted for a simpler approach that aligned with our study objectives. This involved directly importing the curated interactions between lncRNAs, miRNAs, and mRNAs from the selected databases mentioned above. This decision reflects our focus on maintaining an integrity of the curated interactions while ensuring clear visualization of the network.

Gene Ontology-Based Functional Enrichment Analysis

Gene Ontology (GO) is a knowledge base that offers a standardized framework for characterizing gene functions across various species. Our study aimed to explore genes associated with immune-related processes in NSCLC. To accomplish this, we utilized the ClueGO v2.5.10 plug-in, a functional enrichment analysis tool within the Cytoscape software (https://apps.cytoscape.org/apps/cluego), for a targeted GO analysis focused on immune system processes. In particular, the analysis incorporated the Bonferroni step-down approach; a statistical method that adjusts significance thresholds for multiple hypothesis testing to reduce the risk of false positives, for p-value correction, and a two-sided hypergeometric test to enhance the statistical robustness of GO term enrichment.

Results and Discussion
DifferentialExpression Analysis of Genes in NSCLC

The gene expression data retrieved from the GEO database were analyzed using the GEO2R tool, and the resulting DEGs across 120 samples, divided into normal and tumor groups (60 samples each), were obtained (Figure 2). Subsequently, this initial

list of DEGs was refined based on our research focus, forming the basis for further investigation.

Literature Mining

From the intensive literature analysis, we identified significant DEmiRNAs with a potential impact on immune regulation within the tumor microenvironment, specifically targeting those associated with the immune evasion process. This comprehensive study led to the selection of 13 miRNAs, recognized for their involvement in immunosuppression (18), immune cell development (19), interplay in cancer-immune talk (20), and other immunomodulatory roles in NSCLC. Simultaneously, among the lncRNAs collected from the TCGA database, we selected the DElncRNAs that showed significant binding affinity with the 13 chosen DEmiRNAs, as identified through literature mining.

Establishment of the ceRNA-Interaction Network

The screening process uncovered key components essential for constructing the ceRNA network. Based on the 13 miRNAs selected, predictive analysis employing databases and literature studies was conducted. The implicated interactions were primarily associated with NSCLC. Previous investigations have delved into these molecular relationships in NSCLC and also in diverse cancer types. In this study, therefore, interactions from other cancer types, including hepatocellular carcinoma, were incorporated, considering the shared targets.
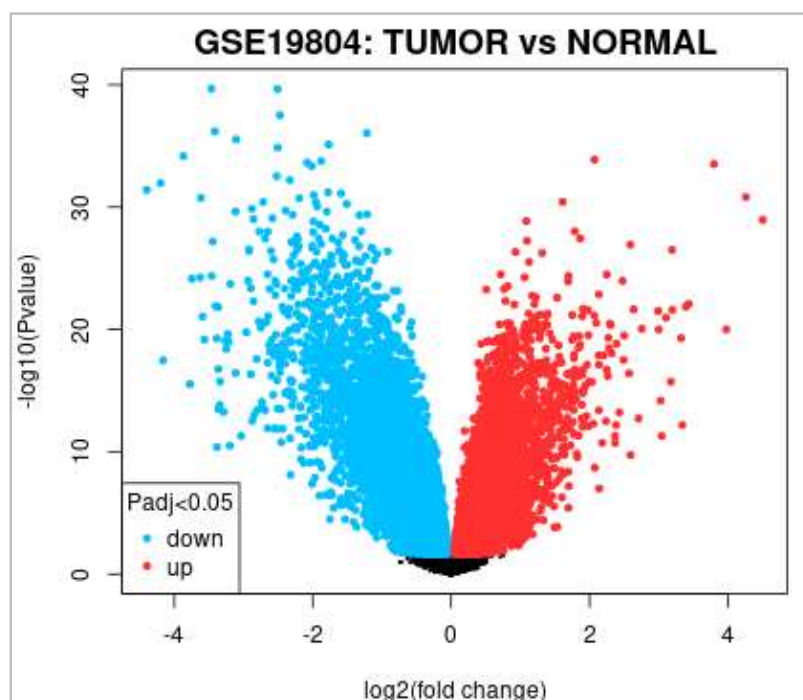
Figure 2: Volcano Plot of Differentially Expressed mRNAs; blue dots represent genes that are significantly downregulated, while red dots indicate genes that are significantly upregulated. The x-axis displays the log2 fold change, and the y-axis displays the negative logarithm of the p-value. Gene above the horizontal line are statistically significant ($p < 0.05$).

Current Trends in Biotechnology and Pharmacy
Vol. 18 (Supplementry Issue 4A) 1 - 17, November 2024, ISSN 0973-8916 (Print), 2230-7303 (Online)
10.5530/ctbp.2024.4s.1

6

Through the identification of potential relationships between miRNA/lncRNA and miRNA/mRNA, we constructed a ceRNA network encompassing 26 lncRNAs, 13 miRNAs, and 143 mRNAs. This network was then visualized using Cytoscape v3.10.0 software. This analytical framework integrated the interacting components, providing an enriched perspective on the regulatory landscape within the established ceRNA network (Figure 3).

Within the network of constructed ceRNA interactions, miR-34a has prominently assumed the role of a central hub miRNA; this centrality is attributed to the extensive relationship it establishes within the network. miR-34a is primarily recognized as a tumor suppressor in NSCLC (21). SIRT1

(Sirtuin 1) has been identified as a proposed target for miR-34a in NSCLC. The study conducted by Yamakuchi et al. explores the intricate interaction between miR-34a and SIRT1. The study has identified that miR-34a is known to inhibit SIRT1, thereby augmenting p53 activity and counteracting SIRT1's conventional role in deacetylating p53 to impede apoptosis (22). Lin et al., in alignment with this perspective, suggested that, in NSCLC, SIRT1 serves as a viable target for miR-34a to induce apoptosis by reducing SIRT1 expression (23). Further exploring the targets of miR-34a revealed key genes, namely FOXP3 (Forkhead Box P3), PRF1 (Perforin 1), and WNT1 (WNT Family Member 1), as expounded by Forough et al. (24). In accordance with findings by Peng et
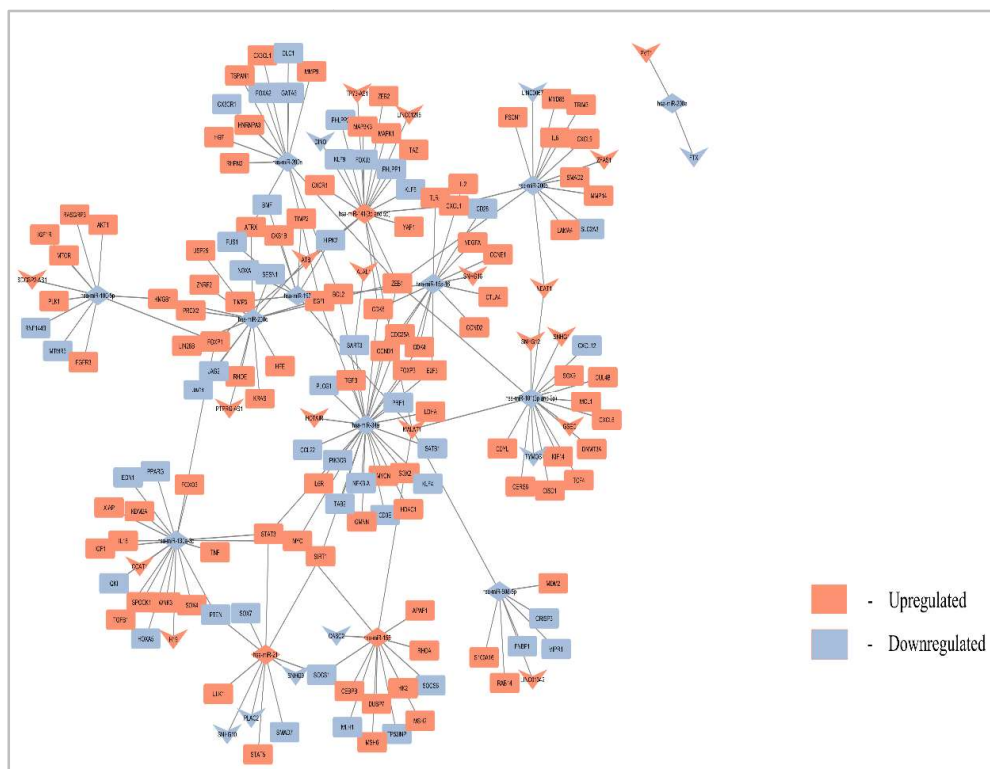
Figure 3: The ceRNA-Interaction Network in Cytoscape; shapes represent the RNA types (V-shape for lncRNAs, diamond for miRNAs, and round rectangle for mRNAs), and colors indicate the regulation type (red color represents upregulated, and blue color represents downregulated).

Non-Small Cell Lung Cancer

Current Trends in Biotechnology and Pharmacy
Vol. 18 (Supplementry Issue 4A) 1 - 17, November 2024, ISSN 0973-8916 (Print), 2230-7303 (Online)
10.5530/ctbp.2024.4s.1

7

al., it was found that the aberrant expression of FOXP3, a regulator of T-cells (Tregs), was identified in lung cancer cells. The interaction between miR-34a and FOXP3 elucidates a downregulatory effect, mitigating the overexpression of FOXP3. This interaction was implicated with relevance to the pathogenesis of rheumatoid arthritis (25). PRF1, involved in T-cell cytotoxicity, may be subject to downregulation by miR-34a. Altered expression of PRF1 may indeed impact T-cell cytotoxic activity, potentially deviating from its presumed anti-tumor immune function. This dynamic suggests a nuanced role for miR-34a in influencing cancer cell viability. Additionally, WNT1, a constituent of the WNT signaling pathway, underscores an oncogenic potential in NSCLC. WNT1 overexpression culminates in the hyperactivation of the WNT1 pathway, contributing to a poor prognosis in NSCLC patients (26). Given that WNT1 is a validated target of miR-34a, the latter's regulatory influence may reduce the expression of WNT1, presenting a prospect for a more favorable outlook in NSCLC patients.

In the context of the ceRNA network, the lncRNA is implicated as having an inhibitory influence on miRNA, directing a reversal in function that leads to the restoration of the initial activity of the target genes. HOTAIR was implicated in lung cancer cells, known to regulate processes such as initiation, proliferation, and invasion(27). miR-34a emerges as a feasible target for the lncRNA HOTAIR identified through the database search. Consequently, it can be inferred that when HOTAIR targets miR-34a, it causes reactivation of the target genes to fulfill their primary functions. This phenomenon, however, assumes a deleterious role in anti-tumor activity, as lncRNA HOTAIR promotes the tumorigenic property by indirectly activating the oncogenic genes through the modulation of miR-34a. This insight is supported by a study conducted by Fang et al. (28).

Most importantly, our study has revealed a novel mechanistic interplay involving the lncRNA ALAL1 (Amplified lncRNA associated with lung cancer 1), the SART3 (Squamous cell carcinoma antigen recognized by T-cells 3) gene, and miR-34a. ALAL1, ascertained in lung cancer cells through a singular study (29), emerges as a frequently amplified oncogenic lncRNA, transcriptionally activated by nuclear factor-kappa B (NF-kB). Primarily functioning within the cytoplasm, ALAL1 exerts its influence on SART3, which further regulates the subcellular localization of the USP4(Ubiquitin-Specific Protease 4) gene. Specifically, within NSCLC cells, overexpressed ALAL1 demonstrates an inverse correlation with immune infiltration, implying a significant role in immune evasion. Concurrently, an additional study highlights the roles of SART3 and miR-34a in NSCLC. SART3 is particularly associated with squamous cell carcinoma, and its overexpression is associated with elevated miR-34a levels, resulting in the downregulation of its target genes, CDK4 and CDK6, triggering a regulatory response to prevent uncontrolled proliferation and imparting a tumor suppressive effect in NSCLC cells(30). Our study proposes a novel hypothesis, stating that ALAL1 as a ceRNA component may indirectly modulate the function of miR-34aby targeting the SART3 gene. This mechanism implies a potential impact on inhibiting cell cycle arrest, exacerbating uncontrolled proliferation, and facilitating tumor growth in NSCLC cells. Beyond this specific interaction, ALAL1's broader role in NSCLC may be critical. Its ability to function as a ceRNA component suggests that it could be a key player in regulating other NSCLC-associated pathways. These compelling insights, through assimilation of existing literature, have been highlighted with plausible interactions between the molecules following the perceptive identification of common targets and mechanisms; however, the absence of experimental validation in this study emphasizes the need to advance this theoretical paradigm.

miR-155 emerges as another key miRNA in NSCLC cells, known for its oncogenic role. It exerts its influence by downregulating tumor suppressor genes like SOCS1 (Suppressor of Cytokine Signaling

Current Trends in Biotechnology and Pharmacy
Vol. 18 (Supplementry Issue 4A) 1 - 17, November 2024, ISSN 0973-8916 (Print), 2230-7303 (Online)
10.5530/ctbp.2024.4s.1

8

1), activating the NF-kB pathway, and cytokine production (31). Its inverse correlation with TGF-β expression influences responses to immune checkpoint inhibitors (32). SOCS1 in NSCLC is known for inhibiting the FAK-dependent signaling pathway (33). Additionally, CASC2 is also associated with tumor growth and poor survival in NSCLC (34). Yuan et al. have elucidated the CASC2/miR-155/SOCS1 axis in hepatocellular carcinoma (HCC) development, emphasizing CASC2's role as a tumor suppressor, impeding cell proliferation and migration by binding to miR-155 (35). This leads to the upregulation of SOCS1 expression, the target gene of miR-155, highlighting the ceRNA function of CASC2. This shared mechanism in HCC suggests that while CASC2 may function as a tumor suppressor in HCC, its oncogenic role in NSCLC could reflect different regulatory dynamics. However, this interaction in NSCLC requires clinical validation to confirm its role.

The ceRNA networks in NSCLC are, thus, a key to identifying treatment targets and advancing innovative therapies. In-depth research on these non-coding elements within ceRNA networks provides a critical understanding of the molecular mechanisms, especially those related to immune escape, in NSCLC.

These ceRNA networks are implicated in substantially influencing the immune escape mechanisms in NSCLC through various strategies. For instance, immune checkpoint molecules such as PD-L1 and CTLA-4 (Cytotoxic T-Lymphocyte Antigen 4) affect the ability of tumor cells to evade immune surveillance (36). They are also known to modulate immune cell infiltration, mainly affecting the function of cytotoxic T cells, regulatory T cells, and myeloid-derived suppressor cells within the tumor microenvironment (37).

Moreover, these ceRNA networks could regulate cytokine and chemokine production, influencing immune cell activation and migration (38). They could also activate immune suppressive pathways such as TGF-β, which inhibits immune cell function, leading to tumor growth and invasiveness (39). Furthermore, ceRNA networks contribute to immune cell exhaustion by activating immune suppressive pathways and contributing to functional impairment, leading to a reduced immune response against tumors (40).

The findings from this study also holdsignificant potential for advancing personalized treatment strategies in NSCLC. Significant biomarkers within the ceRNA network can be identifiedby gaining insights into the molecular mechanisms driving NSCLC progression. These biomarkers could serve as indicators for disease prognosis and treatment response, which could lead to better patient outcomes. Understanding the dysregulated ceRNA networks in NSCLC is another factor that is essential for developing personalized therapies, addressing individual patient profiles, and thereby improving treatment efficiency while minimizing adverse effects. Additionally, drug resistance remains a significant challenge in NSCLC treatment. By delving into the mechanisms underlying resistance pathways, novel therapeutic strategies implicated in overcoming drug resistance could be developed. Our study also provided insights into the impact of interactions between the ceRNA components on immune-related pathways within the TME. This could shed light on immunomodulatory therapies aimed at enhancing anti-tumor immune responses in NSCLC patients.By targeting some of these specific components involved in immune evasion mechanisms, such as the miRNAs highlighted in our study, known to regulate T cell function and tumor infiltrating lymphocytes, and so on, personalized treatment approaches could be implemented to promote the activity of the patient's immune system against tumor cells. The ceRNA regulatory network within our study could also provide insights into the heterogeneity of NSCLC at the molecular level. By characterizing the molecular profiles of individual tumors based on their ceRNA

Current Trends in Biotechnology and Pharmacy
Vol. 18 (Supplementry Issue 4A) 1 - 17, November 2024, ISSN 0973-8916 (Print), 2230-7303 (Online)
10.5530/ctbp.2024.4s.1

9

signatures, the distinct molecular subtypes of patients could be classified, allowing for a more precise treatment approach.

Therefore, our study highlights the potential of ceRNA networks in NSCLC for personalized treatment strategies overall, suggesting the importance of integrating molecular insights into clinical settings to improve NSCLC management (41-45).

GO-BasedFunctional Enrichment Analysis

To gain insights into the immune system's role in NSCLC, we performed a GO analysis restricted to immune system processes within the network of DEGs. The results revealed a significant enrichment of terms related to immune cell differentiation and activation, cytokine signaling, and the immune response to cancer (Figure 4). This suggests the ceRNA network may influence various aspects of the immune response in NSCLC, potentially impacting anti-tumor immunity and immune evasion mechanisms.

The focused exploration into the genes associated with these immune-related processes was utilized for further investigation (Table 1), incorporating insights from another study on Lung Squamous Cell Carcinoma (LUSC). Through an intensive literature study, we established the interconnection of identified pathways with immune cell populations enriched in LUSC, providing a comprehensive understanding of the disease landscape.

Integration of the Immune-Infiltrating Cells and GO Enriched Terms to reveal the interconnecting pathways in LUSC and NSCLC

Lung squamous cell carcinoma (LUSC) stands as a significant subtype within NSCLC, presenting a formidable challenge in cancer research that demands a profound comprehension of its underlying mechanisms. Recent advancements in immunogenic research
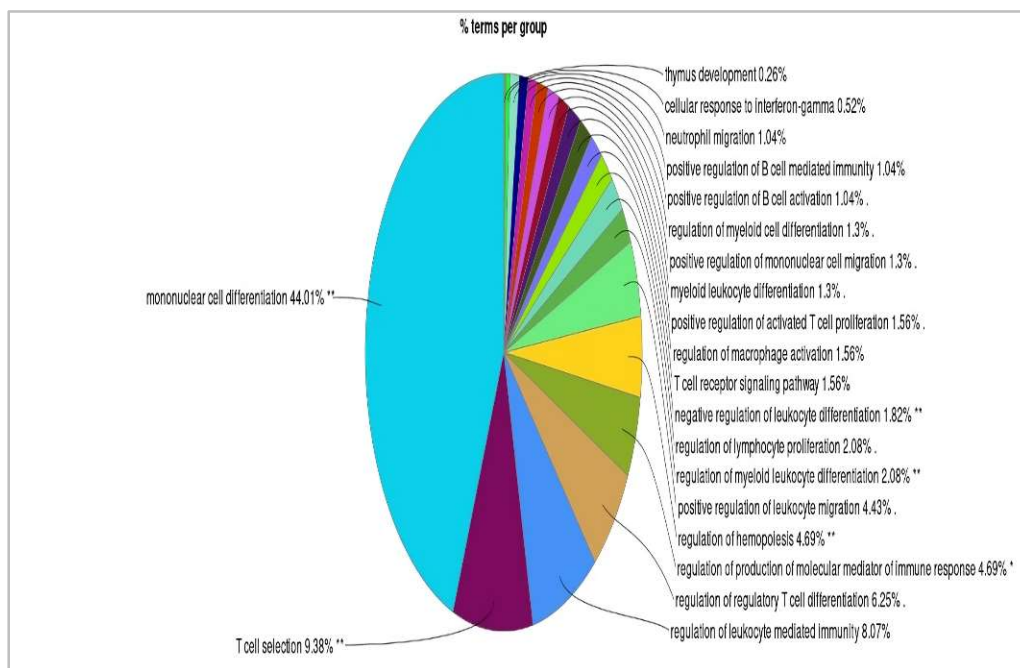
Figure 4: GO Functional Enrichment Analysis of 143 DEGs specifically targeting the immune system processes conducted using ClueGO; Visualization with pie chart. The chart shows the percentage of enriched GO terms within specific cluster identified through the analysis.

Table 1: Enriched GO Terms and their Associated Genes	
GO ID: Description	Associated Genes Found
GO:1903131 Mononuclear cell differentiation	BCL2, CD28, CD3E, CDK6, CEBPB, CTLA4, FOXO3, FOXP1, FOXP3, HMGB1, IL18, IL2, IL6, IL6R, JAG2, KLF6, MMP14, MSH2, MTOR, MYC, PPARG, PRDX2, RHOA, SMAD7, SOCS1, SOX4, STAT3, TGFB1, VEGFA, ZEB1
GO:0045058 T cell selection	BCL2, CD28, CD3E, FOXP3, IL6, IL6R, JAG2, MTOR, RHOA, STAT3
GO:0002703 Regulation of leukocyte mediated immunity	CD28, CX3CR1, CXCL6, FOXP3, HFE, HMGB1, IL18, IL2, IL6, MLH1, MSH2, SMAD7, TGFB1, TLR4, TNF
GO:0045589 Regulation of regulatory T cell differentiation	CD28, CTLA4, FOXO3, FOXP3, IL2, SOCS1, TGFB1
GO:0002700 Regulation of production of molecular mediator of immune response	CD28, FOXP3, HFE, IL18, IL2, IL6, MLH1, MSH2, MYD88, SIRT1, SMAD7, TGFB1, TLR4, TNF
GO:1903706 Regulation of hemopoiesis	CD28, CDK6, CEBPB, CTLA4, FOXO3, FOXP1, FOXP3, HMGB1, HOXA5, IL18, IL2, JAG1, MMP14, MTOR, MYC, NFKBIA, PRDX2, RHOA, SMAD7, SOCS1, SOX4, STAT3, TGFB1, TLR4, TNF, ZEB1
GO:0002687 Positive regulation of leukocyte migration	CX3CL1, CX3CR1, CXCL12, EDN1, HMGB1, IL6, IL6R, MAPK1, MMP14, RHOA, TGFB1, TNF, VEGFA
GO:0045637 Regulation of myeloid cell differentiation	CDK6, CEBPB, FOXO3, FOXP1, HOXA5, JAG1, MTOR, MYC, NFKBIA, STAT3, TGFB1, TLR4, TNF
GO:0050670 Regulation of lymphocyte proliferation	BCL2, CD28, CD3E, CEBPB, CTLA4, FOXP3, HMGB1, IGF1, IL18, IL2, IL6, MYD88, PTEN, TGFB1, TLR4
GO:1902106 Negative regulation of leukocyte differentiation	CDK6, CTLA4, FOXP3, HMGB1, IL2, MYC, PRDX2, SMAD7, SOCS1, TLR4
	(Contd.)

Non-Small Cell Lung Cancer

Current Trends in Biotechnology and Pharmacy
Vol. 18 (Supplementry Issue 4A) 1 - 17, November 2024, ISSN 0973-8916 (Print), 2230-7303 (Online)
10.5530/ctbp.2024.4s.1

11

Table 1: Enriched GO Terms and their Associated Genes (*Contd.*)	
GO ID: Description	Associated Genes Found
GO:0050852 T cell receptor signaling pathway	CD28, CD3E, CTLA4, FOXP3, MAPK1, PLCG1
GO:0043030 Regulation of macrophage activation	CX3CL1, IL6, TLR4
GO:0002573 Myeloid leukocyte differentiation	CDK6, CEBPB, FOXP1, MMP9, MTOR, MYC, PPARG, SIRT1, SOCS1, TGFB1, TLR4, TNF, VEGFA
GO:0071677 Positive regulation of mononuclear cell migration	CX3CR1, CXCL12, HMGB1, RHOA, TGFB1, TNF
GO:0045637 Regulation of myeloid cell differentiation	CDK6, CEBPB, FOXO3, FOXP1, HOXA5, JAG1, MTOR, MYC, NFKBIA, STAT3, TGFB1, TLR4, TNF
GO:0050871 Positive regulation of B cell activation	BCL2, CD28, IL2, IL6, MLH1, MMP14, MSH2, TGFB1, TLR4
GO:0002714 Positive regulation of B cell mediated immunity	CD28, IL2, MLH1, MSH2, TGFB1, TNF
GO:1990266 Neutrophil migration	CCL22, CX3CL1, CXCL1, CXCL6, CXCL9, CXCR1, EDN1, MYD88
GO:0071346 Cellular response to interferon-gamma	CCL22, CX3CL1, EDN1, PPARG, SOCS1, TLR4, TNF
GO:0048538 Thymus development	BCL2, MAPK1, PRDX2

have provided a deeper, more clarified perspective on the tumor microenvironment. Zhao et al. have identified the diverse immune cell populations within LUSC (46). Concurrently, our research delved into the molecular intricacies of NSCLC through gene ontology (GO) analysis. The analysis revealed an intricate network of interconnected pathways that establish links between the immune infiltrating cells and the identified GO pathways.

One such immune-infiltrating cell is the resting CD4 (cluster of differentiation 4) T cells associated with the TP53 mutation in LUSC. The explored key pathways were linked to cytokine secretion and their anti-tumor immune responses. This regulatory influence exerted by resting CD4 memory T

cells is crucial for maintaining effective humoral immune responses. Another study by Blair et al. explored the nuanced engagement of CTLA-4 with specific monoclonal antibodies that had regulatory effects on resting CD4 T cells, causing inhibition of cell proliferation, cytokine production, and cell cycle progression while maintaining cell viability. The specific suppression of IL-2 (interleukin-2) production can modulate the early signaling activities in these cells (47).

Another cell type found was monocytes, known to intricately govern T cell dynamics. Charron et al. have identified the impact of CD28 stimulation on modulating the expression and function of CD46, potentially affecting the interaction between T cells and monocytes (48). Additionally, blocking monocyte migration via CCR2 (C-C motif chemokine receptor 2) inhibition has been found to have diverse impacts on T-cell responses. Specifically, this leads to a reduction in macrophage-based production of cytokines such as IL-6, TNF-α (tumor necrosis factor-alpha), and so on, highlighting the intricate interplay between monocytes and T cell activity (49). They maintain myeloid cell homeostasis and differentiation, regulating immune cell development within the tumor. STAT3 (signal transducer and activator of transcription 3) and TNFs were among the genes identified to significantly contribute to myeloid cell differentiation. A study revealed that TNF played a crucial role in modulating monocyte differentiation and promoting dendritic cell generation in an inflamed microenvironment (50). Moreover, STAT3 is known as a critical regulator that links oncogenic and myeloid-specific activities to dynamic changes in cellular metabolism. The altered metabolic shift caused by increased tumor growth resulting in increased glycolysis was found to impact monocyte differentiation into macrophages (51). Monocytes were also associated with chemotaxis, emphasizing the common chemokine receptors expressed by them, such as CXCR3 (C-X-C motif chemokine receptor 3) and others. These are associated with the modulation of inflammatory response (52).

Neutrophils constitute another distinct category of immune cells present in LUSC tissues, as mentioned in the study explaining the immune cell populations within LUSC. The presence of neutrophils in the advancedTcell stage indicates their crucial role in the immune microenvironment during the later stages of LUSC. Identified as the main sources of reactive oxygen species (ROS) and cytokines, neutrophils contribute to immunosuppression, impacting cytotoxic T-cells. Their significant association with the tumor microenvironment in smokers with NSCLC has also been investigated, revealing both pro- and anti-tumor roles. In NSCLC, tumor-associated neutrophils (TANs) are identified as the main source of MMP-9 (matrix metalloproteinase-9). Research has shown a positive correlation between increased expression levels of MMP-9 and the invasive characteristics of tumor cells. The enrichment analysis performed in our study showed MMP-9s involvement in muscle cell proliferation, which can reflect its role in tissue remodeling and repair. In the context of NSCLC, the dysregulation of MMP-9 can lead to the degradation of extracellular matrix (ECM) components that correlate with tumor invasion and metastasis. The study also revealed that elevated levels of TGF-β in NSCLC cells further drive tumor progression by stimulating epithelial-mesenchymal transition (EMT), angiogenesis, and metastasis.TGF-β also induces immune suppression, influencing dendritic cells (DCs) and promoting regulatory T cell (T-reg) expansion (53).

Resting mast cells, acting as sentinels, are found to be abundant in LUSC tissues. They are critical regulators of the immune response associated with poor overall survival (OS) and progression-free survival (PFS) in LUSC. It is known as a significant biomarker for predicting survival outcomes in LUSC patients (54). Resting mast cell infiltration is markedly suppressed in NSCLC, and its inhibition is correlated with a subgroup at higher risk. The role of mast

cells in NSCLC in general is ambiguous, with studies presenting diverse findings and emphasizing the need to define their prognostic value as therapeutic targets (55). CX3CL-1 (C-X3-C motif chemokine ligand 1) is implicated in orchestrating immune responses, particularly influencing the role of mast cells. It plays a crucial role in coordinating the movement of mast cells to the sites of inflammation (56). Moreover,some vascular endothelial growth factor-positive (VEGF-positive) lungadenocarcinomas were observed to trigger the migration of mast cells within the tumor microenvironment (57).

M2 Macrophages were also found in higher proportions in LUSC and NSCLC tissues, associated with poor survival and contributing to tumor progression, angiogenesis, and immunosuppression in NSCLC patients (58). A study by Fei et al. abstracted the role of distinct functional phenotypes of these macrophages, namely M2a, M2b, M2c, and M2d, within lung cancer in general. Specifically, M2a macrophages secrete high levels of TGF-β and IGFs (insulin-like growth factors), contributing to tissue repair and healing. M2b macrophages produce anti-inflammatory molecules such as IL-6, TNF-α, and so on. M2c was identified as being involved in immunosuppression and tissue repair through the initiation of TGF-β and other molecules. Lastly, M2d macrophages that exhibit low expression of CD206 (mannose receptor C type 1) are activated by leukocyte inhibitory factors and TLR (toll-like receptor) ligands. They contributed to immunosuppression and angiogenesis by producing high amounts of TGF-β and VEGF (59). In the context of NSCLC, a finer classification of M2 macrophage subtypes is crucial for a more precise understanding of their distinct functions leading to NSCLC tumorigenesis.

This analysis elucidates the specific molecular mechanisms in NSCLC, which can further be correlated in the context of LUSC mechanisms. This is particularly pertinent, as the role of these immune-infiltrating cells in LUSC has been underexplored in existing studies. The integration of these findings therefore, contributes to discerning LUSC development and progression.

Conclusion

This work highlights the key regulatory elements and intricate mechanisms governing NSCLC through the ceRNA network, fostering potential for future advancements in navigating the complexities of this disease. The computationally inferred interactions, particularly those involving a newly discovered lncRNA, supported by a lone study, present avenues for experimental validation of their roles in tumor microenvironment. The literature search facilitated the prediction of potential interactions; however, the absence of direct algorithmic applications and the lack of experimental validation introduces a gap in the functional relevance of these associations and may limit the depth of our understanding of the underlying network dynamics. The interpretation of the identified pathways and interactions, therefore, remains contingent upon the available literature. To facilitate the experimental validation of the in-silico findings presented in this study, it is crucial to optimize the protocols for extracting the lncRNAs and miRNAs from various tissue and blood samples. Techniques such as quantitative PCR (qPCR) can be employed to measure the abundance of these specific components.However, these identified components could serve as potential biomarkers, laying the groundwork for subsequent research offering valuable insights that can guide future investigations in the NSCLC domain.

References

1. Kuśnierczyk P. (2023). Genetic differences between smokers and never-smokers with lung cancer. Frontiers in immunology, 14, 1063716.
2. Smolle, E., & Pichler, M. (2019). Non-Smoking-Associated Lung Cancer: A distinct Entity in Terms of Tumor Biology, Patient Characteristics and Impact of Hereditary Cancer Predisposition. Cancers, 11(2), 204.
3. Qin, A., Coffey, D. G., Warren, E. H., & Ramnath, N. (2016). Mechanisms of immune

evasion and current status of checkpoint inhibitors in non-small cell lung cancer. Cancer Medicine, 5(9), 2567–2578.

4. Anichini, A., Perotti, V., Sgambelluri, F., &Mortarini, R. (2020). Immune escape mechanisms in non small cell lung cancer. Cancers, 12(12), 3605.

5. Clark, M. B., Choudhary, A., Smith, M. A., Taft, R. J., & Mattick, J. S. (2013). The dark matter rises: the expanding world of regulatory RNAs. Essays in Biochemistry, 54, 1–16.

6. Yan, H., & Bu, P. (2021). Non-coding RNA in cancer. Essays in Biochemistry, 65(4), 625–639.

7. Braicu, C., Zimta, A.-A., Harangus, A., Iurca, I., Irimie, A., Coza, O., &Berindan-Neagoe, I. (2019). The Function of Non-Coding RNAs in Lung Cancer Tumorigenesis. Cancers, 11(5), 605.

8. Zhao, M., Feng, J., & Tang, L. (2021). Competing endogenous RNAs in lung cancer. Cancer Biology and Medicine, 18(1), 1–20.

9. Wang, L., Zhao, J., Zhu, C., Yang, K., Zhu, L., & Liu, Y. (2022). Construction of a ceRNA Network and Comprehensive Analysis of lncRNA in Hepatocellular Carcinoma. Genes, 13(5), 785.

10. Hajibabaei, S., Nahid Nafisi, Azimi, Y., Reza Mahdian, Fatemeh Rahimi Jamnani, Vahideh Valizadeh, Mohammad Hessam Rafiee, & Azizi, M. (2023). Targeting long non-coding RNA MALAT1 reverses cancerous phenotypes of breast cancer cells through microRNA-561-3p/TOP2A axis. Scientific Reports, 13(1).

11. Cao, S., Wang, Y., Li, J., Lv, M., Niu, H., & Tian, Y. (2016). Tumor-suppressive function of long noncoding RNA MALAT1 in glioma cells by suppressing miR-155 expression and activating FBXW7 function. American Journal of Cancer Research, 6(11), 2561–2574.

12. Wang, X. W., Guo, Q. Q., Wei, Y., Ren, K. M., Zheng, F. S., Tang, J., Zhang, H. Y., & Zhao, J. G. (2019). Construction of a competing endogenous RNA network using differentially expressed lncRNAs, miRNAs and mRNAs in non-small cell lung cancer. Oncology reports, 42(6), 2402–2415.

13. Liu, C., Yang, Z., Deng, Z., Zhou, Y., Gong, Q., Zhao, R., & Chen, T. (2018). Upregulated lncRNA ADAMTS9-AS2 suppresses progression of lung cancer through inhibition of miR-223-3p and promotion ofTGFBR3. 70(6), 536–546.

14. Yang, J., Lin, X., Jiang, W., Wu, J., & Lin, L. (2019). lncRNA LEF1-AS1 Promotes Malignancy in Non-Small-Cell Lung Cancer by Modulating the miR-489/SOX4 Axis. DNA and Cell Biology, 38(9), 1013–1021.

15. Kong, X., Hu, S., Yuan, Y., Du, Y., Zhu, Z., Song, Z., Lu, S., Zhao, C., & Yan, D. (2020). Analysis of lncRNA, miRNA and mRNA-associated ceRNA networks and identification of potential drug targets for drug-resistant non-small cell lung cancer. Journal of Cancer, 11(11), 3357–3368.

16. Liu, H., Wang, S., Zhou, S., Meng, Q., Ma, X., Song, X., Wang, L., & Jiang, W. (2019). Drug Resistance-Related Competing Interactions of lncRNA and mRNA across 19 Cancer Types. Molecular therapy. Nucleic acids, 16, 442–451

17. Seo, D., Kim, D., Chae, Y., & Kim, W. (2020). The ceRNA network of lncRNA and miRNA in lung cancer. Genomics & Informatics, 18(4), e36.

18. Sp, N., Kang, D. Y., Lee, J., & Jang, K. (2021). Mechanistic Insights of Anti-Immune Evasion by Nobiletin through Regulating miR-197/STAT3/PD-L1 Signaling in Non-Small Cell Lung Cancer (NSCLC) Cells. International Journal of Molecular Sciences, 22(18), 9843.

19. Hutter, K., Rülicke, T., Drach, M., Andersen, L., Villunger, A., & Herzog, S. (2020). Differential roles of miR-15a/16-1 and miR-497/195 clusters in immune cell development and homeostasis. The FEBS Journal, 288(5), 1533–1545.

20. Kalkusova, K., Taborska, P., Stakheev, D., & Smrz, D. (2022). The Role of miR-155 in Antitumor Immunity. Cancers, 14(21), 5414.

21. Shi, Y., Liu, C., Liu, X., Tang, D. G., & Wang, J. (2014). The microRNA miR-34a

Current Trends in Biotechnology and Pharmacy
Vol. 18 (Supplementry Issue 4A) 1 - 17, November 2024, ISSN 0973-8916 (Print), 2230-7303 (Online)
10.5530/ctbp.2024.4s.1

15

Inhibits Non-Small Cell Lung Cancer (NSCLC) Growth and the CD44hi Stem-Like NSCLC Cells. PLoS ONE, 9(3), e90022.

22. Yamakuchi, M., Ferlito, M., & Lowenstein, C. J. (2008). miR-34a repression of SIRT1 regulates apoptosis. Proceedings of the National Academy of Sciences, 105(36), 13421–13426.

23. Lin, Q., & Yin, H. (2019). RBM38 induces SIRT1 expression during hypoxia in non-small cell lung cancer cells by suppressing MIR34A expression. Biotechnology Letters, 42(1), 35–44.

24. Taheri, F., Ebrahimi, S. O., Shareef, S., &Reiisi, S. (2020). Regulatory and immunomodulatory role of miR-34a in T cell immunity. Life Sciences, 262, 118209.

25. Peng, J., Yang, S., Ng, C. S. H., & Chen, G. G. (2023). The role of FOXP3 in non-small cell lung cancer and its therapeutic potentials. Pharmacology & Therapeutics, 241, 108333.

26. Bravo, D. T., Yang, Y.-L., Kuchenbecker, K., Hung, M.-S., Xu, Z., Jablons, D. M., & You, L. (2013). Frizzled-8 receptor is activated by the Wnt-2 ligand in non-small cell lung cancer. BMC Cancer, 13, 316.

27. Loewen, G., Jayawickramarajah, J., Zhuo, Y., & Shan, B. (2014). Functions of lncRNA HOTAIR in lung cancer. Journal of hematology & oncology, 7, 90.

28. Zheng, F., Li, J., Ma, C., Tang, X., Tang, Q., Wu, J., Chai, X., Xie, J., Yang, X.-B., & Hann, S. S. (2020). Novel regulation of miR-34a-5p and HOTAIR by the combination of berberine and gefitinib leading to inhibition of EMT in human lung cancer. Journal of Cellular and Molecular Medicine, 24(10), 5578–5592.

29. Athie, A., Marchese, F. P., González, J., Lozano, T., Raimondi, I., Juvvuna, P. K., Abad, A., Marin-Bejar, O., Serizay, J., Martínez, D., Ajona, D., Pajares, M. J., Sandoval, J., Montuenga, L. M., Kanduri, C., Lasarte, J. J., & Huarte, M. (2020). Analysis of copy number alterations reveals the lncRNA ALAL-1 as a regulator of lung cancer immune evasion. The Journal of cell biology, 219(9), e201908078.

30. Sherman, E. J., Mitchell, D. C., & Garner, A. L. (2019). The RNA-binding protein SART3 promotes miR-34a biogenesis and G1 cell cycle arrest in lung cancer cells. 294(46), 17188–17196.

31. Xue, X., Liu, Y., Wang, Y., Meng, M., Wang, K., Zang, X., Zhao, S., Sun, X., Cui, L., Pan, L., & Liu, S. (2016). MiR-21 and MiR-155 promote non-small cell lung cancer progression by downregulating SOCS1, SOCS6, and PTEN. Oncotarget, 7(51), 84508–84519.

32. Dezfuli, N. K., Alipoor, S. D., Dalil Roofchayee, N., Seyfi, S., Salimi, B., Adcock, I. M., &Mortaz, E. (2021). Evaluation Expression of miR-146a and miR-155 in Non-Small-Cell Lung Cancer Patients. Frontiers in Oncology, 11,715677.

33. Jiang, M., Zhang, W., Liu, P., Yu, W., Liu, T., & Yu, J. (2017). Dysregulation of SOCS-Mediated Negative Feedback of Cytokine Signaling in Carcinogenesis and Its Significance in Cancer Treatment. Frontiers in Immunology, 8, 70.

34. Yu, X., Zheng, H., Tse, G., Zhang, L., & Wu, W. K. K. (2018). CASC2: An emerging tumour-suppressing long noncoding RNA in human cancers and melanoma. Cell Proliferation, 51(6).

35. Yuan, Y., Ye, J., Zhang, X., & Liu, Z. (2023). LNCRNA CASC2 regulate cell proliferation and invasion by targeting MIR-155/SOCS1 axis in hepatocellular carcinoma. Journal of Oncology, 2023, 1–9.

36. Jiang, Y., Zhao, L., Wu, Y., Deng, S., Cao, P., Lei, X., & Yang, X. (2022). The Role of NcRNAs to Regulate Immune Checkpoints in Cancer. Frontiers in immunology, 13, 853480.

37. Chen, J. C., Xing, Q. L., Yang, H. W., Yang, F., Luo, Y., Kong, W. J., & Wang, Y. J. (2022). Construction and analysis of a ceRNA network and patterns of immune infiltration in chronic rhinosinusitis with nasal polyps: based on data mining and experimental verification. Scientific reports, 12(1), 9735.

38. Duan, J., Pan, Y., Yang, X., Zhong, L., Jin, Y., Xu, J., Zhuang, J., & Han, S. (2020). Screening of T Cell-Related Long Noncoding

Current Trends in Biotechnology and Pharmacy
Vol. 18 (Supplementry Issue 4A) 1 - 17, November 2024, ISSN 0973-8916 (Print), 2230-7303 (Online)
10.5530/ctbp.2024.4s.1

16

RNA-MicroRNA-mRNA Regulatory Networks in Non-Small-Cell Lung Cancer. BioMed research international, 2020, 5816763.

39. Papoutsoglou, P., & Moustakas, A. (2020). Long non-coding RNAs and TGF-β signaling in cancer. Cancer science, 111(8), 2672–2681.

40. Li, K., & Wang, Z. (2022). Non-coding RNAs: Key players in T cell exhaustion. Frontiers in immunology, 13, 959729.

41. Younes Aftabi, Khalil Ansarin, Dariush Shanehbandi, Khalili, M., Ensiyeh Seyedrezazadeh, Rahbarnia, L., Asadi, M., Amir Amiri-Sadeghan, Zafari, V., Shirin Eyvazi, Nasim Bakhtiyari, & Habib Zarredar. (2021). Long non-codingRNAsas potential biomarkers in the prognosis and diagnosis of lung cancer: A review and target analysis. 73(2), 307–327.

42. Song, Y., Kelava, L., & Kiss, I. (2023). MiRNAs in Lung Adenocarcinoma: Role, Diagnosis, Prognosis, and Therapy. International journal of molecular sciences, 24(17), 13302.

43. Araghi, M., Mannani, R., Heidarnejad Maleki, A., Hamidi, A., Rostami, S., Safa, S. H., Faramarzi, F., Khorasani, S., Alimohammadi, M., Tahmasebi, S., & Akhavan-Sigari, R. (2023). Recent advances in non-small cell lung cancer targeted therapy; an update review. Cancer cell international, 23(1), 162.

44. Omar, H. A., El-Serafi, A. T., Hersi, F., Arafa, E. A., Zaher, D. M., Madkour, M., Arab, H. H., & Tolba, M. F. (2019). Immunomodulatory MicroRNAs in cancer: targeting immune checkpoints and the tumor microenvironment. The FEBS Journal, 286(18), 3540–3557.

45. Leng, D., Yang, Z., Sun, H., Song, C., Huang, C., Ip, K. U., Chen, G., Deng, C.-X., Xiaohua Douglas Zhang, & Zhao, Q. (2023). Comprehensive Analysis of Tumor Microenvironment Reveals Prognostic ceRNA Network Related to Immune Infiltration in Sarcoma. Clinical Cancer Research, 29(19), 3986–4001.

46. Zhao, J., Bao, W., & Cai, W. (2020). Immune Infiltration Landscape in Lung Squamous Cell Carcinoma Implications. BioMed Research International, 2020, 5981870.

47. Blair, P. J., Riley, J. L., Levine, B. L., Lee, K. P., Craighead, N., Francomano, T., Perfetto, S. J., Gray, G. S., Carreño, B. M., & June, C. H. (1998). Cutting Edge: CTLA-4 Ligation Delivers a Unique Signal to Resting Human CD4 T Cells That Inhibits Interleukin-2 Secretion but Allows Bcl-XL Induction. Journal of Immunology, 160(1), 12–15.

48. Charron, L., Doctrinal, A., Ni Choileain, S., & Astier, A. L. (2015). Monocyte:T-cell interaction regulates human T-cell activation through a CD28/CD46 crosstalk. Immunology and cell biology, 93(9), 796–803.

49. Padgett, L. E., Araujo, D. J., Hedrick, C. C., &Olingy, C. E. (2020). Functional Crosstalk Between T Cells and Monocytes in Cancer and Atherosclerosis. Journal of Leukocyte Biology, 108(1), 297–308.

50. Lee, P. Y., Sykes, D. B., Ameri, S., Kalaitzidis, D., Charles, J. F., Nelson-Maney, N., Wei, K., Cunin, P., Morris, A., Cardona, A. E., Root, D. E., Scadden, D. T., &Nigrovic, P. A. (2017). The metabolic regulator mTORC1 controls terminal myeloid differentiation. Science immunology, 2(11), eaam6641.

51. Su, Y., Banerjee, S., Seok Voon White, & Marcin Kortylewski. (2018). STAT3 in Tumor-Associated Myeloid Cells: Multitasking to Disrupt Immunity. International Journal of Molecular Sciences, 19(6), 1803–1803.

52. Costa, C., Traves, S. L., Tudhope, S. J., Fenwick, P. S., Belchamber, K. B. R., Russell, R. E. K., Barnes, P. J., & Donnelly, L. E. (2016). Enhanced monocyte migration to CXCR3 and CCR5 chemokines in COPD. European Respiratory Journal, 47(4), 1093–1102.

53. Aloe, C., Wang, H., Vlahos, R., Irving, L., Steinfort, D., & Bozinovski, S. (2021). Emerging and multifaceted role of neutrophils in lung cancer. Translational Lung Cancer Research, 10(6), 2806-2818.

54. Li, N., Wang, J., & Zhan, X. (2021). Identification of immune-related gene signatures in lung adenocarcinoma and lung

squamous cell carcinoma. Frontiers in Immunology, 12, 752643.

55. Yang, Y., Qian, W., Zhou, J., & Fan, X. (2023). A mast cell-related prognostic model for non-small cell lung cancer. Journal of Thoracic Disease, 15(4), 1948–1957.

56. Ramachandran, S., Verma, A. K., Dev, K., Goyal, Y., Bhatt, D., Alsahli, M. A., Rahmani, A. H., Almatroudi, A., Almatroodi, S. A., Alrumaihi, F., & Khan, N. A. (2021). Role of Cytokines and Chemokines in NSCLC Immune Navigation and Proliferation. Oxidative Medicine and Cellular Longevity, 2021, 1–20.

57. O'Callaghan, D. S., O'Donnell, D., O'Connell, F., & O'Byrne, K. J. (2010). The Role of Inflammation in the Pathogenesis of Non-small Cell Lung Cancer. Journal of Thoracic Oncology, 5(12), 2024–2036.

58. Katarína Balážová, Clevers, H., & Dost, A. F. M. (2023). The role of macrophages in non-small cell lung cancer and advancements in 3D co-cultures. ELife, 12, e82998.

59. Xu, F., Wei, Y., Tang, Z., Liu, B., & Dong, J. (2020). Tumor-associated macrophages in lung cancer: Friend or foe? (Review). Molecular medicine reports, 22(5), 4107–4115.

Utilizing OncomiR and TSmiR as Biomarkers for Screening Breast Cancer

Grace Lydia Phoebe M[1], and Jemmy Christy H[1]

[1]Department of Bioinformatics, Sathyabama Institute of Science and Technology,Tamil Nadu, India
*Corresponding author: jemmychristy.bioinfo@sathyabama.ac.in

Abstract

Breast cancer stands out as a significant threat to women globally, emphasizing the urgent need for reliable diagnostic and prognostic markers.Numerous studies have shown that miRNAs assist as either an oncogene or tumor suppressor. As a result, they are recognized as non-invasive biomarkers for diagnosing and predicting cancer outcomes.Through an in-depth literature review, we have identified numerous upregulated miRNAs, including miR-9, miR-10b, miR-21, miR-29a, miR-92a, miR-148a-3p, miR-155, miR-221, miR-222, and miR-373. Conversely, we have identified downregulated miRNAs, including miR-34a, miR-96, miR-99a, miR-125b, miR-145, miR-200c, miR-203, miR-214, miR-411, and miR-486.We used the miRWalk database to predict target genes associated with each miRNA and constructed a comprehensive network. Additionally, gene ontology (GO) and Kyoto Encyclopedia of Genes and Genomes (KEGG) pathway analyses were conducted to delve deeper into the functional significance and molecular pathways associated with the identified miRNAs target genes. Additionally, we constructed a Protein-Protein interaction networkbased on the miRNA-target genes.Further analysis was directed towards the target genes of OncomiRs (EGFR, MYC, CTNNBI, TP53, CCDNDI, BCL2) and TS-miRs (TP53, CTNNBI, AKT1), exploring their involvement in signaling pathways.This study delves into the utilization of miRNA for the early screening and monitoring of breast cancer.

Keywords: Breast Cancer, Functional Enrichment, Oncomir, TS Mir, PPI Network

Introduction

Despite the existence of various diagnostic modalities, breast cancer continues to exhibit a high prevalence among women. The primary reason lies in the constraints of current screening methods. These include the prevalence of false positives and false negatives, challenges in detecting abnormalities within dense breast tissue, and the restricted frequency of screening intervals (1). As a result, there is a need for alternative methods to identify early-stage breast cancer(BC). This has led to a heightened focus on biomarkers, given their remarkable ability to identify specific molecules or genetic irregularities associated with cancer cells. Conventional biomarkers such as HER2, ER, andPR status are widely utilized in breast cancer diagnosis and classification. While these biomarkers target specific molecular pathways, they may exhibit limited sensitivity and fail to fully capture tumor heterogeneity. Moreover, blood-based markers like CA 15-3 and CA 27.29 may also demonstrate lower sensitivity and specificity compared to tissue-based counterparts. miRNA biomarkers have demonstrated notable sensitivity and specificity across multiple studies, effectively distinguishing between breast cancer patients and healthy individuals, as well as discerning different subtypes and stages of breast cancer.In recent years, there has been a growing emphasis on small non-coding miRNAs as biomarkers. Their variability in tissues and biological fluids compared to normal samples has garnered attention. Their stability renders them ideal for screening and precise prognostication purposes (2). They exert a crucial influence on gene expression by either impeding mRNA translation or

promoting mRNA degradation. Furthermore, miRNAs impact cellular proliferation, migration, invasion, and differentiation, thereby contributing to tumorigenesis through the regulation of oncogenes and tumor suppressor genes.

The dysregulation of Oncomirs and TSmiRs in breast cancer and their potential as biomarkers offer exciting prospects for improving breast cancer detection, diagnosis, prognosis, and treatment. OncomiRs (oncogenic microRNAs) and TS miRs (tumor suppressor microRNAs) have emerged as promising biomarkers for breast cancer screening due to their central roles in modulating essential cellular processes implicated in cancer initiation and progression. Typically, oncomiRs, which inhibit tumor suppressor genes, are upregulated in cancer cells, while TS miRs, which counteract oncogenes, are downregulated. Modulating the levels of these oncomiRs or TS miRs, whether through inhibition or augmentation, can induce significant changes in cancer cell behaviors. OncomiR dysregulation contributes to the uncontrolled growth and survival of cancer cells. In breast cancer, specific oncomiRs have been implicated in various aspects of the disease, including metastasis and resistance to therapy. Identifying and measuring the levels of these oncomiRs in biological samples, such as blood or tissue biopsies, can provide valuable information about the presence and progression of breast cancer.TSmiRs help maintain normal cellular functions by inhibiting processes like cell proliferation and invasion. In breast cancer, the loss of certain TS miRs has been associated with increased tumor aggressiveness and poor prognosis. Therefore, detecting the reduced expression of these miRs in patient samples can indicate cancer development and progression (3). By elucidating common molecular mechanisms and identifying potential therapeutic targets, these findings pave the way for interdisciplinary collaborations and innovative approaches to cancer diagnosis and treatment. Understanding miRNA function in breast cancer offers insights into tumorigenesis, metastasis, and treatment resistance, guiding the development of therapeutic strategies. Exploring miRNA expression across cancers may reveal universal biomarkers and shared tumorigenic pathways.

In this study, we have curated upregulated and downregulated miRNAs through literature mining and constructed a comprehensive miRNA-target regulatory network. The process began with a comprehensive literature review focused on studies investigating miRNA dysregulation in breast cancer. This involved searching relevant databases such as Google Scholar, PubMed, and ScienceDirect conducted on articles over the past five years this involved reviewing articles that contained computational analyses, and experimental validations. Within the literature, miRNAs known to play roles as either oncogenes (OncomiRs) or tumor suppressors (TS miRs) in breast cancer were identified based on reported dysregulation patterns and functional studies. Identified OncomiRs and TS miRs were compiled into lists based on their reported upregulation or downregulation in breast cancer samples compared to normal controls. Further network analysis elucidates how miRNAs intricately regulate the expression of their target genes, thereby exerting an effecton critical processes such as proliferation, differentiation, apoptosis, and development.To delve deeper into the functional roles of miRNA-target interactions within the network, we conducted GO and KEGG pathway analyses. GO analysis elucidates the molecular mechanisms driving biological processes, identifying candidate biomarkers, and facilitating the prioritization of genes for further experimental validation. On the other hand, KEGG pathway analysis involves mapping genes or gene products to their respective pathways and uncovering significantly enriched pathways within the gene list. Furthermore, we conducted a PPI network analysis utilizing the miRNA-target network. Subsequent analysis focused on identifying target genes among OncomiR and

TS-miR, aiding in the exploration of pivotal pathways.This computational approach facilitates the understanding of miRNAs and their associated genes within breast cancer pathways, rendering them viable biomarkers for screening purposes.

Materials and Methods
Literature Mining

A comprehensive literature review was conducted to identify miRNAs associated with breast tumors and their presence in circulating blood. Search engines such as Google Scholar, PubMed, and ScienceDirect were conducted on articles over the past five years.

Mirna-Target Interaction Network

We utilized miRwalk 2.0 (https://mirwalk.umm.uni-heidelberg.de)to forecast miRNA targets. miRWalk is an extensive repository, offering the most extensive collection of predicted and experimentally validated microRNA-target interactions (4). A regulatory network was created to depict the complex interplay among identified miRNAs and their corresponding target genes using Cytoscape (V3.10.1.) (https://cytoscape.org).

Functional Enrichment Analysis

We employed the ClueGO plugin (Version 2.5.9) within Cytoscape (Version 3.10.1) for investigating GOand KEGG pathways. Statistical validation was conducted, with a significance threshold set at P < 0.05, and a kappa score of 0.4 was utilized to ensure the reliability of the enriched terms (5).

Protein-Protein Interaction (PPI) Network

To investigate the interaction among miRNA targets, we utilized the STRING database (Version 12.0) (https://string-db.org/) to construct a PPI network, with a criteria score threshold of ≥ 0.4. The network was visualized using Cytoscape software (Version 3.10.1). Laterhub genes were acquired utilizing the CytoHubba plugin (V 0.1) within Cytoscape.Scoring methods such as Bottleneck and Degree identify and emphasize the central and densely interconnected nodes within thePPI network (6).

Result and Discussion
Literature Mining

Through an exhaustive literature mining approach, we identified elevated expression of miRNAs found in breast tumors, as well as their presence in circulating blood which includeshsa-miR-9, hsa-miR-10b, miR-21, miR-29a, miR-92a, miR-148a-3p, miR-155, miR-221, miR-222, and miR-373(7-11). Conversely, the selected downregulated miRNAs encompassed miR-34a, miR-96, miR-99a, miR-125b, miR-145, miR-200c, miR-203, miR-214, miR-411, andmiR-486(12-16).

Construction of A Mirna-Target Gene Interaction Network

To explore the relationship between miRNAs and their targets and gain insights into regulatory connections and their roles in various breast cancer (BC) processes and pathways, we utilized miRwalk. This tool employs the TarPmiR algorithm, which is a random-forest-based approach for miRNA target site prediction. Our selection criteria focused on identifying targets with a high score of 1 and miRNA binding sites specifically located in the 3'-UTR of the gene, as the 3'-UTR is known for its abundance of miRNA binding sites. This process resulted in the prediction of 215 target genes for oncomiRs and 118 target genes for tumor suppressor (TS) miRNAs, each associated with specific miRNAs. To visualize this intricate miRNA-target network, we utilized Cytoscape software (Figures 1 and 2).

Functional Enrichment Analysis

We utilized the ClueGO plugin within Cytoscape to import the target genes of all oncomiRs and TS miRs, aiming to explore potential GO categories and KEGG pathways. miRNAs are expected to target genes crucial for various biological

processes, molecular functions, and KEGG pathways, some of which are discussed below.

OncomiRs, linked to numerous targets, significantly influence various biological processes in BC. For example, in TNBC, CTNNB1 impacts basal-like and immune subtypes, regulating critical cellular functions like proliferation, migration, and angiogenesis (17). Additionally, miRNAs miR-221/222, miR-21, and miR-29a, along with their associated genes PTEN and TIMP3, activate the AKT pathway, contributing to TRAIL-Activated Apoptotic Signaling (18). Moreover, AKT1 regulates the import of long-chain fatty acids across the plasma membrane, promoting tumor growth in TNBC by disrupting the cell cycle or enhancing apoptosis. Furthermore, heightened fatty acid metabolism is linked to therapy resistance in HER2-positive breast cancer, suggesting potential avenues for treatment (Figure 3 a). Further analysis of molecular functions underscores the importance of several key processes in breast cancer. For instance, the positive regulation of MAP kinase activity, particularly through the MEK1/MAPK1/2 signaling axis and pro-survival autophagy, is critical in overcoming resistance to antiestrogen treatment and enhancing the effectiveness of hormone therapies. Additionally, EGFR activity inhibits the pro- apoptotic function of BimEL,
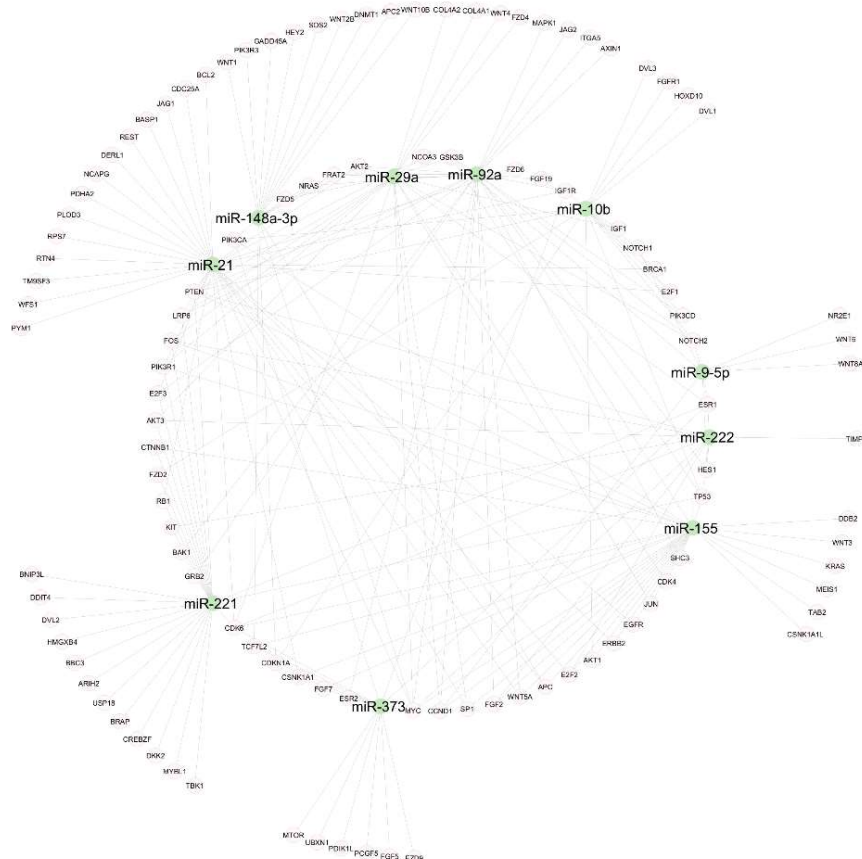
Figure 1: The regulatory network of OncomiRs their target genes: Green nodes represent Upregulated miRNA, where's white nodes represent its target

Grace et al
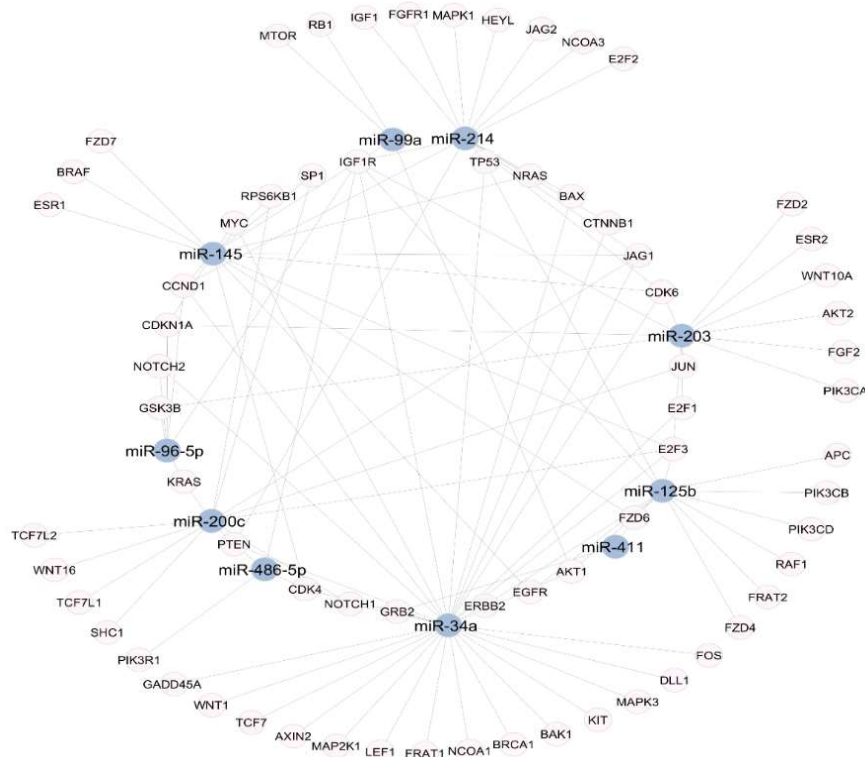
Figure 2: The regulatory network of TS miRs their target genes: Blue nodes represent downregulated miRNA, where's white nodes represent its target
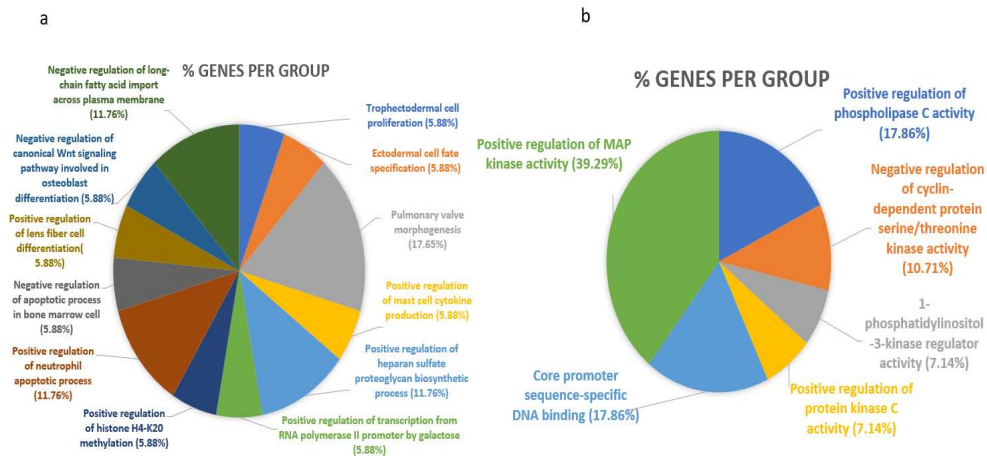
Figure 3: The pie chart depicts the functional connections between (a) biological processes and (b) molecular functions, which are enriched by upregulated miRNAs target genes

Grace et al
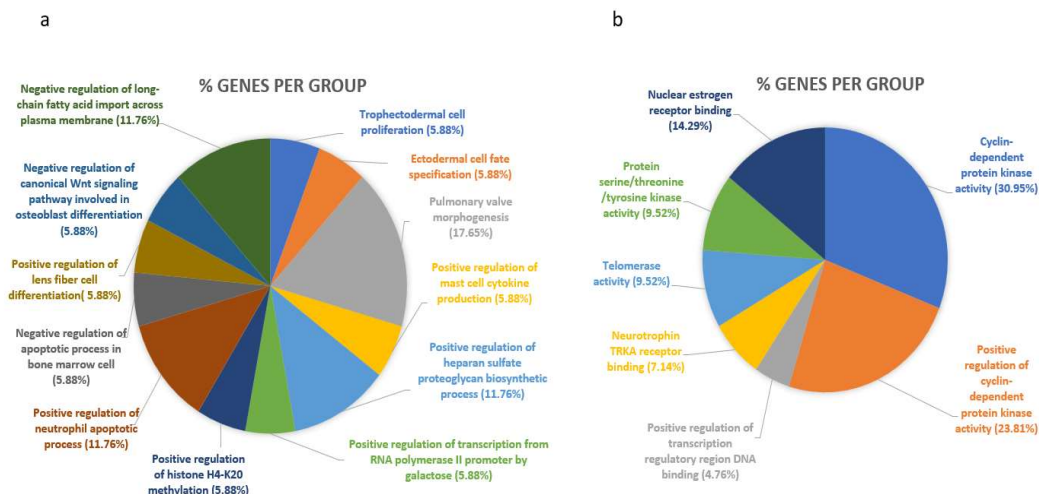
Figure 4: The pie chart depicts the functional connections between (a) biological processes and (b) molecular functions, which are enriched by downregulated miRNAs target genes

a vital regulator of apoptosis in ERα-positive breast cancer cells. Furthermore, the positive regulation of phospholipase C activity, influenced by EGFR, impacts the expression of PLC-γ1, an enzyme involved in EGFR-associated pathways that affect cell migration (19). Lastly, core promoter sequence-specific DNA binding, particularly involving the MYC gene, regulates the transcriptional activity of genes essential for tumor progression, including those involved in cell cycle regulation, apoptosis modulation, and angiogenesis promotion (20) (Figure 3 b).

TS miRNA target genes exhibit significant enrichment in biological processes, particularly in signaling pathways like Ectodermal cell fate specification involving Wnt, Notch, and BMP. These pathways, crucial in regulating ectodermal cell fate and implicated in cancer progression, include the canonical Wntsignaling pathway, notably involving FZD7, which inhibits tumor growth by reducing cell proliferation in TNBC (21). Additionally, LEF1, a downstream component of Wnt/β-catenin signaling, influences stem cell maintenance, organ development, and

EMT. Dysregulation of LEF1 promotes tumorigenesis by enhancing cancer cell proliferation, migration, and invasion, extending its influence to bone marrow cells in breast cancer, where its activation suppresses apoptosis, driving disease progression. Moreover, PIK3CB and PIK3CD, encoding different PI3K isoforms, positively regulate neutrophil apoptosis, prolonging neutrophil survival via PI3K signaling and fostering inflammation, angiogenesis, and tumor cell survival, contributing to tumor progression (22) (Figure 4 a). TS miRNAs are anticipated to target genes essential for a variety of molecular functions. For instance, they may regulate cyclin-dependent protein kinase activity, where AKT1 triggers CDKs by suppressing CDK inhibitors like CDKN1A (p21), thereby facilitating cell cycle advancement(23). Additionally, they might influence positive nuclear estrogen receptor binding, such as the role of Ets1 in mediating interactions between nuclear hormone receptors and coactivators like NCOA1, which intensifies estrogen sensitivity and fosters tumor growth. Furthermore, TS miRNAs could modulate protein serine/threonine/tyrosine kinase

activity, exemplified by RPS6KB1's function in breast cancer, where dysregulation contributes to tumor progression by affecting cellular processes like growth, proliferation, and survival (24) (Figure 4b).

In the KEGG pathway, there are overlapping pathways present in both oncomirs and tumor-suppressive microRNAs (ts-miRNAs). Common microRNA-associated genes are found in both types of pathways. The same gene can demonstrate oncogenic and tumor-suppressive roles, which vary depending on factors such as the cellular environment, specific mutations, interactions with other signaling pathways, and the microenvironment. These factors collectively influence the gene's function, determining whether it promotes tumorigenesis or inhibits tumor growth. Increased expression of E2F1 can enhance mitophagy in breast cancer cells by transcriptionally regulating genes involved in mitochondrial dynamics and quality control, facilitating the removal of damaged mitochondria and maintaining cellular balance. Conversely, decreased E2F1 expression may hinder mitophagy, leading to the accumulation of damaged mitochondria and heightened oxidative stress, factors associated with breast cancer progression. Also, upregulation of TP53 positively influences mitophagy by activating genes involved in mitochondrial quality control, whereas downregulation or loss of TP53 function can impair mitophagy, resulting in mitochondrial dysfunction and increased genomic instability, characteristic of breast cancer development (Figure 5 a). Therefore, while elevated levels of TP53 and E2F1 promote mitophagy and cellular equilibrium, their downregulation or functional loss may disrupt mitophagy, exacerbating breast cancer progression (25).CTNNB1 serves as a pivotal element within adherens junctions, facilitating cell-cell adhesion and signaling processes.Dysregulation of CTNNB1 leads to abnormal initiation of the Wntsignaling pathway, consequently disrupting adherens junctions.This disruption fosters tumor cell invasion and metastasis in breast cancer. Similarly, EGFR signaling modulates the dynamics of adherens junctions and cellular adhesion (26). When EGFR is overexpressed or activated, it disrupts the regulation of adherens junction proteins, contributing to heightened tumor cell motility, invasion, and metastasis in breast cancer (Figure 5 b). As a result, targeting EGFR signalingis avaluable therapeutic method to hinder tumor progression and metastasis in breast cancer. EGFR upregulation enhances hepatocellular carcinoma (HCC) metastasis to breast tissue by promoting cell motility and survival, while downregulation inhibits metastatic potential.
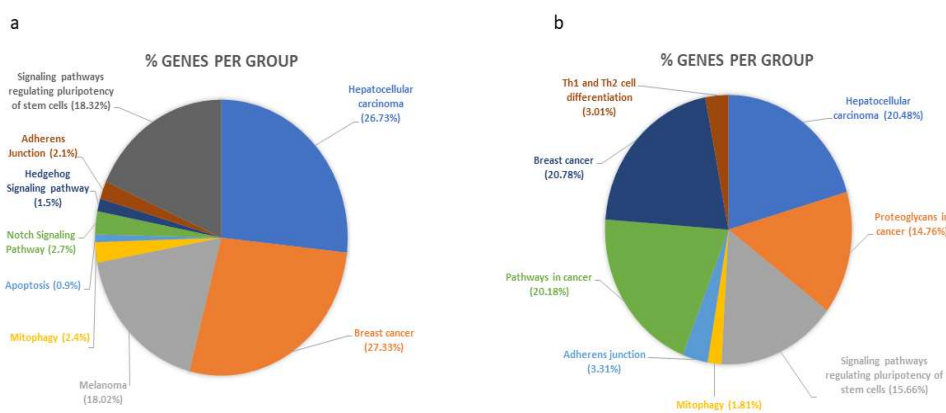
Figure 5: This figure depicts the KEGG pathways associated with target genes regulated by oncomiRs and TS miRNAs.

Utilizing OncomiR and TSmiR as Biomarkers

Current Trends in Biotechnology and Pharmacy
Vol. 17 (Supplementry Issue 3s) 1 - 10, July-Sept 2024, ISSN 0973-8916 (Print), 2230-7303 (Online)
10.5530/ctbp.2024.4s.2

25

a   b
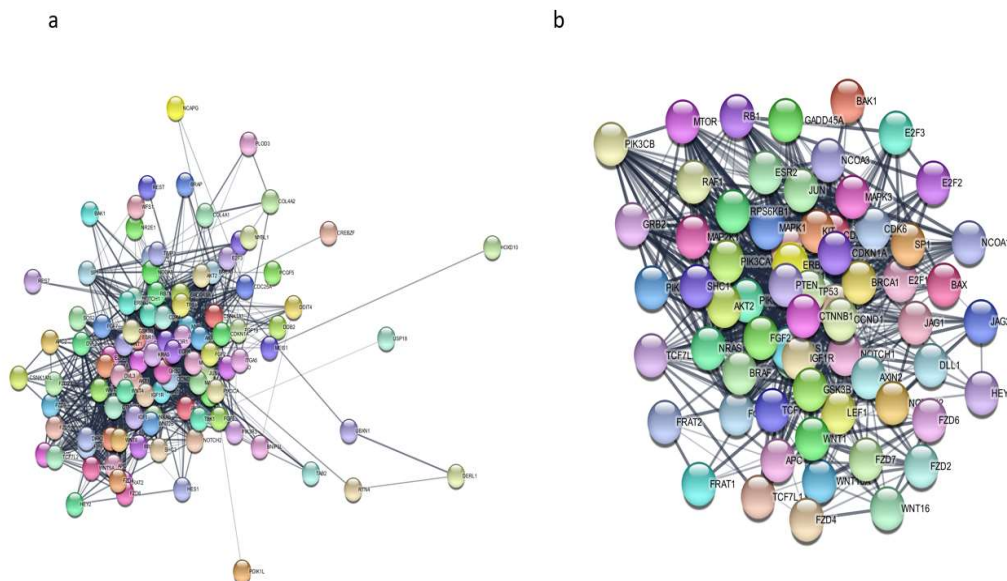
Figure 6: Protein-Protein interaction of miRNA target genes- a) Upregulated miRNA-targets. (b) Downregulated miRNA-targets.

Similarly, AKT1 upregulation aids metastasis via enhanced proliferation and invasion, while its downregulation impedes metastatic spread. EGFR and AKT1 levels significantly influence HCC metastasis to breast tissue, although further research is required to elucidate underlying mechanisms (27).

Protein-Protein Interaction (PPI) Network

The miRNA-target network was employed to build a PPI network, comprising 113 nodes and 140 edges for OncomiR targets, and 69 nodes with 1050 edges for TSmiR targets (Figure 6). The top 10 hub genes ranked by bottleneck and degree for OncomiR and Ts miR-target genes are seen in (Figures 7 and 8). The bottleneck node serves as a critical bridge linking distinct sections of the network. Meanwhile, the degree of a node represents the count of connections it maintains with other nodes within the network. Target genes that were common to both parameters(Bottleneck and degree)for OncomiR (EGFR, MYC, CTNNBI, TP53, CCDNDI, BCL2) and TS-miR (TP53, CTNNBI, AKT1)were chosen.The expression of miRNA along with its corresponding genes and its function areseen in (Tables 1 and 2).

Thus, miRNA emerges as a promising biomarker, functioning as both oncogenes and tumor suppressors, offering a potential breakthrough in early detection methods. Abnormally elevated levels of OncomiRs in cancer promote the proliferation, migration, and metastasis of cancer cells by downregulating the expression of several tumor suppressor genes through direct binding to their corresponding mRNA molecules. Consequently, inhibiting OncomiR function emerges as a promising strategy for cancer treatment. The synthetic anti-miRs, which are complementary to OncomiRs, into cancer cells inhibits the interaction between OncomiRs and their target RNAs.This intervention effectively suppresses cancer cell growth and metastasis. In contrast to OncomiRs, decreased expression of TSmiRs in cancer contributes to the initiation and advancement of malignancy by avoiding the suppression of several cancer-promoting genes targeted for downregulation.
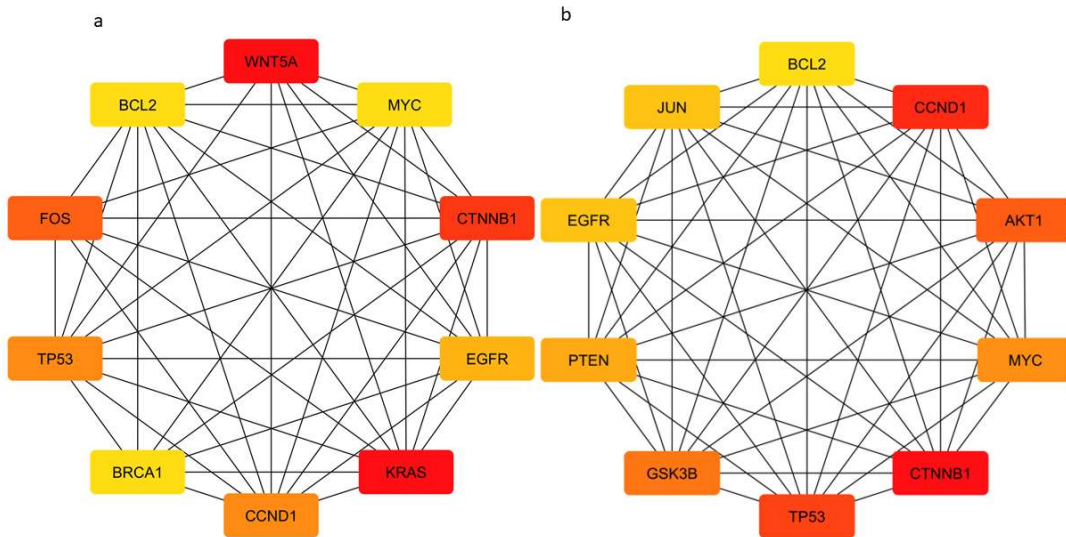
Figure 7: Top 10 hub genes among the upregulated miRNA-targets. (a) Bottleneck centrality. (b) Degree centrality
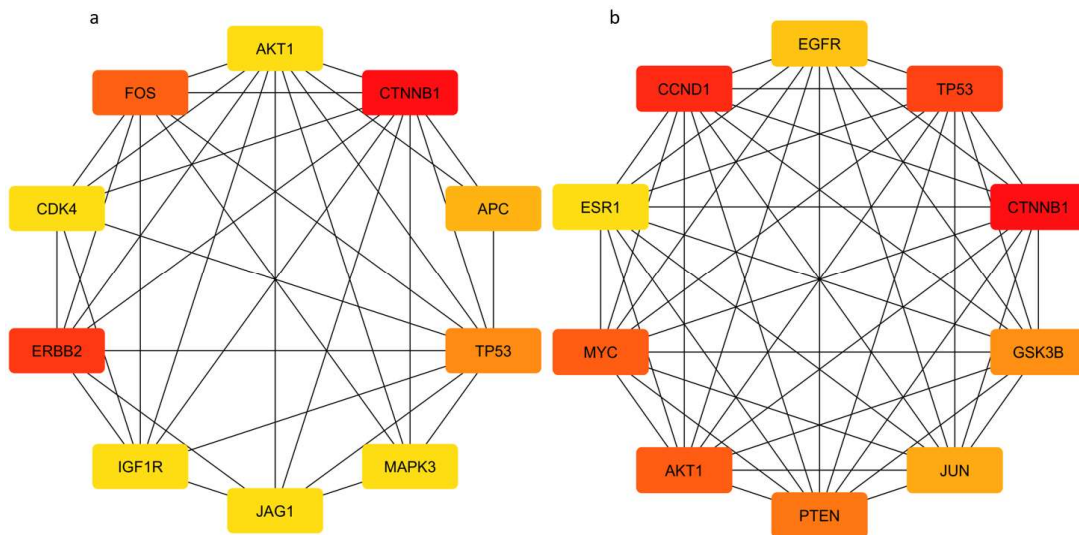
Figure 8: Top 10 hub genes among the downregulated miRNA-targets. (a) Bottleneck centrality. (b) Degree centrality

Utilizing OncomiR and TSmiR as Biomarkers

Table 1: A list of OncomiR targets that involved breast cancer			
Target genes	OncomiR	Function	References
EGFR	miR-21	Suppressed tumour growth and angiogenesis	8
MYC	miR-9	Cell migration, Invasion and metastasis	10
CTNNB1	miR-373	Tumor progression and apoptosis	13
TP53	miR-155	Cell cycle progression, anti-apoptosis, proliferation and metastasis	9
CCDNDI	miR-92a	Proliferation, migration and invasion	14
BCL2	miR-221 and miR-222	Proliferation and metastasis	12

Table 2: A list of TS-miR targets that involved breast cancer			
Target genes	TS miR	Function	References
AKT1	miR-145	Inhibition of EMT	52
CTNNBI	miR-125b	Inhibiting growth and migration	52
TP53	miR-34a	Induction of cell cycle arrest and apoptosis.	20

Conclusion

The findings of this study hold significant promise in the realm of breast cancer screening and prognosis. Breast cancer remains a formidable threat to women worldwide, underscoring the critical need for reliable diagnostic and prognostic markers. Identification of OncomiR and TS miR biomarkers represents a promising avenue for overcoming limitations in current breast cancer screening methods and enhancing patient outcomes through personalized treatment strategies.These biomarkers offer the potential for detecting breast cancer at earlier stages compared to conventional screening techniques like mammography. They can identify molecular changes linked to cancer initiation and progression before tumors become visible on imaging scans, enabling timely intervention and treatment initiation, and ultimately improving survival rates. Moreover, these biomarkers provide valuable molecular insights that can augment the accuracy of breast cancer screening. Their detection can complement existing screening approaches, reducing the likelihood of misdiagnosis and unnecessary procedures. By profiling the expression levels of these biomarkers, clinicians can customize treatment plans to target specific molecular pathways driving tumor growth and advancement, thereby enhancing treatment effectiveness, minimizing adverse effects, and improving patient quality of life. Monitoring changes in miRNA expression following different treatment modalities, including chemotherapy, hormonal therapy, and targeted therapy, could provide valuable information on treatment efficacy and resistance mechanisms. Identifying treatment-specific miRNA signatures associated with favourable or adverse outcomes could facilitate personalized treatment strategies and guide to therapeutic. Additionally, real-time monitoring using these biomarkers enables clinicians to identify patients at higher risk of disease recurrence during follow-up care, allowing for the implementation of proactive management strategies such as intensified surveillance or adjuvant therapies to prevent or delay recurrence and improve long-term prognosis.

Through an extensive literature review and analysis, the study has identified

Current Trends in Biotechnology and Pharmacy
Vol. 17 (Supplementry Issue 3s) 1 - 10, July-Sept 2024, ISSN 0973-8916 (Print), 2230-7303 (Online)
10.5530/ctbp.2024.4s.2

28

a panel of miRNAs that exhibit dysregulation in breast cancer, both as oncogenes and tumor suppressors. The identified upregulated miRNAs, such as miR-9, miR-10b, miR-21, miR-29a, miR-92a, miR-148a-3p, miR-155, miR-221, miR-222, and miR-373, along with downregulated miRNAs like miR-34a, miR-96, miR-99a, miR-125b, miR-145, miR-200c, miR-203, miR-214, miR-411, and miR-486 present a comprehensive profile that could serve as potential non-invasive biomarkers for diagnosing breast cancer and predicting its outcomes. By utilizing the miRWalk database, the study has further elucidated the target genes associated with each miRNA, constructing a network that provides insights into the molecular mechanisms underlying breast cancer development and progression. Moreover, the gene ontology and pathway analyses conducted shed light on the functional significance of these miRNAs and their target genes, revealing their involvement in key biological processes and signalling pathways implicated in breast cancer pathogenesis. The constructed Protein-Protein interaction network adds another layer of understanding by delineating potential interactions among these target genes. Of particular significance is the exploration of target genes associated with OncomiRs and Tumor Suppressor miRNAs (TS-miRs), such as EGFR, MYC, TP53, and AKT1, elucidating their roles in crucial signalling pathways implicated in breast cancer. This deeper insight into the molecular landscape of breast cancer holds immense potential for the development of targeted therapies and personalized treatment strategies. In the context of breast cancer screening, these findings offer a promising avenue for early detection and monitoring. By leveraging the dysregulated miRNAs and their associated target genes, clinicians may be able to enhance the sensitivity and specificity of existing screening methods, enabling earlier detection of breast cancer and facilitating timely interventions. Furthermore, the non-invasive nature of miRNA biomarkers presents an attractive opportunity for routine screening and surveillance, potentially improving patient outcomes through earlier diagnosis and tailored treatment approaches. Further validation on independent cohorts of breast cancer patients and in vitro studies confirm the association between these miRNAs and breast cancer, assessing their predictive or prognostic value. Optimizing protocols for extracting miRNAs from various sample types (e.g., tissue, blood, plasma) is essential to ensure robust and reliable detection. qPCR is a widely used technique that measures the abundance of miRNAs in samples through amplification and quantification of specific nucleic acid sequences. Overall, this study represents a significant step forward in the utilization of miRNA-based biomarkers for breast cancer screening and prognosis, offering novel insights into the molecular mechanisms driving breast cancer progression and highlighting avenues for further research and clinical translation.

References

1. Pu, H., Peng, J., Xu, F., Liu, N., Wang, F., Huang, X., Jia, Y. (2020). Ultrasound and Clinical Characteristics of False-negative Results in Mammography Screening of Dense Breasts. Clin Breast Cancer,20(4):317-325.

2. Zhiguang Yang, and Zhaoyu Liu. (2020). The Emerging Role of MicroRNAs in Breast Cancer. Journal of Oncology, 1687-8450.

3. Nurzadeh, M., Naemi, M., and Sheikh Hasani,S. (2021). A comprehensive review on oncogenic miRNAs in breast cancer. Journal of Genetics, 100 (1).

4. Gupta, S.R.R, Nagar, G., Mittal, P., Rana, S., Singh, H., Singh, R., Singh, A., Singh, I.K.(2023). Breast Cancer Therapeutics and Hippo Signaling Pathway: Novel MicroRNA-Gene-Protein Interaction Networks. OMICS, 27(6): 273-280.

5. Wang, S., Shang, P., Yao, G., Ye, C., Chen, L., and Hu,X. (2022). A genomic and

Current Trends in Biotechnology and Pharmacy
Vol. 17 (Supplementry Issue 3s) 1 - 10, July-Sept 2024, ISSN 0973-8916 (Print), 2230-7303 (Online)
10.5530/ctbp.2024.4s.2

29

transcriptomic study toward breast cancer. Front. Genet, 13:989565.

6. Ahmed, M.M., Ishrat, R., Tazyeen, S., et al.(2021). In Silico Integrative Approach Revealed Key MicroRNAs and Associated Target Genes in Cardiorenal Syndrome. Bioinformatics and Biology Insights, 15.

7. Diansyah, M.N., Prayog, A.A., Sedana, M.P., Savitri, M., Romadhon, PZ., Amrita, P.N.A., Wijaya, A.Y., Hendrata, W.M., and Bintoro, U.Y. (2021). Early detection breast cancer: Role of circulating plasma miRNA-21 expression as a potential screening biomarker. TurkishJournal of Medical Sciences, 51(2), 562-569.

8. Pridko, O., Borikun, T., Rossylna,, O., Rishko, M., Rusyn, A.V.(2022). Expression Pattern of miR-125b-2, -155, -221, AND -320a is Associated With Response of Breast Cancer Patients to Tamoxifen. Experimental oncology, 44:2.

9. Mandar, S., Chaudhary., Vu Pham, V.H.,and Thuc, D. Le. (2021). NIBNA: a network-based node importance approach for identifying breast cancer drivers. Bioinformatics, 37(17), 2521–2528.

10. Kim, J.Y., Jung,E.J., Kim, J. M., Son, Y., Lee,H.S., Kwag, S.J., Park, J. H., Cho,J .K., Kim, H.G., Park,T., Jeong, S. H., Jeong,C.Y., Ju ,Y .T.(2023) . MiR-221 and miR-222 regulate cell cycle progression and affect chemosensitivity in breast cancer by targeting ANXA3. Exp Ther Med, 7;25(3):127.

11. Van der Sijde, F., Homs,M. Y.V., Van Bekkum, M. L., Van den Bosch,T .P. P., Bosscha, K., Besselink, M. G., Bonsing, B .A., De Groot, J .W .B., Karsten, T. M., Groot Koerkamp, B., Haberkorn B. C .M., Luelmo, S .A .C., Mekenkamp, L.J.M., Mustafa,D .A.M., Wilmink, J .W., Van Eijck, C. H. J., Vietsch, E. E. (2021). Serum miR-373-3p and miR-194-5p Are Associated with Early Tumor Progression during FOLFIRINOX Treatment in Pancreatic Cancer Patients: A Prospective Multicenter Study. Int J Mol Sci, 22(20):10902.

12. Hanieh Sadeghi, Aryan Kamal, Marzieh Ahmadi, Hadi Najafi, Ali Sharifi Zarchi, Peyman Haddad, Bahareh Shayestehpour, Leila Kamkar, Masoumeh Salamati, Loabat Geranpayeh, Marzieh Lashkari and Mehdi Totonchi. (2021). A novel panel of blood-based microRNAs capable of discrimination between benign breast disease and breast cancer at early stages. RNA Biology, 18:2, 747-756,

13. Itani, M. M., Nassar, F. J., Tfayli,A.H., Talhouk, R. S., Chamandi, G. K., Itani, A.R .S., Makoukji, J., Boustany, R .M .N., Hou ,L., Zgheib ,N. K .(2021). A Signature of Four Circulating microRNAs as Potential Biomarkers for Diagnosing Early-Stage Breast Cancer. International Journal of Molecular Sciences, 22(11):6121.

14. Takhshid, N., and Fahimi, H., (2021). Diagnostic Potential of miR-30a and miR-200c in Invasive Breast Ductal Carcinoma. Precis Med Clin OMICS, 1(1):e117729.

15. Martínez Illescas, N. G., Leal, S., González, P., et al. (2023). miR-203 drives breast cancer cell differentiation. Breast Cancer Res,2591.

16. Deng, X. J., Zheng, H. L., Ke, X.Q., Deng, M., Ma, Z.Z., Zhu, Y., Cui, Y. Y .(2021). Hsa-miR-34a-5p reverses multidrug resistance in gastric cancer cells by targeting the 3'-UTR of SIRT1 and inhibiting its expression. Cell Signal, 84:110016.

17. Angajala, A., Raymond, H., Muhammad, A., Uddin Ahmed, M.S., Haleema, S., Haque, M., Wang, H., Campbell, M., Martini, R., Karanam, B., Kahn, A.G., Bedi, D., Davis, M., Tan, M., DeanColomb, W., Yates, C. (2022). MicroRNAs within the Basal-like signature of Quadruple Negative Breast Cancer impact overall survival in African Americans. Sci Rep,12(1):22178.

18. Hwang, S.Y., Nguyen, N..H, Kim, T.J., Lee, Y., Kang, M.A., Lee, J.S.(2020). Non-Thermal Plasma Couples Oxidative Stress to TRAIL Sensitization through DR5 Upregulation. International Journal of Molecular Sciences, 21(15):5302.

19. Hagan,M .L., Mander, S., Joseph, C., McGrath, M., Barrett, A., Lewis, A., Hill, W. D., Browning, D., McGeeLawrence, M. E., Cai, H., Liu, K., Barrett, J .T., Gewirtz, D. A., Thangaraju, M., Schoenlein, P.V. (2023).

Upregulation of the EGFR/MEK1/MAPK1/2 signaling axis as a mechanism of resistance to antiestrogen-induced BimEL-dependent apoptosis in ER+ breast cancer cells. Int J Oncol,62(2):20.

20. Teng Huang, Jiaheng Li, San Ming Wang. (2023) . Etiological roles of core promoter variation in triple-negative breast cancer. Genes & Diseases, 10 (1),228-238,

21. Elena Spina, and Pamela Cowin. (2021) . Embryonic mammary gland development.Seminars in Cell and Developmental Biology,114, 83-92.

22. Alexander, M., Mikhailova,M .V., Masjedi, A., Ahmadpour, M.,JadidiNiaragh, F. (2020). Tumor-associated neutrophils as new players in immunosuppressive process of the tumor microenvironment in breast cancer. Life Sciences, 118699.

23. Sofi, S., Mehraj, U., Qayoom, H. et al.(2022). Cyclin-dependent kinases in breast cancer: expression pattern and therapeutic implications. Med Oncol, 39:106.

24. Shaykevich, A., Silverman, I., Bandyopadhyaya, G., Maitra, R. (2023). BRG1: Promoter or Suppressor of Cancer? The Outcome of BRG1's Interaction with Specific Cellular Pathways. International Journal of Molecular Sciences,24(3):2869.

25. Ziegler, D.V., Huber, K., Fajas, L. (2022) . The Intricate Interplay between Cell Cycle Regulators and Autophagy in Cancer. Cancers, 14(1):153.

26. de Bessa Garcia, S.A., Araújo, M., Pereira, T., Freitas, R. (2021). HOXB7 Overexpression Leads Triple-Negative Breast Cancer Cells to a Less Aggressive Phenotype. Biomedicines, 9(5):515.

27. Bang, J., Jun, M., Lee, S., Moon, H., Ro, S.W. (2023) Targeting EGFR/PI3K/AKT/mTOR Signaling in Hepatocellular Carcinoma. Pharmaceutics, 15(8):2130.

Association Between Occupational Pesticide Exposure and Parkinson's Disease Risk: An Observational Study In The South Indian Population

L. Divya Christy[1], Visalakshi Veerapan[1], Jayakrishna T[1], Valli Nachiyar C[2], and Jayshree Nellore[1]*

[1]Department of Biotechnology, School of Biochemical Engineering, Sathyabama Institute of Science and Technology (Deemed to be University), JeppiarNagar, Rajiv Gandhi Salai, Chennai-600119

[2]Dean-publications, Department of Research, Meenakshi Academy of Higher education and Research, West KK Nagar, Chennai-600078

*Corresponding author jayshree.biotech@sathyabama.ac.in

Abstract

The pathways and molecular mechanisms underlying the impact of prolonged pesticide exposure on Parkinson's disease (PD) pathophysiology remain elusive. Given the association of altered expression levels of transcription factors (TFs) such as NURR1 and FOXA1 with PD, any dysregulation in these TFs could disrupt neuronal maintenance mechanisms, potentially increasing susceptibility to PD. We hypothesize that environmental insults such as long pesticide exposure could interact with the genes encoding for the TFs NURR1 and FOXA1 thereby, perturbing the regulatory mechanisms and maintenance of the midbrain dopaminergic neurons. In our study, we used NURR1 and FOXA1 as our biomarkers for PD. The transcriptomes from the peripheral blood lymphocytes collected from the blood samples of rural agricultural workers who were subjected to long-term pesticide exposure amongst the Indian subpopulation were profiled to observe any aberration in the expression levels of NURR1 and FOXA1. We demonstrated a significant downregulation of Nurr1 & Foxa1 mRNA expression in the pesticide exposure group compared with the healthy controls. This data supports that pesticide exposures may be in the initial stage of dopamine neuron degeneration as it is difficult to measure the motor symptoms of PD using the UPDRS scale in the preliminary stages. However, the current study did not identify the risk factor between male and female groups. In conclusion, our findings provide compelling evidence implicating pesticides in PD risk. This is the first human population study indicating that pesticide exposure may elevate PD risk, utilizing transcription factors as markers. Our population-based retrospective cohort study indicates higher long-term PD risks associated with pesticide exposure, potentially constituting an independent PD risk factor.

Keywords: Parkinson's disease, transcription factors, dopamine neurons, DNA damage, pesticide

Introduction

Parkinson's disease arises from a complex interplay of genetic and environmental factors. Environmental influences, particularly long-term pesticide exposure, have been linked to the sporadic onset of PD in various epidemiological studies (1,2). Notably, the herbicide Paraquat shares molecular similarities with MPP^+ (1-methyl-4-phenylpyridinium) and has been found to specially damage dopaminergic neurons, increase neuronal oxidating stress, impair mitochondrial complex I, and disrupt the ubiquitin-proteasome system (3,4). In addition to paraquat, other pesticides such as rotenone, organochlorines, maneb, and organophosphates have also been associated with an elevated risk of PD (5). Studies indicate that pesticides exposure may not only increase

the risk of PD but also contribute to earlier onset of symptoms and premature death in PD patients.Glyphosateexposure, for instance, has been linked to motor, cognitive and psychiatric symptoms,suggesting that pesticides may impact all stages of PD progression (6,7). Beyond observational studies, there are reportssuggesting genetic alterations due to pesticide exposure in PD. A meta-analysis has highlighted an increased risk of alterations in various PD pathogenesis-related genes, including GST, PON-1, MDR1, and SNCA genes. However, the precise mechanism remain to be fully elucidated (8).

In previous studies Slotkin *et al.*(9), it was found that pesticide exposure led to alterations in the expression levels of several genetic risk factors associated with PD. Specifically, organophosphate exposure, a prevalent compound in many pesticides,induced transcriptional changes in genes associated linked to PD in both laboratory cell studies and animal models. Additionally, a separate study highlighted oxidative stress and mitochondrial dysfunction among agricultural workers exposed to organophosphates. These findings suggest a potential mechanism by which pesticide exposure may increase susceptibility to developing neurological symptoms, possibly through oxidative stress-induced mitochondrial dysfunction (10). Despite these insights , the precise pathways and molecular mechanisms underlying the impact of long-term pesticide exposure on PD pathophysiology remain incompletely understood.

Parkinson's disease is characterized by degeneration of dopaminergic neurons in the midbrain, leading to various phenotypic manifestations such as reduced locomotor activity, tremors, and postural instability. Transcriptional factors (TFs) play a crucial role in regulating dopamine synthesis, promoting dopaminergic neuron development during embryonic stages, and maintaining their function in adulthood (11). Among these TFs, NURR1 and FOXA1 are particularly for the survival, differentiation, and maintenance of midbrain dopaminergic neurons in the (12-14). NURR1 regulates nuclear-encoded mitochondrial genes, and its dysfunction contributed to mitochondrial dysfunction, a mechanism PD pathophysiology (15). Ablation of NURR1 and FOXA1 results in rapid neuron loss in regions like the substantia nigra pars compacta (SNpc), characteristic of PD. Additionally, these TFs regulate the expression of dopamine-related markers like the DA transporter (DAT), tyrosine hydroxylase (TH), and vesicular monoamine transporter (VMAT2). Studies have shown decreased NURR1 expression levels in peripheral blood lymphocytes of PD patients (16) and genetic variations in NURR1 and FOXA1 are associated with PD risk . Previous research in the in the Indian subpopulation identified the polymorphisms in exon 4 of NURR1 and exon 3 of FOXA1 in male and female PD patients.Furthermore, alterations in TF expression levels were reported among PD patients (17). These findings underscore the potential of NURR1 and FOXA1 as biomarkers for assessing PDrisk.

Given that alterations in the expression levels TFs NURR1 and FOXA1 are linked to PD, it is hypothesised that pesticide exposure may disrupt molecular mechanisms crucial for neuronal maintenance resulting in susceptibility to developing PD. This study specifically hypothesizes that pesticide exposure can potentially disrupt the intricate molecular mechanisms responsible for neuronal maintenance, potentially affecting these TFs. This study aims to assess the risk of PD development among rural agricultural workers in the Indian subpopulation exposed to pesticides. NURR1 and FOXA1 will be utilised as biomarkers to evaluate their expression levels in pesticide- exposed agricultural workers. By investigating this association, the study aims to shed light on the potential link between pesticide exposure, TF alterations, and PD susceptibility in this demographic.

Materials and Methods
Study Design

All human studies were conducted with prior approval from the ethical issue

committee of the Sathyabama Institute of Science and Technology, Chennai. (Sathyabama University/IHEC/Study no.001). This study utilised a cross-sectional design to examine the effects of prolonged pesticide exposure on the health of agricultural workers in Udumalaipettai, Tirupur district, Tamil Nadu.

Participant Recruitment

Agricultural workers exposed to organochlorines and organophosphates for a minimum of 10 years, aged between35 and 65 years were recruited to participate for the study. Participants were recruited from Udumalaipettai in the Tirupur district of Tamil Nadu.

Inclusion Criteria

The following inclusion criteria were applied:
• Healthy agricultural workers.
• Individuals who had been involved in crop cultivation for at least ten years and had utilised the specified pesticides.
• Age between 35 to 65 years.

Exclusion Criteria

The following exclusion criteria were applied:
• Agricultural workers with pre-existing medical conditions (exception for hypertension and diabetes).
• Individuals above 75 years of age.

The inclusion and exclusion criteria were carefully selected to ensure the enrollment of agricultural workers with significant pesticide exposure while minimizing confounding factors.

Data Collection

Demographic and exposure-related data were collected from the participants through structured questionnaires administered by trained interviewers. Specifically, cases were defined as individuals meeting the following criteria: 1) diagnosed with PD within the past 3 years by a physician; 2) engaged in agriculture and use pesticide and fertilizers; 3)

duration of involvement in agriculture? 4) presence of allergies while handling pesticides and fertilizers; 5) absence of other neurological condition or serious psychiatric diseases; 6) not in the final stages of a terminal illness; 7) willingness to participate in the study.

Blood Sample collection

Blood samples were collected under sterile conditions with 1ml drawn using a sterile syringe and tourniquet assistance. The collected blood was immediately transferred to 3ml vials coated with EDTA. To prevent coagulation, the vials were thoroughly shaken and stored at 4°C. All samples were processed within 24 hours of collection. A total of 40 PBL samples were collected, comprising 17 subjects from the pesticide exposed group with an average age of 51.2 ± 11.19 years and 27 healthy controls (HC) matched by gender, age (55.7 ± 9.2 years), and origin.

1RNA Extraction and cDNA synthesis

Whole blood samples (1 mL) were anticoagulated with ethylene diamine tetra acetic acid (EDTA), and mixed with phosphate-buffered saline (PBS) at a 1:1 ratio. The mixture was then layered over HiSep LSM medium (HiMedia), and centrifuged at 400 ×g for 30 min following the manufacturer's instructions. This process allowed for the isolation of Peripheral blood mononuclear cells (PBMCs), which were subsequently washed in ice-cold PBS for RNA extraction. Total RNA was extracted from PBMCs using the TRIzol Reagent method (Invitrogen) following the manufacturer's protocol. Subsequently, cDNA carried out according to the manufacturer's instructions using Applied Biosystem kit (18).

Expression profiling of Nurr1 and Foxa1

The fluorescent real-time PCR reaction was conducted usingan "Applied Biosystem Step one" instrument and Applied Biosystem power SYBR green with specific primers targeting *Nurr1*and *Foxa1.* The PCR conditions consisted of an initial denaturation step at 95°C for 1 min, followed by 40 cycles

of denaturation at 95°C for 30 sec, annealing at 60°C for 30 sec, and extension at 72°C for 1 min. β-actin was utilised as an internal control for normalisation of gene expression levels. Real-time PCR data were quantitatively analyzed by using the $2^{-\Delta\Delta Ct}$ method (19).

Statistical analysis

In the statistical analysis, X^2 test was employed to assess the differences in the distributions of gender between the pesticide-exposed group and the control subjects. One- or two-way ANOVA was utilised to evaluate differences in the mean values of relative *Nurr1* and *Foxa1* gene expression levels. Additionally, Unconditional multivariable logistic regression analysis was performed to control for potential confounding such as age and gender.This analysis helps determine whether the observed associations between pesticide exposure and gene expression levels remain significant after adjusting for these confounders.

Estimation of the biochemical parameters

The biochemical parameters in the blood samples of agricultural workers were analyzed using a HematologyAnalyzer (biotech). A 20μl blood sample was utilized for this process.A total of 15 parameters were analysed, including the total white blood cell count (WBC), red blood cell count(RBC), red cell distribution width(RDW), granulocytes levels, monocytes level, platelet count, mean platelet volume(MPV), hemoglobin levels, hematocrit levels (HCT) were employed to analyze the proportion of blood made of cells, procalcitonin levels(PCT) to determine the infection levels, mean corpuscular volume(MCV), mean corpuscular hemoglobin (MCH)levels, mean corpuscular hemoglobin concentration(MCHC), platelet distribution width (PDW) for identifying any aberration.

Comet assay

The comet assay was performed on 20 μl blood samples following the protocols outlined by Muniz et al 2007 (20) and Kent et al 1995 (21). DNA damage was assessed by measuring the tail length and tail moment using a UV transilluminator.

Results and Discussion

The study investigated the potential correlation between pesticide exposure and risk PD by examining the expression profiling of Nurr1 and Foxa1, alongside assessing haematological parameters and DNA damage. The participants, predominantly aged over 40 and lacked a family history of PD, were divided into cases and controls. Cases tend to be slightly older than controls, with a higher prevalence of males and fewer years of formal education completed. Furthermore, a large proportion of participants were either non-smokers or former smokers. Throughout agricultural activities, subjects were exposed to various organophosphate pesticides, including dimethoate, oxydemetone ethyl, and quinalphos.

Previous research has suggested a twofold increase in PD risk associated with prolonged exposure to organophosphates compared to other types of pesticide (22, 23). Meta-analysis have consistently demonstrated a significant association between PD and pesticide exposure (24-26). Moreover, certain pesticides have been found to disrupt proteasomal function and promote aggregation of α-synuclein, impacting the dopamine system (3).

Increased rates of gene mutations have been observed in PD patients, with specific genes such as GSTP1, SLC6A3, and MDR1 implicated (27). Animal models exposed to pesticides have exhibited behavioral and motor disturbances resembling with PD (28), along with differential expression of certain genes (29; 17). This study represents the first effort to estimate PD risk and occupational pesticide exposure based on genetic variations using Peripheral blood lymphocytes (PBL).

In our study, we assessed the risk of PD by examining the expression profiling of Nurr1 and Foxa1. Initially, we compared gender-based expression profiles between the pesticide-exposed group and the healthy

Current Trends in Biotechnology and Pharmacy
Vol. 18 (Supplementry Issue 4A) 31 - 40, November 2024, ISSN 0973-8916 (Print), 2230-7303 (Online)
10.5530/ctbp.2024.4s.3

35

Table 1: Gene expression profiling of *Foxa1* and *Nurr1* gene from peripheral blood of agricultural workers. Data are presented as Mean ± SEM, Gene expression was normalized with the beta-actin gene. (ANOVA, *$P<0.05$ relative to control)

Gender	TF	R2	CI-95%	p-Value
Male	Nurr1	0.520	0.15-0.54	0.002
	Foxa1	0.740	0.44-0.90	0.001
Female	Nurr1	0.170	0.04-0.62	0.08
	Foxa1	1.170	0.04-0.56	<0.06

control group (Table 1). Our findings revealed a significant downregulation of Nurr1 expression in males by 26.52% (p<0.05) and in females by 21.09% in the pesticide-exposed group compared to healthy controls. However, no significant changes were observed in female participants. Similarly, Foxa1 expression was significantly downregulated by 54.40% (p<0.05) in the male pesticide-exposed group and by 21.80% (p>0.05) in the female pesticide-exposed group compared to healthy male controls.

The summary Odd Ratios (ORs) for developing PD based on the Nurr1 expression profile indicated a decreased risk in males, with a value of 0.52 (95% CI: 0.15-0.54) (p<0.05), while in females, the OR was 0.172 (95% CI: 0.04-0.62) (p>0.05). Regarding the Foxa1 expression profile, cumulative pesticide exposure in males resulted in an OR of 0.74 (95% CI: 0.44-0.90) (p<0.05), whereas in females, the OR was 1.17 (95% CI: -0.04-0.56) (p>0.05).

These findings suggest that pesticide exposures may indeed contribute to the initial stages of dopamine neuron degeneration, as evidenced by the observed downregulation of Nurr1 and Foxa1 expression. However, it is challenging to assess motor symptoms of PD solely based on these expression profiles.The Unified Parkinson's Disease Rating Scale (UPDRS) is commonly used to evaluate motor symptoms in PD patients, but its utility in assessing early-stage PD solely based on expression profiles of Nurr1 and Foxa1 may be limited. Other factors and clinical assessments may need to be considered for a comprehensive evaluation of PD symptoms and progression.

An in-vitro study assessing the effect of permethrin pesticide exposure reported an increase in Nurr1 expression, which was counteracted by antioxidants (30). While reports do not suggest differential expression of Foxa1, this study revealed varied expression of Foxa1 in individuals after prolonged exposure, indicating its potential as a biomarker for PD progression during pesticide exposure. Although case-control studies have shown a lower risk factor in female groups, this study did not distinguish between male and female risk factors due to gender-specific differences in dopamine neuron degradation initiation (31, 32). Long-term cognitive disturbances were observed in occupationally exposed individuals even after cessation of work, highlighting the need to consider the long-term neurological effects of pesticide usage in agricultural settings.

Our findings are consistent with previous research indicating that high exposure to chemicals and pesticides can lead to changes in hematological parameters, including alterations in hemoglobin levels and increased red blood cell (RBC) and white blood cell (WBC) counts (33). For example, a study by Garca-Garca et al. (34) observed elevated hematological parameters in intensive agriculture workers exposed to pesticides in South-eastern Spain. Similarly, another study noted increased blood parameters in insecticide factory workers (35). In our study, we observed significant changes in RBC and WBC counts among

male agricultural workers aged 45 to 65, indicative of potential hematological effects associated with pesticide exposure. However, such effects were not observed in female employees (Table 2). Disorders such as polycythemia, characterized by abnormal rises in RBC levels, and leukemia, characterized by increased WBC levels, are often associated with elevated WBC and RBC counts (36). Despite these observations, our biochemical analysis did not reveal extreme abnormalities beyond the changes in RBC and WBC counts. It's important to note that while hematological measures provide valuable insights, they

alone may not conclusively establish toxicological evidence. Nonetheless, they serve as additional parameters in understanding potential variations during disease development and progression.

Our study successfully utilized leukocytes from farmers with occupational pesticide exposure to quantify DNA damage employing the comet assay. DNA damage encompasses alterations in the chemical structure and sequence of DNA, which can occur due to exposure to pesticides, leading to lesions that hinder genome transcription and replication. These lesions can result in mutations or aberrant genomes if left

Table 2: Hematological profile of agricultural workers analyzed from the peripheral blood after exposure to pesticides. Data are presented as Mean ± SEM (ANOVA, *$P<0.05$ relative to control)

S. No	Grouping	WBC count (×10^3 µl)	RBC count (×10^6 µl)	PLT (×10^3 µL)	MCV (fl)	MCH (pg)	MCHC (g/dl)
	Ref Range	4.5 – 12	4.2 - 6.5	100 -1610	53 – 68	16 – 23	30 – 34
1	s1	9.2 ± 1.05	9.91 ± 0.80	1582± 82.3	55.8±6.2	17.7± 1.2	31.8± 1.42
2	s2	8.2 ± 1.61	11.47 ± 2.12	866± 30.1	60.1± 7.1	17.5± 0.88	30.6± 1.2
3	s3	13.4 ± 2.63	9.05± 0.55	1119± 43.3	55.9± 6.3	19± 2.34	31.4± 1.38
4	s4	13.8 ± 4.13	9.01± 0.43	621± 24.2	59.2± 6.71	18± 1.7	32.1± 1.5
5	s5	16.4 ± 3.21	8.53± 0.2	1231± 40.2	58.01± 6.53	19.7± 2.6	31.1± 1.31
6	s6	21.9 ± 7.72	7.51± 0.2	1166±38.3	59.3± 6.8	20.1± 2.98	33.2± 1.75
7	s7	12.6 ± 2.32	7.85± 0.28	1338± 30.1	61.01± 7.5	18.5± 2.1	33± 1.7
8	s8	15.5 ± 4.12	9.26± 0.7	1086± 33.1	56.4± 6.43	18.5± 2.2	32.9± 1.64
9	s9	12.4 ± 1.88	8.29± 0.5	1203± 39.7	57.03± 6.62	19.9± 2.87	32.6± 1.6
10	s10	7.9 ± 1.10	8.87± 0.45	1205± 40.0	54.9± 5.8	18.1± 1.81	32.7± 1.68
11	s11	3.7 ± 0.18	8.82± 0.8	1361± 48.6	56.5± 6.5	19.9± 2.87	32.1± 1.58
12	s12	15.5 ± 5.2	6.67± 0.41	854± 27.2	68.4± 8.3	17.8± 1.4	29.1± 0.72
13	s13	13.5 ± 3.33	8.52± 1.0	1416± 60.1	56.9± 6.8	17.5± 0.88	31.4± 1.38
14	s14	6.5 ± 1.07	8.32± 1.1	899± 31.2	57.3± 7.0	18.4± 2.0	30.6± 1.2
15	s15	9.6 ± 2.02	8.25± 0.88	915± 39.9	56.9± 6.8	19.2± 2.5	32.4± 1.68
16	s16	9.4 ± 2.0	7.57± 0.4	232± 20.5	60.2± 7.1	17.8± 1.46	32± 1.7
17	s17	10.9 ± 3.1	8.55± 1.31	1052± 40.1	58.2± 6.95	16.4±	30.7± 1.4

Current Trends in Biotechnology and Pharmacy
Vol. 18 (Supplementry Issue 4A) 31 - 40, November 2024, ISSN 0973-8916 (Print), 2230-7303 (Online)
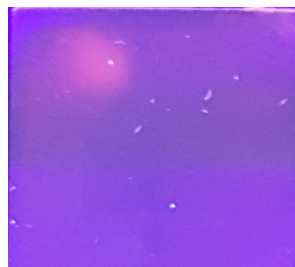10.5530/ctbp.2024.4s.3

37

Figure 1: Comet image of blood sample of agricultural workers after exposure to pesticides visualized under UV transilluminator

unrepaired. Upon observation under a UV transilluminator, the presence of comets was evident in the slides [Figure 1], confirming suspected DNA breakage. This highlights the detrimental impact of repeated exposure to pesticides such as organophosphates and organochlorines on DNA structure, leading to DNA damage (37).

Research by Alves et al. demonstrated that workers exposed to complex pesticide mixes exhibited DNA damage as revealed by the comet assay (38). Additionally, soybean field workers exposed to a cocktail of pesticides reported increased DNA damage measured by the comet assay and other biochemical markers (39). Furthermore, malathion, a highly toxic organophosphate pesticide, was shown to cause genotoxic damage to Daphnia magna cells using the comet assay as a biomarker (40, 41). The comet assay serves as a reliable technique for assessing the genotoxicity and carcinogenesis of various agents in human biomonitoring. Notably, our findings suggest that pesticide exposure at work poses a greater risk of DNA damage compared to drinking polluted water, as evidenced by higher levels observed in exposed individuals than in controls (42, 43).

In summary, our study confirms that long-term pesticide exposure has a detrimental effect on DNA structure, leading to DNA breakage, as evidenced by biochemical parameters and the comet assay. However, elucidating the precise impact and pinpointing the effect in Parkinson's disease (PD) studies can be challenging due to the variability in exposure and residual effects of multiple types of pesticides encountered by agricultural workers over time.

Conclusion

In conclusion, our study provides compelling evidence linking pesticide exposure to the risk of Parkinson's disease (PD). By investigating the association between pesticide exposure and PD risk using transcription factors, we have shed light on a novel aspect of this relationship. Specifically, our findings indicate that exposure to pesticides, particularly organophosphates and organochlorines found in pesticides like Dimethoate, Oxydemetone ethyl, and Quinalphos, significantly increases the long-term risk of developing PD.

However, it is crucial to acknowledge the limitations of our study. The sample size may be limited, potentially impacting the generalizability of our results. Moreover, demographic characteristics and occupational biases among participants may introduce confounding variables that influence the observed associations. The reliance on self-reported or indirect measures for pesticide exposure assessment may also introduce recall bias or misclassification.

Despite these limitations, our study underscores the importance of further research in understanding the complex relationship between pesticide exposure and PD risk. Future studies with larger, more diverse samples and rigorous study designs are warranted to validate our findings and elucidate the underlying mechanisms driving this association.

Overall, our study contributes valuable insights into the potential health impacts of pesticide exposure and highlights the need for continued efforts to mitigate pesticide-related risks in occupational settings. By acknowledging these challenges and limitations upfront, we aim to foster

transparency in the research process and provide a foundation for future investigations in this important area of study.

Authors' Contribution

All authors contributed significantly to the conception and design of the study, as well as the acquisition, analysis, and interpretation of data.

Funding

The authors declare that they did not receive any funds, grants, or other support during the preparation of this manuscript

Conflicts of Interest

The authors declare that they have no conflicts of interest regarding the publication of this manuscript.

Data Availability

The data generated and analyzed in this research article are included in the manuscript, and all references in the text are listed in the reference section.

Publisher's Note

This journal remains neutral concerning jurisdictional claims in published institutional affiliation.

References
1. Angelopoulou, E., Paudel, YN., Papageorgiou, SG., Piperi, C. (2022). Environmental impact on the epigenetic mechanisms underlying Parkinson's disease pathogenesis: a narrative review. Brain Sciences, 12(2):175.
2. Ullah, I., Zhao, L., Hai, Y., Fahim, M., Alwayli, D., Wang, X., Li, H. (2021). Metal elements and pesticides as risk factors for Parkinson's disease-A review. Toxicology Reports, 8:607-16.
3. Xiao, J., Dong, X., Zhang, X., Ye, F., Cheng, J., Dan, G., Zhao, Y., Zou, Z., Cao, J., Sai, Y. (2021). Pesticides exposure and dopaminergic neurodegeneration. Exposure and Health, 13:295-306.
4. Kaur, K., Kaur, R. (2018). Occupational pesticide exposure, impaired DNA repair, and diseases. Ind J Occup Environ Med., 22:74-81.
5. Islam, MS., Azim, F., Saju, H, Zargaran A, Shirzad M, Kamal M, Fatema K, Rehman S, Azad MM, Ebrahimi-Barough S. (2021). Pesticides and Parkinson's disease: Current and future perspective. Journal of Chemical Neuroanatomy, 115:101966.
6. Gamache, PL., Haj Salem, I., Roux-Dubois, N., Le Bouthillier, J., Gan-Or, Z., Dupré, N. (2019). Exposure to pesticides and welding hastens the age-at-onset of Parkinson's disease. Can J Neurol Sci., 46(6):711-6.
7. Caballero, M., Amiri, S., Denney, JT., Monsivais, P., Hystad, P., Amram, O. (2018). Estimated residential exposure to agricultural chemicals and premature mortality by Parkinson's disease in Washington state. Int J Environ Res Public Health., 15(12).
8. Jbaily, H. (2023). Assessing the Impact of Multiple Common Factors on the Development of Parkinson's Disease: An Updated Narrative Review.
9. Slotkin, TA., Seidler, FJ. (2011). Developmental exposure to organophosphates triggers transcriptional changes in genes associated with Parkinson's disease in vitro and in vivo. Brain Res Bull, 86(5-6): 340-7.
10. Huang, M., Bargues-Carot, A., Riaz, Z., Wickham, H., Zenitsky, G., Jin, H., Anantharam, V., Kanthasamy, A., Kanthasamy, AG. (2022). Impact of environmental risk factors on mitochondrial dysfunction, neuroinflammation, protein misfolding, and oxidative stress in the etiopathogenesis of Parkinson's disease. International Journal of Molecular Sciences, 23(18):10808.
11. Tian, L., Al-Nusaif, M., Chen, X., Li, S., Le W. Weidong Le. (2022). Roles of transcription factors in the development and reprogramming of the dopaminergic neurons. Int J Mol Sci., 23(2):845.
12. Tian, L., Al-Nusaif, M., Chen, X., Li, S., Le, W. (2022). Roles of transcription factors in the development and reprogramming of the dopaminergic neurons. International Journal of Molecular Sciences, 23(2):845.

13. Tippabathani, J., Nellore, J. (2021). Temporal changes in key developmental transcription factors in dopamine neurons during MPP+ induced injury and recovery in zebrafish brain. Indian Journal of Biochemistry and Biophysics (IJBB), 58(1):45-55.

14. Prakash, N. (2022). Developmental pathways linked to the vulnerability of adult midbrain dopaminergic neurons to neurodegeneration. Frontiers in Molecular Neuroscience, 15:1071731.

15. Hermanson, E., Joseph, B., Castro, D., Lindqvist, E., Aarnisalo, P., Wallén, Å., Benoit, G., Hengerer, B., Olson, L. and Perlmann, T., (2003). Nurr1 regulates dopamine synthesis and storage in MN9D dopamine cells. Experimental cell research, 288(2), 324-334.

16. Kadkhodaei, B., Alvarsson, A., Schintu, N., Ramsköld, D., Volakakis, N., Joodmardi, E. (2013). Transcription factor Nurr1 maintains fiber integrity and nuclear-encoded mitochondrial gene expression in dopamine neurons. Proc Natl Acad Sci U S A., 110(6):2360-5.

17. Jayakrishna, T., Nellore, J., Radhakrishnan, V., Banik, S., Kapoor, S. (2017). Identification of NURR1 (Exon 4) and FOXA1 (Exon 3) haplotypes associated with mRNA expression levels in peripheral blood lymphocytes of Parkinson's patients in Small Indian population Parkinson's disease 2017.

18. Claudia Rödel adjusted from TRIzol® LS Reagent protocol (Ambion, Cat.# 10296). (2012). Total RNA isolation from 50 zebrafish embryos using TRIzol.

19. Schmittgen, T.D. and Livak, K.J. (2008). Analyzing real-time PCR data by the comparative CT method. Nature protocols, 3(6), 1101-1108.

20. Muniz, JF., McCauley, L., Scherer, J., Lasarev, M., Koshy, M., Kow, YW., Nazar-Stewart, V., Kisby, GE. (2008). Biomarkers of oxidative stress and DNA damage in agricultural workers: a pilot study. Toxicology and applied pharmacology, 227(1):97-107.

21. Kent, CR., Eady, JJ., Ross, GM., Steel, GG. (1995). The comet moment as a measure of DNA damage in the comet assay. International journal of radiation biology, 67(6):655-60.

22. Shrestha, S., Parks, CG., Umbach, DM., Richards-Barber, M., Hofmann, JN., Chen, H.,Blair, A., Freeman, LE., Sandler, DP. (2020). Pesticide use and incident Parkinson's disease in a cohort of farmers and their spouses. Environmental Research, 191:110186.

23. See, WZ., Naidu, R., Tang, KS. (2022). Cellular and Molecular Events Leading to Paraquat-Induced Apoptosis: Mechanistic Insights into Parkinson's Disease Pathophysiology. Molecular Neurobiology, 59(6):3353-69.

24. Barbeau, A., Roy, M., Bernier, G., Campanella, G., Paris, S. (1987). Ecogenetics of Parkinson's disease: prevalence and environmental aspects in rural areas. Can J Neurol Sci., 14(1):36-41.

25. Shrestha, S., Parks, CG., Umbach, DM., Richards-Barber, M., Hofmann, JN., Chen, H., Blair, A., Freeman, LE., Sandler, DP. (2020). Pesticide use and incident Parkinson's disease in a cohort of farmers and their spouses. Environmental Research, 191:110186.

26. Torti, M., Fossati, C., Casali, M., De Pandis, MF., Grassini, P., Radicati, FG., Stirpe, P., Vacca, L., Iavicoli, I., Leso, V., Ceppi, M. (2020). Effect of family history, occupation and diet on the risk of Parkinson disease: A case-control study. Plos one, 15(12):e0243612.

27. Liu, X., Ma, T., Qu, B., Ji, Y., Liu, Z. (2013). Pesticide-induced gene mutations and Parkinson disease risk: a meta-analysis. Genet Test Mol Biomarkers, 17(11):826-32.

28. Anderson, TJ. (2021). The Neurotoxicity of Inhaled Paraquat, a Translationally Relevant Route of Exposure. University of Rochester.

29. Khan, AH., Lee, LK., Smith, DJ. (2022). Single-cell analysis of gene expression in the substantia nigra pars compacta of a pesticide-induced mouse model of Parkinson's disease. TranslNeurosci., 13(1):255-69.

30. Tönges L, Buhmann C, Klebe S, Klucken J, Kwon EH, Müller T, Pedrosa DJ, Schröter N, Riederer P, Lingor P. Blood-

Current Trends in Biotechnology and Pharmacy
Vol. 18 (Supplementry Issue 4A) 31 - 40, November 2024, ISSN 0973-8916 (Print), 2230-7303 (Online)
10.5530/ctbp.2024.4s.3

40

based biomarker in Parkinson's disease: potential for future applications in clinical research and practice. J Neural Transm (Vienna). 2022 Sep;129(9):1201-1217.

31. Bordoni, L., Fedeli, D., Nasuti, C., Capitani, M., Fiorini, D., Gabbianelli, R. (2017). Permethrin pesticide induces NURR1 up-regulation in dopaminergic cell line: is the pro-oxidant effect involved in toxicant-neuronal damage? Comp BiochemPhysiol C ToxicolPharmacol., 201:51-7.

32. Howell, RD., Dominguez-Lopez, S., Ocañas, SR., Freeman, WM., Beckstead, MJ. (2020) Female mice are resilient to age-related decline of substantia nigra dopamine neuron firing parameters. Neurobiol Aging, 95:195-204.

33. Santos, ASE., Krawczyk, N., Parks, CG., Asmus, CFI., Câmara, VM., Lima, J. (20121). Parkinson's disease hospitalization rates and pesticide use in urban and nonurban regions of Brazil. Cad Saúde Colet, 29(4):496-508.

34. Khan, M., Nazir, I., Nazir, S., Wadood, M., Irfan, G., Nasir, SS. (2023). Impact Of Chronic Exposure of Organophosphorus Pesticide On Hematological And Biochemical Parameters Of Agriculture Workers: A Cross Sectional Study. Journal of Pharmaceutical Negative Results, 3059-67.

35. García-García, CR., Parrón, T., Requena, M., Alarcón, R., Tsatsakis, AM., Hernández, AF. (2016). Occupational pesticide exposure and adverse health effects at the clinical, hematological and biochemical level. Life Sci., 145:274-83.

36. Nejatifar, F., Abdollahi, M., Attarchi, M., Roushan, ZA., Deilami, AE., Joshan, M. (2022). Evaluation of hematological indices among insecticides factory workers. Heliyon, 8(3):e09040.

37. Wilson, WW., Shapiro, LP., Bradner, JM., Caudle, WM. (2014). Developmental exposure to the organochlorine insecticide endosulfan damages the nigrostriatal dopamine system in male offspring. Neurotoxicology, 44:279-87.

38. Prathiksha, J., Narasimhamurthy, RK., Dsouza, HS., Mumbrekar, KD. (2023). Organophosphate pesticide-induced toxicity through DNA damage and DNA repair mechanisms. Molecular Biology Reports, 1-5.

39. Alves, JS., da Silva, FR., da Silva, GF., Salvador, M., Kvitko K., Rohr P. (2016). Investigation of potential biomarkers for the early diagnosis of cellular stability after the exposure of agricultural workers to pesticides. An Acad Bras Cienc., 88(1):349-60.

40. Barrón Cuenca, JX. (2020). Genotoxic effects among Bolivian farmers exposed to mixtures of pesticides: population and in vitro based studies.

41. Knapik, LFO., Ramsdorf, W. (2020). Ecotoxicity of Malathion pesticide and its genotoxic effects over the biomarker comet assay in Daphnia magna. Environ Monit Assess. 2020;192(5):264.

42. Bhargavi, B. R., Vellanki, R. K. ., Akurathi, R., & Reddy Kanala, J. (2021). Assessment of eco-genotoxic effects of pesticide mixtures on freshwater fish, Catlacatla. Current Trends in Biotechnology and Pharmacy, 15(1), 44–50. https://doi.org/10.5530/ctbp.2021.1.5

43. Azqueta, A., Ladeira, C., Giovannelli, L., Boutet-Robinet, E., Bonassi, S., Neri, M., Gajski, G., Duthie, S., Del Bo, C., Riso, P., Koppen, G. (2020). Application of the comet assay in human biomonitoring: An hCOMET perspective. Mutation Research/Reviews in Mutation Research, 83:108288.

44. Vazquez Boucard, C., Lee-Cruz, L., Mercier, L., Ramírez Orozco, M., Serrano Pinto, V., Anguiano G. (2017). A study of DNA damage in buccal cells of consumers of well-and/or tap-water using the comet assay: assessment of occupational exposure to genotoxicants. Environ Mol Mutagen, 58(8):619-27.

Mutational Stability Profiling and Functional Analysis of Spike Protein In Indian Sars Cov-2 Delta Variants: An *In Silico* Analysis

Prisho Mariam Paul[1,2], Krupakar Parthasarathy[1]*, Sudhanarayani S Rao[1], Vignesh Sounderrajan[1], Sakthivel Jayaraj[1] and Swetha Sunkar[3]

[1]Centre for Drug Discovery and Development, Sathyabama Institute of Science and Technology, Chennai, Tamil Nadu
[2]Biotechnology Department, CMS College Kottayam, Kerala
[3]Department of Bioinformatics, School of Bio and chemical Engineering, Sathyabama Institute of Science and Technology, Chennai, Tamil Nadu
*Corresponding author: pkrupakar.cddd@sathyabama.ac.in

Abstract

Amidst the global pandemic caused by the SARS-CoV-2 virus, researchers are actively studying its evolution and impact. This research delves into the spike protein of the SARS-CoV-2 Delta variant, using advanced computational methods to analyze mutations and their effects. By examining mutations and their evolutionary connections in the spike protein using data from databases, the study aims to gain insights into the virus's behavior.To gauge the stability of the spike protein variants, we used various methods. We predicted protein sequence disorders using PONDR. We also used the I-Mutant v2.0 bioinformatics tool to assess how mutations affected stability. We then performed functional studies using Protparam and NetPhos to analyze the consequences of these mutations. These analyses identified several key mutations in the spike protein, especially the D614G substitution. This polar-to-nonpolar amino acid change was particularly noteworthy.Our research identified significant mutations in the spike protein of the Delta Indian variant of SARS-CoV-2, including: T19R, E156G, L452R, T478K, P681R, and D950N. Deletions occurred at positions Y145, F157, and R158. Analysis showed increased phosphorylation of the spike protein, hinting at potential regulation by these mutations. Using structural modeling by Spdbv tool, we found that mutations within the Receptor-Binding Domain (RBD) region reduced protein stability. This study enhances our understanding of the mutations and their impact on the function of the Delta Indian variant's spike protein. Our research explores how mutations in the SARS-CoV-2 virus affect how its proteins work and stay stable. By understanding these effects, we can lay the foundation for future studies that design treatments specifically for new SARS-CoV-2 variants. In summary, our work shows that SARS-CoV-2 is constantly evolving, making it crucial to keep track of changes and keep researching to help guide health policies.

Keywords: SARS CoV-2, Spike protein, Mutation, Coronaviruses.

Introduction

The spread of COVID-19 around the world has shown that the severity of the disease can vary a lot. This variation depends on things like age, sex, and where the person lives. Even though there have been many ideas proposed, none of them can fully explain why there are such big differences in COVID-19 symptoms. The virus was first found in Wuhan, China in December 2019 and has since spread all over the world. Scientists are trying to understand how SARS-CoV-2 has changed by comparing the genetic material of the virus from different countries to the original material from Wuhan (1). The Coronaviridae family has two main groups: Letovirinae and Orthocoronavirinae. Orthocoronavirinae has

Current Trends in Biotechnology and Pharmacy
Vol. 18 (Supplementry Issue 4A) 41 - 52, November 2024, ISSN 0973-8916 (Print), 2230-7303 (Online)
10.5530/ctbp.2024.4s.4

42

several types, including alpha, beta, gamma, and delta. Beta-coronaviruses cause respiratory diseases in humans, including SARS-CoV, MERS-CoV, and SARS-CoV-2. Scientists classify variants of these viruses based on how easily they spread, how severe the illness they cause is, how well they can evade immunity, how well they respond to treatment, and how easy they are to detect with tests.Different types of SARS-CoV-2 virus, called variants, are categorized into two groups: Variants of Concern (VOC) and Variants of Interest (VOI). Currently, eleven variants have been identified (Alpha to Lambda). It's likely that more variants will continue to appear in the future(2).

Coronaviruses are viruses that have an outer layer made of fat. Inside, they carry a short strand of RNA that can infect both animals and birds. The RNA in the SARS-CoV-2 virus, which causes COVID-19, is about 30, 000 units long. It contains instructions to make 29 different proteins. These proteins include 16 that help the virus spread and survive, 9 that play a supporting role, and 4 that form the virus's structure. The structural proteins are: Spike (S) glycoprotein: Helps the virus attach to cells. Envelope (E) protein: Forms part of the virus's outer layer. Membrane (M) protein: Forms part of the virus's outer layer and helps assemble new viruses. Nucleocapsid (N) protein: Protects the virus's RNA (3).Coronaviruses have prominent glycoproteins called Spike proteins that extend outside their envelope. These proteins assist in the early stages of viral infection by binding to receptors on host cells. SARS-CoV and SARS-CoV-2 share about 75% similarity in their Spike proteins. These proteins have a molecular weight of about 141, 178 Daltons and are made up of 1, 273 amino acids. The Spike protein has three major parts: an outer ectodomain, a membrane-spanning part, and a brief section within the cell.The Spike protein has two subunits, S1 and S2, which help the virus bind to cells and enter them. It also allows the virus to spread from cell to cell, contributing to the infection's progression(4).

Scientists have identified a specific type of COVID-19 virus (SARS-CoV-2) by looking at the most common changes in its genetic material, especially those in the Spike protein. Viruses like SARS-CoV-2 change their genetic makeup in various ways to increase their chances of staying alive.Despite potential mutations that could weaken the virus, it often regains its strength due to the emergence of "compensatory mutations." To better grasp this process, we analyzed the frequency of mutations in all genes of the SARS-CoV-2 virus.(2) The WHO announced the start of the third wave of the COVID-19 pandemic. The dominant strain is the Delta variant, first seen in India. This variant is better at dodging antibodies, making it more easily spread and possibly causing more severe illness. Experts have also identified a more contagious subvariant of Delta, called Delta plus (B.1.617.2). (5). This research employs bioinformatics tools to assess the impact of mutations on the stability and function of the spike (S) protein found in the SARS-CoV-2 delta variant from India. The analysis is based on the genetic sequence of the virus.

Methodology

Sequence Retrieval

According to the NCBI protein database (http://www.ncbi.nlm.nih.gov/), we obtained 128 full protein sequences from India. Among these, we selected 15 spike protein sequences of the Delta variant strain from different regions for analysis. The reference sequence for comparison is the ancestral strain from Wuhan, China. Table 1

Table 1: Accession id's of all SARS CoV-2 sequences that were used in this study
NCBI Accession id(Spike Protein)
YP_009724390.1 QYM90002.1QYM89991.1QYM89980.1 QYM89969.1QYM89958.1QYM89445.1QYM89434.1QYM89423.1QYM89412.1QYM89401. 1QYM88739.1QYM88727.1QYM88716.1QYM88705.1QYM88694.1

Mutational Stability Profiling and Functional Analysis

contains the accession numbers for all spike protein sequences.

Multiple Sequence Analysis and Phylogenetic analysis

We used BioEdit to align the amino acid sequences of spike protein variants. Conserved sites were verified using ClustalW. Sequence comparisons were conducted with MEGA(Molecular Evolutionary Genetics Analysis). The Neighbour-Joining method was utilized to study evolutionary history (6), with 1000 replicates used to create the bootstrap consensus tree (7).

Mutational analysis

PONDR, a predictor of natural disordered regions available at (http://www.pondr.com/), forecasts regions of disorder within protein sequences. These disordered regions can impact the specificity or affinity of protein binding (8). PONDR relies on five different algorithms, including VLXT, XL1_XT, and VSL2. The VLXT predictor combines three feedforward neural networks: VL1, N-terminus (XN), and C-terminus (XC) predictors. XL1 focuses on disorder regions of more than 39 amino acids (9), while VSL2 predicts both long and short disordered regions.

The iMutant 2.0 server is used to compare the stability of wild type and mutant proteins by calculating the effect of mutations. It predicts the outcome based on changes in Gibbs free energy (10). ΔG is calculated by subtracting the energy of the unfolded state from the energy of the folded state. The difference between the ΔG of the wild type and mutant type is referred to as $\Delta\Delta G$. If both values are negative, the protein's energy and stability decrease. A positive $\Delta\Delta G$ value indicates that the mutant sequence has a higher ΔG and stabilizes the protein. All mutations were conducted at 25 °C, close to the global average temperature, and pH 7, which does not impact any type of mutation. Learn more about the iMutant 2.0 server at (https://folding.biofold.org/imutant/i-mutant2.0.

html). Changing these values has an impact on protein stability.

Physicochemical properties of S-proteins

The S-proteins' physical and chemical characteristics were analyzed using Expasy'sProtParam tool (http://expasy.org/tools/protparam.html). This included predicting the theoretical isoelectric point (pI), extinction coefficient, instability index, molecular weight, aliphatic index, and grand average hydropathy (GRAVY) of the spike protein.

Post-Translational Modification

The NetPhos tool available at (http://www.cbs.dtu.dk/services/NetPhos/) can predict Serine, Threonine, and Tyrosine phosphorylation sites. Similarly, the NetNGlyc tool found at (www.cbs.dtu.dk/services/NetNGlyc/) is used to predict glycosylation sites on spike proteins.

Structural Analysis

The ACE2 bound to the spike protein of SARS CoV-2 was obtained from the PDB database (ID: 6M0J). The RBD region of the spike protein was extracted using the Autodock tool, and a specific mutation was introduced using Spdbv. The stability of the structure was then assessed by performing energy calculations after the mutation insertion.

Results and Discussions

Multiple Sequence Analysis of Spike protein delta variants

We compared 15 spike protein sequences of Indian delta variant strain from different regions of India with the reference sequence from Wuhan, China. Total 29 mutations are identified in sequences. Result of multiple sequence alignment is shown in Figure 1. Each variation and its proportion is displayed in Figure 2. Substitution of amino acid occurs in non polar amino acids and polar amino acids. Also a polar to non polar and non polar to amino acid substitution is identified in multiple sequence alignment. The D614G mutation is the most notable change from a polar to a non-polar amino acid, and it is a significant mutation. Additionally, there are other important mutations observed, such
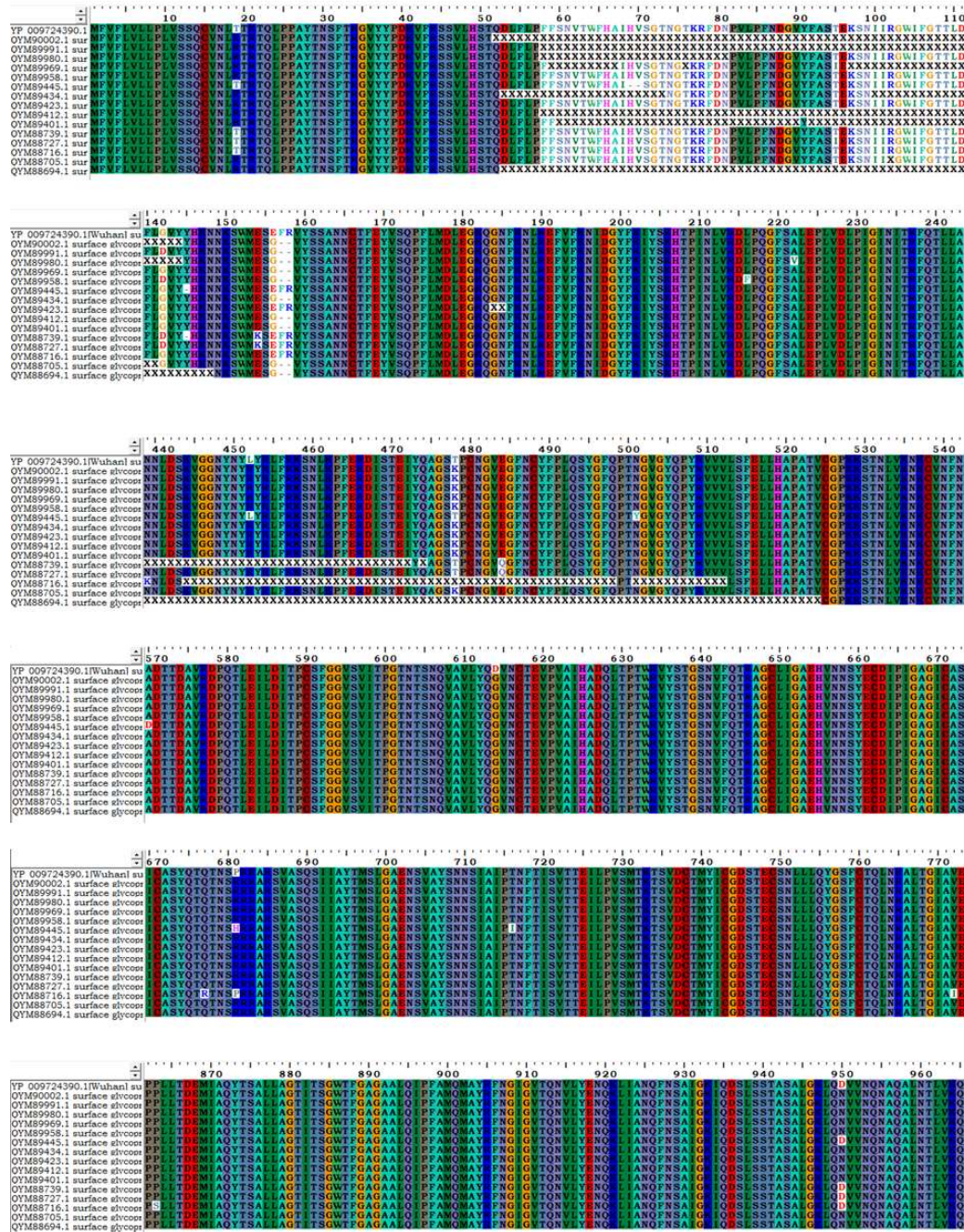
Figure 1: Multiple Sequence Analysis of SARSCoV- 2 Spike protein

Mutational Stability Profiling and Functional Analysis
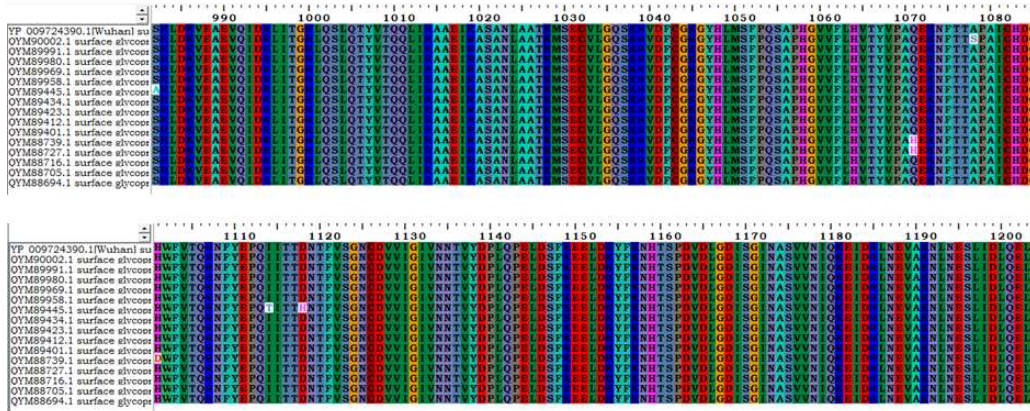
Figure 1: Multiple Sequence Analysis of SARSCoV- 2 Spike protein (*Contd.*)
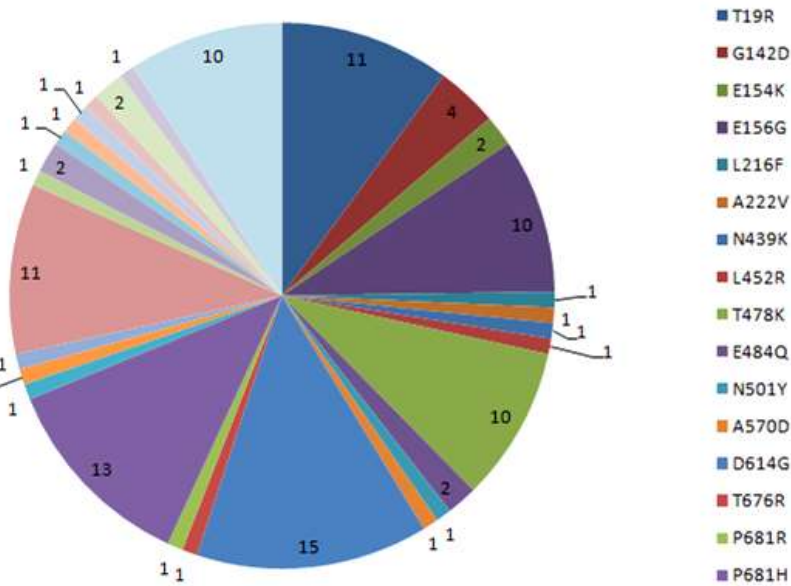
Figure 2: Proportion of variation in Sequences of SARS CoV-2

as the T19R switch from polar to polar, E156G switch from polar to non-polar, L452R switch from non-polar to polar, T478K switch from polar to polar, P681R switch from non-polar to polar, and D950N switch from polar to polar. Furthermore, there are deletions of Y145 in two sequences, as well as deletions of F157 and R158 in ten sequences.

Phylogenetic Analysis

Phylogenetic analyses of spike proteins were done with MegaX tool. Neighbor Joining method was used to interpret the evolutionary history (6). The bootstrap consensus tree inferred from 1000 replicates is taken to represent the evolutionary history of the taxa

Paulet al

analyzed(7). Branches corresponding to partitions reproduced in less than 50% bootstrap replicates are collapsed. A Poisson correction method is used to calculate the evolutionary distances and is represented as units of the number of amino acid substitutions per site (11). 16 amino acid sequences are involved in this analysis. All ambiguous positions were removed for each sequence pair (pairwise deletion option). There were a total of 1273 positions in the final dataset. Resulting tree is shown in Figure 3. Result demonstrated that only one sequence is positioned in same clade of Wuhan strain. All other sequences are showed in different clade based on similarity.

Mutational analysis

PONDR (http://www.pondr.com/) Predictor of Natural Disordered Regions predicts the disordered region upon sequences. For predicting disordered region in this study, we took three algorithms XL1-XT, VLXT, VSL2. We consider the region which has been predicted by 3 algorithms as a disordered region of protein. The resulting disordered region is shown in Table 2.

To calculate the effect of mutation on protein stability between wild type and mutant protein the iMutant 2.0 server (https://folding.biofold.org/imutant/i-mutant2.0. html)

is used. Each mutation was considered separately for prediction. Table 3 showed the mutation stability of each mutation which identified after multiple sequence analysis. For analyzing mutational stability the individual mutation took the Wuhan protein as the reference.

Physicochemical properties of S-proteins

Protparamanalysis resulted that spike protein is an acidic peptide due to the theoretical pI range from 6.2 to 6.8 (percentage of acidic amino acid). The instability indexes of all sequences are below 40 and it showed that all protein was a stable peptide.Positive factors for the increased thermo stability of proteins are represented by aliphatic index and this factor is range from 69.33 to 84.67 which showed that all proteins are thermostable. GRAVY is ahydropathy index which augmented with theincrease in the positive score. GRAVY value of all protein is approximately near to -0.079. So this interpret that all proteins were hydrophilic in nature. Protparam result of all spike protein is given in Table 4.Due to some ambiguous sequence Protparam tooldid not calculates the pI of some sequencesand it was shown as undefined. The mutation causes very less variation in physiochemical properties. But further studies on this will reveal more details of physiochemical parameters.
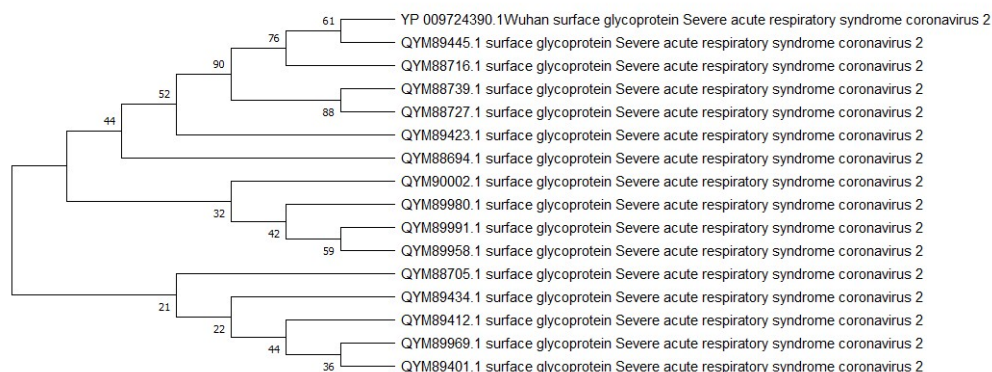
Figure 3: Phygenetic Analysis of SARS CoV-2 Delta variant Spike protein

Mutational Stability Profiling and Functional Analysis

Current Trends in Biotechnology and Pharmacy
Vol. 18 (Supplementry Issue 4A) 41 - 52, November 2024, ISSN 0973-8916 (Print), 2230-7303 (Online)
10.5530/ctbp.2024.4s.4

47

Table 2: PONDR – Disordered regions in the sequences		
Sl.No.	Protein Name (total length)	XL1-XT ,VLXT, VSL2
1	YP_009724390.1(Wuhan)	679-689, 945-950
2	QYM90002.1	677-687, 700, 938-953
3	QYM89991.1	677-687, 700-702, 938-953
4	QYM89980.1	677-687, 700-702, 938-953
5	QYM89969.1	677-687, 700-702, 938-953
6	QYM89958.1	677-687, 700-702, 938-953
7	QYM89445.1	681-685, 942-946
8	QYM89434.1	93-96, 677-687, 700-702, 938-953
9	QYM89423.1	679-689, 940-955
10	QYM89412.1	677-687, 700-702, 938-953
11	QYM89401.1	677-687, 700-702, 938-953
12	QYM88739.1	677-687, 700-703, 944-948
13	QYM88727.1	679-689, 702-704, 945-950
14	QYM88716.1	678-689, 702-704, 945-950
15	QYM88705.1	677-687, 700-702, 938-953
16	QYM88694.1	677-687, 700-702, 938-953

Table 3: Stability of the induced Mutant with reference to wild type SARS CoV-2 Wuhan strain					
Mutation Stability					
T19R	Decrease ↓	E484Q	Decrease ↓	P863S	Decrease ↓
G142D	Decrease ↓	N501Y	Increase ↑	D950N	Decrease ↓
E154K	Decrease ↓	A570D	Decrease ↓	S982A	Decrease ↓
E156G	Decrease ↓	D614G	Decrease ↓	A1070H	Decrease ↓
L216F	Decrease ↓	T676R	Decrease ↓	A1078S	Decrease ↓
A222V	Increase ↑	P681R	Decrease ↓	H1101D	Decrease ↓
N439K	Decrease ↓	P681H	Decrease ↓	I1114T	Decrease ↓
L452R	Decrease ↓	T716I	Decrease ↓	D1118H	Decrease ↓
T478K	Decrease ↓	V772I	Decrease ↓		

Post-Translational Modification

NetPhos and NetNGlyc are used for predicting modification sites. Our result showed that spike protein is highly phosphorylated. All variant strains also have the same result. So, mutation is not affected in post translational modification.

Structural Analysis

After mutational analysis, study identified five mutations in RBD region of spike protein. They are N439K, L452R, T478K, E484Q, and N501Y. Using Spdbv inserted these mutations in RBD region and calculated the energy.

Current Trends in Biotechnology and Pharmacy
Vol. 18 (Supplementry Issue 4A) 41 - 52, November 2024, ISSN 0973-8916 (Print), 2230-7303 (Online)
10.5530/ctbp.2024.4s.4

48

Table 4: Protparam result for the SARS CoV-2 Spike protein sequences

Protein id	Theoretical Isoelectric Point(pI)	Instability index	Aliphatic index	Grand average hydropathy(GRAVY)
YP_009724390.1(Wuhan)	6.24	33.01	84.67	-0.079
QYM90002.1	Undefined	30.19	74.38	-0.086
QYM89991.1	Undefined	30.46	76.14	-0.085
QYM89980.1	Undefined	31.48	78.44	-0.069
QYM89969.1	Undefined	32.66	80.06	-0.091
QYM89958.1	6.78	32.75	84.19	-0.091
QYM89445.1	6.35	32.82	84.65	-0.078
QYM89434.1	Undefined	30.87	76.6	-0.097
QYM89423.1	Undefined	32.24	80.84	-0.076
QYM89412.1	Undefined	30.78	76.68	-0.091
QYM89401.1	Undefined	30.75	76.37	-0.087
QYM88739.1	Undefined	31.41	78.61	-0.045
QYM88727.1	6.8	32.81	84.67	-0.084
QYM88716.1	Undefined	29.16	72.05	-0.031
QYM88705.1	Undefined	32.79	83.19	-0.094
QYM88694.1	Undefined	28.09	69.33	-0.047

Table 5: Phosphorylation and Glycosylation sites in the SARS CoV-2 Sequences

NetPhos (Phosphorylation sites) and NetNGlyc(Glycosylation sites)

Phosphorylation sites

13, 19, 29, 46, 50, 51, 71, 73, 76, 91, 95, 108, 109, 112, 116, 151, 160, 161, 162, 170, 172, 200, 204, 208, 221, 240, 247, 250, 255, 256, 279, 286, 302, 305, 313, 316, 349, 351, 359, 366, 375, 376, 380, 383, 396, 415, 449, 469, 470, 473, 477, 494, 514, 523, 531, 547, 553, 555, 572, 573, 588, 591, 596, 599, 602, 604, 612, 630, 632, 637, 640, 659, 660, 673, 676, 678, 680, 686, 689, 691, 698, 707, 721, 734, 735, 741, 746, 758, 768, 778, 789, 791, 803, 813, 875, 881, 917, 929, 937, 939, 940, 961, 968, 974, 975, 982, 998, 1003, 1009, 1021, 1027, 1030, 1037, 1100, 1138, 1147, 1155, 1161, 1170, 1196, 1209, 1215, 1242, 1252, 1261

Glycosylation sites

17, 61, 74, 122, 149, 165, 234, 282, 331, 343, 603, 616, 657, 709, 717, 801, 1074, 1098, 1134, 1158, 1173, 1194

For SARS CoV-2 RBD region showed the energy -10337.443 kcal/mol and after inserting mutation it showed -9755.156 kcal/mol. So it revealed that mutation decreases the stability of the structure Figures 4 and 5.

Due to mutations, the SARS CoV-2 virus has spread more easily. The virus's low genetic diversity suggests a recent origin. Mutations' impact increases over time, as seen in HIV-1. The virus's novelty is indicated by the presence of acommon phenotypic
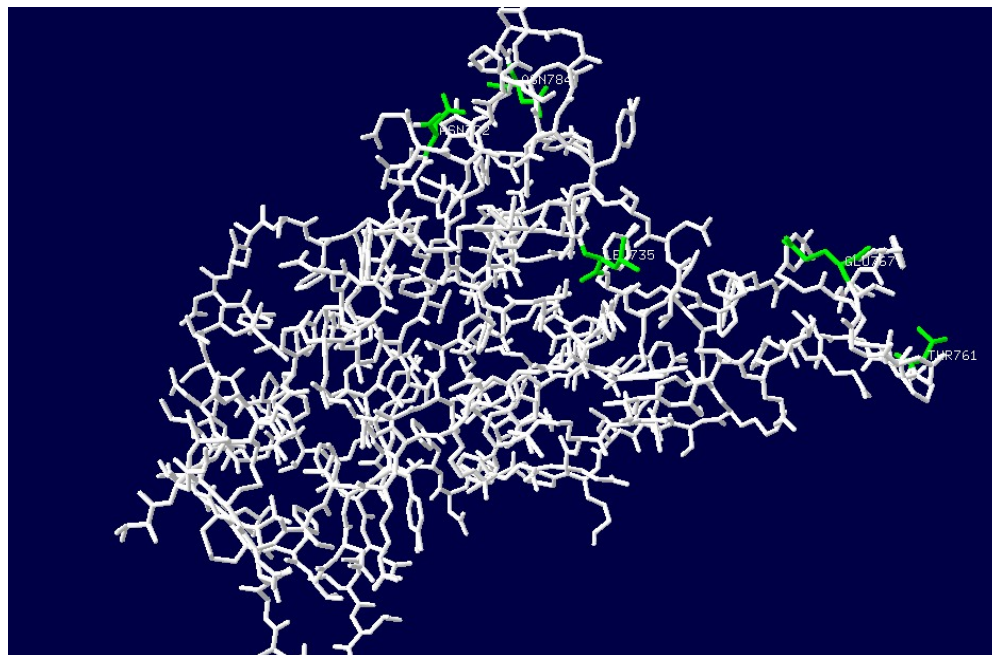
Mutational Stability Profiling and Functional Analysis
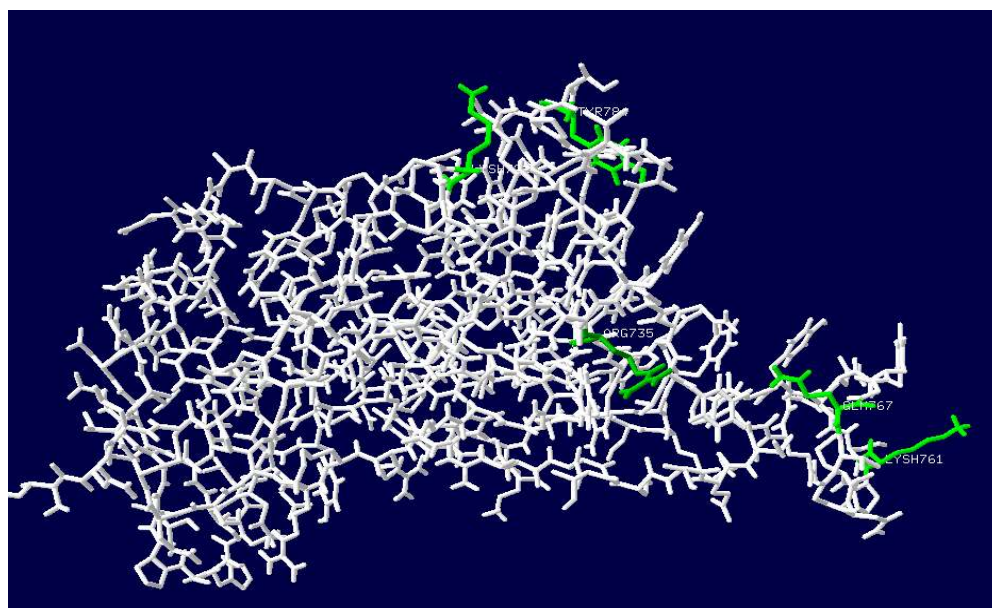
Figure 4: RBD Structure of CoV-2 before mutation

Figure 5: RBD Structure of CoV-2 after induced Mutation

Paulet al

Current Trends in Biotechnology and Pharmacy
Vol. 18 (Supplementry Issue 4A) 41 - 52, November 2024, ISSN 0973-8916 (Print), 2230-7303 (Online)
10.5530/ctbp.2024.4s.4

50

mutation(12). If a virus has a single unique mutation that often means, it's new. The pattern of mutations in spike protein shows how all the possible changes in these proteins have built up over time. Generally, most mutations make the proteins less stable, which drives the virus to change further to become more stable and avoid being killed off by the immune system (13).

Protein mutations weaken their stability, both functionally and structurally. Research indicates that proteins with smaller cores are more susceptible to mutations. Mutations can destabilize proteins, causing structural changes that alter their conformation. These changes can disrupt protein function and stability (14). Similarly, in the case of HIV-1, drug resistance is a significant concern in the use of combination therapies. Through sequence analysis of drug-resistant strains, it has been discovered that the majority of mutations destabilize the virus (15).The destabilizing mutations in SARS CoV-2 are the main reason for strain diversification and huge variation of the virus. Some mutations affect the phenotype of protein and viral transmissibility (16). Protein stability change due to mutation leads to evolvability of virus and increases genetic diversity (17).To predict intrinsic disorder regions of S protein in this study 3 prediction methods are used. VSL2, XL1-XT and VLXT (18). All three predictive models used characteristics derived from amino acid compositions. Since the S protein's primary role is to bind to host proteins, these disordered areas may impact how the virus spreads. Mutations in the receptor-binding area include L452R, T478K, E484Q, and N501Y.

Phosphorylation sites have prominent role in coronavirus. Phosphorylation plays a vital role in the retention of spike protein at cell surface. For assembling the trimer phosphorylation sites on S protein is needed (19). Glycosylation has a vital role in antigenicity, fusogenic, and immunomodulatory activities of the spike protein (20).Previous studies show that these positions are conserved and these can be considered as inhibitory sites.

The SARS-CoV-2 delta variant, which originated in India, has spread to multiple countries and is known for having three unique mutations: E156del/R158G in the N-terminal domain and T478K in an important receptor binding domain. The T478K mutation in the S gene's functional domain may be linked to the transmissibility and severity of this variant. However, despite efforts, researchers have not been able to precisely locate this specific mutation site in the δ variant through detailed protein structure analyses, possibly due to limitations in laboratory conditions as compared to the complex viral infection process in hosts. Additionally, these mutations could impact the way the virus interacts with other molecules, possibly resulting in stronger interactions with different amino acids (21).

Conclusion

Since December 2019, COVID-19, caused by the SARS CoV-2 virus, has become a global pandemic. A major challenge in developing specific treatments is that the virus evolves over time, creating new strains with different protein sequences. This study used various computer-based methods to examine and analyze mutations in ten SARS CoV-2 proteins. By grouping and comparing protein sequences, researchers identified variations in the virus. They also assessed the impact of these mutations on protein structure and function using mutational profiling and analysis.Understanding the nature of specific viral residues can guide the development of antiviral drugs to combat a broader spectrum of mutations. This knowledge is crucial because mutations can lead to drug resistance, requiring combinatorial therapies like those used for HIV-1. These therapies combine multiple drugs to prevent resistance and increase efficacy(22).Other respiratory viruses have also been treated successfully through therapies that combine multiple drugs (23).

Current Trends in Biotechnology and Pharmacy
Vol. 18 (Supplementry Issue 4A) 41 - 52, November 2024, ISSN 0973-8916 (Print), 2230-7303 (Online)
10.5530/ctbp.2024.4s.4

51

The COVID-19 pandemic, caused by the SARS-CoV-2 virus, has posed a major public health challenge globally. The virus's tendency to mutate rapidly makes it essential to develop treatment strategies that can adapt to these changes. This study used advanced computer simulations to analyze mutations in key viral proteins. This analysis revealed important variations in the virus's genetic makeup, which can affect protein structure and function. By identifying specific viral "weak spots" and their role in drug resistance, this research provides valuable information for designing more effective antiviral treatments.Like successful strategies against viruses like HIV-1, proactively anticipating and countering emerging mutations is crucial for fighting COVID-19. This helps healthcare professionals adapt to the virus's changing nature, preventing its spread and minimizing its global impact. Researchers can customize vaccines to target specific mutations, such as those found in the Delta Indian variant, in order to enhance their effectiveness against new variants. By honingin on crucial mutations, vaccine makers could enhance the range and strength of vaccines, potentially expanding protection against different strains of SARS-CoV-2. Studying how mutations affect the stability and function of the spike protein can help develop treatment options like monoclonal antibodies or antiviral drugs. These therapies could target spike protein areas made susceptible by mutations, potentially blocking the virus from entering host cells or improving virus elimination.

Competing interest
All authors declare that there is not any actual or potential conflict of interest including anyfinancial, personal, or other relationships with other people or organizations within five years ofbeginning the submitted work.

Author Contributions
All authors contributed to the study conception and design. Material preparation, data collection and analysis were performed by [Prisho Mariam paul], [Vignesh Sounderrajan], [Krupakar Parthasarathy], [Sudhanarayani S Rao], [Sakthivel Jayaraj] and [Shwetha Sunkar] The first draft of the manuscript was written by [Prisho Mariam paul] and all authors commented on previous versions of the manuscript. All authors read and approved the final manuscript.

Data Availability
The datasets generated during and/or analysed during the current study are available from the corresponding author on reasonable request.

References
1. Biswas, S. K., & Mudi, S. R. (2020). Genetic variation in SARS-CoV-2 may explain variable severity of COVID-19. Medical Hypotheses, 143, 109877.
2. Kannan, S. R., Spratt, A. N., Cohen, A. R., Naqvi, S. H., Chand, H. S., Quinn, T. P., et al. (2021). Evolutionary analysis of the Delta and Delta Plus variants of the SARS-CoV-2 viruses. Journal of Autoimmunity, 124, 102715.
3. Gao, T., Gao, Y., Liu, X., Nie, Z., Sun, H., Lin, K., et al. (2021). Identification and functional analysis of the SARS-COV-2 nucleocapsid protein. BMC Microbiology, 21(1), 58.
4. Satarker, S., &Nampoothiri, M. (2020). Structural Proteins in Severe Acute Respiratory Syndrome Coronavirus-2. Archives of Medical Research, 51(6), 482–491.
5. Arora, P., Kempf, A., Nehlmeier, I., Graichen, L., Sidarovich, A., Winkler, M. S., et al. (2021). Delta variant (B.1.617.2) sublineages do not show increased neutralization resistance. Cellular & Molecular Immunology, 18(11), 2557–2559.

Current Trends in Biotechnology and Pharmacy
Vol. 18 (Supplementry Issue 4A) 41 - 52, November 2024, ISSN 0973-8916 (Print), 2230-7303 (Online)
10.5530/ctbp.2024.4s.4

52

6. Saitou, N., & Nei, M. (1987). The neighbor-joining method: A new method for reconstructing phylogenetic trees. Molecular Biology and Evolution, 4(4), 406–425.

7. Felsenstein, J., & Kishino, H. (1993). Is there something wrong with the bootstrap on phylogenies? A reply to Hillis and Bull. Systematic Biology.

8. Dunker, A. K., Brown, C. J., Lawson, J. D., Iakoucheva, L. M., & Obradović, Z. (2002). Intrinsic Disorder and Protein Function. Biochemistry, 41(21), 6573–6582. https://doi.org/10.1021/bi012159.

9. Romero, P., Obradovic, Z., & Dunker, A. K. (1997). Sequence data analysis for long disordered regions prediction in the calcineurin family. Genome Informatics, 8, 110–124.

10. Capriotti, E., Fariselli, P., &Casadio, R. (2005). I-Mutant2.0: Predicting stability changes upon mutation from the protein sequence or structure. Nucleic Acids Research, 33(Web Server issue), W306-W310.

11. Zuckerkandl, E., & Pauling, L. (1965). Evolutionary divergence and convergence in proteins. Evolving Genes and Proteins, 97–166.

12. Storz, J. F. (2018). Compensatory mutations and epistasis for protein function. Current Opinion in Structural Biology, 50, 18–25.

13. Serohijos, A. W. R., Rimas, Z., &Shakhnovich, E. I. (2012). Protein biophysics explains why highly abundant proteins evolve slowly. Cell Reports, 2(2), 249–256.

14. Hadfield, J., Megill, C., Bell, S. M., Huddleston, J., Potter, B., Callender, C., et al. (2018). Nextstrain: Real-time tracking of pathogen evolution. Bioinformatics, 34(23), 4121–4123.

15. Olabode, A. S., Avino, M., Ng, G. T., Abu-Sardanah, F., Dick, D. W., & Poon, A. F. Y. (2019). Evidence for a recombinant origin of HIV-1 Group M from genomic variation. Virus Evolution, 5(1), 039.

16. Chen, G., Wu, D., Guo, W., Cao, Y., Huang, D., Wang, H., et al. (2020). Clinical and immunological features of severe and moderate coronavirus disease 2019. Journal of Clinical Investigation, 130(5), 2620–2629.

17. Petit, C. M., Melancon, J. M., Chouljenko, V. N., Colgrove, R., Farzan, M., Knipe, D. M., et al. (2005). Genetic analysis of the SARS-coronavirus spike glycoprotein functional domains involved in cell-surface expression and cell-to-cell fusion. Virology, 341(2), 215–230.

18. Peng, K., Radivojac, P., Vucetic, S., Dunker, A. K., & Obradovic, Z. (2006). Length-dependent prediction of protein intrinsic disorder. BMC Bioinformatics, 7, 208.

19. Davidson, A. D., Williamson, M. K., Lewis, S., Shoemark, D., Carroll, M. W., Heesom, K. J., et al. (2020). Characterisation of the transcriptome and proteome of SARS-CoV-2 reveals a cell passage induced in-frame deletion of the furin-like cleavage site from the spike glycoprotein. Genome Medicine, 12(1), 68.

20. Fung, T. S., & Liu, D. X. (2018). Post-translational modifications of coronavirus proteins: Roles and function. Future Virology, 13(6), 405–430.

21. Jhun, H., Park, H. Y., Hisham, Y., Song, C. S., & Kim, S. (2021). SARS-CoV-2 Delta (B.1.617.2) Variant: A Unique T478K Mutation in Receptor Binding Motif (RBM) of Spike Gene. Immune Network, 21(5), e32. https://doi.org/10.4110/in.2021.21.e32.

22. McFadden, K., Fletcher, P., Rossi, F., Kantharaju, Umashankara, M., Pirrone, V., et al. (2012). Antiviral breadth and combination potential of peptide triazole HIV-1 entry inhibitors. Antimicrobial Agents and Chemotherapy, 56(2), 1073–1080.

23. Hayden, F. G. (1996). Combination antiviral therapy for respiratory virus infections. Antiviral Research, 29(1), 45–48.

Exploring Molecular Interactions and Pathways in Major Depressive Disorder (MDD): A Comparative Analysis of Patients With and Without Anxiety

Manisha Koyimadatha[1], and D. Alex Anand[1]

[1]Department of Bioinformatics, Sathyabama Institute of science and Technology, Tamil Nadu, India
*Corresponding author: danielalexanand@gmail.com

Abstract

Major Depressive Disorder (MDD) presents as an intricate mental health issue often associated with Anxiety. In this study, we used data from Gene Expression Omnibus (GEO) to investigate how anxiety acts as a comorbidity to MDD at the molecular level. We used NCBI GEO Accession ID: GSE98793 for this study. This microarray dataset examines the gene expression profiles associated with MDD both with and without anxiety. As the outcome of the study, a total of 15 significantly upregulated Differential Expressed Genes (DEGs), 4 significantly down regulated Differential Expressed Genes (DEGs) were found in MDD with anxiety data's and 5 significantly upregulated Differential Expressed Genes (DEGs), 18 significantly down regulated Differential Expressed Genes (DEGs) were found in MDD without anxiety data were obtained from the dataset. After protein-protein interaction networks were generated using STRING DB, the molecular associations for MDD were visualised using Cytohubba, a Cytoscape plugin. We performed a functional enrichment analysis using the DAVID Functional Annotation tool to identify the biological processes and pathways associated with the up-regulated and down-regulated genes in the anxiety and non-anxiety groups. ARG1, CRISP3, DEFA4, LCN2, BPI, and LTF were discovered in the anxiety group, while HLA-DQB1, FAM3B, GATB, and HLA-DQA1 were discovered in the non-anxiety group. The Kyoto Encyclopedia of Genes and Genomes (KEGG) pathway and Gene Ontology (GO) were used to analyse differentially expressed genes (DEGs). Interestingly, factors like Staphylococcus aureus infection, the intestinal immune network's role in producing IgA, the steps involved in processing and presenting antigens, and the development of Th1 and Th2 cells are all processes that play a role in the illness and its comorbidity.

Keywords: MDD, DEG's, Biomarkers, Pathways, Therapeutic targets

Introduction

Major Depressive Disorder (MDD) is a common mental health conditioncharacterised by an overpowering sensation of sorrow, despair, and a total loss of interest or pleasure in formerly fun things (1). While depression can manifest on its own, it often coexists with anxiety, creating a complex and challenging clinical presentation(2,3).As per the World Health Organization (WHO), depression stands as the foremost cause of disability globally, impacting more than 264 million individuals across all age groups(4).MDD frequently coexists with various other mental health conditions, such as anxiety disorders, obsessive-compulsive disorder (OCD), post-traumatic stress disorder (PTSD), and substance-related disorders(5).

Anxiety disorders manifest through symptoms like worrying, fears related to social interactions and performance, sudden or triggered panic attacks, anticipatory anxiety, and avoidance behaviors. Also, it's prevalence includes Generalized anxiety disorder (6.2%), social anxiety disorder (13%), and panic disorder (5.2%). Anxiety

disorders are associated with physical symptoms, such as palpitations, shortness of breath, and dizziness. Anxiety disorders are among the most common mental health illnesses globally, with an estimated global prevalence of around 3.8%. Anxiety disorders are among the most common mental health illnesses globally, with an estimated global prevalence of around 3.8 %(5).

The combination of MDD with anxiety not only exacerbates the severity of symptoms but also complicates diagnosis and treatment strategies (3,4).The co-occurrence of MDD with anxiety is common, with epidemiological studies demonstrating a high rate of comorbidity between the two disorders. When MDD and anxiety coincide, the severity of symptoms tends to increase, leading to greater impairment in functioning, heightened risk of suicide, and greater resistance to treatment(6).

Due to the intricate nature of Major Depressive Disorder (MDD) and its co-occurrence with anxiety, there is a critical need for research aimed at elucidating the underlying molecular mechanisms and pathways involved in both conditions. Understanding the molecular interactions and pathways associated with MDD with and without anxiety can provide valuable insights into the biological underpinnings of these disorders, potentially leading to the development of more targeted and effective treatment approaches(5,6).

Despite the recognition of MDD with anxiety as a distinct clinical entity, its diagnosis and management present several challenges (1). The overlapping symptomatology between MDD and anxiety, leading to diagnostic confusion and potential underestimation of the severity of either condition. Additionally, treatment approaches for MDD with anxiety often require careful consideration of pharmacological and psychotherapeutic interventions tailored to address both sets of symptoms effectively. The complexity of managing comorbid MDD and anxiety underscores the need for further research to elucidate underlying mechanisms, improve diagnostic accuracy, and develop more targeted treatment strategies to optimize outcomes for individuals affected by these debilitating disorders (4,6).

Materials and Methods

DataSet

We obtained 68 series and 688 samples pertaining to human Major Depressive Disorder by using the search query "Gene Expression AND (("Major Depressive disorder" OR "MDD") AND (Human OR Homosapien))" in the GEO Datasets database (https://www.ncbi.nlm.nih.gov/geo/) (MDD). Based on a comprehensive analysis, we downloaded gene expression profiles using the GSE98793series, which was based on the GPL570 [HG-U133 Plus 2] Affymetrix Human Genome U133 Plus 2.0 Array. There were no human or animal subjects in any of the studies, and the results are publicly accessible online (7,8).

Analysis of DEG's

Using the GEO2R online analytical application (http://www.ncbi.nlm.nih.gov/geo/geo2r), we compared patients with MDD with and without anxiety to healthy controls. Based on Differentially Expressed Genes (DEGs), the investigation was conducted.We used logFC and corrected P-values as part of the investigation. If a gene's absolute logFC was more than or equal to 1.0 and its adjusted P-value was less than 0.05, it was considered a DEG (9).

Interaction Network:

The DEGs were inserted into the Search Tool for the Retrieval of Interacting Genes (STRING) database (https://string-db.org/)to create a PPI network. The STRING database received multiple gene names from the microarray analysis, both upregulated and downregulated. The database created a PPI network with nodes representing proteins and edges indicating connections between them using these gene names (10).

Current Trends in Biotechnology and Pharmacy
Vol. 18 (Supplementry Issue 4A) 53 - 66, November 2024, ISSN 0973-8916 (Print), 2230-7303 (Online)
10.5530/ctbp.2024.4s.5

55

Hub Genes Identification

The PPI network topology was then examined using Cytoscape (version 3.10.1; http://www.cytoscape.org/). With the use of the CytoHubba plugin function in Cytoscape, the degree of every protein node was determined. Hub genes were defined as those having ten or more gene degrees in the PPI network. The resulting visualizations provided insight into the key molecular interactions associated with MDD, highlighting potential biomarkers or therapeutic targets for further investigation(7,8).

Gene Ontology

Gene ontology was used to analyse the top ten genes in MDD with and without anxiety that were shown to be up and down-regulated. The DAVID Functional Annotation Tool (https://david.ncifcrf.gov/) was used for this analysis. The DAVID tool was used for analysis once gene symbols that corresponded to the top DEGs were uploaded. Three categories exist for classifying gene functions: molecular function (MF), cellular component (CC), and biological process (BP) (9).

Functional Enrichment Analysis

Using the DAVID Functional Annotation Tool (https://david.ncifcrf.gov/), pathway enrichment analysis was performed on the top 10 genes identified in MDD with and without anxiety. This analysis aimed to reveal molecular pathways and signalling cascades influenced by dysregulated genes, shedding light on the pathophysiological mechanisms in MDD. Statistical significance of enriched pathways was determined by adjusted p-values (< 0.05) through appropriate tests. Post-analysis, dysregulated genes and enriched pathways were visualized using the Science and Research plot (SR plot, https://www.bioinformatics.com.cn/en), illustrating fold change and statistical significance of gene expression data related to both MDD with and without Anxiety. Similarly, the GOpathway enrichment bubbleplot(https://www.bioinformatics.com.cn /plot_basic_gopathway_enrichment_bubblepl ot081en) from the KEGG database depicted enriched pathways graphically, with bubble size indicating the number of involved genes and color representing statistical significance(10).

Results & Discussion
Identification of DEG's

The Gene Expression profile gene series dataset (GSE98793) was used in this study. The GSE98793 contained total of 128 samples in that 64 with generalised anxiety disorder, diagnosed by the MINI questionnaire, and 64 without anxiety disorder and 64 healthy controls (Table 1). A total of 45119 DEGs were screened from GSE98793 according to the criterion of $P < 0.05$ and $—logFC— \geq 1.0$. In this 18 upregulated DEG's, 5 downregulated DEG's for MDD with Anxiety and 6 upregulated DEG's, 19 downregulated DEG's for MDD without Anxiety were identified (Table 2). We were able to identify all DEGs by comparing samples of MDD with and without anxiety with samples of normal, healthy individuals (2).

Interaction Network and Hub Gene Identification

Analyzed PPI network in MDD with anxiety revealed 14 nodes and 39 edges for upregulated genes and 4 nodes with 1 edge for downregulated genes. In MDD without anxiety, identified 4 nodes and 1 edge for upregulated genes, and 17 nodes with 40

Table 1: Data from GEO Major Depressive Disorder (MDD) With and Without Anxiety						
Reference	Sample	GEO	Platform	Normal	MDD with Anxiety	MDD without Anxiety
Leday GGR, 2018	Whole Blood Samples	GSE98793	GPL570	64	64	64

Table 2: Screening DEG's in MDD with and without Anxiety		
Gene Regulation	MDD with Anxiety	MDD without Anxiety
Upregulated	OLFM4 CEACAM8 MMP8 LTF LCN2 HLA-DQA1 CRISP3 MMP8 CEACAM6 ARG1 DEFA4 CEACAM6 BPI CNTNAP3P2 CNTNAP3 CNTNAP3B TDRD9	HLA-DQB1 FAM3B GATM HLA-DQA1
Downregulated	ERAP2 HLA-DQB1 FAM3B HLA-DQA1	CD177 CEACAM6 PF4V1 TNNT1 GRB10 SDHD LTF FOLR3 MMP8 CEACAM8 TMEM176A ARG1 LCN2 DEFA4 TMEM176B OLFM4 HLA-DRB4 BPI

edges for downregulated genes (Figure 1). The methodological approach chosen for constructing the hub network using Cytoscape, Cytohubba was Degree centrality, as it identifies nodes with the highest number of connections within the biological network, indicating their potential significance in regulating cellular processes and disease mechanisms. For MDD with anxiety, upregulated genes included MMP8, LCN2, CEACAM8, OLFM4, LTF, CRISP3, DEFA4, BPI, CEACAM6, and ARG1. For MDD without anxiety, downregulated genes comprised CEACAM8, MMP8, LCN2, DEFA4, OLFM4, LTF, BPI, CEACAM6, CD177, and FOLR3(10,11) (Figure 2).

Current Trends in Biotechnology and Pharmacy
Vol. 18 (Supplementry Issue 4A) 53 - 66, November 2024, ISSN 0973-8916 (Print), 2230-7303 (Online)
10.5530/ctbp.2024.4s.5

57

The network includes MDD with anxiety revealed 14 nodes and 39 edges for upregulated genes (a). In MDD without anxiety, identified 17 nodes with 40 edges for downregulated genes (b) (10,11)

Color of node indicates degree of connectedness. The top nine hub genes score from 1 to 9 on the pseudocolor scale, which ranges from red to yellow. On a scale from lowest to greatest, the colours red, orange, and yellow denote the various degrees (10,11).

The matrix metalloproteinase family includes matrix metalloproteinase 8, or collagenase 2, an enzyme that is essential for wound healing, inflammation, and tissue remodelling. Anxiety and Major Depressive Disorder (MDD) patients may have
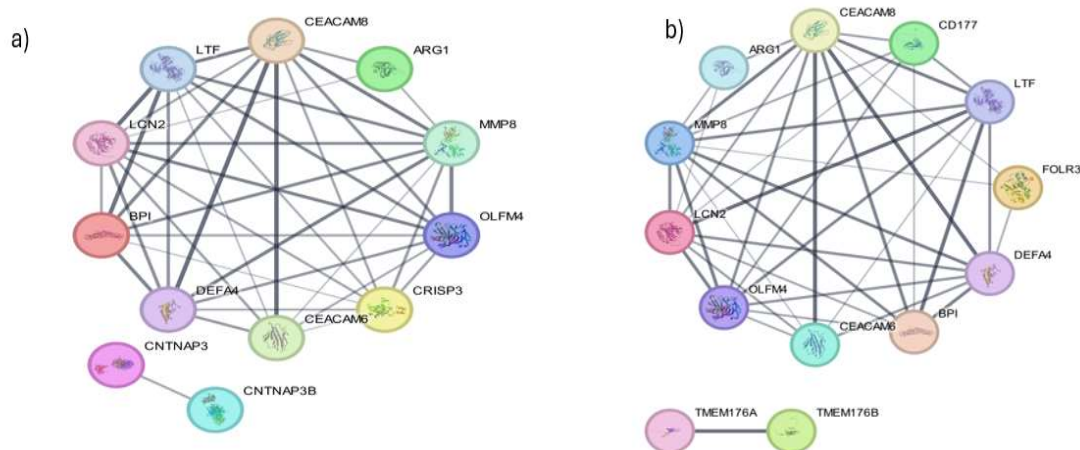

Figure 1: STRING protein-protein interactions network of 20 upregulated and 22 downregulated genes
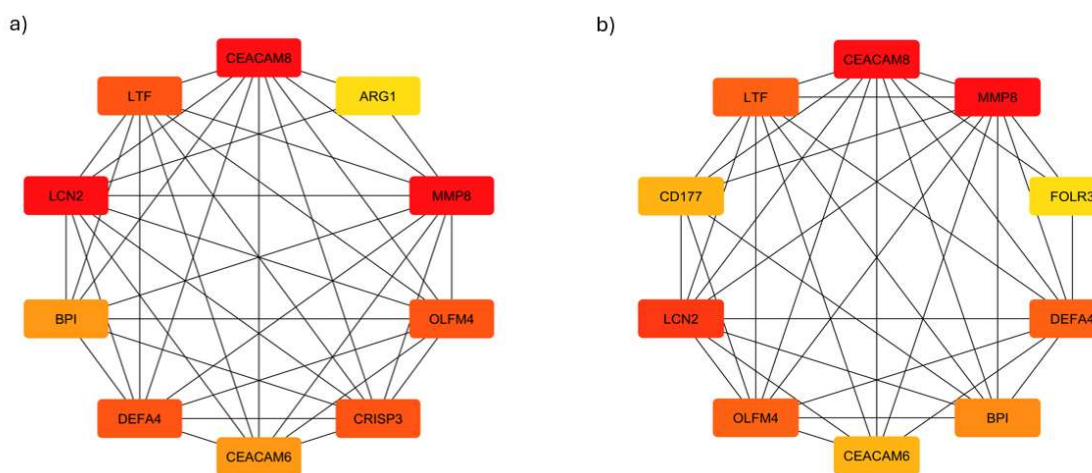

Figure 2: Subnetwork of top nine hub genes from protein-protein interactions network using Cytoscape software

Current Trends in Biotechnology and Pharmacy
Vol. 18 (Supplementry Issue 4A) 53 - 66, November 2024, ISSN 0973-8916 (Print), 2230-7303 (Online)
10.5530/ctbp.2024.4s.5

58

abnormalities in tissue remodelling processes or increased inflammatory activity, as shown by the overexpression of MMP8 in these patients. Conversely, the downregulation of MMP8 in MDD without anxiety suggests differences in the inflammatory profile or tissue remodeling dynamics specific to this subtype of depression, involving inflammatory and stress response pathways (12).

Tissue inhibitors of metalloproteinases are one of the variables that affect the activity of matrix metalloproteinase 8, which mostly breaks down collagen in the extracellular matrix (TIMPs). Natural inhibitors known as TIMPs bind to matrix metalloproteinases (MMPs) and control their activity. In conditions like MDD with anxiety, the balance between MMPs and their inhibitors, such as TIMPs, influences MMP8 activity. Dysregulation of this balance, characterized by decreased TIMP levels relative to MMPs, could elevate MMP activity, potentially contributing to pathological processes like inflammation, tissue remodeling, and neurodegeneration (12,13). Neutrophil gelatinase-associated lipocalin, also known as lipocalin-2 (LCN2), is one member of the lipocalin family of proteins (NGAL). LCN2 is essential for the movement of iron, the response to inflammation, neurogenesis, and neuroprotection. A specific pathway involving lipocalin-2 (LCN2) in major depressive disorder are Neuroinflammation pathways, Neuroprotection and Neurogenesis pathways, Stress Response pathways, Iron Metabolism pathways(14).

CEACAM8, also known as CD66b or CCG, is a member of the family of carcinoembryonic antigen-related cell adhesion molecules. It is primarily expressed on the surface of neutrophils and plays a role in various immune processes. Some Key roles are Neutrophil activation, Inflammatory Response, Cell Adhesion and Migration, Microbial Defence. If CEACAM8 is indeed dysregulated in MDD with or without anxiety, its functions could potentially impact several pathways implicated in the pathophysiology of depression such as Neuroinflammation,

stress response, Blood Brain Barrier integrity. CEACAM8-mediated neutrophil activation might contribute to the inflammatory response and neuroinflammation in MDD, whereas its role in regulating neutrophil adhesion and migration could influence immune cell trafficking and tissue inflammation (15,16).

OLFM4, or olfactomedin 4, is a glycoprotein within the olfactomedin family, engaging in diverse biological processes and implicated in cancer, inflammation, and tissue development. Its role in cell adhesion and migration, inflammation response, neurogenesis, neuroplasticity, and dysregulation of the WNT signalling pathway are among its notable roles. Neuronal function and mood regulation may be affected by OLFM4-mediated modulation of Wnt signalling, which has been associated with depression. (16–18). A member of the transferrin family, Lactotransferrin (LTF), often referred to as lactoferrin, is a multifunctional glycoprotein. With the ability to inhibit inflammation, fight germs, and regulate immunity, it is involved in many different biological processes. It involves in some pathways such as Neuroinflammation, Neuroprotection and iron metabolism. LTF-mediated inhibition of inflammatory cytokines and oxidative stress could have anti-inflammatory and neuroprotective effects, whereas its promotion of immune cell activity could enhance immune responses against pathogens (19).

The male reproductive system, the pancreas, the kidney, the prostate, salivary glands, and other organs all produce cysteine-rich secretory protein 3 (CRISP3), a member of the CRISP family of proteins. CRISP3 has been implicated in several biological processes, such as Regulation of Fertility, Immune modulation, Anti-microbial activity, and Regulation of cell signalling. It involves in some pathways such as Neuroinflammation, Neuroprotection and Neurotransmitter Regulation (20).

DEFA4, also known as defensin alpha 4, is a member of the defensin family of antimicrobial peptides. Small cationic

peptides called defensins are essential for the innate immune system's protection against microbiological infections. It involves in biological process such as antimicrobial activity, Immune modulation, Inflammatory response, and Epithelial Barrier function. It involves in some pathways such as Neuroinflammation, Stress response and Gut-Brain Axis (20).

BPI, or bactericidal/permeability-increasing protein, is a protein primarily known for its antimicrobial properties. As a component of the innate immune system, it starts to break down the cell membranes of a variety of Gram-negative bacteria to function as a strong antibacterial agent against them. It involves in biological process such as antimicrobial activity, Inflammatory Response and Endotoxin Neutralization. It involves in some pathways such as Neuroinflammation, Stress Response and Gut-Brain Axis (21).

CEACAM6, short for carcinoembryonic antigen-related cell adhesion molecule 6, is one of the many members of the CEACAM family. It is a glycoprotein that is primarily involved in cell adhesion and signalling processes. It involves in biological process cell Adhesion, Immune Regulation and Signal Transduction. It involves in some pathways such as Neuroinflammation, Stress response, Cell Adhesion and Neuroplasticity (22).

One enzyme that may convert arginine to ornithine and urea is ARG1, which stands for Arginase1. Important to the effort to eliminate excess ammonia from the body, it is part of the urea cycle. Additionally, ARG1 is involved in regulating arginine availability for various cellular processes, including protein synthesis, nitric oxide (NO) production, and immune function. It involves in some pathways such as Neuroinflammation, Nitric oxide signalling and Immune Dysregulation (23).

One of the members of the family of receptors that facilitate the absorption of folates into cells is FOLR3, which is another name for folate receptor gamma (FR-gamma). While the placenta is the most common site of expression, other tissues, including the brain, have also shown signs of its presence. The transport of folates across cell membranes is facilitated by folate receptors, which are essential in folate metabolism. It involves in biological process such as Folate transport, Neurotransmitter synthesis and one carbon metabolism. It involves in some pathways such as Neurotransmitter dysfunction and Epigenetic Regulation (24).

CD177, also known as neutrophil specific antigen NB1, is a glycoprotein receptor primarily expressed on the surface of neutrophils. It plays a role in neutrophil biology and immune responses, Endothelial Adhesion, and Inflammatory Responses. It involves in some pathways such as Neuroinflammation, Blood-Brain Barrier dysfunction and Stress Response (25).

Functional Enrichment Analysis of DEG's

GO function analyses and the KEGG pathway enrichment analysis DEGs were carried out by DAVID. The enriched GO terms were categorized into biological process (BP), cellular component (CC), and molecular function (MF) ontologies.

The majority of DEGs associated with MDD with anxiety in BP are Anti-bacterial humoral response, Innate Immune Response and Cellular response to polysacchrides. These process posses the intricate interplay between the immune system and mental health, particularly in mood disorders like MDD. Anxiety disorders frequently co-occur with MDD, indicating shared underlying mechanisms. Dysregulation of innate immune responses, characterized by the activation of immune cells and the release of pro-inflammatory cytokines, may contribute to the development and maintenance of depressive and anxious symptoms. Moreover, heightened cellular responses to bacterial components such as LPS and increased antibacterial humoral responses suggest a state of chronic inflammation, which has been implicated in the etiology of both mood and anxiety disorders(26).

CC indicated significant enrichment in Extracellular space, Extracellular region,

specific granule lumen involved in intercellular communication and signaling pathways in the pathophysiology of this condition.The importance of the extracellular environment, including the space between cells and within specific cellular compartments, in regulating various physiological processes, including immune responses and neuroinflammation. The dysregulation of genes associated with these cellular components may reflect alterations in communication between immune cells, glial cells, and neurons, contributing to the development and maintenance of depressive and anxious symptoms. Furthermore, the specific enrichment of genes in granule lumens suggests a potential role for secretory pathways and vesicle trafficking mechanisms in mediating cellular responses to stress and inflammatory stimuli in MDD with anxiety(27).

MF analysis showed enrichment in Lipopolysaccharide Binding, Iron ion binding, and Serine type endo peptidase activity.This suggests potential link between immune dysregulation, oxidative stress, and neuroinflammation in the pathophysiology of this condition. Lipopolysaccharide (LPS) binding proteins are integral components of the innate immune response, recognizing bacterial cell wall components and initiating inflammatory signaling pathways. The upregulation of genes involved in LPS binding may reflect heightened immune activation and chronic low-grade inflammation observed in individuals with MDD and anxiety. Additionally, iron ion binding proteins are critical for various physiological processes, including neurotransmitter synthesis and oxidative stress regulation. Dysregulation of iron metabolism and increased iron accumulation have been implicated in both mood disorders and anxiety disorders, contributing to oxidative stress and neuronal damage. Furthermore, the enrichment of serine-type endopeptidase activity suggests potential alterations in proteolytic processing and regulation of neuroinflammatory mediators, further implicating immune-inflammatory pathways in MDD with anxiety(27).

According to GO analysis, BP was more abundant in Major Depressive Disorder (MDD) without Anxiety. This covers functions such as the MHC class-II protein complex, the adaptive immune response, and the processing and presentation of polysaccharide antigen by MHC class-II. The MHC class-II protein complex plays a pivotal role in antigen presentation to CD4+ T cells, crucial for coordinating the adaptive immune response. Dysregulation of MHC-II expression or function may disrupt antigen presentation, potentially contributing to neuroinflammation. Aberrant adaptive immune responses, characterized by T cell dysfunction, cytokine signaling alterations, and antibody production irregularities, have been implicated in the chronic low-grade inflammation. Disturbances in the processing and presentation of polysaccharide antigens by MHC class-II molecules could disrupt immune homeostasis observed in MDD without the comorbidity Anxiety(28).

The CC analysis revealed an enrichment in the lumenal side of the endoplasmic reticulum membrane, the MHC class II protein complex, and the integral component of the lumenal side of the endoplasmic reticulum membrane. Dysregulation within the endoplasmic reticulum (ER) can instigate cellular stress responses like the unfolded protein response (UPR), pivotal for maintaining protein homeostasis. In MDD pathogenesis, ER dysfunction may ensue, fostering the accumulation of misfolded proteins, consequently activating the UPR. Prolonged ER stress can lead to neuronal apoptosis, fuel neuroinflammation, disrupt synaptic plasticity and neurotransmitter signaling, thereby undermining neural circuits involved in mood regulation. Additionally, ER stress perturbs neurotrophic factor levels, including brain-derived neurotrophic factor (BDNF), exacerbating neuronal vulnerability, and further compromising cognitive function. Furthermore, ER-mitochondria crosstalk disruption, attributable to ER stress, fosters mitochondrial dysfunction and oxidative stress, amplifying neuronal damage and depressive symptomatology.

Molecular Interactions and Pathways in Major Depressive Disorder (MDD)

The MHC class II protein complex implies perturbations in immune regulation. The MHC class II molecules are instrumental in antigen presentation to CD4+ T cells, a process pivotal for immune response coordination. Dysfunctions in MHC class II expression or function could contribute to aberrant immune responses, inflammation and these mechanisms implies in MDD without the comorbidity Anxiety(29).

The MFanalysis revealed an enrichment for peptide antigen binding, MHC class II protein complex binding, and MHC class II receptor activation (8,9).The enrichment in peptide antigen binding indicates alterations in the recognition and binding of specific antigens, potentially implicating dysregulation in immune response pathways. In MHC class II protein complex binding signifies disturbances in the interaction between antigens and MHC class II molecules, which are essential for antigen presentation to immune cells. Dysfunctions in this process may lead to impaired immune recognition and response, contributing to chronic inflammation observed in MDD. In MHC class II receptor activation suggests alterations in downstream signaling pathways following interaction with MHC class II molecules. This activation may modulate immune cell function and cytokine production, further influencing neuroinflammatory processes implicated in MDD without the comorbidity Anxiety(30).

Ten improved biological mechanisms, cellular constituents, and molecular operations. The X-axis shows the molecular functions, while the vertical axis shows the number of genes.

KEGG pathway analysis revealed that the differentially expressed genes (DEGs) associated MDD with Anxiety patients were primarily concentrated in pathways related to Inflammatory Bowel Disease (IBD), Rheumatoid Arthritis (RA), Th1 and Th2 Cell differentiation, Phagosome, Systemic Lupus erythematosus (SLS). Simultaneously, there was enrichment in similar pathways for autoimmune thyroid disease, inflammatory bowel disease, viral myocarditis, and major depressive disorder without anxiety (Figures 3 and 4)(7,8).

These are the top ten DEG-enriched KEGG pathways. The pathways are shown on the vertical axis, while the number of genes is shown on the X-axis.

The association between Inflammatory Bowel Disease (IBD) and the co-occurrence of MDD with Anxiety underscores the roles of the DEFA4 and LCN2 genes. DEFA4 encodes human defensin 4, which has antimicrobial functions in the gut, while LCN2 encodes lipocalin-2, which is involved in regulating inflammation and iron homeostasis. Changes in the expression of these genes may influence intestinal inflammation and gut microbiota composition, which could play a role in the pathogenesis of IBD. Furthermore, their roles in the neuroimmune axis might be relevant to understanding MDD with Anxiety, a condition that is frequently observed alongside IBD(31).

The CRISP3, LCN2, and DEFA4 genes are important for elucidating the complex relationship between Rheumatoid Arthritis (RA) and MDD with Anxiety. Changes in CRISP3, LCN2, and DEFA4 genes are linked to Rheumatoid Arthritis (RA) through their involvement in inflammatory pathways and immune system dysfunction. Evidence also suggests their potential connection to mood and anxiety disorders, likely due to their roles in neuroinflammation and immune responses relevant to psychiatric conditions. This underscores the bidirectional relationship between inflammation and mood disorders, indicating that genetic variations affecting immune regulation may impact susceptibility to mood and anxiety disorders as well(32).

The roles of the CRISP3, LCN2, and DEFA4 genes in the differentiation of Th1 and Th2 immune cells may be informative regarding the immune aspects of MDD with Anxiety. Dysregulation of Th1/Th2 balance can perpetuate chronic inflammation and neuroinflammation observed in major depressive disorder (MDD) and anxiety by disrupting the immune system's ability to

Figure 3: Gene ontology analysis performed using DAVID on DEG's identified from MDD with and without anxiety samples

Figure 4: KEGG pathway enrichment analysis performed using DAVID and KEGG Bubble on DEG's identified from MDD with and without anxiety samples

Molecular Interactions and Pathways in Major Depressive Disorder (MDD)

regulate inflammation. When this balance is skewed, it can lead to persistent activation of inflammatory responses throughout the body, exacerbating symptoms of depression and anxiety. Additionally, dysregulated Th1/Th2 balance can result in neuroinflammation, contributing to changes in brain chemistry and function associated with MDD and anxiety. Ultimately, these immune dysregulations worsen symptoms, impair neurotransmitter function, and perpetuate the underlying conditions(33).

LCN2 and BPI are key regulators in the phagosome pathway, which is essential for pathogen clearance and cellular debris removal. Variations in the expression of these genes could potentially influence this pathway, leading to altered immune responses. Such changes may be implicated in the development of MDD with Anxiety, although the exact mechanisms linking immune function to psychiatric conditions remain to be clarified(34).

In Systemic Lupus Erythematosus (SLE), the genes LCN2 and DEFA4 are involved in immune regulation and inflammation, which are prominent features of SLE. While dysregulation of these genes is associated with SLE, their role in MDD with Anxiety is complex and potentially involves multiple pathways. It is hypothesized that immune and inflammatory processes influenced by these genes might also play a role in psychiatric symptoms observed in SLE; however, this relationship is not fully understood and warrants further investigation(35).

DEFA4 encodes alpha-defensin, integral to innate immunity and inflammatory responses, while LCN2 encodes lipocalin-2, a mediator of both innate immunity and neuroinflammation. In conditions such as Inflammatory Bowel Disease (IBD), characterized by heightened immune activation and gut inflammation, DEFA4 and LCN2 may exacerbate systemic inflammation and influence the neuroimmune axis, potentially impacting mood, and anxiety regulation. This association is significant in Major Depressive Disorder (MDD), where neuroinflammation is implicated, suggesting a link between immune dysregulation and psychiatric symptoms. Understanding DEFA4 and LCN2's roles in the neuroimmune axis could shed light on the co-occurrence of MDD with Anxiety, particularly in individuals with conditions like IBD, where shared inflammatory pathways may contribute to gastrointestinal and psychiatric symptoms. This underscores the bidirectional relationship between immune activation, neuroinflammation, and mood disorders, highlighting the need to consider the interconnectedness of physical and mental health in these comorbid conditions(36).

Conclusion

Our study explores the complex relationship between Major Depressive Disorder (MDD) with and without Anxiety, uncovering the underlying molecular mechanisms and pathways associated with these comorbid conditions. Through analyzing differentially expressed genes (DEGs) and conducting functional enrichment studies, we identified distinct molecular signatures and biological pathways characteristic of each condition. The identification of DEGs associated with MDD with Anxiety and MDD without Anxiety offers valuable insights into the unique molecular profiles of these disorders. Notably, we observed dysregulation of genes involved in immune response, inflammation, neurogenesis, and stress regulation, highlighting the intricate interplay between the immune system and mental health.

Functional enrichment analysis revealed pathways enriched in immune dysregulation, inflammatory processes, and neuroinflammation, emphasizing the crucial role of the immune system in the pathophysiology of MDD with Anxiety. Furthermore, the identification of specific pathways such as Inflammatory Bowel Disease, Rheumatoid Arthritis, and Th1/Th2 Cell Differentiation further clarifies the complex connections between psychiatric disorders and immune-mediated conditions.

Current Trends in Biotechnology and Pharmacy
Vol. 18 (Supplementry Issue 4A) 53 - 66, November 2024, ISSN 0973-8916 (Print), 2230-7303 (Online)
10.5530/ctbp.2024.4s.5

64

Our findings contribute to a deeper understanding of the molecular underpinnings of MDD with and without Anxiety, laying a foundation for the development of more targeted and effective treatment approaches. By elucidating the molecular mechanisms driving these disorders, our study paves the way for personalized interventions addressing the underlying pathophysiology and optimizing outcomes for individuals affected by these debilitating conditions. However, further validation through in vitro and in vivo studies is necessary for full comprehension.

References

1. Karrouri, R., Hammani, Z., Otheman, Y., & Benjelloun, R. (2021). Major depressive disorder: Validated treatments and future challenges.World Journal of Clinical Cases, 9(31), 9350–9367.

2. Park, S. C., & Kim, D. (2020). The Centrality of Depression and Anxiety Symptoms in Major Depressive Disorder Determined Using a Network Analysis.Journal of Affective Disorders, 271, 19–26.

3. Kalin, N. H. (2020). The critical relationship between anxiety and depression.American Journal of Psychiatry, 177, 365–367.

4. Cohen, Z. D., & Derubeis, R. J. (2018). Treatment Selection in Depression. Annual Review of Clinical Psychology, 14, 209–236.

5. Thaipisuttikul, P., Ittasakul, P., Waleeprakhon, P., Wisajun, P., &Jullagate, S. (2014). Psychiatric comorbidities in patients with major depressive disorder. Neuropsychiatric Disease and Treatment, 10, 2097–2103.

6. Hopwood, M. (2023). Anxiety Symptoms in Patients with Major Depressive Disorder: Commentary on Prevalence and Clinical Implications. Neurology and Therapy, 12, 5–12.

7. Zhang, G., Xu, S., Zhang, Z., Zhang, Y., Wu, Y., An, J., et al. (2020). Identification of Key Genes and the Pathophysiology Associated with Major Depressive Disorder Patients Based on Integrated Bioinformatics Analysis. Frontiers in Psychiatry, 11:192.

8. Chen, Y., Zhou, F., Lu, W., Zeng, W., Wang, X., & Xie, J. (2022). Identification of potential Mitogen-Activated Protein Kinase-related key genes and regulation networks in molecular subtypes of major depressive disorder. Frontiers in Psychiatry, 13:1004945.

9. Zhang, G., Xu, S., Yuan, Z., & Shen, L. (2020). Weighted gene coexpression network analysis identifies specific modules and hub genes related to major depression. Neuropsychiatric Disease and Treatment, 16, 703–713.

10. Cheng, Y., Sun, M., Wang, F., Geng, X., & Wang, F. (2021). Identification of Hub Genes Related to Alzheimer's Disease and Major Depressive Disorder. American Journal of Alzheimer's Disease and Other Dementias, 36:15333175211046123.

11. Malgaroli, M., Calderon, A., & Bonanno, G. A. (2021). Networks of major depressive disorder: A systematic review. Clinical Psychology Review, 85,102000.

12. Cathomas, F., Lin, H. Y., Chan, K. L., Li, L., Parise, L. F., Alvarez, J., et al. (2024). Circulating myeloid-derived MMP8 in stress susceptibility and depression. Nature, 626, 1108–1115.

13. Bobińska, K., Szemraj, J., Czarny, P., &Gałecki, P. (2016). Role of MMP-2, MMP-7, MMP-9 and TIMP-2 in the development of recurrent depressive disorder. Journal of Affective Disorders, 205, 119–129.

14. Akter, S., Emon, F. A., Nahar, Z., ShalahuddinQusar, M., Islam, S. M. A., Shahriar, M., et al. (2023). Altered IL-3 and lipocalin-2 levels are associated with the pathophysiology of major depressive disorder: a case-control study. BMC Psychiatry, 23(1),830.

15. Bouzid, A., Almidani, A., Zubrikhina, M., Kamzanova, A., Ilce, B. Y., Zholdassova, M., et al. (2023). Integrative bioinformatics and artificial intelligence analyses of transcriptomics data identified genes

Current Trends in Biotechnology and Pharmacy
Vol. 18 (Supplementry Issue 4A) 53 - 66, November 2024, ISSN 0973-8916 (Print), 2230-7303 (Online)
10.5530/ctbp.2024.4s.5

65

associated with major depressive disorders including NRG1. Neurobiology of Stress, 26:100555.

16. Sun, Y., Li, J., Wang, L., Cong, T., Zhai, X., Li, L., et al. (2022). Identification of Potential Diagnoses Based on Immune Infiltration and Autophagy Characteristics in Major Depressive Disorder. Frontiers in Genetics, 13:702366.

17. Tian, C. (2021). Exploring the Relationship between Gut Microbiota and Major Depressive Disorders. E3S Web of Conferences, 12(1):20977.

18. Xu, K., Zheng, P., Zhao, S., Wang, J., Feng, J., Ren, Y., et al. (2023). LRFN5 and OLFM4 as novel potential biomarkers for major depressive disorder: a pilot study. Translational Psychiatry, 13(1):188.

19. Nagy, C., Vaillancourt, K., &Turecki, G. (2018). A role for activity-dependent epigenetics in the development and treatment of major depressive disorder. Genes, Brain and Behavior, 17(3):e12446.

20. Gonzalez, S. N., Sulzyk, V., Weigel Muñoz, M., &Cuasnicu, P. S. (2021). Cysteine-Rich Secretory Proteins (CRISP) are Key Players in Mammalian Fertilization and Fertility. Frontiers in Cell and Developmental Biology, 9:800351.

21. Gao, K., Su, M., Sweet, J., & Calabrese, J. R. (2019). Correlation between depression/anxiety symptom severity and quality of life in patients with major depressive disorder or bipolar disorder. Journal of Affective Disorders, 244, 9–15.

22. Hasselbalch, H. C., Skov, V., Larsen, T. S., Thomassen, M., Riley, C., Jensen, M. K., et al. (2010). High Expression of Carcinoembryonic Antigen-Related Cell Adhesion Molecule(CEACAM) 6 In Primary Myelofibrosis. Blood, 116(21), 4116–4116.

23. Zhao, S., Bao, Z., Zhao, X., Xu, M., Li, M. D., & Yang, Z. (2021). Identification of Diagnostic Markers for Major Depressive Disorder Using Machine Learning Methods. Frontiers in Neuroscience, 15:645998.

24. Ohnishi, J., Ayuzawa, S., Nakamura, S., Sakamoto, S., Hori, M., Sasaoka, T., et al. (2017). Distinct transcriptional and metabolic profiles associated with empathy in Buddhist priests: A pilot study. Human Genomics, 11(1):21.

25. Lévy, Y., Wiedemann, A., Hejblum, B. P., Durand, M., Lefebvre, C., Surénaud, M., et al. (2021). CD177, a specific marker of neutrophil activation, is associated with coronavirus disease 2019 severity and death. iScience, 24(7):102711.

26. Gaspersz, R., Lamers, F., Wittenberg, G., Beekman, A. T. F., Van Hemert, A. M., Schoevers, R. A., et al. (2017). The role of anxious distress in immune dysregulation in patients with major depressive disorder. Translational Psychiatry,7(12):1268.

27. Fries, G. R., Saldana, V. A., Finnstein, J., & Rein, T. (2023). Molecular pathways of major depressive disorder converge on the synapse. Molecular Psychiatry, 28, 284–297.

28. Tubbs, J. D., Ding, J., Baum, L., & Sham, P. C. (2020). Immune dysregulation in depression: Evidence from genome-wide association. Brain, Behavior, and Immunity - Health, 7:100108.

29. Deng, Z., Suyama, K., Kang, K. H., & Li, Y.(2022). Comprehensive analysis of endoplasmic reticulum stress and immune infiltration in major depressive disorder. Front Psychiatry,13:1008124.

30. Jurewicz, M. M., & Stern, L. J. (2019). Class II MHC antigen processing in immune tolerance and inflammation. Immunogenetics, 71, 171–187.

31. Hu, S., Chen, Y., Chen, Y., & Wang, C. (2021). Depression and Anxiety Disorders in Patients with Inflammatory Bowel Disease. Frontiers in Psychiatry, 12:714057.

32. Peterson, S., Piercy, J., Blackburn, S., Sullivan, E., Karyekar, C. S., & Li, N. (2019). The multifaceted impact of anxiety and depression on patients with rheumatoid arthritis. BMC Rheumatology, 28;3:43.

33. Hou, R., & Baldwin, D. S. (2012). A neuroimmunological perspective on anxiety

disorders. Human Psychopharmacology, 27, 6–14.

34. Tang, M., Liu, T., Jiang, P., & Dang, R. (2021). The interaction between autophagy and neuroinflammation in major depressive disorder: From pathophysiology to therapeutic implications. Pharmacological Research, 168:105586.

35. Zhang, L., Fu, T., Yin, R., Zhang, Q., & Shen, B. (2017). Prevalence of depression and anxiety in systemic lupus erythematosus: A systematic review and meta-analysis. BMC Psychiatry, 17(1):70.

36. Liu, W., Zheng, Y., Zhang, F., Zhu, M., Guo, Q., Xu, H., et al. (2021). A Preliminary Investigation on Plasma Cell Adhesion Molecules Levels by Protein Microarray Technology in Major Depressive Disorder. Frontiers in Psychiatry, 12:627469.

Computational Evaluation of Curcumenol as a Potential Inhibitor against Calcineurin Protein

Nivya R. M.*, and Amitha Joy

Department of Biotechnology, Sahrdaya College of Engineering and Technology, APJ Abdul Kalam Technological University of Kerala, Kerala

*Correspondingauthor: nivya@sahrdaya.ac.in

Abstract

Calcineurin protein is a multifunctional serine-threonine protein phosphatase vital to several cellular functions, such as immune response control, signal transduction, and cardiac function. Its relevance in preserving cellular homeostasis is highlighted by its involvement in T-cell activation, calcium signalling pathways, etc. The dysregulation of the calcineurin protein has been reported to be linked with neurodegenerative diseases, and hence calcineurin inhibitors may be beneficial as a treatment option. Existing FDA-approved calcineurin inhibitors are used under stringent guidelines and require careful monitoring because of possible side effects and toxicity. Consequently, as a therapeutic option, the discovery and development of novel calcineurin inhibitors is imperative. For this reason, the current study aims to characterize the calcineurin inhibitory action of curcumenol, a naturally occurring chemical by employing diverse *in-silico* techniques. Curcumenol was checked for its ADME-T and molecular interactional stability and was predicted to have impressive inhibitory potential with a docking score of -9.1kcal/mol and a mean RMSD of the backbone atoms of the Calcineurin-curcumenol complex as 4.55Å when simulated in a molecular dynamics system for 100ns. The*in-silico*findings were further justified using *in vitro* Calcineurin Phosphatase activity assayto quantitively analyse the inhibitory efficacy of curcumenol, defined in terms of IC_{50} value,which was found to be 0.113 µM. The overall study suggested that curcumenol holds the characteristic molecular and interactional properties and hence can be developed as a prospectiveand safe calcineurin inhibitor which can be ultimately employed as a promising therapeutic candidate against neurodegenerative diseases.

Keywords: Natural inhibitor, Molecular Docking, Molecular dynamics simulation, Inhibitory concentration 50

Introduction

Calcineurin is a heterodimeric, eukaryotic protein and functions as a direct mediator between calcium signaling and other phosphorylating states in several physiological pathways. Its structural components include a catalytic subunit known as Calcineurin A with an active site that is blocked by an autoinhibitory peptide, and a regulatory subunit with a calmodulin-binding site known as calcineurin B (1). The binding of calmodulin to the regulatory subunit is facilitated by a rise in cellular calcium concentration, which then displaces the autoinhibitory peptide from the active site and hence activates the calcineurin protein.It plays vital roles in many physiological processes, including memory and cognition, apoptosis, muscle and cardiac function, cell cycle regulation, T-cell activation, and transcription regulation. More significantly, it is the only calcium-dependent phosphatase found in the brain and is abundantly expressed within the brain, particularly in the forebrain (2). Hence, the regulation of calcineurin expression and its activation plays an essential part in a variety of developmental and differentiating processes (3). Consequently, its dysregulation can play a major role in the pathogenesis of diseases affecting the diverse organ systems; some of these diseases have already been

documented, and they include skeletal muscle hypertrophy, autoimmune diseases, neurodegenerative diseases, spermatogenesis, inflammatory bowel disease, allergies and asthma, diabetes, liver fibrosis, and more (4).

Given calcineurin's well-studied ability to activate immune system T cells, typically through the NFAT pathway, its inhibitors are designed to prevent unintended immune activation. At the moment, calcineurin inhibitors are used as a class of immunosuppressants in clinical applications. The FDA-approved calcineurin inhibitors like cyclosporin, tacrolimus, voclosporin, and pimecrolimus are used to treat autoimmune diseases including connective tissue disorders, lupus nephritis, idiopathic inflammatory myositis, interstitial lung disease, atopic dermatitis, as well as during solid organ transplantation to manage the unwanted immune reaction (5).

Recently these inhibitors, especially cyclosporin and tacrolimus have demonstrated their ability of neuroprotection in different neurodegenerative cell line models as well as animal models such as forebrain ischemia in rat models, mouse models of Alzheimer's disease, rotenone-treated rat models, etc (6,7,8). However, the concern lies in the direct application of these inhibitors against a neurodegenerative disease as they possess significant toxicity as well as innate side effects (9). Therefore, there is a strong need to find and develop new calcineurin inhibitors to provide treatment for numerous distinct neurodegenerative conditions.

Repurposing of drugs is becoming a revolutionary trend in drug discovery which in turn facilitates the use of natural products with substantial potential involving a wide range of pharmacological activity, and considerable structural diversity, as well as less toxicity (10, 11). Curcumenol which is a sesquiterpene primarily isolated from the rhizomes of *Curcuma zedoaria*is one such natural active molecule that has the potential to be developed as a promising medication (12). It is known to possess innumerable medicinal properties like antimicrobial properties, applicability as an anti-inflammatory agent for intervertebral disc degeneration, and anti-cancerous activity in lung cancer disease models. Its employment in the future clinical setting will be highly favored due to reduced cytotoxicity and adverse effects (13).

The protective effect of different bioactive components extracted from *Curcuma zedoaria* on oxidative stress in neuroblastoma glioma hybrid cell lines, induced by hydrogen peroxide has previously been studied. In the same study, it was found that increasing the concentration of curcumenol enhanced this protective effect (14). The mechanism underlying this, nonetheless, remains unknown. Accordingly, exploring curcumenol's inhibitory effects on the calcineurin protein may reveal information on the underlying neuroprotective processes. The current study hereby aims at the evaluation of curcumenol as a potential calcineurin inhibitor using different *in silico* techniques mainly including molecular docking studies and molecular dynamics simulation studies for predicting the molecular interactional behaviour in the simulated virtual systems mimicking the physiological environment and to further confirm its inhibitory efficiency via *in vitro* assays. The study consequently proposes the hypothesis that if curcumenol can be proved to be a potential calcineurin inhibitor then it can be developed further for its employment as a prospective neuroprotective remedy.The current therapeutic strategies against diverse neurodegenerative conditions like Alzheimer's disease, Parkinson's disease, Huntington's disease, etc, demand serious attention and the application of sophisticated research and development approaches is imperative.In this context, this work can open new avenues for the development of novel therapeutic options.

Materials and Methods

Retrieval of the 3D structure of Curcumenol and Prediction of ADME-Toxicity

The present work commenced by retrieving 3D structural data of curcumenol

Current Trends in Biotechnology and Pharmacy
Vol. 18 (Supplementry Issue 4A) 67 - 76, November 2024, ISSN 0973-8916 (Print), 2230-7303 (Online)
10.5530/ctbp.2024.4s.6

69

from PubChem (15). The structural data in both SMILES, as well as ".sdf" formats, were downloaded. The 3D structure in ".sdf" format was further converted to ". pdbqt" via the OpenBabel tool (16). The structural data in SMILES format were used as the input for predicting the ADME properties and toxicity details via the open web servers SWISS-ADMEand ProToxII accordingly (17, 18). The predicted properties and toxicity profiles were studied thoroughly and understood the possibility of employing curcumenol as a possible drug candidate.

Retrieval of the 3D structure of Calcineurin protein and evaluation of molecular interactional stability

Further, the 3D structure of the Calcineurin protein was retrieved from RCSB-PDB with PDB id 1MF8 (19). The initial preparation of the protein structure was done and Binding Site coordinates were predicted using Biovia Discovery Studio (20). The protein structure in ".pdbqt" was used for docking against the 3D structure of curcumenol in ".pdbqt" using POAP, which is a software pipeline based on GNU Parallel that is configured to operate Open Babel and the AutoDock suite in highly ideal parallelization (21). The docking score obtained was studied and determined whether the calcineurin-curcumin interaction was spontaneous or not. The 2-D interaction diagram was then used to study the key residues of protein and curcumenol involved in the interaction along with the type of interactions. Further, the interactional behavior was scrutinized in a virtual dynamic system mimicking a physiological system using Desmond Maestro, Molecular Dynamics Simulation platform, procured from Schrodinger.Inc (22). The simulation event analysis panel of the software facilitated the analysis of structural stability and behavioral pattern of calcineurin alone and when interacted with curcumenol for a while of 100ns by converting the trajectory data into performance metrics like RMSD (Root mean square deviation) as well as Radius of Gyration plots.

In vitro confirmation of Calcineurin inhibition by curcumenol

The computational analysis of the molecular inhibitory ability of curcumenol was then validated via _in vitro_ assay using the calcineurin phosphatase activity kit provided by Abcam (ab139461) (23). Calcineurin protein is a phosphatase that removes the phosphate group from its substrates. Hence when curcumenol is added to the reaction mixture if it has an inhibitory effect then there will be a decrease in the released phosphate concentration. The phosphate release was detected by adding the malachite green solution and measuring the absorbance at a wavelength of 620nm after 30 mins of incubation at dark. A standard phosphate graph was further plotted to derive equations to calculate the Phosphate release and Percentage inhibition. Varying concentrations of curcumenol ranging from 1 mM, 100 µM, 10 µM, 1 µM and 0.1 µM were assayed and the regression plot was obtained by plotting concentration against percentage inhibition which was then employed to get the minimum inhibitory concentration (IC_{50}) of curcumenol against calcineurin protein.
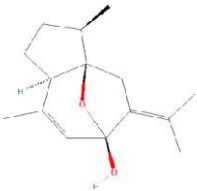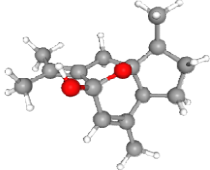
Results and Discussion

Owing to the implicit side effects and toxicity demonstrated by the currently available FDA approved calcineurin inhibitors, the present study intended to evaluate the potential of curcumenol as a possible candidate via diverse computational evaluations.

Retrieval of the 3D structure of Curcumenol and Prediction of ADME-Toxicity

For that objective, the structural data of curcumenol was initially retrieved from the PubChem Database (Table 1).

Besides having the intended biological activity, a prospective chemical must also have appropriate or ideal pharmacokinetics and safety features to be taken into consideration as a possible medicine. Therefore, we used the Swiss-ADME _in silico_ toolset to examine the curcumenol, to find appropriate

Current Trends in Biotechnology and Pharmacy
Vol. 18 (Supplementry Issue 4A) 67 - 76, November 2024, ISSN 0973-8916 (Print), 2230-7303 (Online)
10.5530/ctbp.2024.4s.6

70

Table1: Chemical structure of Curcumenol (https://pubchem.ncbi.nlm.nih.gov/compound/ 167812)	
2D structure	
3D structure	
SMILES format	CC1CCC2C13CC(=C(C)C)C(O3) (C=C2C)O

pharmacokinetics, drug-likeness, and ideal medicinal chemistry properties (24). Hence in the preliminary screening, curcumenol was found to be soluble, blood-brain barrier permeable, highly gastrointestinal absorbable, and possess no cytochrome inhibition, as predicted by the SWISS-ADME website. With a bioavailability score of 0.55, which is discussed to be ideally admissible and readily absorbed by the human body as stated by other authors, curcumenol is predicted to be successfully developed as an oral drug (25). Curcumenol is further predicted to be Lipinski's rule-following compound in addition to Mugge's, Egan's, and Verber's Rules which shows that curcumenol can be developed as an oral drug candidate with good pharmacokinetic druggability characteristics (26).The ProTox II webserver estimated that curcumenol has an LD_{50} value of 6000 mg/kg for acute oral toxicity, placing it in class 6 toxicity. According to the globally harmonized system of categorization and labeling of substances (GHS), class 6 toxicity is classified as non-toxic. Additionally, it was determined to be inert in terms of immunotoxicity, cytotoxicity, mutagenicity, hepatotoxicity, and carcinogenicity (27). Overall, curcumenol's toxicity profile was favorable. Hence it was concluded that
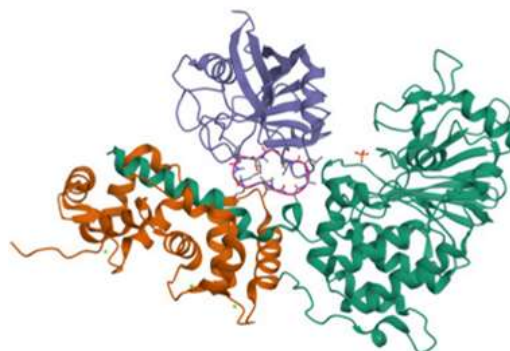

Figure 1: 3D Structure of the human calcineurin-cyclosporin-cyclophilin complex with PDBid: 1MF8. (https://www.rcsb.org/ structure/1MF8)

curcumenol is a promising candidate for drug development under clinical conditions, according to initial screening based on ADME and toxicity predictions.

Retrieval of the 3D structure of Calcineurin protein and evaluation of molecular interactional stability

Consequently, the PDB file containing the 3.10 Å resolution protein structure of the human calcineurin-cyclosporin-cyclophilin complex (PDB id: 1MF8) has been retrieved from the Protein Data Bank (Figure 1). The retrieved .pdb file was prepared and binding site coordinates were found using Biovia Discovery studio as x: -36.754, y: 15.366, and z: 23.538.

The docking score obtained via POAP software for curcumenol against calcineurinprotein in terms of binding energy was -9.1 kcal/mol, which indicated the better inhibitory capability of curcumenol in a static environment against the calcineurin protein. The inhibition constant (Ki) was then found using equation (1), where ΔG is the Binding energy, R (universal gas constant) has the value of 1.985×10^{-3} kcal/molK, and T (temperature) is 298.15 K and it was found to be 2.1 (Figure 2).

$$Ki = \exp^{(\Delta G/RT)} \qquad (1)$$

A chemical is generally considered to be more active if its docking score is more negative. Consequently, curcumenol can be contemplated as an active inhibitor of curcumenol reviewing the discussions made in similar studies (28).

The 2D interaction diagram of calcineurin-curcumenol complex was then analyzed using Biovia Discovery studio and key interactions including van der Waals, Conventional Hydrogen bond, Alkyl, and Pi-alkyl bonds, were found to be the common

interactional forces seen in most stable target protein-drug complexes (29). The major underlying interactions were conventional hydrogen bonds with residue Val: D: 9, van der Waals interaction with residues Asn: B: 122, Thr: C: 73 and Ser: A: 353, and alkyl bonds with residues Met: B:118, Trp: A: 352, Phe: A: 356, Pro: A: 355 and Val: B: 119 of calcineurin protein (Figure 3).

Ultimately, molecular dynamics simulation was used to verify the effectiveness of curcumenol as a molecular
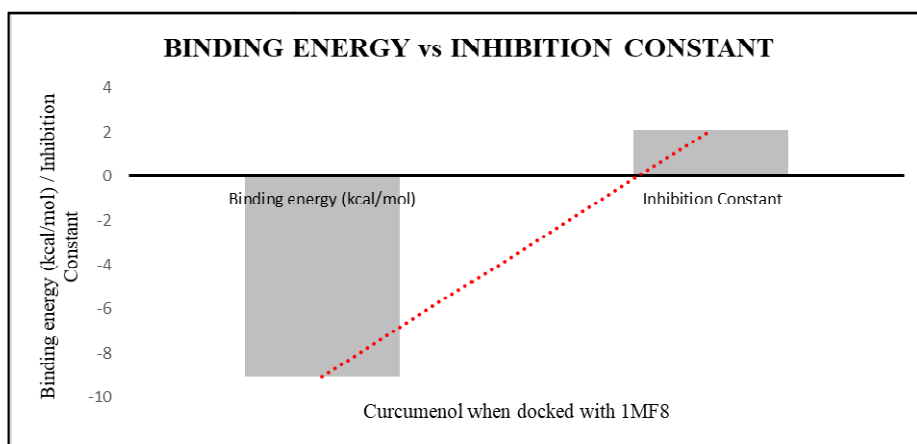

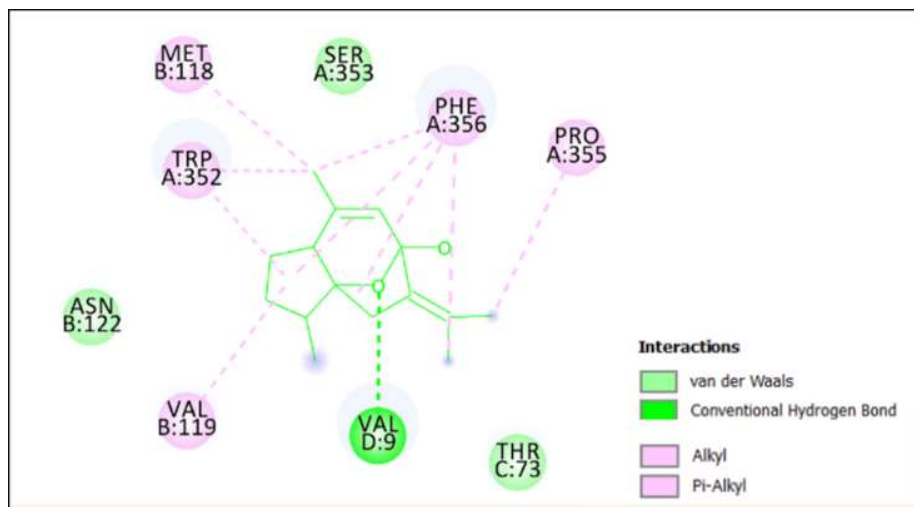**Figure 2:** Binding energy vs Inhibition constant

Figure 3: 2D interactional Diagram

Nivyaet al

inhibitor against calcineurin in a simulated SPC-solvated system. Molecular biology and drug development have benefited greatly from the application of molecular dynamics (MD) simulations in recent years. These simulations provide a fine temporal resolution and complete atomic information on the behavior of proteins and other biomolecules (30).This information can hence be deducted for evaluating the applicability of our candidate molecule as a potential inhibitor. Consequently, the interactional stability of curcumenol with calcineurin in a dynamic virtualcondition mimicking the physiological environment was studied for 100ns, which revealed the behavior of trajectories in terms of performance metrices like Root mean square deviation and Radius of Gyration. The mean RMSD (Root mean square deviation) for trajectories of backbone atoms was obtained as;5.032 Å for calcineurin protein alone and 4.55 Å, when complexed with curcumenol, correspondingly. The small and relatively comparable values of RMSD of apoprotein and holoprotein implied that the backbone atoms had relatively constant movement in the dynamic physiological

condition. Reports state that RMSD should ideally be zero, but deviance results from statistical errors. Therefore, the more spatially comparable the two compared structures are, the smaller the variance. The more configurations deviate from the reference structure, the worse the RMSD value becomes (31). In the current study, as shown in Figure 4, the blue line indicates the plot of reference structure or structure of the protein (1MF8) alone and the red line indicates the structure to be evaluated or 1MF8-curcumenol complex structure. The plot showed that both structures were following the same trajectories for most time in simulation with very negligible deviations. Further, the radius of gyration (ROG) of atom trajectories within the simulated period was used to assess the compactness of the structures of calcineurin alone and the calcineurin curcumenol complex. Plotting the RMSD and ROG provided additional evidence of the interactional stability. Moreover, all plots indicated the overall structural stability in a significant manner as scrutinized by other authors (Figure 5) (31).
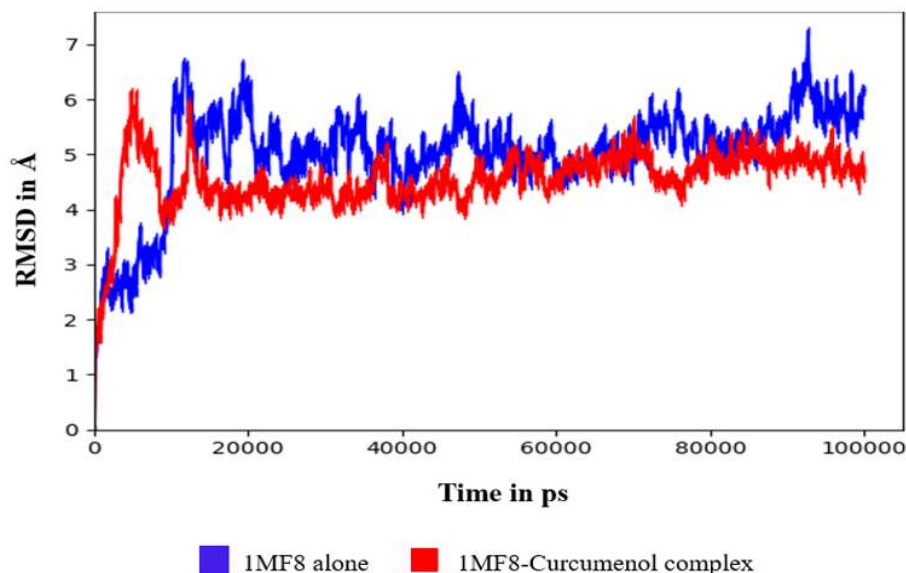
Figure 4: Root mean square deviation of backbone atoms of calcineurin protein alone and curcumenol-calcineurin complex

Computational Evaluation of Curcumenol

***In vitro* confirmation of Calcineurin inhibition by curcumenol**

The computational evaluations carried out hence predicted that curcumenol is a possible calcineurin inhibitor by having fairly acceptable molecular inhibitory and interactional characteristics. Accordingly, the inhibitory efficacy of curcumenol was lastly assayed using real-time *in vitro* assay employing a calcineurin phosphatase activity kit. The inhibitory effect was calculated based on the decrease in released phosphate concentration, which was obtained using equation (2) derived from the standard phosphate graph (Figure 6).

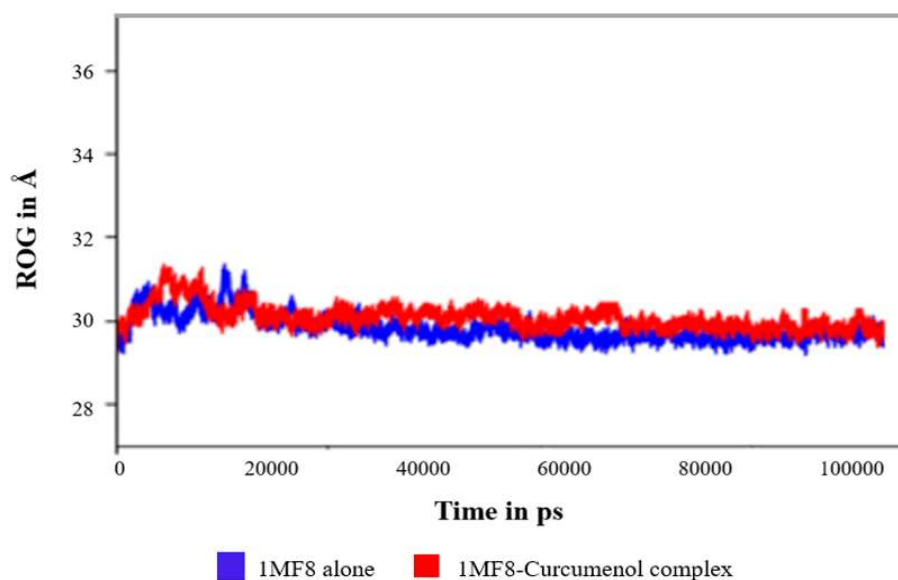**Figure 5:** Radius of Gyration Plot of backbone and sidechain atoms of calcineurin protein alone and curcumenol-calcineurin complex
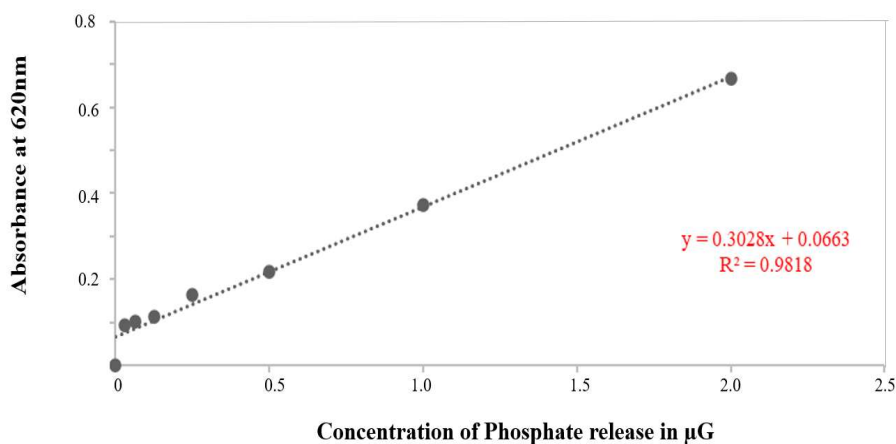

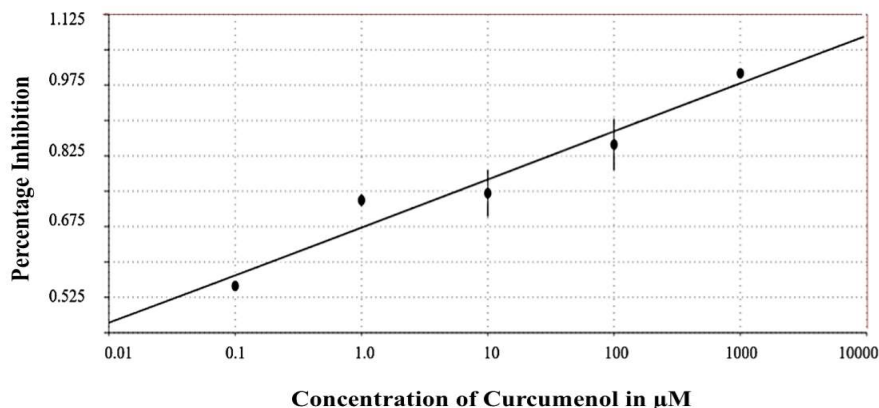**Figure 6:** Phosphate Standard Curve

Nivyaet al

Current Trends in Biotechnology and Pharmacy
Vol. 18 (Supplementry Issue 4A) 67 - 76, November 2024, ISSN 0973-8916 (Print), 2230-7303 (Online)
10.5530/ctbp.2024.4s.6

74

Figure 7: Percentage Inhibition Regression Curve

$$\text{Phosphate Released} = \frac{(\text{OD at 620nm} - \text{Y intercept})}{\text{Slope}}$$

(2)

Curcumenol in 5 different concentrations was used to assay its inhibitory effect. The percentage inhibition was consequently calculated using equation (3).

$$\text{Percentage Inhibition} = \frac{(\text{Positive control} - \text{Test well})}{\text{Positive control}} * 10$$

(3)

The percentage inhibition was plotted against the concentration of curcumenol to obtain the regression plot and the minimum inhibitory concentration value of curcumenol as 0.113 μM using the online software AAT Bio Quest IC_{50} Calculator (Figure 7) (32).

The low IC_{50} value of curcumenol that was found is similar to the investigative calcineurin inhibitors reported by other authors (33). After analyzing all of these data, it was determined that curcumenol possessed adequate inhibitory activity. These characteristics were predicted by *in silico* studies and replicated through *in vitro* assays, in the current study. Thus, more thorough research on curcumenol may be necessary to assess and develop it as a potential treatment for diverse neurodegenerative diseases.

Conclusion

The application of calcineurin inhibitors is suggested as the best course of treatment for a variety of ailments, including neurodegenerative conditions like Parkinson's Disease, Alzheimer's disease, Amyotrophic Lateral Sclerosis, Huntington's disease, Transmissible spongiform encephalopathies, and so on. Current FDA-approved calcineurin inhibitors must be administered by rigorous guidelines and need to be closely monitored due to potential toxicity and side effects. Therefore, finding new calcineurin inhibitors is essential. According to the results of the current study, curcumenol possesses the necessary molecular and interactional characteristics as a potential calcineurin inhibitor. Its effectiveness as a potent calcineurin inhibitor was ultimately confirmed using *in vitro* assay. In light of these findings, we conclude by proposing further research and investigations on advancing curcumenol's potential as a treatment option against neurodegenerative diseases.

Acknowledgement

References

1. Rusnak, F., and Mertz, P. (2000). Calcineurin: form and function, Physiological reviews, 80(4): 1483–1521.

2. Creamer, T. P. (2020). Calcineurin. Cell Communication and Signaling, 18(1).

3. Schulz, R. A., andYutzey, K. E. (2004). Calcineurin signaling and NFAT activation in cardiovascular and skeletal muscle development. Developmental biology, 266(1): 1-16.

4. Chen, L., Song, M., and Yao, C. (2022). Calcineurin in development and disease. Genes and Diseases, 9(4): 915-927.

5. Lee, J. U., Kim, L. K., and Choi, J. M. (2018). Revisiting the Concept of Targeting NFAT to Control T Cell Immunity and Autoimmune Diseases. Frontiers in immunology, 9: 2747.

6. Uchino, H., Minamikawa-Tachino, R., Kristián, T., Perkins, G., Narazaki, M., Siesjö, B.K. and Shibasaki, F., (2002). Differential neuroprotection by cyclosporin A and FK506 following ischemia corresponds with differing abilities to inhibit calcineurin and the mitochondrial permeability transition. Neurobiology of disease, 10(3): 219-233.

7. Sullivan, P.G., Sebastian, A.H. and Hall, E.D. (2011) "Therapeutic window analysis of the neuroprotective effects of cyclosporine-A after traumatic brain injury," Journal of Neurotrauma, 28(2): 311–318.

8. Singh, S., Ganguly, U., Pal, S., Chandan, G., Thakur, R., Saini, R. V., Chakrabarti, S. S., Agrawal, B. K., and Chakrabarti, S. (2022). Protective effects of cyclosporine A on neurodegeneration and motor impairment in rotenone-induced experimental models of Parkinson's disease. European journal of pharmacology, 929: 175129.

9. Naesens, M., Kuypers, D. R., and Sarwal, M. (2009). Calcineurin inhibitor nephrotoxicity. Clinical Journal of the American Society of Nephrology, 4(2): 481-508.

10. Pushpakom, S., Iorio, F., Eyers, P.A., Escott, K.J., Hopper, S., Wells, A., Doig, A., Guilliams, T., Latimer, J., McNamee, C. and Norris, A. (2019). Drug repurposing: progress, challenges and recommendations. Nature reviews Drug discovery, 18(1): 41-58.

11. Newman, D. J., and Cragg, G. M. (2016). Natural products as sources of new drugs from 1981 to 2014. Journal of natural products, 79(3): 629-661.

12. U. C. Rahayu, D., Hartono, and Sugita, P. (2018). Antibacterial activity of curcumenol from rhizomes of Indonesian Curcuma aeruginosa (Zingiberaceae). Rasayan Journal of Chemistry, 11(2): 762–765.

13. Zhang R, Pan T, Xiang Y, Zhang M, Xie H, Liang Z, Chen B, Xu C, Wang J, Huang X, Zhu Q, Zhao Z, Gao Q, Wen C, Liu W, Ma W, Feng J, Sun X, Duan T, Lai-Han Leung E, Xie T, Wu Q, Sui X. (2021). Curcumenol triggered ferroptosis in lung cancer cells via lncRNA H19/miR-19b-3p/FTH1 axis. Bioactive materials, 13: 23–36.

14. Hamdi, O. A. A., Ye, L. J., Kamarudin, M. N. A., Hazni, H., Paydar, M., Looi, C. Y., and Awang, K. (2015). Neuroprotective and Antioxidant Constituents from Curcuma zedoaria Rhizomes. Records of Natural Products, 9(3): 349-355

15. Kim, S., Chen, J., Cheng, T., Gindulyte, A., He, J., He, S., Li, Q., Shoemaker, B. A., Thiessen, P. A., Yu, B., Zaslavsky, L., Zhang, J., and Bolton, E. E. (2023). PubChem 2023 update. Nucleic Acids Res., 51(D1): D1373–D1380.

16. O'Boyle, N. M., Banck, M., James, C. A., Morley, C., Vandermeersch, T., & Hutchison, G. R. (2011). Open Babel: An open chemical toolbox. Journal of cheminformatics, 3: 33.

17. Daina, A., Michielin, O., and Zoete, V. (2017). SwissADME: a free web tool to evaluate pharmacokinetics, drug-likeness and medicinal chemistry friendliness of small molecules. Scientific reports, 7: 42717.

18. Banerjee, P., Eckert, A. O., Schrey, A. K., and Preissner, R. (2018). ProTox-II: a webserver for the prediction of toxicity of chemicals. Nucleic acids research, 46(W1), W257–W263.

19. Jin, L., and Harrison, S. C. (2002). Crystal structure of human calcineurin complexed with cyclosporin A and

human cyclophilin. Proceedings of the National Academy of Sciences, 99(21): 13522–13526.

20. SYSTÈMES, D. (2016). BIOVIA Discovery Studio Dassault Systems BIOVIA, Discovery Studio Modeling Environment, Release 2017. Dassault Systemes

21. Samdani, A., and Vetrivel, U. (2018). POAP: A GNU parallel based multithreaded pipeline of open babel and AutoDock suite for boosted high throughput virtual screening. Computational biology and chemistry, 74: 39–48.

22. Ivanova, L., Tammiku-Taul, J., García-Sosa, A. T., Sidorova, Y., Saarma, M., and Karelson, M. (2018). Molecular dynamics simulations of the interactions between glial cell line-derived neurotrophic factor family receptor GFRα1 and small-molecule ligands. ACS Omega, 3(9): 11407–11414.

23. Zhang, H. L., Zhao, B., Han, W., Sun, Y. B., Yang, P., Chen, Y., Ni, D., Zhang, J., and Yin, D. M. (2021). Acetylation of calmodulin regulates synaptic plasticity and fear learning. The Journal of Biological Chemistry, 297(3): 101034.

24. Ononamadu, C. J., and Ibrahim, A. (2021). Molecular docking and prediction" of ADME/drug-likeness properties of potentially active antidiabetic compounds isolated from aqueous-methanol extracts of Gymnemasylvestre and Combretum micranthum. Biotechnologia, 102(1): 85–99.

25. Martin, Y.C. (2005). A bioavailability score, Journal of Medicinal Chemistry, 48(9): 3164–3170.

26. Benet, L. Z., Hosey, C. M., Ursu, O., and Oprea, T. I. (2016). BDDCS, the Rule of 5 and drugability. Advanced drug delivery reviews, 101: 89–98.

27. Bhat, V., and Chatterjee, J. (2021). The use of in silico tools for the toxicity prediction of potential inhibitors of SARS-COV-2. Alternatives to Laboratory Animals, 49(1–2): 22–32.

28. Macip, G., Garcia-Segura, P., Mestres-Truyol, J., Saldivar-Espinoza, B., Ojeda-Montes, M. J., Gimeno, A., Cereto-Massagué, A., Garcia-Vallvé, S., and Pujadas, G. (2022). Haste makes waste: A critical review of docking-based virtual screening in drug repurposing for SARS-CoV-2 main protease (M-pro) inhibition. Medicinal research reviews, 42(2): 744–769.

29. Dhorajiwala, T., Halder, S., and Samant, L. (2019). Comparative in silico molecular docking analysis of L-threonine-3-dehydrogenase, a protein target against African trypanosomiasis using selected phytochemicals. Journal of Applied Biotechnology Reports, 6(3): 101–108.

30. Hollingsworth, S. A., and Dror, R. O. (2018). Molecular Dynamics Simulation for All. Neuron, 99(6): 1129–1143.

31. Arnittali, M., Rissanou, A.N. and Harmandaris, V. (2019) 'Structure of biomolecules through molecular dynamics simulations', Procedia Computer Science, 156: 69–78.

32. AAT Bioquest, Inc Quest Graph™ IC50 Calculator. Accessed on 26 February 2024, (Available online: www.aatbio.com/tools/ic50-calculator).

33. Mukherjee, A., Cuanalo-Contreras, K., Sood, A., and Soto, C. (2022). Development of a novel pharmacophore model to screen specific inhibitors for the serine-threonine protein phosphatase calcineurin. Biochemistry and Biophysics Reports, 31: 101311.

Synthesis of phyto-hydroxyapatite using *Ocimum sanctum* and its characterization

Srividya S[1*], Jitya R[2], Premjanu N[3], Malathy B R[3], Revathy R[4], and Sridevi. G[4]

[1]Department of Biochemistry, Sathyabama Dental College and Hospital
[2]CRRI, Sathyabama Dental College and Hospital
[3]Department of Biochemistry, Sathyabama Dental College and Hospital
[3]Department of Microbiology, Sathyabama Dental College and Hospital
[4]Department of Pharmacology, Sathyabama Dental College and Hospital
[4]Department of Physiology, SRM Dental College and Hospital
*Corresponding author: srividyabiomed@gmail.com

Abstract

Hydroxyapatite is a mineral naturally occurring in the form of calcium apatite which is important to make biocompatible bone grafts, dental implants and dental fillings. The objective of the study is to synthesize a herbal hydroxyapatite using *Ocimum sanctum* (Basil) leaf aqueous extract ofto impart the anti-inflammatory, anti-oxidant and anti-microbial properties to hydroxyapatite to improve its applications. The formed phyto-hydroxyapatite (phyto-HAP) was subjected to various characterization using Fourier transform infrared spectroscopy (FTIR), scanning electron microscopy (SEM) and X-ray diffraction (XRD) studies. The aqueous leaf extract of *Ocimum sanctum* was subjected to anti-microbial, anti-oxidant and anti-inflammatory activity. The results showed that the synthesized phyto-hydroxyapatite has the crystalline structure similar to natural hydroxyapatite with the bioactive compounds of *Ocimum sanctum* which could make HAP a more effective material to be used in dentistry as filling materials, as herbal bone grafts, as composite herbal dental grafts, as coating material for dental implants, in orthopaedics and in other biomedical applications.

Keywords: *Ocimum sanctum*, Phyto hydroxyapatite, Hydroxyapatite, Herbal Bone graft, Dental implant, Basil leaf, Dental filling material.

Introduction

Hydroxyapatite (HAP) is a versatile biomaterial explored by the researchers worldwide in making bone implants. Because of its ability to differentiate osteoblast, being biocompatible, ability to bond with osseous tissues, and natural occurrence in the human body, HAP has been widely applied in areas of dentistry and tissue engineering.This property of HAP promotes its application in various biomedical fields(1, 2).

When HAP is incorporated in scaffolds, shows excellent osteoconduction by integrating with bone without eliciting an immune response (3).Although synthetic HAP shows great promise in bone tissue engineering, its low fracture toughness, brittleness, and weak mechanical strength make it unsuitable for load-carrying applications (4-7). Moreover, there is a possibility of infection occurring in the implant site as HAP doesn't exhibit antimicrobial property by its own (8). To overcome this, researchers showed great interest in designing and developing biomaterials with the infusion of indigenous herbs which indeed stabilizes the composition and property of the biomaterials through its phytochemicals without inducing any side effects to the host and also imparting antimicrobial and anti-inflammatory properties to HAP. Herbal biomaterials have gained momentum in orthopedic requirements, biomedical applications and also in dentistry. Dental implants are at the

risk of failure due to deposits of oral pathogens. Attempts are made by the researchers to develop coating materials for preventing biofilm formation on dental implants by using zinc oxide coated hydroxyapatite (9). This gave the idea of synthesizing hydroxyapatite with herbs having antimicrobial property which on coating with dental implants or prepared as dental or bone grafts can prevent infection in the implant site.

Indigenous herbs with various therapeutic purposes are abundant in India which can be used as medication sources in a conjugated form (10). Phenols, Tannins, Saponins, and Flavonoids are the significant bioactive compounds found in medicinal plants imparting the therapeutic value to the plant (11). Among these, *Ocimum sanctum* (Holy basil), a well-known traditional herb for many years in India belongs to the family Labiateae, used in treating headaches, common colds, inflammation, heart disease, stomach disorders, various forms of poisoning and malaria (12,13). Holy basil or Tulasi possess a strong aroma with an astringent taste and also considered as the queen of herbs (14). Several research articles showed that *Ocimum sanctum L* is a promising herb containing antioxidant, antiarthritic, antimicrobial (15, 16), anti-inflammatory, anticancer and antistress properties. Kalaiselvi et al used *Moringa oliefera* flower extract and capped with hydroxyapatite to form nano rods. The herbal hydroxyapatite nano rod was characterized and the results supported that, the inclusion of the plant extract favours in stabilizing the hydroxyapatite (17). Based on this, the objective of this study is to synthesize hydroxyapatite with the phytochemicals of *Ocimum sanctum* an insitu method to incorporate the bioactive compounds of *Ocimum* into hydroxyapatite and to characterize theirstructural, morphological and other biological activities namely antimicrobial, antioxidant and anti-inflammatory activities. This novel phyto-HAP with the biological activities of *Ocimum sanctum* can be applied in the field of dentistry, dental implant coating, bone grafts and in orthopedic applications.

Materials and Methods

Chemicals

Ethanol of 95% purity, calcium nitrate tetra hydrate, Di-ammonium Hydrogen Phosphate, and ammonia were purchased from Sigma Aldrich.

Preparation of *Ocimum sanctum* leaf aqueous Extract

2.0 g of *Ocimum sanctum* leaf was collected and rinsed with deionized water. Then it was subjected to boiling in deionized water for 10 min and filtered. The obtained *Ocimum sanctum* aqueous filtrate was used for the synthesis of Phyto-HAP.

***In situ* synthesis of phyto hydroxyapatite**

On modifying the approach employed by Nayar et al (18), 30 ml of the *Ocimum sanctum* aqueous filtrate was taken and mixed with350 ml of 0.4 M alkaline calcium nitrate tetra hydrate. The mixture was kept for incubation at 30°C for 24 h. The resulting solution was added to 400 ml of 0.156 M alkaline diammonium hydrogen phosphate salt solution. The reaction mixture was stirred for 7 days at an ambient temperature of 30 ±0.5 °C. After ageing, the precipitate was collected, rinsed with de-ionized water and dried at 80°C.

The obtained phyto-HAP was subjected to Fourier transform infrared (FT-IR) spectra were performed by pelleting the phyto-HAP with KBr (Nicolet 400) and the peaks were obtained in the region 400– 4000 cm^{-1}. X-ray diffraction (XRD) studies for phyto-HAP was done usingThermofisher ARL Equinox 3000 with Cu Kα radiation running at 45 kV and 40 mA with an angular 2θ range of 20–80° and a sampling interval of 0.002°. Scanning electron microscopy (SEM) studies were performed using JOEL by mounting the sample on a copper disc and images were recorded at 20 kV.

Current Trends in Biotechnology and Pharmacy
Vol. 18 (Supplementry Issue 4A) 77 - 87, November 2024, ISSN 0973-8916 (Print), 2230-7303 (Online)
10.5530/ctbp.2024.4s.7

79

Antimicrobial activity

Media and inoculum

To perform antimicrobial activity, bacterial strains namely *Staphylococcus aureus* ATCC 25923, *Pseudomonas aeruginosa* ATCC 27853, *Escherichia coli* ATCC 25922, and *Klebsiella pneumoniae* ATCC 67120 and for fungus *Candida albicans* (ATCC 10231) were used in this study. Müller-Hinton agar (MHA) was used in cultivating the bacteria at 35°C for 24 h. For fungi cultivation, Sabouraud dextrose agar (SDA) was used.

Preparation of Sabouraud Dextrose Agar (SDA)

6.5 g of the medium should be dissolved in 100 ml of purified water. For the medium to fully dissolve, heat it while stirring often and bring it to a boil for one minute. The content should be 15 minutes autoclaved and cooled. Place petri plates with the sterile agar in them.

Preparation of Mueller Hinton Agar (MHA)

15.2 g of the medium should be dissolved in 400 ml of purified water. For the medium to fully dissolve, heat it while stirring often and bring it to a boil for one minute. Autoclave the contents for 15 minutes at 121 °C, then let them cool to room temperature. Mueller Hinton Agar should be poured onto sterilized petri plates on a level, horizontal surface at a constant depth. *Pseudomonas aeruginosa, Escherichia coli, Staphylococcus aureus, Klebsiella pneumoniae*, and *Candida albicans* are the chosen test microorganisms.

Well Diffusion Method

The antibacterial activity was assessed using the agar well-diffusion method. On Sabouraud Dextrose Agar (SDA) and Mueller Hinton Agar (MHA) plates, 8-hour-old broth cultures of the appropriate fungi and bacteria were swabbed respectively using sterile cotton swabs. Using a sterile cork borer, wells (10 mm in diameter and about 2 cm apart) were drilled into each of these plates. *Ocimum sanctum* extract

stock solution was created at a concentration of 1 mg/ml. The wells received around 100 µl of the extract, which was added, and was left to diffuse at room temperature for two hours. They set up control trials using inoculums devoid of plant extract. For bacterial pathogens, the plates were maintained at 37°C for 18–24 h, and for fungal pathogens, the temperature was maintained at 28°C for 48 h. The inhibitory zone's diameter (in mm) and activity index were both determined (19).

In vitro Anti Oxidant Activity

DPPH radical scavenging activity

According to the methodology of Braca et al, the scavenging activity for DPPH free radicals was measured (20). A mixture of 0.1 ml of plant extract/ascorbic acid in various doses (50 – 500 µg) and 3 ml of 0.004% DPPH solution in ethanol was made. Here, different concentrations of ascorbic acid (50 – 500 µg) was taken as a positive control standard. The mixture was well mixed and given 30 minutes to stabilize at room temperature. The absorbance at 517 nm was measured in order to quantify the decolorization of DPPH. The plant extract was substituted with 0.1 ml of ascorbic acid so as to make positive control. By contrasting the absorbance values of the experimental and control tubes, it was possible to calculate the proportion of DPPH radicals that the extract/compound successfully inhibited (21).

$$\text{DPPH Scavenged (\%)} = \frac{(A \text{ cont} - A \text{ test})}{A \text{ cont}} \times 100$$

Where A test is the absorbance for the presence of the sample in the extracts and A cont is the absorbance of the control reaction. The extract's antioxidant activity was quantified as IC_{50}. The amount of extract (measured in µg/ml) needed to inhibit the production of DPPH radicals by 50% is known as the IC_{50} value. The inhibition curve was reported as a percentage of mean inhibition divided by the standard deviation and plotted for repeated experiments. SPSS 2022 One Way Anova was used to plot the different concentrations of DPPH radical-

scavenging activity (%) against *Ocimum sanctum* extract concentration (µg/ml) which will determine the IC_{50} value of each extract.

Anti-inflammatory activity

Protein Denaturation method

The protein denaturation approach was used to demonstrate anti-arthritic and anti-inflammatory efficacy **In vitro**. Using this procedure, 0.05 ml of *Ocimum extract* (50–250 µg/ml) was combined with 0.45 ml of 5% bovine serum albumin in distilled water. The reaction mixture's pH was brought down to 6.3 by adding 1N hydrochloric acid. The mixture was heated to 57°C for three minutes after being incubated for twenty minutes at 37 °C. After cooling the mixture, 2.5 milliliters of phosphate buffer were added. 0.05 ml of distilled water was taken asnegative control by replacing plant extract, and for product control bovine serum albumin was substituted with distilled water (22-24). At 600 nm, the reaction mixture's turbidity was measured.200 µg of diclofenac sodium was taken as standard. Protein denaturation inhibition percentage was calculated as follows,

Percentage Inhibition = 100 – (Test OD – Product Control OD/ Control OD) x 100

100% protein denaturation is considered as negative control. 200 µg/mlof Diclofenac sodium is taken as a positive control and the results were calculated.

Statistical Analysis

The antimicrobial, anti-inflammatory, and DPPH activity findings were shown as the mean±standard deviation of three independent tests (n = 3). Using the statistical software program SPSS, version 22.0, a one-way analysis of variance ($p<0.05$) was performed by comparing the means and then Duncan's multiple range analysis.

Results and Discussion

The present study aims to synthesize phyto-hydroxyapatite using *Ocimum sanctum* and characterize it using FTIR, XRD, SEM EDX, Antioxidant, Anti-inflammatory and anti microbial properties. While researchers have made various attempts in making different biomaterial, infusion of medicinal herbs in biomaterial makes it more versatile in its applications. With substantial scientific evidence, the herbal biomaterials can be applied not only in basic or applied research, instead it can be taken to clinical research.

Herbs possessing both antioxidant, anti microbial and anti-inflammatory properties like *Ocimum sanctum* benefits the biomaterials to overcome the inflammatory response and infection in the implant site. This was demonstrated by Santin et al in his study by using soy bean extract in bone fillers and showed that the extract with antioxidant and anti-inflammatory properties reduces the inflammatory response in the implant site and promotes the osteoblast differentiation of the bone fillers in invivo models (25).

Fourier Transform Infrared Spectroscopy (FTIR)

The FTIR spectra of Phyto-HAP was shown in Figure 1. The phosphate bandsv3 PO_4^{3-} were observed at 670 cm^{-1} and874.1 cm^{-1}. v1 phosphate band was observed at 963.5 cm^{-1}, 1019 cm^{-1} and 1088.4 cm^{-1} which attributes the anti-symmetric bending motion in Phyto-HAP. The peak at 872.2 cm^{-1}, also indicates the CO_3^{2-} stretching band in Phyto-HAP. 3379 cm^{-1} and 1638 cm^{-1} peak values corresponds to the phenolic group and the amide group of *Ocimum sanctum* which is due to the presence of euginolin *Ocimum sanctum* (26). The peak at 1422 cm^{-1} shows the presence of aliphatic amines of *Ocimum sanctum* (27). The bands reveal that, the prepared Phyto-HAP contains both the chemical compounds of *Ocimum sanctum* and Hydroxyapatite. Kumar et al prepared a bone graft using hydroxyapatite with the herb *Cassia occidentalis* and characterized it invitro using FTIR, in which the peak values obtained for hydroxyapatite were similar to our findings (28). Moreover, the phenols and amines of *Ocimum sanctum* imparts antimicrobial and anti-inflammatory property

Current Trends in Biotechnology and Pharmacy
Vol. 18 (Supplementry Issue 4A) 77 - 87, November 2024, ISSN 0973-8916 (Print), 2230-7303 (Online)
10.5530/ctbp.2024.4s.7

81

to Phyto-HAP and which may support thephyto-HAP to overcome the inflammation and infection in the implant site, when it is introduced in a bone graft or a dental implant.

X ray Diffraction Analysis

Figure 2 shows the X-ray diffraction (XRD) pattern of phyto-HAP which shows the presence of peaks at 25.92º, 32.13º, 39.67º, 46.76º, 49.53º, 53.12, 64.07º, 77.17º, and 87.80º indicates the reflection from 002, 210, 300, 130, 222, 321, 511, 513, and 244 crystal planes, respectively, which were compared with JCPDS (740566) data and it clearly indicates the presence of phyto-HAP. The results of XRD analysis obtained in the present investigation are in good agreement with the reported results (29). The results
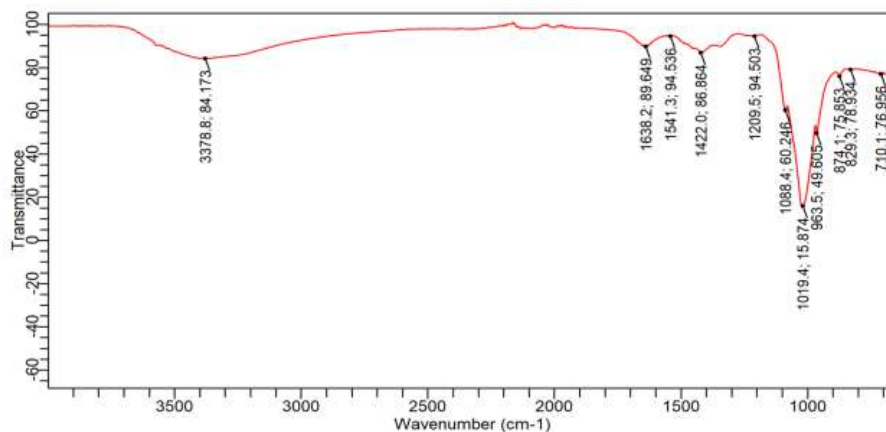

Figure 1: Shows the FTIR pattern of Phyto-hydroxyapatite (Phyto-HAP)
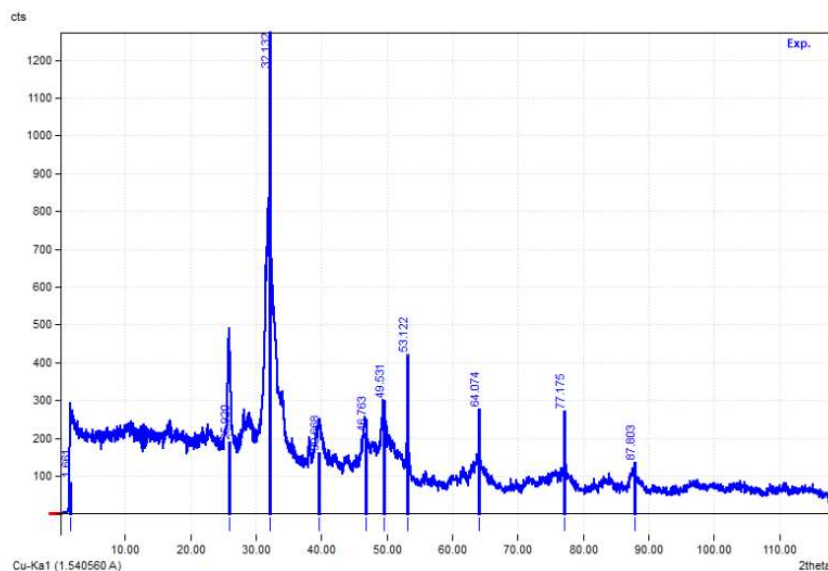
Figure 2: Shows the XRD pattern of Phyto-hydroxyapatite

Srividya et al

obtained in our study are in accordance with the study conducted by Rabiei et al who did a comparative analysis on the crystal structure of hydroxyapatite through XRD analysis and showed the reflections obtained for hydroxyapatite (30). These results supports that the prepared phyto-HAP is similar to natural hydroxyapatite and could be used in coatings of dental implants or can be incorporated in bone grafts.

Scanning Electron Microscopy

The Figure 3 shows the SEM image of phyto hydroxyapatite. The image shows white crystalline deposits of hydroxyapatite along with the phyto chemicals of *Ocimum sanctum*. The standard EDX spectra reveals the calcium and phosphate presence with a ratio of 1.66 which corresponds to the living bone ratio of 1.67(31). Our previous study on the bone graft prepared with the incorporation of *Ormocarpum sennoides*, exhibited a stoichiometric ratio of 1.66 for hydroxyapatite which showed an effective ossification property with the anti-

inflammatory properties of the incorporated herb *Ormocarpum sennoides* (32). Similarly, Chandrasekar et al also demonstrated that the synthesized nano hydroxyapatite showed a Ca/P ratio of 1.68 which was so close to our study findings (33).

Anti microbial activity

The current study assessed the antibacterial activity of an aqueous extract of *Ocimum sanctum* leaves against a variety of Gram positive and Gram negative bacteria as well as a fungus that was thought to be a human pathogenic microbe. Using the agar well diffusion method, the plant extract's susceptibility was evaluated. According to Table 1, our initial research revealed that *Ocimum sanctum* aqueous leaf extract with a concentration of 100 mg/l was effective against human pathogens that were isolated locally, including *E. Coli and Staphylococcus aureus* each with a zone of inhibition 19mmand for, *Klebsiella species*the resistance zone was 16 mm, and for *Pseudomonas aeruginosa*

Figure 3: Shows the SEM image of Phyto-hydroxyapatite with EDX

Phyto-Hydroxyapatite Using *Ocimum Sanctum*

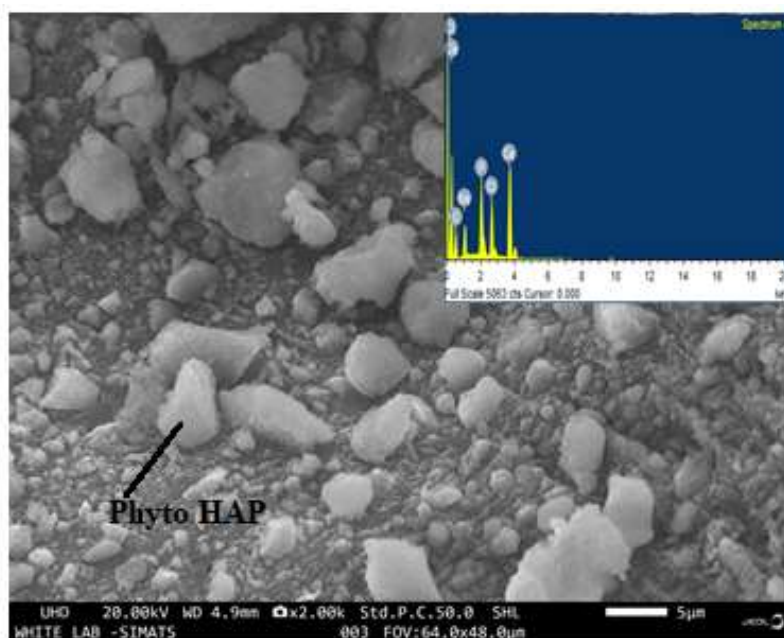21 mm was exhibited. There were no zone formation for *Candida albicans* which was in accordance with the study conducted by Khan et al who reported that the aqueous extract of *Ocimum sanctum* showed no inhibition against candida albicans (34). The findings of this study are in accordance with the study performed by Ashish Ranjan Singh et al who has reported anti-microbial activity for aqueous, methanolic and ethanolic extracts of *Ocimum sanctum* (35). Hence, the antimicrobial property of *Ocimum sanctum* may be imparted to hydroxyapatite which help to overcome the infections at the implant site or can prevent any biofilm formation on dental implants or bone grafts.

Antioxidant Assay

DPPH Radical Scavenging Activity

At varying doses, *Ocimum sanctum* demonstrated efficient scavenging of the free radicals in a dose-dependent manner. The DPPH free radical scavenging activity is a widely recognized model for mitigating lipid oxidation (36). It was previously believed that antioxidants' capacity to donate hydrogen was the reason behind their impact on DPPH radical scavenging (37). The aqueous extract of *Ocimum sanctum* at varying concentration 50, 100, 200, 300, 400 and 500 µg/ml exhibited 71.15%, 75.59%, 81.11%, 83.57%, 85.19% and 91.76% inhibition respectively. The standard drug ascorbic acid at the same dosage showed 80.9%, 89.64%, 92.73%, 95.58%, 101.62% and 102.81% inhibition respectively. The IC_{50} value for *Ocimum sanctum* was found to be 35.13 µg/ml and for Standard ascorbic acid was 30.9 µg/ml Table 2. The aqueous extract of *Ocimum sanctum* was able to scavenge the free radicals significantly when compared with standard ascorbic acid.Gupta et al studied the antioxidant activity of ethanolic-water extract of *Ocimum sanctum*

	Table 1: Shows the antimicrobial activity of *Ocimum sanctum*	
S. No	Selected Pathogens	Zone of Inhibition in millimeter (mm)
1	*Escherichia coli*	19 $\pm$ 0.5
2	Candida albicans	No Zone
3	*Klebsiella sp*	16 $\pm$ 0.4
4	*Staphylococus aureus*	19 $\pm$ 0.5
5	*Pseudomonas aeruginosa*	21$\pm$ 0.4
The experiments were performed in triplicates and the values are expressed as Mean $\pm$ SEM		

	Table 2: Shows the antioxidant activity of *Ocimum sanctum*	
Concentration (µg/ml)	DPPH inhibition % of Positive control-Ascorbic acid	DPPH inhibition % of*Ocimum sanctum*
50	80.9 ±2.38	71.15±1.24
100	89.64±2.21	75.59±1.21
200	92.73±0.35	81.11±1.35
300	95.58±1.65	83.57±1.36
400	101.62±2.69	85.19±1.45
500	102.81±2.41	91.76±1.58
IC_{50} (µg/ml)	35.13 µg/ml	30.9 µg/ml

Current Trends in Biotechnology and Pharmacy
Vol. 18 (Supplementry Issue 4A) 77 - 87, November 2024, ISSN 0973-8916 (Print), 2230-7303 (Online)
10.5530/ctbp.2024.4s.7

84

S. No	Conc. (µg/ml)	*Ocimum sanctum* Extract (% inhibition of protein denaturation) (%)	Diclofenac Sodium (% inhibition of protein denaturation) (%)
		Table 3: Shows the anti-inflammatory activity of *Ocimum sanctum*	
1	50	23.82 ± 2.06	
2	100	37.62 ± 2.17	
3	200	49.93 ± 1.77	87.69 ± 1.0
4	300	57.62 ±2.34	
5	400	62.71 ±2.21	
6	500	70.37 ± 1.63	
7	1000	77.12 ± 1.54	

The experiments were performed in triplicates and the values are expressed as Mean ± SEM. Diclofenac sodium was used as positive control.

and reported an IC_{50} value of the extract as 34.21 µg/ml. the results are matching with our study (38)

Anti-inflammatory Activity

Denaturation of protein is usually caused by inflammation. Non-steroidal Anti-inflammatory drugs like Diclofenac sodium are considered as good anti-inflammatory drug but in long term it induces side effects in the body (39). As an alternative, traditional herbs like Tulsi can be a suitable substitute for Diclofenac sodium as many researchers have studied about its anti-inflammatory property. Surender singh et al studied about the anti-inflammatory and anti-arthritic activity of *Ocimum sanctum* and found that it significantly reduced the inflammatory edema in rats (40). In this study, *Ocimum sanctum* extract was tested for anti-inflammatory efficacy *In vitro* at different doses inhibiting bovine serum albumin. A dose-dependent rise in percentage inhibition was observed in *Ocimum sanctum* extract at concentrations between 50 and 1000 µg/ml, indicating the extract's potential to prevent denaturation of albumin. These results were comparable to those of diclofenac sodium (200 µg/ml) as mentioned in Table 3. At 50 µg/ml, *Ocimum sanctum* extract was able to prevent denaturation by 23.82%. *Ocimum* extract

progressively raised its percentage of denaturation inhibition in a dose-dependent way. The extract was preventing denaturation by 77.12% at 1000 µg/ml, which was almost identical to the 200 µg/ml denaturation inhibition caused by diclofenac sodium. *Ocimum sanctum* extract's anti-inflammatory properties may be attributable to the extract's bioactive compound octadecenoic acid and hexadecenoic acid (24)

Conclusion

The infusion of native herbs in biomaterial makes it a versatile composite for its utilization in various biomedical applications. In this study, the bioactive compounds of *Ocimum sanctum* (Holy basil) leaves were incorporated in the synthesis of hydroxyapatite by an insitu method. The various characterization of the phyto-HAP reveals the inclusion of bioactive compounds of basil leaves and the chemical composition of Hydroxyapatite. Moreover, this combination can help to achieve osteoconduction with the anti-inflammatory, anti-microbial and antioxidant properties of the basil leaves.

Acknowledgement

Conflicts of Interest

The authors declare no conflict of interest.

References

1. Ojo, S.A., Abere, D.V., Adejo, H.O., Robert, R.A., & Oluwasegun, K.M. (2023). Additive manufacturing of hydroxyapatite-based composites for bioengineering applications. Bioprinting, 32, e00278.

2. Murugesan, V., Vaiyapuri, M., &Murugeasan, A. (2022). Fabrication and characterization of strontium substituted chitosan modify hydroxyapatite for biomedical applications. Inorganic Chemistry Communications, 142, 109653.

3. Muzzarelli, R.A.A. (2011). Chitosan composites with inorganic, morphogenetic proteins and stem cells, for bone regeneration. Carbohydrate Polymers, 83, 1433–1445.

4. Dragomir, L., Antoniac, A., Manescu, V., Robu, A., Dinu, M., Pana, I., Cotrut, C.M., Kamel, E., Antoniac, I., Rau, J.V., et al. (2023). Preparation and characterization of hydroxyapatite coating by magnetron sputtering on Mg–Zn–Ag alloys for orthopaedic trauma implants. Ceramic International, 49, 26274–26288.

5. Elabbasy, M.T., Algahtani, F.D., Alshammari, H.F., Kolsi, L., Dkhil, M.A., Abd El-Rahman, G.I., El-Morsy, M.A., &Menazea, A.A. (2022). Improvement of mechanical and antibacterial features of hydroxyapatite/chromium oxide/graphene oxide nanocomposite for biomedical utilizations. Surface and Coatings Technology, 440, 128476.

6. Radovanovi´c, Ž., Joki´c, B., Veljovi´c, D., Dimitrijevi´c, S., Koji´c, V., Petrovi´c, R., &Jana´ckovi´c, D. (2014). Antimicrobial activity and biocompatibility of Ag+ - and Cu2+-doped biphasic hydroxyapatite/α-tricalcium phosphate obtained from hydrothermally synthesized Ag+ - and Cu2+-doped hydroxyapatite. Applications of Surface Science, 307, 513–519.

7. Zhang, Z., Wang, T., Zhang, S., Yao, K., Sun, Y., Liu, Y., Wang, X., & Huang, W.A. (2021). Novel La3+ doped MIL spherical analogue used as antibacterial and anticorrosive additives for hydroxyapatite coating on titanium dioxide nanotube array. Applications of Surface Science, 551, 149425.

8. Nisar, A., Iqbal, S., Atiq Ur Rehman, M., Mahmood, A., Younas, M., Hussain, S.Z., Tayyaba, Q., & Shah, A. (2023). Study of physico-mechanical and electrical properties of cerium doped hydroxyapatite for biomedical applications. Material Chemistry and Physics, 299, 127511.

9. Abdulkareem, E.H., Memarzadeh, K., Allaker, R.P., Huang, J., Pratten, J., & Spratt, D. (2015). Anti-biofilm activity of zinc oxide and hydroxyapatite nanoparticles as dental implant coating materials. Journal of Dentistry, 43(12), 1462–1469.

10. Gurib, F.A. (2006). Medicinal plants: Traditionals of yesterday and drugs tomorrow. Molecular Aspects of Medicine, 27, 1-93.

11. Krishnaiah, D., Sukla, A.R., Sikand, K., & Dhawan, V. (2009). Effect of herbal polyphenols on artherogenic transcriptome. Molecular Cell Biochemistry, 278, 177-184.

12. Shetty, S., Udupa, S., & Udupa, L. (2008). Evaluation of Antioxidant and Wound Healing Effects of Alcoholic and Aqueous Extract of Ocimum sanctum Linn in Rats. Evid. -Based Complement. Alternative Medicine ECAM, 5, 95–101.

13. Cohen, M.M. (2014). Tulsi—Ocimum sanctum: A herb for all reasons. Journal of Ayurveda and Integrated Medicine, 5, 251–259.

14. Marja, P.K., Anu, I.H., Heikki, J.V., Jussi-Pekka, R., Kalevi, P., Tytti, S.K., et al. (1999). Antioxidant activity of plant extracts containing phenolic compounds. Journal of Agricultural Food Chemistry, 47(10), 395462.

15. Geeta, Vasudevan, D.M., Kedlaya, R., Deepa, S., & Ballal, M. (2001). Activity of Ocimum sanctum (the traditional Indian medicinal plant) against the enteric pathogens. Indian Journal of Medical Sciences, 55, 434- 8, 472.

16. Singh, S., Malhotra, M., & Majumdar, D.K. (2005). Antibacterial activity of *Ocimum sanctum* L. fixed oil. Indian Journal of Experimental Biology, 43, 835-7.

17. Kalaiselvi, V., Mathammal, R., Vijayakumar, S., & Vaseeharan, B. (2018). Microwave assisted green synthesis of Hydroxyapatite nanorods using Moringa oleifera flower extract and its antimicrobial applications. International Journal of Veterinary Science and Medicine, 6, 286–295.

18. Nayar, S., & Guha, A. (2009). Waste utilization for the controlled synthesis of nanosized hydroxyapatite. Materials Science and Engineering C, 29(4), 1-4.

19. Mehrishi, P., Agarwal, P., Broor, S., & Sharma, A. (2020). Antibacterial and antibiofilm properties of medicinal plant extracts against multi-drug resistant Staphylococcus species and non-fermenter bacteria. Journal of Pure and Applied Microbiology, 14(1), 403-413.

20. Braca, A., Tommasi, N.D., Bari, L.D., Pizza, C., Politi, M., & Morelli, I. (2001). Antioxidant principles from Bauhinia terapotensis. Journal of Natural Products (Lloydia), 64, 892–895.

21. Trevisan, M.T., Vasconcelos Silva, M.G., Pfundstein, B., Spiegelhalder, B., & Owen, R.W. (2006). Characterization of the volatile pattern and antioxidant capacity of essential oils from different species of the genus Ocimum. Journal of Agricultural Food Chemistry, 54, 4378-82.

22. Kelm, M.A., Nair, M.G., Stasburg, G.M., & DeWitt, D.L. (2000). Antioxidant and cyclooxygenase inhibitiory phenolic compounds from *Ocimum sanctum* Linn. Phytomedicine, 7, 7-13.

23. Singh, S. (1998). Comparative evaluation of anti-inflammatory potential of fixed oil of different species of Ocimum and its possible mechanism of action. Indian Journal of Experimental Biology, 36, 1028-31.

24. Srivastava, A., Subhashini, & Keshari, A.K., & Srivastava, R. (2021). Phytochemical and GC-MS Analysis of Hydro Ethanolic Leaf Extract of *Ocimum sanctum* (L.). Pharmacognosy Research, 13(4), 233-237.

25. Santin, M., Morris, C., Standen, G., Nicolais, L., & Ambrosio, L. (2007). A new class of bioactive and biodegradable soybean-based bone fillers. Biomacromolecules, 8, 2706-2711.

26. Balamurughan, M.G., Mohanraj, S., Kodhaiyolii, S., & Pugalenthi, V. (2014). *Ocimum sanctum* leaf extract mediated green synthesis of iron oxide nanoparticles: spectroscopic and microscopic studies. Journal of Chemical and Pharmaceutical Sciences, 4, 201-204.

27. Williams, L.A.D., Connar, A.O., Latore, L., Dennis, O., Ringer, S., Whittaker, J.A., et al. (2008). The *In vitro* anti-denaturation effects induced by natural products and non-steroidal compounds in heat-treated (immunogenic) bovine serum albumin is proposed as a screening assay for the detection of anti-inflammatory compounds, without the use of animals, in the early stages of the drug discovery process. West Indian Medical Journal, 57, 327-31.

28. Santhosh Kumar, B., Hemalatha, T., Deepachitra, R., Narasimha Raghavan, R., Prabu, P., & Sastry, T.P. (2015). Biphasic calcium phosphate–casein bone graft fortified with Cassia occidentalis for bone tissue engineering and regeneration. Bulletin of Material Science, 38(1), 259–266.

29. Bouyer, E., Gitzhofer, F., & Boulos, M.I. (2000). Morphological study of hydroxyapatite nanocrystal suspension. Journal of Material Science: Materials in Medicine, 11, 523-528.

30. Rabiei, M., Palevicius, A., Monshi, A., & Nasiri, S. (2020). Comparing Methods for Calculating Nano Crystal Size of Natural Hydroxyapatite Using X-Ray Diffraction. Nanomaterials, 10(9), 1-21.

31. Poologasundarampillai, G., Ionescu, C., Tsigkou, O., Murugesan, M., Hill, R.G., & Stevens, M.M. (2010). Synthesis of bioactive class II poly (gamma-glutamic acid)/silica hybrids for bone regeneration. Journal of Material Chemistry, 20, 8952–8961.

Phyto-Hydroxyapatite Using *Ocimum Sanctum*

32. Srividya, S., Sastry, T.P., Santhosh Kumar, B., & Hemalatha, T. (2015). Osteopotential Bone Implant Containing Porous Biphasic Calcium Phosphate Impregnated With Casein, Egg Yolk and Ormocarpum sennoides - An *In vitro* Study. International Journal of Pharma and Bio Sciences, 6(1), 275 - 282.

33. Chandrasekar, A., Sagadevan, S., &Dakshnamoorthy, A. (2013). Synthesis and characterization of nano-hydroxyapatite (n-HAP) using wet chemical technique. International Journal of Physical Science, 8, 1639–1645.

34. Khan, A., Ahmad, A., Manzoor, N., & Khan, L.A. (2010). Antifungal Activities of *Ocimum sanctum* Essential Oil and its Lead Molecules. Natural Product Communications, 5(2), 345-349.

35. Singha, A.R., Bajaj, V.K., Sekhawat, P.S., & Singh, K. (2013). Phytochemical estimation and Antimicrobial activity of Aqueous and Methanolic extract of *Ocimum sanctum* L. Journal of Natural Product and Plant Resourses, 3(1), 51-58.

36. Viturro, C., Molina, A., & Schmeda-Hischmann, G. (1999). Free radical scavengers from Mutisia friesiana (Asteraceae) and Sanicula graveolens (Apiaceae). Phytotherapy Research, 13, 422.

37. Gupta, S., Mediratta, P.K., Singh, S., Sharma, K.K., & Shukla, R. (2006). Antidiabetic, antihypercholesterolaemic and antioxidant effect of *Ocimum sanctum* (Linn) seed oil. Indian Journal of Experimental Biology, 44, 300-4.

38. Gupta, S., Kumar, M.N.S., Duraiswamy, B., Chhajed, M., & Chhajed, A. (2012). In-Vitro Antioxidant And Free Radical Scavenging Activities Of *Ocimum sanctum*. World Journal of Pharmacy and Research, 1(1), 78-94.

39. Deshpande, V., & Jadhav, M. (2009). *In vitro* anti-arthritic activity of Abution indicum. J Pharm Res, 2, 644-5.

40. Singh, S., & Majumdar, D.K. (1995). Anti-inflammatory and Antipyretic Activities of *Ocimum sanctum* Fixed Oil. International Journal of Pharmacognosy, 33(4), 288-292.

Antibiofilm activity of ethanolic root extract of *Vetiveria zizanioides* against dental pathogens

N. Premjanu[1]*, Rizwana Khatun M R[2], S. Srividya[3], B.R. Malathy[4], and R. Revathy[5]

[1]Department of Biochemistry, Sathyabama Dental College and Hospital
[2]CRRI, Sathyabama Dental College and Hospital, Chennai 600119
[3]Department of Biochemistry, Sathyabama Dental College and Hospital
[4]Department of Microbiology, Sathyabama Dental College and Hospital
[5]Department of Pharmacology, Sathyabama Dental College and Hospital
*Corresponding author: janu6kishore@gmail.com

Abstract

Biofilm infections, shielded from antibiotics and immune defences, pose a major health threat. Plants offer potential solutions due to their diverse bioactive compounds. This study investigated the root extract of *Vetiveria zizanioides* for its composition and tested for its ability to inhibit biofilms, fight bacteria and fungi, reduce inflammation, and combat oxidative stress in pathogens. The anti-biofilm properties were assessed using test tube method and a crystal violet assay. Phytochemical composition was analysed via Gas Chromatography-Mass Spectrometry (GC-MS). Antimicrobial activity was tested against *Staphylococcus aureus, Escherichia coli, Pseudomonas aeruginosa, Klebsiella pneumonia* and *Candida albicans* using both agar well plate and micro broth dilution methods. Antioxidant and anti-inflammatory effects were determined by DPPH and protein denaturation assays, respectively. The ethanolic extract contained 17 identified compounds, primarily sesquiterpenes and fatty acids. Major compounds were identified as 17-hydroxy-3,20-dioxopregna-1,4,ol, z,z-8,10-hexadecadien-1-ol, formic acid, campesterol, cedren-13-ol, It inhibited biofilm formation in various pathogens, with the strongest effect against *Staphylococcus aureus* (75%) and the weakest against *Pseudomonas aeruginosa* (25%). The extract also displayed antimicrobial activity against all tested bacteria and fungi, with the best activity against *Staphylococcus aureus* (23mm inhibition zone). Additionally, it exhibited dose-dependent antioxidant and anti-inflammatory properties. These findings suggest *Vetiveria zizanioides* extract has significant potential for combating biofilm-related infections. Future research should focus on isolating and purifying active compounds, assessing their safety and long-term effects, and exploring their potential as therapeutic agents.

Keywords: *Vetiveria zizanioides,* anti-biofilm, antimicrobial, antioxidant and anti-inflammatory

Introduction

The oral microbiome consists of inter-kingdom microorganisms, which includes a few viruses, fungal species and roughly 700 different bacterial species belonging to 13 independent phyla (1). These interactions collectively determine the composition of the oral microbiome. Microorganisms in the oral microbiomei interact synergistically, mutualistically, and antagonistically, collectively shaping its composition (2). The oral cavity supports the growth of a diverse microbiome, due to its, humid, warm and nutrient-rich surroundings. The composition of the oral microbiota is influenced by factors such as saliva composition, diet, hygiene habits, and the anatomical structure of the oral cavity. This results in a vast diversity of microorganisms

Current Trends in Biotechnology and Pharmacy
Vol. 18 (Supplementry Issue 4A) 88 - 105, November 2024, ISSN 0973-8916 (Print), 2230-7303 (Online)
10.5530/ctbp.2024.4s.8

89

within the oral microbiome, which occupy distinct ecological niches including the cheek, palate, tongue surface, teeth, gingiva, and periodontal pocket (3). Alterations in factors like saliva composition, diet, and hygiene habits can result in an imbalance of the oral microbiota, known as dysbiosis (3). Moreover, the complex interaction among the oral microbiome, the body's immune response, and dietary patterns plays a pivotal role in the creation of harmful biofilms within theoral cavity (4). These biofilms, characterized by their ability to adhere to dental surfaces, are implicated in the pathogenesis of various oral infections, significantly impacting dental health and well-being (4). Both Gram-positive and Gram-negative bacteria have the capability to form biofilms on various surfaces, including the hard surfaces of teeth and the soft tissues of oral mucosa, like epithelial cells, dental surfaces as well as medical devices such as dental implants, orthodontic prostheses(5). Among the most prevalent bacterial species involved in biofilm formation are *Enterococcus faecalis, Staphylococcus aureus, Staphylococcus epidermidis, Streptococcus viridans, Escherichia coli, Klebsiella pneumoniae, Proteus mirabilis, and Pseudomonas aeruginosa* (6).

The process of pathogenic oral biofilm development follows a sequential pattern. Initially, a salivary pellicle forms, originating from salivary glycoproteins that adhere to the tooth surface. Subsequently, initial adhesion occurs as early colonizer bacteria in saliva recognize binding proteins within the acquired pellicle and attach to them. As the biofilm grows, various bacterial species become incorporated, leading to biofilm maturation. Finally, the bacteria disperse from the biofilm and spread to colonize new surfaces (7). These Bacterial biofilms secrete a complex mixture of polysaccharides, proteins, fatty acids, extracellular DNA and proteins mainly composed of D-amino acids collectively referred to as extracellular polymeric substance (EPS) (8). EPS plays several crucial roles in biofilm development and function, including stabilizing the biofilm structure, mediating adhesion and resistance, preventing water loss, acting as a resin, retaining and digesting nutrients, balancing production and degradation, enabling communication and quorum sensing, and even serving as a carbon and energy source (9). These resilient communities of bacteria safe guard themselves from conventional antibiotics and immune defences, leading to chronic, challenging infections.

The National Institutes of Health (NIH) reports that a staggering 80% of microbial infections in the human body are caused by biofilm-associated microorganisms (10). The primary challenge with biofilm-related infections lies in the detection of causative species, as biofilm samples often yield culture-negative results. This issue, attributed to the robust integration or uncultivability of bacteria within biofilms, extends to implant and catheter-related infections, where bacterial identification is notably difficult. Historically, biofilm bacteria have been deemed unculturable. Moreover, certain pathogenic bacteria, unable to thrive in culture media, are thought to become virulent within the host or environmental conditions, leading to infection (11). The pervasive role of bacterial biofilms in chronic infections is well-documented, with a wide array of conditions such as otitis, diabetic foot ulcers, rhinosinusitis, chronic pneumonia in cystic fibrosis, osteomyelitis, and infective endocarditis being attributed to these microbial structures (12). Approximately two-thirds of hospital-acquired infections are attributed to *S. aureus Pseudomonas aeruginosa*, and *Klebsiella pneumoniae*. These infections often involve biofilms on medical devices like dental implants, which can result from contact with infected individuals or during surgeries, leading to severe health outcomes. Chronic conditions such as periodontitis and urinary tract infections are also linked to biofilms, which are difficult to treat due to their resistance to antibiotics and the immune system. The onset of biofilm-related infections involves microbial contamination, a compromised

immune response near the device, and a generally weakened immune function (13). *Candida* infections, including invasive candidiasis, have increased in severity and are a major cause of morbidity and mortality in healthcare settings, particularly among older adults and newborns. *Candida* is a natural inhabitant of oral cavity and a part of oral microbiota. The interaction between *Candida* and its host relies on yeast virulence and host-related elements, including comorbidities, immunity, and age. *Candida* frequently contributes to biofilm-related infections, particularly in the context of medical devices. The liberation of yeast cells from biofilms can result in widespread infection or fungemia (14). These infections collectively exert a significant health toll, are not only prevalent but also annually contribute to considerable mortality and morbidity worldwide. In recognition of this growing threat, a significant increase in research efforts is imperative to develop effective strategies for preventing and managing these complex infections(15). Plants provide promising avenues owing to the production of varied novel bioactive secondary metabolites. In this context, the current study is intended to explore one such plant namely *Vetiveria zizanioides.*

Vetiveria zizanioides commonly known as vetiver, is a perennial long tufted grass belonging to the family Poaceae. It is native to India and well-recognized in southern India, where it goes by various names such as khus, vetiver, and vala in different Indian languages Vetiver is an aromatic and ornamental plant, widely used for bathing and perfumery purposes which has been acknowledged since ancient times. Numerous studies have explored its chemical composition, with sesquiterpenes being the primary components found in the roots and phenolic compounds in the leaves(16). *Vetiveria zizanioides* contains a variety of chemical constituents, including ß-vetivone, vetivone, vetivene, vetiverol, vetivenate, vetivenyl, vetivazulene, khusimol, iso-khusimol, khositone, khusimone, tripene-4-ol,

terpenes, benzoic acid, ß-humulene, and epizizianalThe predominant component in the roots is valencene, constituting 30.36%, while the shoots and leaves primarily contain 9-octadecenamide, 1,2-benzenedicarboxylic acid, and diisooctyl ester. Analysis reveals a rich presence of terpenoids in the plant's volatile oil, with three monoterpenes, two sesquiterpenes, and one triterpene identified in the shoot volatiles, and a predominance of sesquiterpenes in the root volatiles (17). Vetiver serves multiple purposes, including being aromatic, antifungal, cooling, antiemetic, diaphoretic, haemostatic, expectorant, diuretic, and stimulant. It has also been used traditionally for managing conditions such as hysteria, insomnia, skin diseases, asthma, amentia, amenorrhea, antispasmodic effects, kidney problems, gallstones, and as a mosquito repellent. Additionally, vetiver exhibits antioxidant and anti-inflammatory properties (18). Laboratory studies have demonstrated vetiver's antimicrobial activity, particularly against pathogens like *Staphylococcus aureus* and *Escherichia coli*. It exerts bacteriostatic and fungistatic effects, inhibiting bacterial growth (19). Furthermore, Vetiver oil's inherent aroma characteristics contribute to its pleasant odour, is known for its sedative properties. Traditionally, *Vetiveria zizanioides* has been employed in aromatherapy to mitigate stress, anxiety, nervous tension, and insomnia (20).

Given its rich chemical composition and diverse bioactive properties, *Vetiveria zizanioides* offers a multifaceted approach to combating biofilm infections by combining antibacterial, antifungal, antioxidant, and anti-inflammatory activities. This comprehensive action can help address the diverse challenges posed by biofilms, including antimicrobial resistance and inflammatory responses. Studying its efficacy against biofilms, forming pathogens, can provide valuable insights into its therapeutic potential in combating biofilm-related infections.

This research endeavours to explore the antibiofilm potential of *Vetiveria*

Antibiofilm Activity of *Vetiveria zizanioides*

zizanioides root extract against dental pathogens. Objectives encompass elucidating its phytochemical profile, assessing antimicrobial efficacy against prevalent oral pathogens, and evaluating anti-inflammatory and antioxidant properties. Furthermore, this research seeks to investigate the extract's ability to inhibit biofilm formation, offering valuable insights into natural agents for managing oral biofilm-related diseases.

Materials and Methods

Preparation of ethanolic extracts of *Vetiveria zizanioides*

Dried roots of *Vetiveria zizanioides* were powdered and then 40 g of the powder was soaked in 400 mL of ethanol. For extraction, the extract was continuously stirred at room temperature for 48 hours using a magnetic stirrer. Then the ethanol extract was filtered using Whatman filter paper (No.1). The filtrates were concentrated under reduced pressure at 45-50°C using a rotary evaporator and stored at 4°C until analysis.

Phytochemical analysis by Gas chromatography–mass spectrometry (GC-MS)

1 μl volume of ethanol extract from *Vetiveria zizanioides* was utilized for GC/MS analysis. The analysis was conducted using a GC QP 2010 instrument by SHIMADZU, which consisted of an AOC-20i autosampler and a gas chromatograph connected to a mass spectrometer (GC-MS). The GC-MS mass spectrum interpretation relied on the National Institute Standard and Technology (NIST) database

Antimicrobial activity in Vetiver Root Extract

Media and inoculum

For antimicrobial activity, *Staphylococcus aureus* ATCC 25923, *Escherichia coli* ATCC 25922, *Pseudomonas aeruginosa* ATCC 27853 and *Klebsiella pneumoniae* ATCC 67120 and *Candida albicans* (ATCC 10231) were used in this investigation. The bacteria used were cultivated on Müller-Hinton agar (MHA) at 35°C for 24 h. The fungi were cultivated on Sabouraud dextrose agar (SDA).

Antimicrobial activity by agar diffusion test

Sterile petri dish plates were prepared, each containing 20 ml of sterilized Müller-Hinton agar for antibacterial testing and 20 ml of sterilized Sabouraud dextrose agar (SDA) for antifungal testing. The media in these plates was allowed to solidify. Fresh culture suspensions of bacteria and fungi (100 μl each) were swabbed onto their respective plates. Using a sterile gel puncher, wells of 10 mm diameter were created approximately 2 cm apart on the agar surface. A stock solution of plant extract at a concentration of 1 mg/ml was added to each well, allowing it to diffuse at room temperature. The plates were then incubated for 24 hours, and afterward, the inhibitory zones' diameters around each well were measured and recorded (21).

Minimum inhibitory concentration (MIC) by microbroth dilution method

The minimum inhibitory concentration (MIC) was assessed using the microbroth dilution method on slants (1 ml). Plant extracts were serially diluted by factors of two, resulting in concentrations of 50, 25, 12.5, and 6.25 mg/ml. To these dilutions, 100 μl of microorganism suspension was added. The tubes were then incubated at 37°C for 24 hours. After incubation, sub-cultures were prepared on Mueller Hinton agar for bacteria and Sabouraud dextrose agar (SDA) for fungi. Bacterial and fungal growth was observed the following day. The MIC was defined as the lowest concentration of plant extract that inhibited bacterial or fungal growth in the subcultures. (21).

DPPH Radical Scavenging Assay

The DPPH Radical Scavenging Assay is a widely used method for assessing the antioxidant activity of plant extracts. This assay relies on the capacity of antioxidants to reduce

Current Trends in Biotechnology and Pharmacy
Vol. 18 (Supplementry Issue 4A) 88 - 105, November 2024, ISSN 0973-8916 (Print), 2230-7303 (Online)
10.5530/ctbp.2024.4s.8

92

the stable free radical DPPH (2,2-diphenyl-1-picrylhydrazyl) to its corresponding hydrazine form. The reduction of DPPH is accompanied by a colour change from purple to yellow, which can be quantified spectrophotometrically at a wavelength of 517 nm. For the assay ascorbic acid is taken as standard. Dissolve 250 mg of ascorbic acid in 50 mL of distilled water to create a 5 mg/mL stock solution. Then, dilute 10 mL of the stock solution with 100 mL of distilled water to obtain a 500 µg/mL working standard of ascorbic acid. Various concentrations of working standard of ascorbic acid and the ethanolic extract of *Vetiveria zizanioides* (50-500µg/ml) were prepared. Then mixed 100 µl of plant extract and ascorbic acid of each concentration with 300 µl of the DPPH solution followed by incubation of the mixture at room temperature for 30 minutes. The absorbance of the mixture was measured at 517 nm using a spectrophotometer. The Inhibition Percentage was calculated using the following formula (22):

Inhibition% = ((Ablank - Asample) / Ablank) × 100
where:
A blank is the absorbance of the blank (DPPH solution without plant extract).
A sample is the absorbance of the sample (DPPH solution with plant extract).

Anti-inflammatory activity by Protein Denaturation Assay

The albumin denaturation assay followed the method outlined by Williams et al. with minor adjustments. (23) During the preparation of the reaction mixture, various concentrations of *Vetiveria zizanioides* ethanolic extract (ranging from 50 to 500 µg/ml) were used. 0.05 ml of the plant extract was combined with 0.45 ml of 5% bovine serum albumin and incubated at 37°C for 20 minutes. Subsequently, the reaction mixture was heated to 57°C for 3 minutes, followed by the addition of 2.5 ml of 0.5 M phosphate buffer (pH = 6.3) to each sample. Copper-alkaline reagent and 1% (v/v) Folin-Ciocalteu's reagent were then introduced and incubated for 10 minutes. The

absorbance was measured at 650 nm. The results were compared to those obtained using diclofenac sodium (at a concentration of 200 µg/ml) as a reference drug.

% Inhibition of denaturation = (1-D/C) X100. Where D is the absorbance of test sample and C is the absorbance of negative control (without the test sample or reference drug).

Determination of Biofilm Formation by test tube method and crystal violet assay

Sterile test tubes were prepared, with 100 µl of Mueller Hinton agar for bacterial testing and Sabouraud dextrose agar (SDA) for fungal testing. Fresh bacterial and fungal suspensions (at a concentration of 1.0 McFarland) were added (100 µl each) to the tubes and incubated for 48 hours at 37°C. To assess biofilm formation, the tube contents were washed with 200 µl of normal saline, followed by the addition of 200 µl of 0.1% crystal violet stain and another 20 minute incubation. Subsequently, each tube was thoroughly washed with deionized water, and 96% ethanol (200 µl) was added. The optical density (OD) of the adherent microorganisms was measured using a spectrometer at 630 nm. Biofilm formation was quantified using the following formula (21).

OD ≤ ODc= No biofilm producer
ODc< OD ≤ 2 × ODc= Weak biofilm producer
2 × ODc< OD ≤ 4 × ODc= Moderate biofilm producer
4 × ODc< OD= Strong biofilm producer.
ODc: Optical density of growth control

Determination of Anti Biofilm Activity using modified crystal violet assay

Sterile test tubes were prepared, with 100 µl of Mueller Hinton agar for bacterial testing and Sabouraud dextrose agar (SDA) for fungal testing. To each test tube, 100 µl of *Vetiveria zizanioides* ethanolic extract was added. Fresh bacterial and fungal suspensions (at a concentration of 1.0 McFarland) were introduced (100 µl each) and incubated for 48

hours at 37°C. To assess biofilm inhibition, the tube contents were washed with 200 µl of normal saline, followed by the addition of 200 µl of 0.1% crystal violet stain and another 20-minute incubation. Subsequently, each tube was thoroughly washed with deionized water, and 96% ethanol (200 µl) was added. The optical density (OD) of the adherent microorganisms was measured using a spectrometer at 630 nm. Biofilm inhibition was calculated using the following formula (21).

OD of bacteria= [(OD growth control – OD sample) / OD growth control] × 100.

Results and Discussion

For the phytochemical study of *Vetiveria zizanioides* roots, ethanol was used as an extraction solvent The phytochemicals present in the ethanolic extract were characterized and identified by GC-MS analysis. A total of 17 compounds were identified. The major identified compounds are presented in (Table 1 & Figure 1). The identified

Table 1:GC-MS analytical report of ethanolic extract of *Vetiveriazizanioides*						
Retention time	Area	Area %	Name of the compound	Chemical formula	Molecular weight (g/mol)	Chemical nature
30.848	159902	1.72	Gamma.-Gurjunenepoxide-(2)	$C_{15}H_{24}O$	220.3505	Sesquiterpene Epoxide.
31.587	345155	3.72	Cedren-13-Ol,8-	$C_{15}H_{24}O$	220.3505	Sesquiterpene Alcohol
32.913	281695	3.03	Trans-ValerenylAcetate	$C_{15}H_{24}O_2$	236.35	Sesquiterpene Ester
33.3	199040	2.14	Pentacyclo(3.3.0.02,4.03,7.06,8)Octane	C_8H_8	104.15	Hydrocarbon
33.579	989073	10.66	FormicAcid	HCOOH	46.03	CarboxylicAcid
35.724	134330	1.45	Acetamide,2-(Diethylamino)-N-(2,	C_2H_5NO	59.07	Amides
37.428	135866	1.46	DibutylPhthalate	$C_{16}H_{22}O_4$	278.35	Phthalate
38.411	153308	1.65	HexadecanoicAcid,EthylEster	$C_{18}H_{36}O_2$	284.4772	Fatty Acid Ester
41.408	1185808	12.78	Z,Z-8,10-Hexadecadien-1-Ol	$C_{16}H_{30}O$	238.41	Fatty Alcohol
41.484	555876	5.99	OctadecanoicAcid	$C_{18}H_{36}O_2$	284.48	Saturated Fatty Acid
41.6	217456	2.34	2-AminoethanethiolHydrogenS	$C_2H_7NS_2$	77.15	Thiol
41.91	136229	1.47	EthylOleate	$C_{20}H_{38}O_2$	310.51	Fatty Acid Ester
48.124	169715	1.83	Bis(2-Ethylhexyl)Phthalate	$C_{24}H_{38}O_4$	390.56	Phthalate
48.865	3922276	42.26	17-Hydroxy-3,20-Dioxopregna-1,4,Ol	$C_{21}H_{32}O_5$	372.47	Sterol.
51.25	184809	1.99	(2E)-6Acetoxy-2-Methylhexenal	$C_9H_{14}O_3$	170.09	Sesquiterpene Epoxide
53.1	327350	3.53	Campesterol	$C_{29}H_{50}O$	426.72	Sterol
54.162	184094	1.98	Stigmasterol	$C_{29}H_{48}O$	412.69	Sterol

Current Trends in Biotechnology and Pharmacy
Vol. 18 (Supplementry Issue 4A) 88 - 105, November 2024, ISSN 0973-8916 (Print), 2230-7303 (Online)
10.5530/ctbp.2024.4s.8

94

compounds represent a mix of steroids, fatty alcohols, carboxylic acids, sterols, and terpenes.The major ones being 17-hydroxy-3,20-dioxopregna-1,4,ol, (42.26), Z,z-8,10-hexadecadien-1-ol,(12.78), Formic acid(10.66), Octadecanoic Acid (5.99), Cedren-13-ol (3.72) and Campesterol, (3.53). These compounds could disrupt microbial membranes, inhibit essential enzymatic processes, or interfere with cell signalling pathways. Cedren-13-ol disrupts bacterial

cell membranes, increasing membrane permeability. This interference affects vital cellular processes, making bacterial cells more vulnerable to damage and death. Formic acid triggers a rapid intracellular burst of reactive oxygen species (ROS), resulting in oxidative damage and cell death. This process affects both metabolic activity and membrane integrity (24). Moreover in *Candida* species formic acid triggers programmed cell death by activating caspase, resulting in apoptosis-like cell demise(25).Octadecanoic acid due to its amphiphilic nature disrupts bacterial cell membranes and also interferes with fatty acid metabolism, energy metabolism pathways,

including the citrate cycle(26). Similar to our findings a study conducted by Kannappan and colleagues discovered that *Vetiveria zizanioides* root extract contains sesquiterpenes as a prominent constituent (27). Yet in another study Krishnaveni revealed the presence of Saponins, Flavanoids and Phenols in *Vetiveria zizanioides* root extract (19).

Antimicrobial activity of *Vetiveria zizanioides* ethanolic root extract

The Vetiver ethanolic extract exhibited a significant antimicrobial activity as shown in Figures 1 & 2. The observed variations in the zone of inhibition highlight the differential sensitivity of the tested microorganisms to the Vetiver ethanolic extract. *Staphylococcus aureus* exhibited the highest sensitivity, followed by *Candida albicans, Escherichia coli, Klebsiella pneumoniae,* and *Pseudomonas aeruginosa. Staphylococcus aureus* displayed the largest zone of inhibition at 23 mm, suggesting a robust and effective inhibition of growth by the Vetiver extract against this Gram-positive
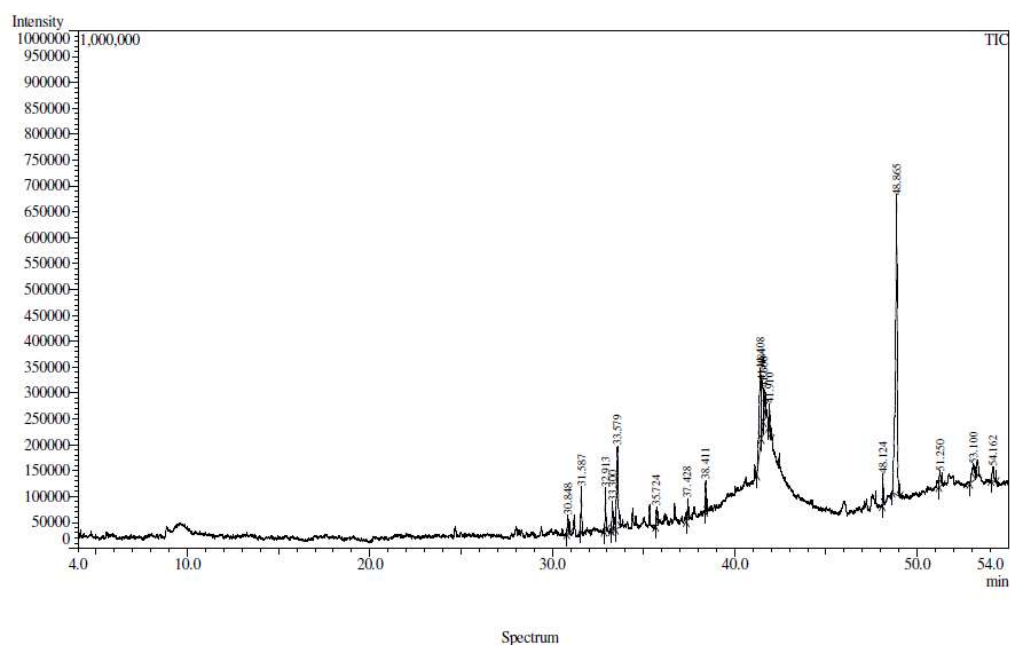

Figure1: Chromatogram of ethanolic extract of *Vetiveriazizanioides*

Antibiofilm Activity of *Vetiveria zizanioides*

Current Trends in Biotechnology and Pharmacy
Vol. 18 (Supplementry Issue 4A) 88 - 105, November 2024, ISSN 0973-8916 (Print), 2230-7303 (Online)
10.5530/ctbp.2024.4s.8

95

bacterium. The Vetiver ethanolic extract exhibited antimicrobial effect against *E. Coli and Klebisilla pneumoniae*, resulting in a zone of inhibition measuring 16 mm. The Vetiver ethanolic extract exhibited a moderate antimicrobial effect against *Pseudomonas aeruginosa*, resulting in a zone of inhibition measuring 11mm. Against the fungal pathogen *Candida albicans*, the Vetiver extract demonstrated a significant zone of inhibition measuring 19 mm, suggesting notable antifungal activity. The findings of this study corroborate the observational evidence thatGram-positive bacteria exhibit greater susceptibility to plant Extracts compared to Gram-negative bacteria. These disparities can be attributed to the structural differences in cell walls Gram-positive bacteria possess a single-layered cell wall, while Gram-negative bacteria have a multilayered structure. Consequently, the passage of active compounds through the Gram-negative cell wall may be hindered (28). Gram-Negative Bacteria possess an effective permeability barrier in the form of a thin lipopolysaccharide exterior membrane, which restricts the penetration of plant extracts. While Gram-

positive bacteria possess a mesh-like peptidoglycan layer, this structure renders it more susceptible to permeation by the extracts (29). The outer membrane of Gram-negative bacteria has narrow porin channels within this membrane which limits the penetration of hydrophobic molecules. Moreover, the limited fluidity of the lipopolysaccharide leaflet impedes the inward diffusion of lipophilic products. Additionally, Gram-negative bacteria exhibit high intrinsic resistance due to the presence of efflux systems in their outer membrane, which limits antimicrobial diffusion into the cells (30).

Our results are in accordance with Krishnaveni who exhibited that the *Vetiveria zizanioides* extract, at a concentration of 50%, exhibits strong antibacterial activity against the positive pathogenic microorganism *Staphylococcus aureus*, surpassing its effect on the negative pathogenic microorganism *Escherichia coli* (19). But in another study by Subhadra Devi et al, contrary to our findings, exhibited that ethanolic extract of *Vetiveria zizanioides* inhibited gram negative bacteria than gram positive bacteria (20). Yet in another study by Muthukrishnan et al the antimicrobial activity
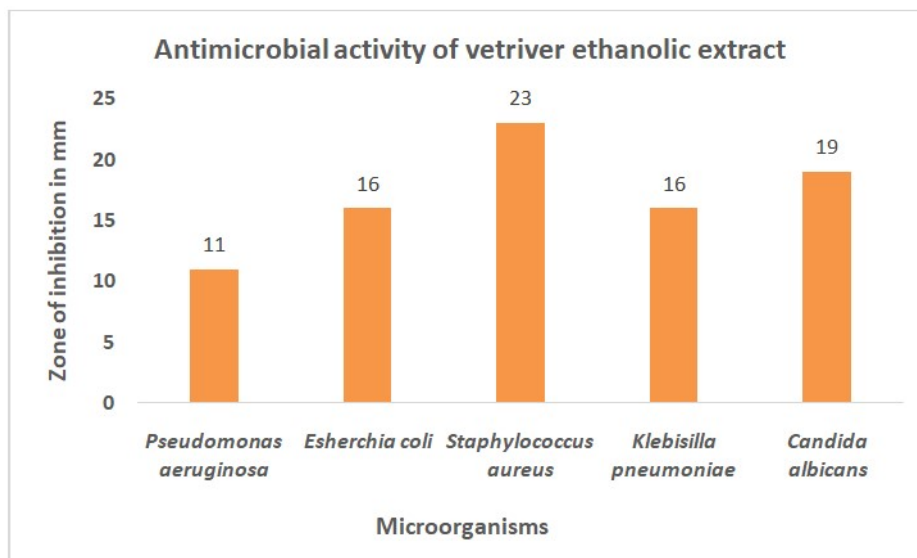

Figure 2: Antimicrobial activity of *Vetiveriazizanioides*root extract

Premjanu et al

of *Vetiveria zizanioides* chloroform extract showed the maximum zone of inhibition for *E. coli, S. aureus*, and *P. aeruginosa* was found to be 20 mm, 24 mm and 25 mm respectively. Whereasf or *Klebsiella pneumoniae*, *Salmonella typhi*, *Staphylococcus faecalis,* and *Enterococcus faecalis*, the zone of inhibition measured 21 mm. *Candida albicans* exhibited a 28 mm zone of inhibition, while against *Cryptococcus neoformans*, it was 22 mm (31). These results were similar to our research outcomes.

Minimum Inhibitory Concentration (MIC) of *Vetiveria zizanioides* ethanolic extract

The Minimum Inhibitory Concentration (MIC) of *Vetiveria zizanioides* ethanolic extract is depicted in Table 2. The results indicate variations in the sensitivity of different microorganisms to the *Vetiver* ethanolic extract. *Escherichia coli* and *Staphylococcus aureus* are common Gram-negative and Gram-positive bacteria, respectively, associated with various infections. A MIC of 12.5 mg/mL for both indicates that the extract is more potent against these bacteria suggesting higher susceptibility compared to the other tested pathogens. It suggests a higher efficacy, as lower concentrations (12.5 mg/mL) are sufficient to inhibit their growth. *Pseudomonas aeruginosa* is a notoriously resilient Gram-negative bacterium often associated with nosocomial infections and antibiotic resistance. *Klebsiella pneumoniae* is another Gram-negative bacterium frequently implicated in hospital-acquired infections. *Klebsiella pneumoniae* and *Pseudomonas aeruginosa* showed a MIC of 50mg/ml, indicating a moderate inhibitory

effect. The extract has the ability to inhibit both gram positive bacteria and gram-negative bacteria. For *Candida albicans*, the MIC is 25 mg/mL. This suggests that this fungus is moderately sensitive to the extract, requiring a slightly higherconcentration (25 mg/mL) compared to *E. coli* and *S. aureus*, but lower than *P. aeruginosa and K. pneumoniae*.The extract's ability to inhibit both bacteria *(P. aeruginosa, E. coli, S. aureus, K. pneumoniae)* and a fungus (*C. albicans*) suggests a broad-spectrum antimicrobial potential, making it versatile for different types of infections.

Mahajan et al. reported MIC values against *Staphylococcus aureus* and *Pseudomonas aeruginosa* ranging from 6.25 to 25 mg/ml. In our study, the MIC was 12.5 mg/ml and 50 mg/ml, respectively, against all biofilm-producing microorganisms (32). Meanwhile, Priya et al. found a minimum inhibitory concentration of 12.5 mg/ml for *Staphylococcus aureus*, whereas for *Acinetobacter baumannii* and *Pseudomonas aeruginosa*, the MIC was 25 mg/ml (21), which is similar to our findings. In our study *Staphylococcus aureus* exhibited the same MICbut for *Pseudomonas aeruginosa*, the MIC was 50mg/ml which is slightly higher compared to their result. Similarily, yet in another study by Alireza et al., the reported minimum inhibitory concentration (MIC) was 25mg/mL for *Staphylococcus aureus* and 50mg/mL for *Pseudomonas aeruginosa* (33), findings that align with our own research outcomes. In our study *Pseudomonas aeruginosa*, the MIC was 50 mg/ml which is same but for *Staphylococcus aureus* it is slightly lower compared to their result. It suggests a higher

Table2: Minimum Inhibitory Concentration (MIC) of *Vetiveriazizanioides*ethanolic extract	
Microorganism	Minimum Inhibitory Concentration (MIC)
Pseudomonasaeruginosa	50mg/mL
Escherichia coli	12.5mg/mL
Staphylococcus aureus	12.5mg/mL
Klebsiellapneumoniae	50mg/mL
Candida albicans	25 mg/mL

Antibiofilm Activity of *Vetiveria zizanioides*

97

efficacy, as lower concentrations (12.5 mg/mL) are sufficient to inhibit their growth.

Antioxidant activity using DPPH radical scavenging activity

The results demonstrate a concentration-dependent increase in DPPH inhibition percentage with escalating concentrations of Vetiver ethanolic extract as shown in Table 3. This suggests a positive correlation between the extract's concentration and its antioxidant activity. At the lowest concentration of 50 µg, the DPPH inhibition percentage was 56.25%, indicating a substantial ability to scavenge free radicals. As the concentration increased, reaching 80.25 % at 500 µg, the radical scavenging potential increased significantly.The antioxidant activity of standard Ascorbic acid also demonstrates a concentration-dependent increase in DPPH inhibition percentage. However, the antioxidant activity of the extract is lower than standard Ascorbic acid. The antioxidant activity of the extract may be due to the presence of phytochemicals such as 17-hydroxy-3,20-dioxopregna-1,4,ol, Z,z-8,10-hexadecadien-1-ol,Formicacid, Octadecanoic Acid,Cedren-13-ol and, Campesterol. It is thought to do this by scavenging free radicals and by protecting cells from oxidative damage. The antioxidant potency of Vetiver oil is attributed to cedr-8-en-13-ol, its most abundant compound. This compound restores cellular levels of SOD (superoxide dismutase), GPX (glutathione peroxidase), and CAT (catalase) activities (34). Campesterol functions as an antioxidant by elevating phenolic and flavonoid levels, neutralizing free radicals through electron-proton transfer processes, enhancing DPPH scavenging, chelating metals, and activating enzymes like catalase, superoxide dismutase, and glutathione peroxidase. Additionally, it inhibits oxidases (35). Researcher Muthukrishnan & Manogaran has demonstrated that *Vetiveria zizanioides* is a source of various phytochemicals with antioxidant capabilities, including alkaloids, flavonoids, tannins, saponins, and phenols. The presence of these compounds enhances the plant's ability to neutralize free radicals, thereby under scoring its significant antioxidant properties (31). The findings of Subhadra devi study align with the observational evidence, similar to our own results. They have shown that the ethanolic extract of *Vetiveria zizanioides* roots exhibits potent antioxidant activity across various in vitro assays, including reducing power, superoxide anion radical scavenging, deoxyribose degradation, total antioxidant capacity, total phenolics, and total flavonoid composition. Moreover, the extract effectively scavenges free radicals such as O_2, H_2O_2, OH, and NO in a dose-dependent manner (36). Similarly, in a study Luqman et al compared two *Vetiveria zizanioides* genotypes, KS1 exhibited superior antioxidant properties, including higher ferric reducing antioxidant power (FRAP), DPPH inhibition, total phenolic content (TPC), and reducing power (RP) potential compared to the gulabi genotype. As the extract

Table3: Antioxidant activity using DPPH radical scavenging activity		
Concentrationinmicrogram	DPPHinhibitionpercentageofAscorbicacid	DPPHinhibitionpercentageofVetriver extract
50	60.25±0.23	56.25±0.34
100	68.16±0.43	64±0.23
200	72.16±0.13	69.16±0.43
300	76.85±0.33	72.85±0.25
400	80.63±0.25	75.625±0.13
500	85.97±0.25	80.25±0.25
IC_{50}	117.80	125.07

concentration increased, antioxidant activity also increased (37), which were similar to our findings. Antioxidants play a crucial role in mitigating oxidative stress, which is implicated in various diseases. The observed antioxidant potential of Vetiver ethanolic extract suggests its possible role in promoting health by counteracting oxidative damage.

Anti-inflammatory activity by Protein Denaturation Assay

The denaturation of proteins is one of the causes of inflammation. The Vetiver ethanolic extract exhibited a significant anti-inflammatory activity as shown in Figure 3.

The results demonstrate a clear dose-response relationship between the concentration of Vetiver ethanolic extract and the inhibition percentage. As the concentration increased, there was a corresponding increase in inhibitory activity. At the lowest concentration of 50 μg, the inhibition was 39.14%, indicating a moderate inhibitory effect. However, as the concentration increased to 500 μg, the inhibition reached 82.61%,demonstrating a substantial enhancement in inhibitory activity. The concentration of 500 μg resulted in an inhibition percentage of 82.61%, approaching the positive control's inhibition of 86.96%. These results were comparable to those of diclofenac sodium (200 μg/ml) as mentioned in Figure 3. This suggests that the extract's inhibitory potential may reach a plateau beyond a certain concentration. Campesterol, regulates interleukins and immune responses, by effectively modulating both pro-inflammatory and anti-inflammatory cytokines (38) The phytochemical present in the extract stimulates the antioxidant enzyme system, reduces the oxidative stress and maintains a balance between oxidants and antioxidants, which is crucial in combating inflammation (18). A study conducted by Su-Tze Chou et al on the essential oil of *Vetiveria zizanioides* (VZ-EO) exhibited anti-inflammatory properties by modulating the expression of inflammation-related enzymes (HO-1, iNOS, and COX-2) and cytokines (TNF-α, IL-1β, and IFN-β) in LPS-stimulated RAW 264.7 macrophages. Additionally, VZ-EO's antioxidant activity contributes to its anti-inflammatory effects, as it reduces LPS-induced superoxide anion production and
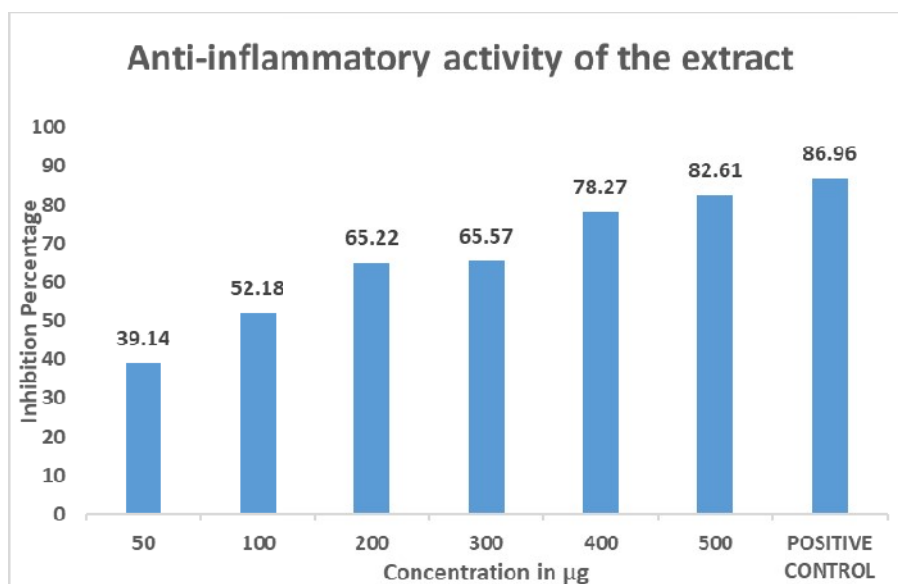

Figure3: Anti-inflammatory activity of *Vetiveriazizanioides*ethanolic extract

Antibiofilm Activity of *Vetiveria zizanioides*

malondialdehyde(MDA)levels (39).In another study by Mohammad et al the ethanol extracts of *H. procumbens* and *U. dioica*, both individually and in combination, were assessed for their anti-denaturation effects using an albumin denaturation assay. The results demonstrated concentration-dependent inhibition of protein (albumin) denaturation by these extracts (40), which were similar to our findings. In a study the essential oil of *Vetiveria zizanioides* was evaluated using standard inflammation models, including acetic acid-induced writhing, carrageenan-induced paw edema, and the formalin test. The oil demonstrated effects similar to aspirin, reducing abdominal writhing, formalin-induced pain, and carrageenan-induced inflammation. This suggests its analgesic and anti-inflammatory potential. The proposed mechanism, based on the study's results, involves the inhibition of leukocyte migration to the inflammation site, preventing the progression and chronicity of inflammation, indicating its broader anti-inflammatory applications(41). While the ethanolic vetiver extract may exhibit anti-inflammatory properties, it is essential to recognize and address its limitations, which includes potency, mechanism of action, safety profile, bioavailability, and clinical evidence. These considerations are crucial for assessing its suitability and potential in therapeutic applications for inflammation.

Biofilm Formation

Adhesion to a biotic or abiotic surface is considered to be the initial step in the formation of biofilm by microorganisms. The results indicate varying levels of biofilm formation among the tested microorganisms as shown in Figure 4.

Staphylococcus aureus exhibited the highest biofilm formation rate, suggesting a higher risk of persistent infections associated with this pathogen. The high biofilm formation by *Staphylococcus aureus* and *Pseudomonas aeruginosa* underscores the clinical challenges posed by these pathogens in terms of treatment resistance and recurrence. *Klebsiella pneumoniae* and *Candida albicans* exhibited a moderate biofilm formation rate indicating an intermediate ability to form biofilms compared to other microorganisms. *Escherichia coli* demonstrated a lower ability to form biofilm, aligning with its usual presentation as an acute, rather than chronic, infection.
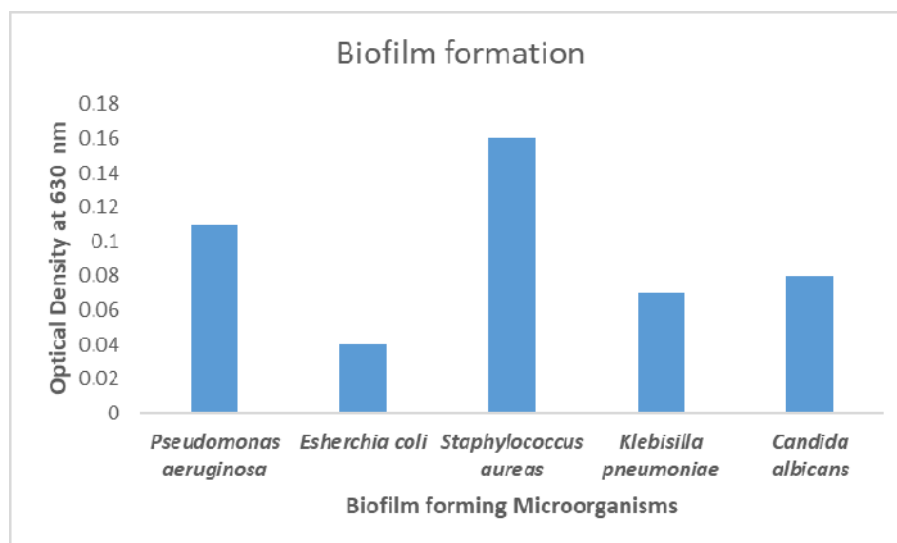

Figure4: Biofilm formation by test microorganisms

Premjanu et al

Nair and his colleagues selected 3 species frequently associated with denture stomatitis, namely *Candida albicans, Staphylococcus aureus* and *Streptococcus mutans* for their biofilm forming capability for the experiment. The study demonstrated that both fungal and bacterial species can coexist and form biofilms in the same environment (42)**.** The result coincides with our outcome. Similar to our findings, in a separate investigation, *Candida albicans*, in conjunction with *Pseudomonas aeruginosa*, *Escherichia coli*, *Staphylococcus aureus*, and *Klebsiella pneumoniae*, demonstrated the ability to form biofilms. *C. albicans* engages in physical attachment, extracellular signaling, and metabolic cross-feeding interactions with co-existing oral bacteria. These multidimentional interactions contribute to the complex biofilm architecture (43).

The equilibrium between the host and the microbiome relies on multiple factors, including the lifestyle, host's genotype, physiology and immune system efficiency (44). Additionally, the preferences of the inhabited niche, such as variations in pH,

temperature, and nutrient availability, play a significant role. These factors collectively influence the biofilm formation capabilities of these microorganisms and composition of the microflora (45).

Anti-Biofilm activity of *Vetiveria zizanioides* ethanolic root extract

The study shows that the *Vetiveria zizanioides* ethanolic root extract is capable of inhibiting the biofilm formation as depicted in Figure 5. The varying degrees of biofilm inhibition highlight the microorganism-specific response to the Vetiver ethanolic extract. The highest inhibition observed against *Staphylococcus aureus* and *Escherichia coli* suggests a potent impact on both Gram-positive and Gram-negative bacteria. The substantial biofilm inhibition against *Staphylococcus aureus* is particularly relevant due to the role of this pathogen in chronic infections. The extract's ability to inhibit biofilm formation may contribute to mitigating the challenges posed by persistent infections *Candida albicans*, a fungal pathogen causing oral and genital infections,
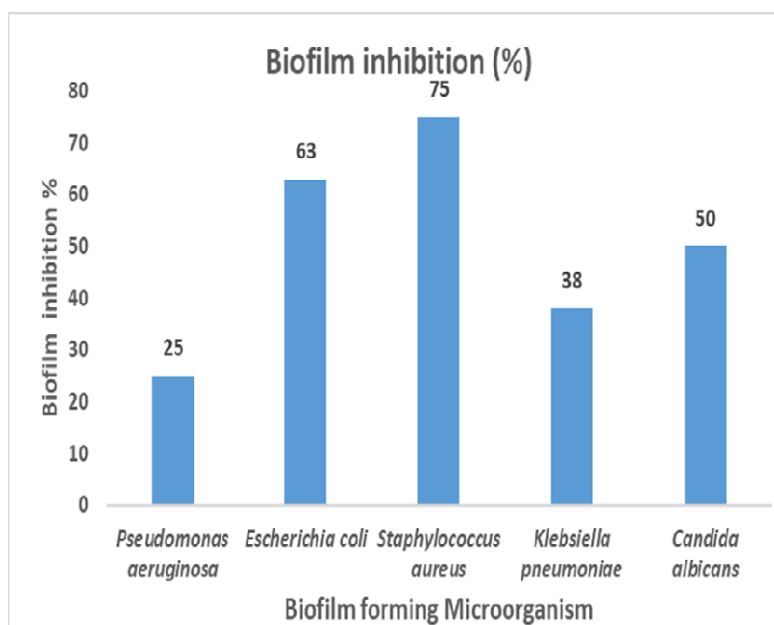

Figure5: Anti-Biofilm activity of *Vetiveriazizanioides*ethanolic root extract

Antibiofilm Activity of *Vetiveria zizanioides*

displayed a moderate biofilm inhibition of 50%. The observed biofilm inhibition activity against *Candida albicans* suggests the extract's antifungal potential. This is significant, considering the increasing prevalence of fungal infections and the role of biofilms in their pathogenesis.

Many crude plant extracts were capable of inhibiting biofilm formation by *Staphylococcal sp.* such as *Quercus cerris, Alnus japonica, Rubus ulmifolius, Coriandrum sativum, Mentha piperita and Pimpinella anisum* (46-49). In another study, by Muhammad Shahid et. al. the methanolic extract of *Elettaria Cardamomum* and *Cichorium Intybus* exhibited the highest inhibition of biofilm formation against *Staphylococcus aureus* (55.92%), while the lowest inhibition was observed with the aqueous extract of *Cichorium Intybus* (AqEC) against *Escherichia coli* (20%) (50), which were similar to our findings. Elmasri et al demonstrated that sesquiterpenes found in the plant *Teucrium polium* play a crucial role in inhibiting biofilm formation in *Staphylococcus aureus*. These sesquiterpenes achieve this effect by modulating the membrane fatty acid composition (51). Similarly, *V. zizanioides* root extract (VREX) prevents the biofilm formation of MRSA and its clinical strains by down regulating of the genes responsible for adhesion (27).

In our study the phytochemicals present in *Vetiveria zizanioides* roots extract represent a mix of steroids, fatty alcohols, carboxylic acids, sterols, and sesquiterpenes. To inhibit biofilm growth, various compounds utilize six primary mechanisms: substrate deprivation, membrane rupture, binding to adhesion complexes and cell walls, protein binding, interaction with eukaryotic DNA, and inhibition of viral fusion (52). Active secondary metabolites found in both aqueous and alcoholic extracts specifically target one or more stages of biofilm formation, thereby reducing bacterial virulence associated with biofilm production. The distinct modes of action of each compound contribute to the extract's antibacterial and antibiofilm properties.

Phenolic compounds can damage cell structure and membranes, inhibiting bacterial protein synthesis. Flavonoids, with antibacterial properties disrupt cell wall formation by suppressing cytoplasm function, interrupt nutrient exchange, thereby inhibiting bacterial energy supply, inhibit enzymes that produce quorum-sensing signals, disrupting cell communication during biofilm formation. Steroids cause lysosome leakage and membrane phospholipid disruption, reducing cell membrane integrity and leading to cell lysis (53). Sesquiterpenes, natural compounds, exhibit versatile mechanisms in inhibiting biofilm formation by interfering with initial adhesion thereby disrupting bacterial attachment to surfaces. Secondly, they modulate the gene expression by, downregulating adhesion-related genes (*sdrD*, *spa*, *agr*, *hld*) and upregulating capsular polysaccharide genes (*cap5B*, *cap5C*). Thirdly they disrupt cell membrane, modulate metabolic process and interfere with cell signalling (54). Protein denaturation through the use of proteinase K resulted in decreased biofilm thickness and modified composition. This approach holds potential as an adjunctive strategy for biofilm management by specifically targeting biofilm proteins (55). VREX demonstrates a comprehensive range of antibiofilm effects: it inhibits biofilm formationinmethicillin-resistant *Staphylococcus aureus* (MRSA) and its clinical counterparts, preserves cellular viability, exerts microscopic impact on biofilm structure, suppresses the synthesis of key biofilm components (α-hemolysin toxin, exopolysaccharide, and slime), regulates adhesin genes (clfA,fnbA,and fnbB,) responsible for initial attachment, and contains sesquiterpenes as major constituents(27). Thereby, the antibiofilm activity of *Vetiveria zizanioides* may be attributed to the presence of these phytochemicals in the ethanolic extract.

The reported scientific data supports the antibacterial and antifungal effects of *Vetiveria zizanioides*, suggesting it could prevent biofilm development by pathogenic entities. Biofilms resist typical antimicrobials,

posing a significant healthcare challenge. Vetiver extract's properties may inhibit bacteria and fungi in biofilms, reducing their formation and negative impact on host tissues. Furthermore, the antioxidant and anti-inflammatory properties of vetiver extract can contribute to mitigating the inflammatory response associated with biofilm infections, promoting tissue healing, and reducing the risk of complications. Consequently, by targeting biofilm-forming microorganisms and modulating the host immune response, vetiver extract shows promise as a natural remedy with potential antibiofilm activity, offering a multifaceted approach to combating biofilm-related infections. The current research suggests that it could serve as mouth rinses, irrigation solutions, and intracanal medicaments. These applications are vital for the dental industry, particularly in developing effective plaque-control strategies (56).

Vetiveria zizanioides, while showing potential as an antibiofilm agent, faces several challenges. These include a lack of extensive clinical evidence, a narrower activity spectrum, difficulties in standardization and quality control, the potential for resistance development, absence of regulatory approval, and undefined dosing guidelines. Addressing these issues through further research and clinical trials is crucial for its potential use against biofilm-associated infections.

Conclusion

In this study ethanolic extract of *Vetiveria zizanioides* was studied for its phytochemical constituents by using GC MS analysis. 17 compounds were identified from *Vetiveria zizanioides* roots extract. They represent a mix of steroids, fatty alcohols, carboxylic acids, sterols, and sesquiterpenes. This diversity in chemical nature contributes to the extract's multifaceted biological activities, including antioxidant, antimicrobial, anti-inflammatory, and antibiofilm properties. Each compound class may contribute to specific biological effects, and the synergistic interactions among these compounds enhance the overall efficacy of the *Vetiver*

root extract. These compounds have been shown to interfere with the formation and structure of dental biofilms, and to inhibit the growth and metabolism of dental pathogens. The concentration-dependentresponses observed in antioxidant and inhibitory assays suggest the potential utility of *Vetiver* root extract in various applications, including pharmaceuticals, nutraceuticals, and functional foods. Hence it may be used in treating various biofilm-related infection. Despite the promise of *Vetiveria zizanioides* as an antibiofilm agent, it confronts obstacles such as insufficient clinical validation, limited antibacterial and antifungal range, standardizationchallenges, possible resistance emergence, lack of official sanction, and indeterminate dosage protocols. Future research is essential to ascertain its efficacy and safety for human use, which should encompass the isolation and refinement of active antibiofilm constituents, along with assessments of their ADMET profiles and long-term human impacts.

References
1. Kilian, M., Chapple, I. L. C., Hanning, M., Marsh, P. D., Meuric, V., Pedersen, A. M. L., et al. (2016). The oral microbiome: An update for oral healthcare professionals. British Dental Journal, 221(10), 657–665.
2. Arzmi, M. H., Dashper, S., & McCullough, M. (2019). Polymicrobial interactions of *Candida albicans* and its role in oral carcinogenesis. Journal of Oral Pathology & Medicine, 48(7), 546-551.
3. Krzyściak, W., Jurczak, A., &Piątkowski, J. (2016). The role of human oral microbiome in dental biofilm formation. In Microbial Biofilms - Importance and Applications (pp. 229-382).
4. Su, Y., Yrastorza, J. T., Matis, M., Cusick, J., Zhao, S., Wang, G., & Xie, J. (2022). Biofilms: Formation, research models, potential targets, and methods for prevention and treatment. Advances in Science, 9(29), e22032912.
5. Deo, P. N., & Deshmukh, R. (2019). Oral microbiome: Unveiling the

fundamentals. Journal of Oral and Maxillofacial Pathology, 23, 122–128.

6. Chen, M., Yu, Q., & Sun, H. (2013). Novel strategies for the prevention and treatment of biofilm-related infections. International Journal of Molecular Sciences, 14(9), 18488–18501.

7. Milho, C., Silva, J., Guimarães, R., Ferreira, I. C. F. R., Barros, L., & Alves, M. J. (2021). Antimicrobials from medicinal plants: An emergent strategy to control oral biofilms. Applied Sciences, 11, 40205.

8. Gupta, P., Sarkar, S., Das, B., Bhattacharjee, S., &Tribedi, P. (2016). Biofilm, pathogenesis, and prevention – A journey to break the wall: A review. Archives of Microbiology, 198(1), 1–156.

9. Soria, S., Angulo-Bejarano, P. I., & Sharma, A. (2020). Biofilms: Development and molecular interaction of microbiome in the human oral cavity. Current Research and Future Trends in Microbial Biofilms, 61–75.

10. Jamal, M., et al. (2018). Bacterial biofilm and associated infections. Journal of the Chinese Medical Association, 81, 7–118.

11. Brown, M. R. W., & Barker, J. (1999). Unexplored reservoirs of pathogenic bacteria: Protozoa and biofilms. Trends in Microbiology, 7(1), 46-50.

12. Burmølle, M., Thomsen, T. R., Fazli, M., Dige, I., Christensen, L., Homøe, P., et al. (2010). Biofilms in chronic infections - a matter of opportunity - monospecies biofilms in multispecies infections. FEMS Immunology and Medical Microbiology, 59(3), 324-336.

13. Stewart, P. S., & Bjarnsholt, T. (2020). Risk factors for chronic biofilm-related infection associated with implanted medical devices. Clinical Microbiology and Infection, 26(8), 1034-1038.

14. Fulgêncio, D. L. A., da Costa, R. A., Guilhelmelli, F., Silva, C. M. S., Ortega, D. B., de Araujo, T., et al. (2021). In vitro antifungal activity of pelgipeptins against human pathogenic fungi and *Candida albicans* biofilms. AIMS Microbiology, 7(1), 28-39.

15. Percival, S. L., Suleman, L., Vuotto, C., & Donelli, G. (2015). Healthcare-associated infections, medical devices, and biofilms: Risk, tolerance, and control. Journal of Medical Microbiology, 64, 323–334.

16. Dos Santos, D. S., et al. (2014). Seasonal phytochemical study and antimicrobial potential of *Vetiveria zizanioides* roots. Acta Pharmaceutica, 64, 495–501.

17. Huang, J., Li, H., Yang, J., Chen, Y., Liu, Y., Li, N., et al. (2004). Chemical components of *Vetiveria zizanioides* volatiles. Ying Yong Sheng Tai Xue Bao, 15(1), 170-172.

18. Grover, M., Behl, T., Bungau, S., & Aleya, L. (2021). Potential therapeutic effect of *Chrysopogon zizanioides* (Vetiver) as an anti-inflammatory agent. Environmental Science and Pollution Research, 28(28), 155.

19. Krishnaveni, V. (2016). Analysis of chemical components and antimicrobial activity on vetiver extract for home textile applications. Journal of Textile Science and Engineering, 6, 259.

20. Subhadra Devi V, K Asok Kumar, M. Uma Maheswari, A T Siva Shanmugam, & R Sankar Anand Devi et al. (2010). In vitro antibacterial activity of ethanolic extract of *Vetiveria zizanioides* root. International Journal of Pharmaceutical Sciences and Research, 1(9), 120-124.

21. Priya Mehrishi, Priti Agarwal, Shobha Broor, & Amisha Sharma (2020). Antibacterial and antibiofilm properties of medicinal plant extracts against multi-drug resistant Staphylococcus species and non-fermenter bacteria. Journal of Pure and Applied Microbiology, 14(1), 403-413.

22. Noor, N., Sarfraz, R. A., Ali, S., & Shahid, M. (2014). Antitumor and antioxidant potential of some selected Pakistani honeys. Food Chemistry, 143, 362–366.

23. Williams, L. A., O'Connor, A., Latore, L., Dennis, O., Ringer, S., Whittaker, J. A., et al. (2008). The in vitro anti-denaturation effects induced by natural products and non-steroidal compounds in heat-treated (immunogenic) bovine serum albumin is proposed as a screening assay for the detection of anti-inflammatory compounds,

without the use of animals, in the early stages of the drug discovery process. West Indian Medical Journal, 57, 327–3.

24. Du, L. (2012). Toxicity Mechanism of Formic Acid is Directly Linked to ROS Burst and Oxidative Damage in Yeast Saccharomyces cerevisiae. In Advanced Materials Research (Vols. 550–553, pp. 1060–1065).

25. Lastauskienė, E., Zinkevičienė, A., Girkontaitė, I., et al. Formic Acid and Acetic Acid Induce a Programmed Cell Death in Pathogenic *Candida* Species. Curr Microbiol 69, 303–310.

26. Masayuki Taniguchi, Akihito Ochiai, Kiyoshi Takahashi, Shunichi Nakamichi, Takafumi Nomoto, Eiichi Saitoh, et al. (2015). Antimicrobial activity and mechanism of action of a novel cationic α-helical octadecapeptide derived from α-amylase of rice. Biopolymers, 104(2), 73-83.

27. Kannappan, A., Gowrishankar, S., Srinivasan, R., Pandian, S. K., & Ravi, A. V. (2017). Antibiofilm activity of *Vetiveria zizanioides* root extract against methicillin-resistant *Staphylococcus aureus*. Microbial Pathogenesis, 110, 313-324.

28. Premjanu, N., & C. Jaynthy. (2017). Identification and characterization of antimicrobial metabolite from an endophytic fungus, Colletotrichum gloeosporioides, isolated from Lannea corammendalica. International Journal of ChemTech Research, 7(1), 369-374.

29. Rameshkumar, K. B., George, V., &Shiburaj, S. (2007). Chemical constituents and antibacterial activity of the leaf oil of cinnamomumchemungianum Mohan et Henry. Journal of Essential Oil Research, 19(1), 98–100.

30. Simões, M., Bennett, R. N., & Rosa, E. A. S. (2009). Understanding antimicrobial activities of phytochemicals against multidrug resistant bacteria and biofilms. Natural Product Reports, 26, 746–757.

31. Suriyavathana Muthukrishnan & Punithavathi Manogaran (2018). Phytochemical analysis and free radical scavenging potential activity of *Vetiveria zizanioides* Linn. Journal of Pharmacognosy and Phytochemistry, 7(2), 1955 -1960.

32. Maharjan, D., Singh, A., Lekhak, B., Basnyat, S., & Gautam, L. S. (2011). Study on antibacterial activity of common spices. Nepal Journal of Science and Technology, 12, 312-317.

33. Vasiee, A., Tabatabaei Yazdi, F., & Mortazavi, S. A. (2016). The antibacterial activity of Coriandrum (Coriandrum sativum) on pathogenic microorganisms "In vitro". Iranian Journal of Infectious Diseases and Tropical Medicine, 20(71), 59-66.

34. Hsin-Yi, P., Lai, C.-C., Lin, C.-C., & Chou, S.-T. (2014). Effect of *Vetiveria zizanioides* essential oil on melanogenesis in melanoma cells, downregulation of tyrosinase expression, and suppression of oxidative stress. Scientific World Journal, 2014, 1–9.

35. Sundaram Sanjay, S., Shukla, A. K. (2021). Mechanism of Antioxidant Activity. In: Potential Therapeutic Applications of Nano-antioxidants. Springer, Singapore. Pp. 83-99.

36. Subhadradevi, V., Asokkumar, K., Umamaheswari, M., Sivashanmugam, A., &Sankaranand, R. (2010). In vitro antioxidant activity of *Vetiveria zizanioides* root extract. Tanzanian Journal of Health Research, 12(4), 274-279.

37. Luqman, S., Kumar, R., Kaushik, S., Srivastava, S., Darokar, M. P., & Khanuja, S. P. (2009). Antioxidant potential of the root of *Vetiveria zizanioides* (L.) Nash. Indian Journal of Biochemistry and Biophysics, 46(1), 122-125.

38. Nazir, S., Chaudhary, W. A., Mobashar, A., Anjum, I., Hameed, S., & Azhar, S. (2023). Campesterol: A Natural Phytochemical with Anti Inflammatory Properties as Potential Therapeutic Agent for Rheumatoid Arthritis: A Systematic Review. Pakistan Journal of Health Sciences, 4(05), 1-8.

39. Chou, S.-T., Lai, C.-P., Lin, C.-C., & Shih, Y. (2012). Study of the chemical composition, antioxidant activity, and anti-inflammatory activity of essential oil from *Vetiveria zizanioides*. Food Chemistry, 134, 262–268.

Antibiofilm Activity of *Vetiveria zizanioides*

40.   Haghparast Cheshmeh Ali, M. R., Khosroyar, S., & Mohammadi, A. (2018). Evaluation of in vitro anti-inflammatory activity of Harpagophytum procumbens and Urtica dioica against the denaturation of protein. Plant Archives, 18(1), 161-166.

41.   Lima, G. M., Quintans-Júnior, L. J., Thomazzi, S. M., Almeida, E. M. S. A., Melo, M. S., Serafini, M. R.et al (2012). Phytochemical screening, antinociceptive and [sic]. Revista Brasileira de Farmacognosia, 22(2), 443-450.

42.   Nair VV, Karibasappa GN, Dodamani A, Prashanth VK (2016) Microbial contamination of removable dental prosthesis at different interval of usage: An in vitro study. J Indian Prosthodont Soc 16: 346-351.

43.   RapalaKozik, M., Surowiec, M., Juszczak, M., Wronowska, E., Kulig, K., Bednarek, A.. et al (2023). Living together: The role of Candida albicans in the formation of polymicrobial biofilms in the oral cavity. Yeast, 40, 303–317.

44.   Rizzetto, L., De Filippo, C., & Cavalieri, D. (2014). Richness and diversity of mammalian fungal communities shape innate and adaptive immunity in health and disease. European Journal of Immunology, 44(11), 3166–3181.

45.   Zheng, D., Liwinski, T., &Elinav, E. (2020). Interaction between microbiota and immunity in health and disease. Cell Research, 30(6), 492–506.

46.   Bazargani, M. M., & Rohloff, J. (2016). Antibiofilm activity of essential oils and plant extracts against Staphylococcus aureus and Escherichia coli biofilms. Food Control, 61, 156-164.

47.   Hobby, G., Quave, C., Nelson, K., Compadre, C., Beenken, K., & Smeltze, M. (2012). Quercus cerris extracts limit Staphylococcus aureus biofilm formation. Journal of Ethnopharmacology, 144, 812–815.

48.   Lee, J-H., Park, J-H., Cho, H., Joo, S., Cho, M., & Lee, J. (2013). Anti-biofilm activities of quercetin and tannic acid against Staphylococcus aureus. Biofouling, 29, 491–9.

49.   Quave, C., Estévez-Carmona, M., Compadre, C., Hobby, G., Hendrickson, H., Beenken, K., et al. (2012). Ellagic acid derivatives from Rubus ulmifolius inhibit Staphylococcus aureus biofilm formation and improve response to antibiotics. PLoS ONE, 7(1), e28737.

50.   Shahid, M., Kashif, M., Khan, K., Rehman, A. U., Anjum, F., Abbas, M., & Ali, M. (2022). Anti-Inflammatory and Biofilm Inhibition Potential of Methanolic and Aqueous Extract of Elettaria Cardamomum and Cichorium Intybus. Journal of Biological Regulators and Homeostatic Agents, 36(5), 1281-1289.

51.   Elmasri, W. A., Hegazy, M. E., Aziz, M., Koksal, E., Amor, W., Mechref, Y., et al. (2014). Biofilm blocking sesquiterpenes from Teucrium polium. Phytochemistry, 103, 107–113.

52.   Lu, L., Hu, W., Tian, Z., Yuan, D., Yi, G., Zhou, Y., et al. (2019). Developing natural products as potential anti-biofilm agents. Chinese Medicine, 14(1), 1-17.

53.   Soesanto, S., Hepziba, E. R., Yasnill, &Widyarman, A. S. (2023). The Antibacterial and Antibiofilm Effect of Amoxicillin and Mangifera indica L. Leaves Extract on Oral Pathogens. Contemporary Clinical Dentistry, 14(2), 145-151.

54.   Salinas, C., Florentín, G., Rodríguez, F., Alvarenga, N., & Guillén, R. (2022). Terpenes Combinations Inhibit Biofilm Formation in Staphylococcus aureus by Interfering with Initial Adhesion. Microorganisms, 10(8), 1527.

55.   Karygianni, L., Paqué, P. N., Attin, T., & Thurnheer, T. (2021). Single DNase or Proteinase Treatment Induces Change in Composition and Structural Integrity of Multispecies Oral Biofilms. Antibiotics, 10(4), 400.

56.   Karygianni, L., Cecere, M., Skaltsounis, A. L., Argyropoulou, A., Hellwig, E., Aligiannis, N et al. (2014). High-Level Antimicrobial Efficacy of Representative Mediterranean Natural Plant Extracts against Oral Microorganisms. BioMed Research International, 2014, 839019.

A cost-effective superabsorbent polymer composite for prospective wound healing applications

Bharti[1]*, **Priyanka Tyagi[2]**, **and Mainak Basu[3,4]**

[1]School of Engineering & Sciences, GD Goenka University, Gurgaon, India
[2]Department of Botany, Maitreyi College, University of Delhi, New Delhi, 110021 India
[3]School of Engineering & Sciences, GD Goenka University, Gurgaon, India
[4]SciCept Advanced Technologies (OPC) Pvt. Ltd., Kolkata, India
*Corresponding author: bhatnagarbharti1996@gmail.com

Abstract

Wound healing is essential for maintaining the physiological functions of the skin. Any disruption of the skin may lead to wound formation, which can result in mortality if left unattended. The most regular or standard therapy is to cover the wound with a dressing, which reduces the risk of infection and secondary damage. Wound healing is a continuous process accompanied by many other associated biological processes. Available market products to aid in wound healing, have some disadvantages, such as the formation of blisters, pain, and delayed healing. The present work is focussed on the development of a new material based upon the theory of super-absorption using cheap and food grade products. These materials are called hydrogels, which can absorb a substantial amount of water and have several applications. One of the applications is for wound healing as the absorption of bloodallows the agglomeration of the platelets, and other proteins which accelerates the wound healing process Although lyophilized hydrogels are lightweight and capable of absorbing large volumes of water, they are extremely brittle and lack structural integrity when absorbed. In this study, we have used Sodium Carboxymethyl Cellulose (NaCMC) and Polyvinyl Alcohol (PVA) polymers with a crosslinker (Boric Acid) to form apolymer composite capable of considerable water absorption to accelerate the wound healing process while retaining the benefits of strong mechanical characteristics, biodegradability, good water absorption, retention, and biocompatibility at a low cost. FTIR and DSC studies have been performed to estimate the chemical composition of the polymer composite and good crosslinking was observed with increasing amounts of the crosslinker.

Keywords: Wound healing, Hydrogel, Crosslinking, Mortality, Lyophilized

Introduction

The skin performs several functions that are required for ideal health and vitality, and as a general defence against external elements. Any disruption in the skin can cause wound formation (laceration, burns, etc.) and increase the chance of mortality, if left unattended (1). Chronic wounds, which can be caused by pressure ulcers, burns, and diabetic foot ulcers, take longer to heal than acute wounds because the normal skin regeneration phases are disrupted and inflammation is extended.(2). Each type of wound has some exudate, which is frequently observed in chronic wounds (particularly venous leg ulcers, diabetic foot ulcers, and certain pressure ulcers(3). This understanding has generated an increasing interest in biomaterial engineering, which focuses on the development of innovative wound dressings to accelerate wound healing (4).

An ideal wound dressing should have the ability to absorb wound exudates, have good porosity and antimicrobial capacity, and

provide a moist environment to the wound area. (5). Wound dressings can be made from a variety of natural and synthetic materials that are capable of displaying the beneficial behaviors mentioned above, and various forms are currently available on the market. The available solutions can be subdivided into (i) Film (thin, elastic, semipermeable, and transparent) (6,7)for superficial wounds; (ii) Hydrocolloid dressings (two layers; outside semipermeable and interior hydrocolloid (8)); (iii) Foam dressings, which are suitable to moderately and extensively leaking wounds (2) and (iv) Hydrogels are 3D networks of hydrophilic polymers with high water content(9).

Conventional dressings keep the wound area dry and absorb all exudate from the wound. (10), causing saturation. As a result, exudates leak out of the dressing, promoting bacterial attack. The scab covers the entire wound region, decreasing the speed of epithelialization and inhibiting the healing process. These dressings are known as dry dressings (10), which have several limitations, in that they do not favour keratinocyte migration and fibroblast formation. The construction and design of current wound dressings rely on the concept of generating a humid environment surrounding the wound zone (11).

Various biopolymers have been designed and implemented for the applications mentioned above with high biodegradability, biological compatibility, low cost, and the ability to accelerate wound healing (6,9). Many synthetic polymers used for wound healing (12) that have a high water absorption capacity, are also designed to be biodegradable. Recently, there has been growing interest in the use of derivatives of some biopolymers because of their ability to absorb a significant amount of water, gelling ability, and accelerating wound healing (13,14), specifically, the use of nanomaterials has also played a crucial role in the medical industry. Various nanomaterials have been used to form wound hydrogels or scaffolds (through the chelation process), along with antimicrobial activity. (15). In previous studies, different composites have been prepared as superabsorbents. (2). In all of the aforementioned studies, the materials have been developed with the intention of or exploit super absorbency as a property. Although this yields a highly superabsorbent material, it also reduces the mechanical strength, which reduces its effectiveness for wound healing. This is due to the reduced mechanical strength upon super-absorption, which probably leads to leaching into the open wound. In turn, this requires a cytotoxic study of the material that may or may not be beneficial for the stated purpose. Thus, in this study, the choice of materials to develop polymer composites was made with the intention of utilising materials that are already available in commercial space, but utilised in a different manner to allow for both super-absorption as well as higher mechanical strength upon the same.

Uncontrolled bleeding remains the leading cause of preventable mortality following any sort of trauma, whether on the battlefield or in a civilian trauma scenario. Approximately half of the deaths occur before reaching the hospital (16). The problem becomes more complicated when the pattern of injuries becomes significantly more complex. In all these cases, the application of topical hemostatic drugs can be life-threatening. Hence, wound dressings should have the ability to rapidly stop bleeding. However, hemostatic dressings are not accessible everywhere, and hence, are the genesis of this work. Some of the favorable properties of such dressings would include the ability to absorb a considerable amount of water, non-leeching, or low toxicity of the component chemical species in the material, and preferably, the ability to load and discharge specific chemical compounds that can aid in wound healing.

The premise of this study is based on the principle of super-absorption, where the material can absorb a considerable amount of water, which for some of the necessary conditions for the acceleration of the wound-healing process. Hence, in this work, we have used a class of chemical compounds

called 'Hydrogels' which are extremely lightweight, and can absorb considerable amounts of water but are extremely fragile and incapable of structural integrity in the water-absorbed state.

In recent years, polymers derived from natural sources have gained considerable attention because of their biodegradability, cost-effectiveness, and prospect of abundant supply. Despite these advantages, the primary problem with composites derived from the aforementioned materials is their mechanical weakness. Hence, we chose polyvinyl alcohol (PVA) and sodium carboxymethyl cellulose (Na-CMC) as precursors for the polymeric superabsorbent composite. PVA is a semi-synthetic polymer with excellent water absorption properties (17) and tissue adherence capabilities (18), which are also used in many biomedical applications (19). Several previous studies have used PVA-based wound dressings (20-23). However, in the majority of the work, the presence of only PVA, provided some disadvantages in terms of the dissolution of the hydrogel under water absorption. However, when a composite was devised with a crosslinker and other polymers, the mechanical strength increased, but the water absorption capability decreased. Thus, the addition of a second polymer was necessary for stability, of the composite. Na-CMC is a derivative of cellulose used in the food industry (24) and also possesses the ability to absorb and retain considerable amount of water (25 - 27). Considering this fact, the present study was designed to prepare a novel polymer composite to ascertain some of its physical parameters and determine its potential use as a composite for the wound healing process.

The predecessor materials (namely Na-CMC and PVA), mentioned above have significant superabsorbent capability, but minimal mechanical strength, for application as a wound dressing. Thus, to enhance the mechanical strength and maintain super-absorption of the material, a polymer composite has been envisioned with the predecessor materials. To maintain mechanical stability, a cross-linker is required to form the bridge-linkages between the different chains of the constituent polymers. This in turn, may reduce the absorption capability of the composite because the cross-linker would utilise the same chemical sites for cross-linking as those used for hydrogen bonding with the water molecule. The aim of this article is to study the effects of the absorption of the polymer composite of Na-CMC and PVA on the amount of the crosslinker used. Another preliminary study investigated in this article is the loading of the polymer composite with a material that can be released into the wound during the healing procedure. The aforementioned polymeric superabsorbent materials with a crosslinking agent (Boric acid (BA)) were fabricated in various concentrations to test their absorption capability. Boric Acid is a good precursor of boron which has been reported as beneficial for tissue regeneration and is recognised as a predominant element for homeostasis of the human body. Past research studies have shown that boron interacts with collagenase, elastase and trypsin-like enzymes to enhance the production of an Extracellular matrix (28).

The polymer composite has been developed using a simple heating and stirring method to keep costs low. Further, the semi-solid product is cooled, freeze dried and lyophilized to produce the necessary product. The product samples were then tested for their water absorption, water retention and, porosity estimation (as the samples were lyohpilized), minimal chemical structural identification (via FTIR) and the response to ambient temperature (DSC).

Materials and Methods

The primary material utilized in this study, as mentioned aboveis Na-CMC (High Viscocity, 500-600 cps, P-Code: 13440) by Molychem Mumbai, India, which is available as a powder suitable for use in the food industry. Na-CMC powder is superabsorbent

and can retain or absorb a significant amount of water. And another material is PVA (P-Code: 16945) by Molychem Mumbai, India, which is available in a small crystalline form and is also a biodegradable polymer that is soluble in hot water. However, the absorbent material lacks mechanical stability and can be effectively utilized as a wound healing dressing. Thus, to enhance the mechanical stability, Na-CMC and PVA were crosslinked using boric acid as the crosslinking agent, as shown in Figure 1. The effectiveness of the gelling agent determines the quality of the of the final polymer material to maintain the delicate balance between mechanical stability and water absorption capability.

All the gelling agents were mixed with Na-CMC, heated, and stirred for a period of 1.5-2 hours at 70° -80ºC, to initiate polymerization. Among all the gelling agents, a combination of Boric Acid, Na-CMC and PVA provided optimal crosslinking to maintain the mechanical stability and retain the capability to absorb water. However, it must be noted that the water absorption capacity of the polymerized and lyophilized Na-CMC composite is lower than that of the Na-CMC powder, the latter of which lacks mechanical strength. To enhance antibacterial activity, menthol was added to the mixture after the polymer blend was prepared.

The constituent chemical species of the polymer composite that is Na-CMC, PVA, Boric Acid and menthol individually provide sufficient biocompatibility and antibiotic properties. Menthol is also known to have anti-inflammatory properties, which is conducive for wound healing. Thus, it is an estimate that the polymer composite would also be biocompatible and have the necessary antibiotic properties, required for biomedical applications.

Preparation of Boric acid crosslinked polymer composite

Sodium Carboxymethyl Cellulose (Na-CMC) and Polyvinyl Alcohol (PVA) were dissolved in warm water with different concentrations of boric acid, which was used as the crosslinking agent. To test the efficacy of the crosslinking agent on the water absorption capability of the final product, five samples were developed (as shown in Table 1), which consisted of one (SC_1) without the use of boric acid, to test the efficacy of the proposed polymer sample for water absorption. SC_2–SC_4 were developed using different concentrations of BA. A previous study showed that boric acid inhibited Candida and CA growth, reduced microbial diversity, and improved the microecological flora of mouse skin (29). It
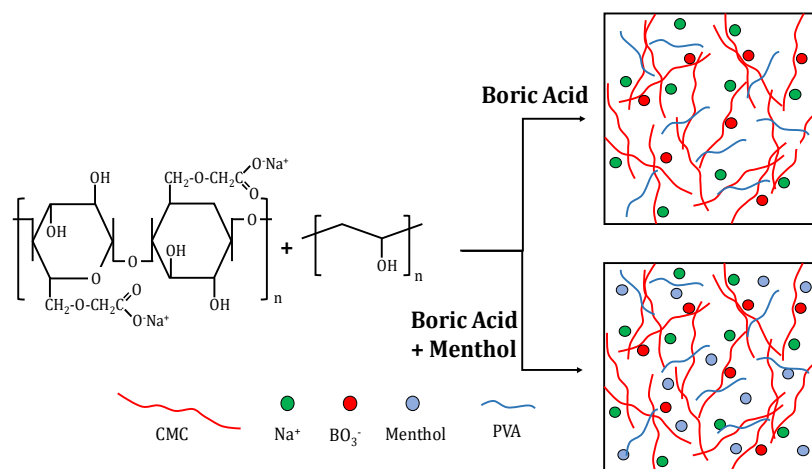

Figure 1: The preparation of the proposed polymers using Na-CMC and PVA

Bharti et al

must be noted that there are some alternative crosslinking agents like citric acid, $CaCl_2$ and additives like gelatin which can be used to increase the adherence power and biocompatibility. However, in this study our choice of Boric Acid is based upon its potential advantage in the acceleration of the wound healing process due to the presence of the Borate ion (30).SC_5 had a specific concentration of BA (0.5 g of menthol in 100% ethanol). The components, with differing concentrations as mentioned in the table, were dissolved in 100 ml of distilled water and magnetically stirred for 1.5-2h to obtain a well-blended reaction mixture. For samples containing menthol, the menthol solution was added dropwise at room temperature, and the effective concentration was determined analogous on a previous study (31). The mixture was poured into a petri dish, kept at -40ºC for 12 h, and then freeze dried (Labconco Freeze Dryer for 24 h). The weight of the components was taken as the weight percentage of 100 ml of water. A flowchart of sample fabrication is shown in Figure 2.

It must be noted that the samples derived from this fabrication process, is required to be Lyophilized before the commencement of further tests.

Characterization Methodologies

Several tests were performed to characterize the stated samples in terms of the characteristics required for wound healing. These include, the following:

(i) Fourier Transform Infra-Red Spectroscopy (FTIR)

(ii) Differential Scanning Calorimetry (DSC)

(iii) Liquid Absorption to estimate the amount of water that can be absorbed.

(iv) Porosity indicator to test for the quantity of liquid which may be absorbed.

(v) Water Retention for the ability to hold onto the water, to accelerate the wound healing.

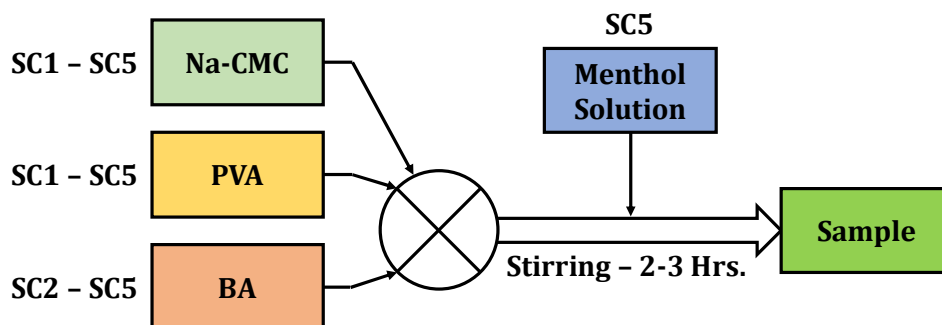| Table 1: Composition of SC1 – SC5 Polymer Blends (wt. % age in 100 ml of water)				
Sample No.	Na-CMC (wt. %age)	PVA (wt. %age)	Boric Acid (wt. %age)	Menthol (wt. in 100% Ethanol)
SC_1	6%	3%	Nil	N/A
SC_2	6%	3%	0.5%	N/A
SC_3	6%	3%	1%	N/A
SC_4	6%	3%	2%	N/A
SC_5	6%	3%	2%	0.5g

Figure 2: The flowchart for the fabrication of the Na-CMC polymer Samples

Phyto-Hydroxyapatite Using *Ocimum Sanctum*

Current Trends in Biotechnology and Pharmacy
Vol. 18 (Supplementry Issue 4A) 106 - 120, November 2024, ISSN 0973-8916 (Print), 2230-7303 (Online)
10.5530/ctbp.2024.4s.9

111

Fourier Transform Infra-Red Spectroscopy (FTIR)

The FT-IR spectroscopy mainly used to identify the functional groups in prepared samples. Samples are being placed directly into the infrared beam. When we run the sample IR beam pass through the sample, the transmitted energy is measured and a spectrum is generated. Prepared samples in this study are in lyophilized form of hydrogel. And the generated spectrum of every prepared sample was observed.

Differential Scanning Calorimetry (DSC)

DSC technique is being used for thermal analysis that measures the temperature and heat flow related to material transformations over time and at different temperatures.

Liquid absorption

Wound dressings should have a good fluid absorption capacity to avoid tissue dehydration in the wound bed and cell death, as well as to promote angiogenesis and heal injured tissues. The polymeric scaffold samples were tested for water absorption capacity at room temperature by weight variation after immersing a piece of pre-weighed sample in water until it was completely saturated with the liquid. Distilled water at 37 °C was used for immersion, after which the samples were removed, and any extra water on the surface was absorbed using filter paper. The capacity of water absorption of the prepared polymeric sample was determined by using the following equation (4)

$$Liquid\ Absorption\ (\%) = \left(\frac{W_1 - W_0}{W_0}\right) * 100 \quad (1)$$

Where W_0 and W_1 represent the weight of the scaffold before and after water absorption.

Porosity Estimate

Porosity is a crucial physical indicator for ideal wound dressing because it influences exudate absorption capacity, colonization rate, cell structure, and angiogenesis. The liquid displacement method was used to determine the porosity of the samples (32). The samples, were weighed under dry condition (W_0), before soaking in absolute ethanol to reach a saturation point. After 30 minutes, the samples were removed from ethanol and weighed again W_1.

The porosity of the samples was calculated by using the following equation[4]:

$$Porosity\ \% = \left(\frac{W_1 - W_0}{\rho V}\right) * 100 \quad (2)$$

Where ρ is the density of the sample and V is the volume of the dry sample under consideration.

Water Retention

Water retention activity is an important parameter for hydrogel-based wound-healing polymers, which operate based on the principle of water absorption. The longer the polymer sample is capable of holding water, the better are the conditions that lead to wound healing. in order to perform the experiment, the samples were dried at 37°C in an oven for 24 h to remove any traces of water that could influence the recording. The weights recorded at this stage were W_0. The samples were then completely soaked in deionized water for 24 h, and the water retention was measured based on sample weighing at predefined intervals (W_i, where i = 1,2,3…, N), while the samples were placed in a 37 °C oven. The water retention rate of the samples was calculated using the following formula (4):

$$Retention\ (\%) = \frac{W_i}{W_0} * 100….. \quad (3)$$

Results and Discussions

The results obtained from different avenues, as mentioned in Section 2.2, are summarized as follows:

Fourier Transform Infra-Red Spectroscopy (FTIR)

The prepared hydrogels were characterized using FT-IR spectroscopy, as shown in Figure 3. In this study, FTIR spectroscopy was used to investigate the
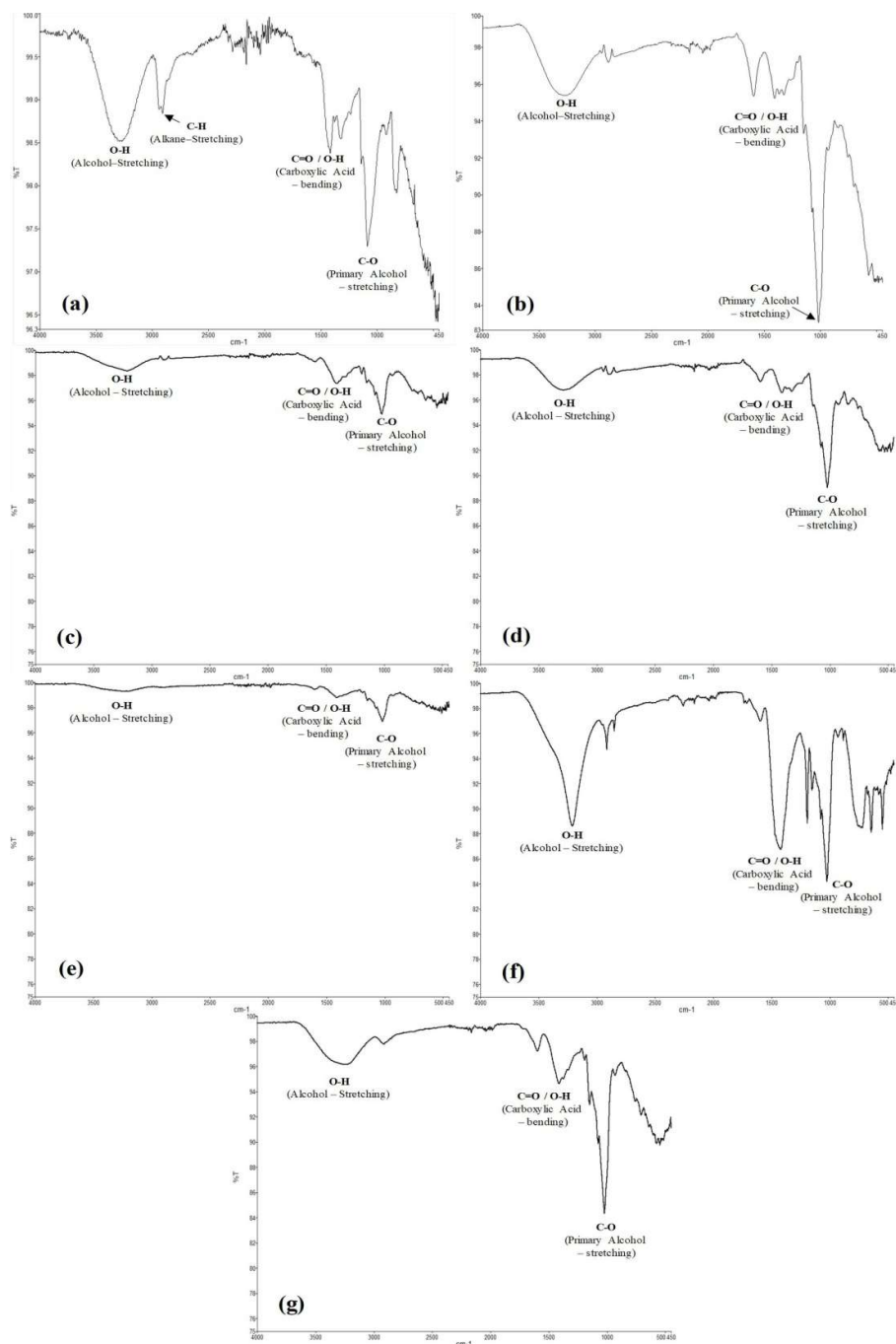
Figure 3: The FTIR spectra of (a) Pure PVA; (b) Pure Na-CMC; (c) SC_1; (d) SC_2; (e) SC_3; (f) SC_4; (g) SC_5

chemical structure of the lyophilized composite and the probable interactions between the functional groups of PVA and NaCMC polymer blend scaffold. The aim of this study was to determine the number of sites available for water absorption via hydrogen bonding. From Figure 1, it is necessary to mention that during the blending process, the sites on both molecules that participate in the polymerization are also sites that are required for hydrogen bonding with water for its absorption. Although a greater number of bonds dictates that the mechanical strength is comparatively higher, it also dictates that the number of absorption sites and, in turn, the absorption capability of the material is reduced. Hence, the study of FTIR can be indicative of the number of available sites for water absorption with varying mechanical strengths.

Additionally, in this technique, a crosslinker, boric acid, was used for the crosslinking of PVA and the NaCMC polymer. Blend polymer compatibility is indicated by changes in the vibrational frequency of the peaks in the system. Figure 3(a) shows the FTIR spectrum of pure PVA, which is characterized by broad O-H stretching. The spectra of the Na-CMC/PVA and boric acid blends in Figure 3 (c) show that the OH bands in the PVA: NaCMC blend system broadened in size with decreased intensity, which indicates a reduction in PVA crystallinity. The O-H, C-O, C-H, and C =O vibrational peaks were used to identify the distinctive bands of the prepared samples, which contributed to the formation of hydrogen bonds within the hybrid polymer matrix. PVA polymers have a strong propensity for hydrogen bonding with other polymers, including CMC, which contains many electronegative groups. It is important to note that the PVA structure contains carbonyl functionalities owing to the remaining acetate groups from the hydrolysis of polyvinyl acetate that remained after PVA synthesis. The FTIR spectra showed that the response of hydrophilic functional groups, such as C=O, C-O, and O-H, decreased across increasing BA concentration while, the bandwidths of the C=O and O-H groups increased.It should be emphasized that while using a cross-linker decreases the number of available sites for cross-linking in each precursor molecule, there are instances where this can lead to the formation of porous spaces. These porous areas are capable of absorbing and retaining more water than would be possible in a non-porous structure. As the FTIR absorption percentage of the specific groups havedecreased with increasing BA concentration, it can be estimated that the cross linker has provided effective crosslinking between the different polymer molecules, to create porous spaces which can absorb, and hold large quantities of water. This can also be estimated from the increased absorption of the incident IR radiation corresponding to the different functional groups and the porosity estimation values of the different samples mentioned later.

Differential Scanning Calorimetry (DSC)

DSC of the samples is important for understanding the thermal stability of the compounds and their prospective water absorption capability before and after heating. Although the nominal temperatures for the fabricated materials, when utilized in prospective wound healing applications, are around the body temperature, it is also necessary to determine their glass transition and melting points to ascertain their range of operation.

DSC thermograms of the samples prepared using different concentrations of PVA, NaCMC, boric acid, and menthol. The DSC profiles of the prepared polymer composites shown in Figure 4 have endothermic peaks because of physical changes in the samples, which confirms the retention of moisture content in the samples owing to the hydrophilicity of the polymer system.

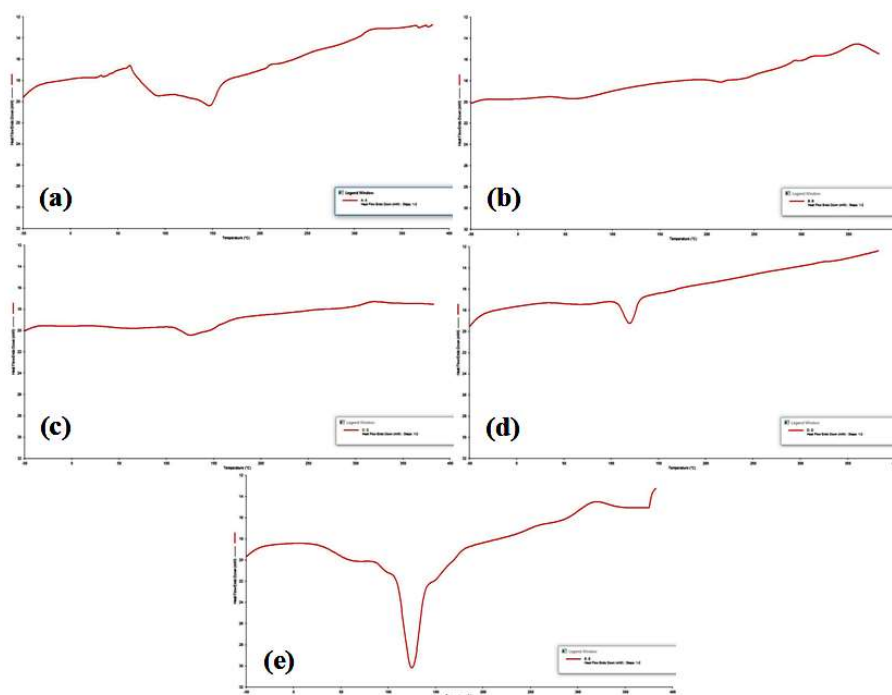Sample SC_1, which includes only PVA and NaCMC, showed two main

Current Trends in Biotechnology and Pharmacy
Vol. 18 (Supplementry Issue 4A) 106 - 120, November 2024, ISSN 0973-8916 (Print), 2230-7303 (Online)
10.5530/ctbp.2024.4s.9

114

Figure 4: The DSC Thermographs of Samples (a) SC_1; (b) SC_2; (c) SC_3; (d) SC_4 and (e) SC_5

transitions corresponding to the glass transition temperature of approximately 700^0C and the melting temperature of approximately 140^0C. SC_2 and SC_3 showed a single short and broad endothermic peak at 125^0C because of the 'powdered' nature of the sample. SC_4 showed a marginally narrow endothermic peak at 125^0C. SC_5, which contained PVA, NaCMC, boric acid, and menthol, showed a sharp endothermic peak at 125^0C because of the crystalline nature of menthol in the sample. An increase in the thermal stability with an increase in the concentration of boric acid in the prepared scaffold suggests conformational changes in the alkyl chains of the polymer, and this increase in crosslinking causes an increase in the thermal stability Table 2.

It may be estimated that the sharpening of the 125^0C endothermic melting peaks for samples SC_3 to SC_5 is characteristic of the increased number of uniform bond formation between the cross linker and the predecessor materials. However, in SC_5 the loading of menthol also contributes to a much sharper melting peak, as the same would evaporate while the sample also melts and changes phase.

Liquid absorption studies

Figure 5 shows the comparative weights of each sample under dry and water-soaked conditions, as mentioned in Section 2.2.3.

The data and the corresponding Liquid Absorption (%) is tabulated in Table 3.

From the above data, it can be estimated that with increased crosslinking, the porosity of the samples increased, allowing a large volume of water to be absorbed. However, Sample SC5, which contains menthol, does not absorb water readily because of the insolubility of menthol in water and SC4 sample absorb and retained a good amount of water.

Phyto-Hydroxyapatite Using *Ocimum Sanctum*

Table 2: FTIR frequency range and functional groups present in the prepared polymeric sample

Sample	Functional Group (cm^{-1})			
	O-H (Alcohol-Stretching)	C-H (Alkane-Stretching)	C+O / O-H (Carboxylic Acid/Alcohol-Bending)	C-O (Primary Alcohol-Stretching)
Pure PVA	~3330 (Broad)	~2860 (Relatively Sharp)	~1713 (Relatively Sharp)	~1085 (Relatively Sharp)
Pure Na-CMC	~3330 (Broad)	Not Prominent	~1350 (Relatively Broad)	~1050 (Relatively Sharp)
SC_1	~3330 (Broad)	Not Prominent	~1350 (Relatively Broad)	~1050 (Relatively Sharp)
SC_2	~3330 (Broad)	Not Prominent	~1350 (Relatively Broad)	~1050 (Relatively Sharp)
SC_3	~3330 (Broad)		~1350 (Relatively Broad)	~1050 (Relatively Sharp)
SC_4	~3330 (Broad)	~2860 (Relatively Sharp)	~1450 (Relatively Broad)	~1050 (Relatively Sharp)
SC_5	~3330 (Broad)		~1450 (Relatively Broad)	~1050 (Relatively Sharp)

Table 3: Liquid Absorption Test Data

	SC_1	SC_2	SC_3	SC_4	SC_5
W_0	100 mg	100 mg	100 mg	100 mg	100 mg
W_1	560 mg	620 mg	650 mg	700 mg	700 mg
Liq. Abs. (%)	460	520	550	600	600

Table 4: The estimated melting temperatures of the samples

Sample	SC_1	SC_2	SC_3	SC_4	SC_5
DSC melting temperature	140^0C	N/A	120^0C	125^0C	125^0C

Table 5: Porosity Estimate Test Data

	SC_1	SC_2	SC_3	SC_4	SC_5
W_0	100 mg	100 mg	100 mg	100 mg	100 mg
W_1	290 mg	300 mg	612 mg	650 mg	650 mg
Porosity Est. (%)	~5.9	~6.25	~16	~17.18	~17.18

Table 6: Water Retention of the samples (all weights in milligrams)

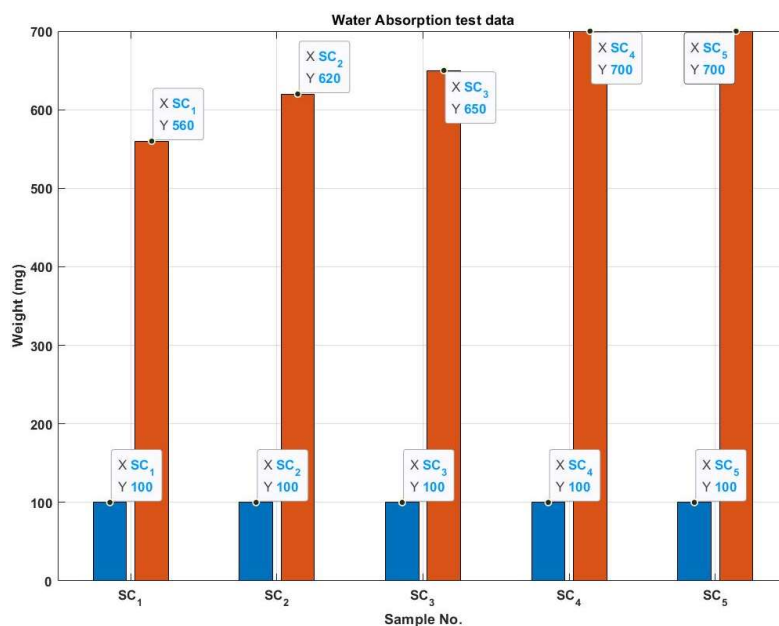|	SC_1			SC_2			SC_3			SC_4			SC_5		
	Wt.	Ret. (%)	Loss (%)	Wt.	Ret. (%)	Loss (%)	Wt.	Ret. (%)	Loss (%)	Wt.	Ret. (%)	Loss (%)	Wt.	Ret. (%)	Loss (%)
W_0	100	N/A	N/A	100	N/A	N/A	100	N/A	N/A	100	N/A	N/A	100	N/A	N/A
W_1	560	--	--	620	--	--	650	--	--	700	--	--	700	--	--
W_2	500	89.3	10.7	610	98.4	1.6	473	72.7	27.3	640	91.4	8.6	685	97.8	2.2
W_3	450	80.4	10	547	88.2	10.3	430	66.2	9.1	640	91.4	0.0	590	84.3	13.9

Bharti et al

Figure 5: The water Absorption test data showing the weights of the different samples under dry and soaked conditions
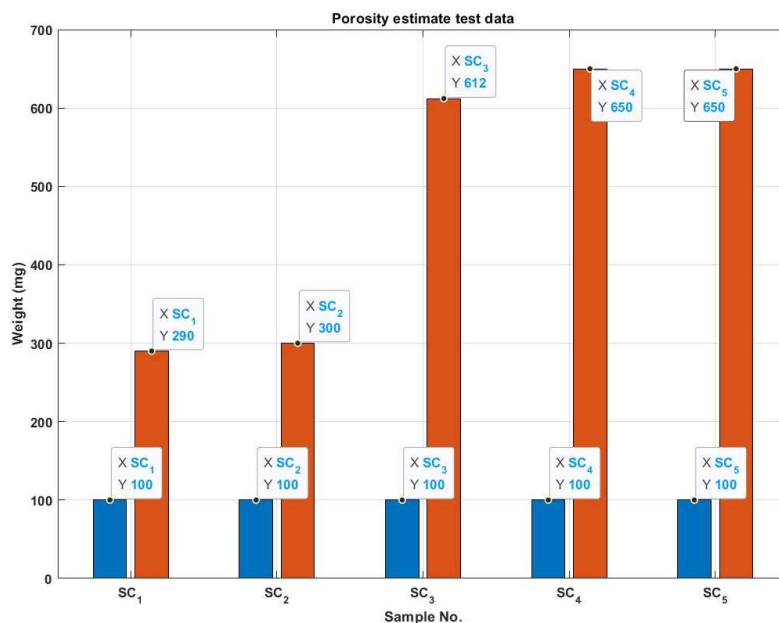

Figure 6: The porosity estimates test data showing the weights of the different samples under dry and ethanol-soaked conditions

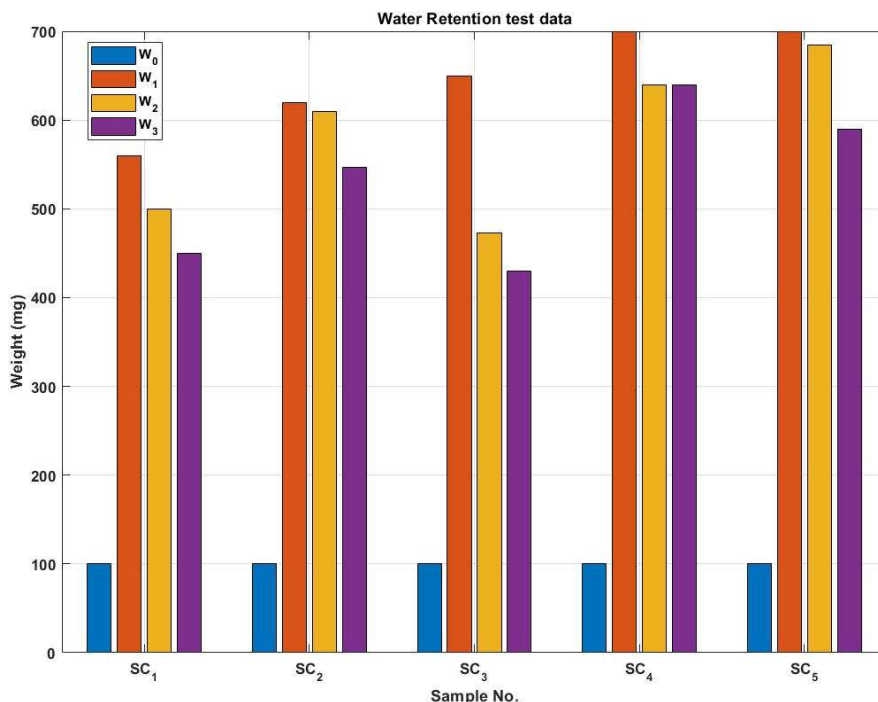Phyto-Hydroxyapatite Using *Ocimum Sanctum*

Figure 7: The water retention study data showing the weights of the different samples under dry and subsequent conditions every 30 minutes

Porosity Estimate studies

Figure 6 and Table 5 shows the porosity estimate study on the scaffold samples with ethanol as mentioned. The volume of each lyophilized scaffold sample used for the testing was ~ 2cm^3.

The corresponding data and the porosity estimate for the different scaffold samples are tabulated in Table 4.

In a similar manner of the data as compared to the water absorption test, scaffold SC5 shows a higher percentage of porosity and the crosslinking

Water Retention studies

To evaluate the water retention ability of the scaffold samples, their weights were measured at predefined intervals. Four instances of the weights were taken, each after a period of 30 minutes. Figure 7 shows the data pertaining to water retention of each sample.

The tabulated data and the estimated water retention percentage have been tabulated in Table 6.

Although it is difficult to estimate a standard water retention value, all samples showed a promising capability of retaining a significant amount of water absorbed. The loss percentage was calculated as a relative factor to estimate the rate of water loss every 30 min in an 370^{0}C oven. Some samples showed an increase in the loss rate, while others showed a decreasing trend. This can occur because of an innumerable number of conditions, which also include the effective area open to the heat of the oven.

The polymer composite material proposed in this article was developed with the beneficial properties mentioned in Section 1. In addition, several conditions were followed to implement the same in a cost-effective manner. The choice of materials has been restricted to natural

Current Trends in Biotechnology and Pharmacy
Vol. 18 (Supplementry Issue 4A) 106 - 120, November 2024, ISSN 0973-8916 (Print), 2230-7303 (Online)
10.5530/ctbp.2024.4s.9

118

derivatives, which are already in use in the biomedical domain. This would ensure an abundant material supply while simultaneously reducing cytotoxicity in the body. Both composite precursors mentioned in this article are either used by the food industry or have biomedical applications, thereby justifying their low, if not non-existent, cytotoxic nature. However, it must be noted that the toxic effects of such a polymer composite still need to be studied for its leeching (seep-out) and overall cytotoxic properties. Owing to the use of food/biomedical-grade materials that are widely available in commercial space, it may be assumed that the cost of the final product per weight would be comparable to the sum of the cost per weight of the individual chemicals. As the production process merely relies on stirring and heating without the addition of any specialized chemicals, the final cost of the product per unit weight would be considerably lower than that currently available in commercial space.

It is also to be noted that the water absorption and porosity estimation studies have to be performed under exacting condition and timings in order to acquire accurate data. There are many possible factors which can cause variations which includes the ratios of the materials, time period and blending procedures, Lyophilization conditions and storage of the material. In order to avoid any discrepancies in the data, all materials were prepared under the same blending procedures, i.e. 70-80^{0}C for 1.5-2 hr. with equal initial volume (100ml) and were directly freeze dried and lyophilized.

The prepared polymer composite showed promisingresults as a superabsorbent and was mechanically stable, which provided a template on which to build it. After this next phase of the work, which is currently ongoing, the development of loading in this kind of material or embedding in other kinds of biocompatible polymers so that it can be embedded in the skin for direct application.

Conclusion

Recently, considerable focus has been directed towards natural polymer-based hydrogels and their potential applications in the biomedical domain, largely due to their biocompatibility, biodegradability, abundance in nature, and customizable mechanical properties. In this study, The choice of the materials is governed by many different factors. For the present work, ease of availability dictated the use of long-chain polymers, and materials which are already used in the food or biomedical industry. Hence the choice of Na-CMC and PVA as mentioned before. This allows the cost of development and the unit cost of the final product to be lowered, while also ensuring availability. Coupled with the cost effective procedure of heating and stirring, the cost per unit weight of the material can be kept low in competition with contemporary solutions. NaCMC and PVA were used as gelling agents with the crosslinker boric acid and were formulated into NaCMC-BA-PVA to develop a biocompatible material with broad-range effects for wound application. Properties such as complexation, blending, and thermal stability were determined using FTIR and DSC. The FTIR results demonstrated that the polymer composite was successfully prepared through blending and casting polymerization, and the shatter value of the polymeric structure increased with increasing boric acid content. The factors affecting the water absorbency, retention, and porosity were also investigated. It was observed that under optimal synthesis conditions, the polymeric composites (SC4 and SC5) exhibited the best water absorbency with increased amounts of boric acid and good porosity. The crosslinking behavior and ability to absorb water increased with an increase in the amount of crosslinking agent. Boric Acid is capable of considerable water absorption to accelerate the wound healing process while retaining the benefits of strong mechanical characteristics, biodegradability, good water retention, absorption, and biocompatibility at a low cost. Good crosslinking was observed with increasing amounts of the crosslinker. The

Current Trends in Biotechnology and Pharmacy
Vol. 18 (Supplementry Issue 4A) 106 - 120, November 2024, ISSN 0973-8916 (Print), 2230-7303 (Online)
10.5530/ctbp.2024.4s.9

119

proposed chemical composite was devised as a template to build and develop a cost-effective superabsorbent polymer composite that may have prospective wound healing applications. Further comprehensive cell and animal studies are required to be performed to translate the prepared polymer composite for clinical use. These additional studies will provide valuable insights into its safety, efficacy, and long-term performance, thereby advancing its clinical application, but the preliminary studies mentioned in this article suggest that the proposed composite may be a good dressing for hemostatic wound healing.

References

1. Zhang, H., Qin, H., Li, L., Zhou, X., Wang, W., & Kan, C. (2017). Preparation and characterization of controlled-release avermectin/castor oil-based polyurethane nanoemulsions. Journal of agricultural and food chemistry, 66(26), 6552-6560.

2. Arefian, M., Hojjati, M., Tajzad, I., Mokhtarzade, A., Mazhar, M., &Jamavari, A. (2020). A review of Polyvinyl alcohol/Carboxymethyl cellulose (PVA/CMC) composites for various applications. *Journal of Composites and Compounds*, *2*(3), 69-76.

3. Mustoe, T. (2004). Understanding chronic wounds: a unifying hypothesis on their pathogenesis and implications for therapy. *The American Journal of Surgery*, *187*(5), S65-S70.

4. Monfared-Hajishirkiaee, R., Ehtesabi, H., Najafinobar, S., &Masoumian, Z. (2023). Multifunctional chitosan/carbon dots/sodium alginate/zinc oxide double-layer sponge hydrogel with high antibacterial, mechanical and hemostatic properties. *OpenNano*, *12*, 100162.

5. Guo, S. a., & DiPietro, L. A. (2010). Factors affecting wound healing. *Journal of dental research*, *89*(3), 219-229.

6. Degreef, H. J. (1998). How to heal a wound fast. *Dermatologic clinics*, *16*(2), 365-375.

7. Tenorová, K., Masteiková, R., Pavloková, S., Kostelanská, K., Bernatonienė, J., & Vetchý, D. (2022). Formulation and evaluation of novel film wound dressing based on collagen/microfibrillated carboxymethylcellulose blend. *Pharmaceutics*, *14*(4), 782.

8. Takeuchi, T., Ito, M., Yamaguchi, S., Watanabe, S., Honda, M., Imahashi, T., Yamada, T., & Kokubo, T. (2020). Hydrocolloid dressing improves wound healing by increasing M2 macrophage polarization in mice with diabetes. *Nagoya Journal of Medical Science*, *82*(3), 487.

9. Liang, Y., He, J., & Guo, B. (2021). Functional hydrogels as wound dressing to enhance wound healing. *ACS nano*, *15*(8), 12687-12722.

10. Shi, C., Wang, C., Liu, H., Li, Q., Li, R., Zhang, Y., Liu, Y., Shao, Y., & Wang, J. (2020). Selection of appropriate wound dressing for various wounds. *Frontiers in bioengineering and biotechnology*, *8*, 182.

11. Junker, J. P., Kamel, R. A., Caterson, E., & Eriksson, E. (2013). Clinical impact upon wound healing and inflammation in moist, wet, and dry environments. *Advances in wound care*, *2*(7), 348-356.

12. Kohli, N., Sharma, V., Brown, S. J., & García-Gareta, E. (2019). Synthetic polymers for skin biomaterials. In *Biomaterials for Skin Repair and Regeneration* (pp. 125-149). Elsevier.

13. Kanikireddy, V., Varaprasad, K., Jayaramudu, T., Karthikeyan, C., & Sadiku, R. (2020). Carboxymethyl cellulose-based materials for infection control and wound healing: A review. *International Journal of Biological Macromolecules*, *164*, 963-975.

14. Miranda, Í. K. S. P. B., Santana, F. R., Camilloto, G. P., Detoni, C. B., Souza, F. V. D., de Magalhães Cabral-Albuquerque, E. C., Alves, S. L., Neco, G. L., de Lima, F. O., & de Assis, S. A. (2021). Development of membranes based on carboxymethyl cellulose/acetylated arrowroot starch containing bromelain extract carried on nanoparticles and liposomes. *Journal of Pharmaceutical Sciences*, *110*(6), 2372-2378.

15. Ataide, J. A., Zanchetta, B., Santos, É. M., Fava, A. L. M., Alves, T. F., Cefali, L. C., Chaud, M. V., Oliveira-Nascimento, L., Souto, E. B., & Mazzola, P. G. (2022).

Nanotechnology-Based Dressings for Wound Management. *Pharmaceuticals*, *15*(10), 1286.

16. Moore, E. E., Moore, H. B., Kornblith, L. Z., Neal, M. D., Hoffman, M., Mutch, N. J., Schöchl, H., Hunt, B. J., &Sauaia, A. (2021). Trauma-induced coagulopathy. *Nature Reviews Disease Primers*, *7*(1), 30.

17. Ray, R., Das, S. N., & Das, A. (2021). Mechanical, thermal, moisture absorption and biodegradation behaviour of date palm leaf reinforced PVA/starch hybrid composites. *Materials Today: Proceedings*, *41*, 376-381.

18. Chen, X., & Taguchi, T. (2020). Enhanced skin adhesive property of hydrophobically modified poly (vinyl alcohol) films. *ACS omega*, *5*(3), 1519-1527.

19. Jiang, S., Liu, S., & Feng, W. (2011). PVA hydrogel properties for biomedical application. *Journal of the mechanical behavior of biomedical materials*, *4*(7), 1228-1233.

20. Adeli, H., Khorasani, M. T., &Parvazinia, M. (2019). Wound dressing based on electrospun PVA/chitosan/starch nanofibrous mats: Fabrication, antibacterial and cytocompatibility evaluation and in vitro healing assay. *International Journal of Biological Macromolecules*, *122*, 238-254.

21. Chopra, H., Bibi, S., Kumar, S., Khan, M. S., Kumar, P., & Singh, I. (2022). Preparation and evaluation of chitosan/PVA based hydrogel films loaded with honey for wound healing application. *Gels*, *8*(2), 111.

22. Tamer, T. M., Alsehli, M. H., Omer, A. M., Afifi, T. H., Sabet, M. M., Mohy-Eldin, M. S., & Hassan, M. A. (2021). Development of polyvinyl alcohol/kaolin sponges stimulated by marjoram as hemostatic, antibacterial, and antioxidant dressings for wound healing promotion. *International journal of molecular sciences*, *22*(23), 13050.

23. Xu, F., Zou, D., Dai, T., Xu, H., An, R., Liu, Y., & Liu, B. (2018). Effects of incorporation of granule-lyophilised platelet-rich fibrin into polyvinyl alcohol hydrogel on wound healing. *Scientific Reports*, *8*(1), 14042.

24. Behra, J. S., Mattsson, J., Cayre, O. J., Robles, E. S., Tang, H., & Hunter, T. N. (2019). Characterization of sodium carboxymethyl cellulose aqueous solutions to support complex product formulation: A rheology and light scattering study. *ACS Applied Polymer Materials*, *1*(3), 344-358.

25. Akalin, G. O., &Pulat, M. (2018). Preparation and characterization of nanoporous sodium carboxymethyl cellulose hydrogel beads. *Journal of Nanomaterials*, *2018*.

26. Kundu, J., Mohapatra, R., & Kundu, S. (2011). Silk fibroin/sodium carboxymethylcellulose blended films for biotechnological applications. *Journal of Biomaterials Science, Polymer Edition*, *22*(4-6), 519-539.

27. Moumni, H., & Cherif, E. (2024). The Drug Paracetamol and Sodium Carboxymethyl Cellulose Interactions and Their Importances for Pharmaceutical and Biomedical Applications. *Journal of Macromolecular Science, Part B*, 1-14.

28. Coskun, M. (2023). Success in treating wounds with local boric acid: a case study. *Journal of wound care*, *32*(10), 686-690.

29. Liu, Q., Liu, Z., Zhang, C., Xu, Y., Li, X., & Gao, H. (2021). Effects of 3% boric acid solution on cutaneous Candida albicans infection and microecological flora mice. *Frontiers in Microbiology*, *12*, 709880.

30. Yang, Q., Chen, S., Shi, H., Xiao, H., & Ma, Y. (2015). In vitro study of improved wound-healing effect of bioactive borate-based glass nano-/micro-fibers. Materials Science and Engineering: C, 55, 105-117.

31. Rozza, A. L., Beserra, F. P., Vieira, A. J., Oliveira de Souza, E., Hussni, C. A., Martinez, E. R. M., Nóbrega, R. H., & Pellizzon, C. H. (2021). The use of menthol in skin wound healing—Anti-inflammatory potential, antioxidant defense system stimulation and increased epithelialization. *Pharmaceutics*, *13*(11), 1902.

32. Khorasani, M. T., Joorabloo, A., Moghaddam, A., Shamsi, H., and MansooriMoghadam, Z. (2018). Incorporation of ZnO nanoparticles into heparinised polyvinyl alcohol/chitosan hydrogels for wound dressing application. *International Journal of Biological Macromolecules*, *114*, 1203-1215.

Phyto-Hydroxyapatite Using *Ocimum Sanctum*

Computational Studies on *Diospyros Ebenum* and *Oldenlandia Umbellata* Phytochemicals as Novel Fatty Acid Synthase Inhibitors

Athista. M[1], and Swetha Sunkar[1]*, C. Valli Nachiyar[2], and Krupakar Parthasarathy[3]

[1]Department of Bioinformatics, Sathyabama Institute of Science and Technology, Chennai, Tamil Nadu
[2]Department of Research, Meenakshi Academy of Higher Education and Research, India
[3]Centre for Drug Discovery and Development, Sathyabama Institute of Science and Technology, Chennai, Tamil Nadu, India
*Corresponding author: swethauk78@gmail.com

Abstract

Obesity is a global health concern associated with severe diseases, including atherosclerosis, osteoarthritis, coronary artery disease, and cerebrovascular disorders. These conditions pose significant risks such as restricted blood flow, coronary heart disease, and mortality. Fatty acid synthase (FAS), a key enzyme in lipogenesis, plays a pivotal role in fat accumulation and is a primary target for therapeutic intervention. Orlistat, a widely used drug that targets and inhibits fatty acid synthase activity to treat obesity; however, prolonged use may result in unintended health issues. This study aimed to identify natural compounds from *Diospyros ebenum* (Ceylon ebony) and *Oldenlandia umbellata* (chay root) that inhibit fatty acid synthase. Through comprehensive *in silico* analyses, including ADMET studies, toxicity profiling, pharmacophore analysis, ligand-receptor interactions, and molecular simulations, we found phytochemicals from these plants to be non-toxic with favourable pharmacological properties. Molecular interaction studies demonstrated efficient binding to the fatty acid synthase site, suggesting potential for inhibiting enzyme activity and reducing fat accumulation. In conclusion, *Oldenlandia umbellata* exhibited greater efficacy compared to *Diospyros ebenum*, suggesting its ability as a promising source of anti-obesity agents. These findings offer valuable insights for further experimental investigation.

Introduction

Obesity, characterized by an imbalance between energy intake and expenditure resulting in excess fat accumulation, has become a global public health concern affecting nearly one-third of the world's population. This condition, associated with metabolic disorders such as hypertension, dyslipidemia, and hyperglycemia, poses a significant risk for diseases like diabetes, cardiovascular disorders, and cancer. The escalating prevalence of obesity underscores the urgency to address its detrimental health effects. While surgical weight loss interventions effectively reduce morbidity and mortality risk, they may evoke negative emotions. Some anti-obesity drugs exist, but they come with potential side effects. The need for developing safe and efficient weight management treatments to prevent obesity (1) requires a comprehensive understanding of the mechanism.

Adipocytes play a crucial role in maintaining nutritional homeostasis by storing triglycerides (TG) when there's an energy surplus and releasing fatty acids during fasting or periods of heightened energy demand to support other tissues. The process of adipocyte differentiation from multipotent mesenchymal stem cells is guided by specific adipogenic transcription

factors. Mature adipocytes can expand in size by synthesizing and storing triglycerides through the process of lipogenesis when there is an excess of available nutrients. This facilitates the storage of fat in existing fat cells (2). To maintain physiological conditions, it is essential to control the transcription of genes associated with lipid synthesis and storage. This includes overseeing the activity of crucial genes such as fatty acid synthase (FAS), acetyl-CoA carboxylase (ACC), and genes involved in the accumulation of lipids (3).

Orlistat, an FDA-approved weight loss drug available globally, targets fatty acid synthase (FAS), a key enzyme for lipid synthesis and an important anti-obesity drug target (4). By inhibiting FAS, orlistat reduces the breakdown of dietary triglycerides into absorbable free fatty acids and monoglycerides, preventing fat absorption. Although side effects, notably gastrointestinal, such as oily stool, may occur early in treatment, they often diminish as therapy progresses (5). Hence, there is a growing interest in exploring alternative approaches for treating and managing the disease. Natural compounds derived from sources such as plants are gaining attention due to their rich repository of structurally diverse metabolites, holding potential applications ranging from medicine to industry(6). We computationally screened phytochemicals from medicinal plants *Diospyros ebenum,* (*D.ebenum*) and *Oldenlandia umbellata* (*O.umbellata*) to assess their potential to inhibit the activity of the enzyme FAS. We compared their efficacy with the standard drug, orlistat, to analyze their inhibitory capabilities.

D. ebenum, traditionally used for treating diarrhoea and dyspepsia, possesses leaves with diuretic, laxative, carminative, and styptic properties, making them beneficial for digestive and wound-healing conditions. Additionally, its dried flowers have been employed in treating urinary and skin infections, showcasing hepatoprotective and antidiabetic properties(7). In Indian Siddha medicine, *O.umbellata* is traditionally employed to address health issues such as bronchitis,

asthma, tuberculosis, and hemoptysis. Scientific research has highlighted its pharmacological effects, revealing potential antibacterial, anti-inflammatory, antipyretic, hepatoprotective, antioxidant, and antitussive activities(8).

Utilizing computational screening expedites drug discovery by efficiently analyzing extensive compound libraries, predicting ligand properties, and pinpointing potential therapeutics. Recent advances in ligand discovery enhance the development of safer and more effective small-molecule treatments. Employing computational technologies enables cost-effective and rapid identification of diverse, potent, and target-specific ligands, transforming the landscape of drug discovery. Molecular docking and simulation play crucial roles, enabling prediction of molecular interactions, aiding in drug candidate identification, and advancing our understanding of biochemical processes for novel treatments (9,10)

Evaluating the inhibitory binding potential of phytochemicals from *D. ebenum* and *O. umbellata* on FAS activity is vital for assessing their role as anti-obesity agents. Understanding their impact on FAS activity through docking and simulation is crucial for devising innovative therapeutic strategies against obesity-related conditions. The study aims to employ computational methods to assess these phytochemicals, comparing their efficacy with orlistat. The hypothesis suggests that these natural compounds may offer safer and more effective options for obesity management. Additionally, the research seeks to identify bioactive compounds from these plants for potential development into anti-obesity drugs. Through computational approaches, this research helps to gain valuable insights into the effectiveness of *D. ebenum* and *O. umbellata* phytochemicals in binding to FAS to prevent fat accumulation and manage obesity. This exploration aims to contribute significantly to the understanding and potential treatment of obesity-related disorders, leveraging the therapeutic potential of natural compounds.

Diospyros ebenum and *Oldenlandia umbellata* Phytochemicals

Materials and Methods

Target and Ligand Identification

The enzyme FAS plays a pivotal role as the limiting factor in triglyceride biosynthesis, establishing it as a significant therapeutic target endorsed by the World Health Organization (WHO). This research leveraged the Protein Data Bank (PDB), an openly accessible online structure database, to obtain both the sequence and structural details of the protein (11). After this, a comprehensive exploration of literature and the natural phytocompounds database led to the identification of various bioactive and phytochemical compounds present in the medicinal plants, *D. ebenum* and *O. umbellata*. Essential information such as monoisotopic mass, molecular formula, and other relevant details concerning these compounds was sourced from PubChem (12).

Analysis of ADMET descriptors

To evaluate the druggability of the compounds, it is essential to study their absorption, distribution, metabolism, excretion, and toxicity (ADMET) properties. The ADMET descriptors algorithm in Discovery Studio software was used to analyze the ADMET properties of the phytocompounds. This includes models to predict human intestinal absorption based on polar surface area and partition coefficient values, aqueous solubility levels based on a regression model, and blood-brain barrier penetration with prediction levels defining logBB ranges. Additionally, the software incorporates confidence ellipses to model intestinal absorption relative to physicochemical parameters. This comprehensive approach aids in evaluating the drug's suitability for clinical trials by analyzing its pharmacokinetic characteristics (13). Predicting these factors helps determine whether the molecule interacts with the receptor flexibly or rigidly (14).

In silico predictive toxicology assessments

The TOPKAT (Toxicity Prediction Komputer Assisted Technology version) module within Discovery Studio was utilized to assess various properties, including rodent carcinogenicity, Ames mutagenicity, developmental toxicity potential, rat oral median lethal dose (LD_{50}), biodegradability, and skin sensitization, for all potential compounds. The model selected compounds that met the validation criteria for the query, and the results were documented. These pharmacological properties played a crucial role in the selection of appropriate drug candidates aimed at reducing the activity of FAS(15).

Pharmacophore analysis for drug discovery

A pharmacophore model was generated for the selected compounds. The pharmacophore mapping module of the Discovery Studio 2016 software was employed to analyze a chemical library consisting of bioactive compounds from plants and synthetic drugs. (16). This model, derived from the structural features of an active compound, guided the filtration and screening of molecular databases. The effective pharmacophore incorporated crucial ligand properties, including hydrogen bond acceptors, hydrogen bond donors, hydrophobicity, and aromaticity (17).

Molecular docking

Molecular docking and visualization studies were conducted using the LibDock program in Discovery Studio. LibDock, a high-throughput algorithm by Diller and Merz, employs polar and apolar features as "Hotspots" for flexible docking. The protocol, utilizing the CHARMm force field, allowed ligands to be docked and scored with default parameters. A 2D diagram was generated to identify interacting residues. Ligands were prepared with three-dimensional coordinates for docking analysis (18,19).

Molecular simulation

The ligand-protein interaction dynamics were assessed to identify active amino acid residues at the FAS binding site. Using the CABS Flex 2.0 server, coarse-
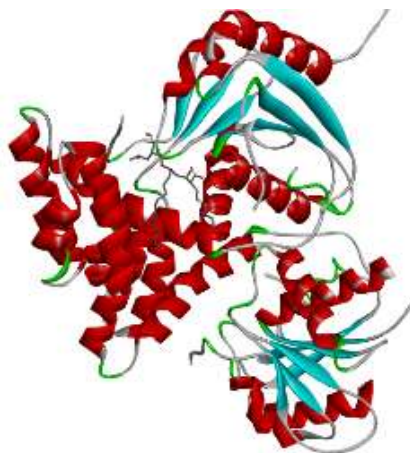
Current Trends in Biotechnology and Pharmacy
Vol. 18 (Supplementry Issue 4A) 121 - 137, November 2024, ISSN 0973-8916 (Print), 2230-7303 (Online)
10.5530/ctbp.2024.4s.10

124

Figure 1: The complex of Drug orlistat and the catalytic domain (thioesterase) of human FAS

grained simulations were performed to analyse the protein's stable structure. Parameters included 50 cycles, a global weight of 1.0, and a temperature of 1.4. RMSF values, reflective of protein flexibility, were recorded over a 10 ns simulation to evaluate the conformational stability of the protein and the protein-ligand complex (20,21).

Result and discussion

Target Selectionand Ligand Identification

Fatty acid synthase (FAS), a key enzyme in lipogenesis, was investigated using UniProt for basic information. The crystal structure (PDB ID: 2PX6) of the thioesterase domain of human FAS, inhibited by Orlistat, was obtained from the PDB, offering valuable structural insights shown in Figure 1 (22).

A total of 30 bioactive compounds were sourced, with 14 from *D. ebenum* and 16 from *O. umbellata*, obtained from the IMPPAT database and extensive literature review (Table 1). These compounds exhibited diverse bioactivities, encompassing proteins, lipids, carbohydrates, alkaloids, sterols, terpenoids, polypeptides, flavonoids, and saponins. Previous research confirms

the bioactivity of these phytochemicals, underscoring their potential medicinal and therapeutic applications (23, 24). The drug Orlistat is also chosen for the comparative study. The identified bioactive components were assessed for drug development cues. Further evaluation included ADMET properties, toxicity analysis, and pharmacophore examination to determine the most promising candidates for drug development to manage obesity.

Integrating ADMET in Drug Discovery and Development

In drug discovery, assessing the compound's absorption, distribution, metabolism, excretion, and toxicity (ADMET) is pivotal. An ideal drug candidate should not only exhibit efficacy against the therapeutic target but also possess favourable ADMET properties at a therapeutic dose. Table 1 details the ADMET results for the bioactive compound and the drug Orlistat, while Figure 2 depicts the polar surface area (2D PSA) and AlogP plots. Predictions based on 2D PSA and AlogP, with 95% and 99% confidence ellipses, determine intestinal absorption and blood-brain barrier penetration in the ADMET study. All molecules demonstrate excellent human intestinal absorption (HIA) and aqueous solubility, emphasizing their potential as well-absorbed compounds with good absorption characteristics in aqueous media (25). The pharmacokinetic properties of the studied molecules were assessed using six predetermined ADMET models in Discovery Studio. Optimal cell permeability criteria included PSA < 140 Å2 and AlogP98 < 5, as per the model (11). Prior research on ADMET (Absorption, Distribution, Metabolism, Excretion, and Toxicity) studies has disclosed valuable information about ADMET descriptors along with their corresponding rules and keys. When assessing the druggability of compounds, an in-depth evaluation of their ADMET properties (absorption, distribution, metabolism, excretion, and toxicity) is essential. These

Diospyros ebenum and *Oldenlandia umbellata* Phytochemicals

Table 1: ADMET profiling of the compounds present in *D. ebenum*, *O. umbellata,* and the drug orlistat

Compounds	ADMET solubility	ADMET solubility level	ADMET absorption level	ADMET AlogP98	ADMET BBB level	ADMET PPB	ADMET PSA 2D	Molecular weight (g/mol)
D. ebenum								
Ellagic acid	-3.452	3	1	1.584	4	<90%	135.723	302.19
1,4-Naphthoquinone	-2.748	3	0	1.757	2	<90%	34.601	302.19
Elliptinone	-4.987	2	0	3.612	4	<90%	110.834	158.15
Ebenone	-5.194	2	0	4.391	4	<90%	97.048	442.72
Betulin	-7.151	1	1	6.312	0	<90%	41.631	442.72
Ursolic acid	-7.617	1	1	6.492	4	≥90%	58.931	456.7
Betulinic acid	-7.567	1	2	6.546	4	<90%	58.931	412.69
Alpha-Amyrin	-8.808	0	3	7.349	4	≥90%	20.815	426.72
Bauerenol	-8.807	0	3	7.349	4	≥90%	20.815	360.36
Lupeol	-8.757	0	3	7.403	4	<90%	20.815	426.72
Alpha-Amyrenone	-9.625	0	3	7.449	4	≥90%	17.3	424.7
Stigmasterol	-7.963	1	3	7.639	4	≥90%	20.815	382.71
Beta-Sitosterol	-8.256	0	3	8.084	4	≥90%	20.815	426.72
1-Hexacosanol	-7.284	1	3	11.007	4	≥95%	20.815	374.34
O.umbellata								
Scan-doside	-0.096	4	3	-3.326	4	<90%	189.799	594.52
scandoside methyl ester	0.013	5	3	-3.1	4	<90%	177.914	390.34
Asperulosidic acid	-0.551	4	3	-2.947	4	<90%	195.214	123.11
Deacetylasperuloside	-0.066	4	3	-2.742	4	<90%	157.098	432.38
Nicotiflorin	-5.098	2	3	-0.916	4	<90%	249.29	208.21
Ruberythric acid	-3.244	3	3	-0.842	4	<90%	216.03	240.21
Nicotinic acid	-0.494	4	0	0.309	3	<90%	49.377	208.21
Purpurin	-2.812	3	0	2.082	3	<90%	97.048	534.47
Alizarin	-3.096	3	0	2.324	3	≥90%	76.232	284.26
1,3-Dimethoxy-2-hydroxy-9,10-anthraquinone	-3.743	3	0	2.533	3	<90%	73.277	254.24
Alizarin 1-methyl ether	-3.654	3	0	2.55	2	≥90%	64.347	260.29
Anthraquinone	-4.15	2	0	2.808	1	≥90%	34.601	256.21

Current Trends in Biotechnology and Pharmacy
Vol. 18 (Supplementry Issue 4A) 121 - 137, November 2024, ISSN 0973-8916 (Print), 2230-7303 (Online)
10.5530/ctbp.2024.4s.10

126

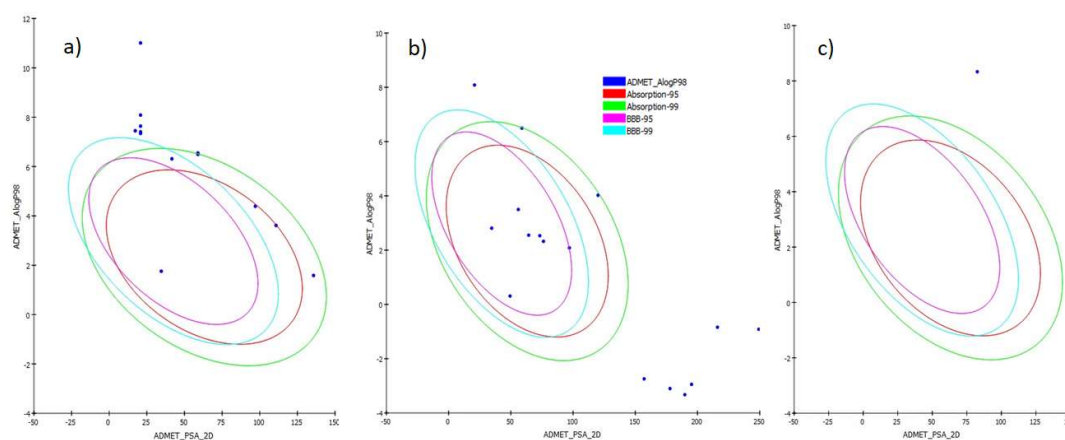| Table 1: ADMET profiling of the compounds present in *D. ebenum*, *O. umbellata,* and the drug orlistat (*Contd*.)							
D. ebenum							
Cedrelopsin	-4.058	2	0	3.497	1	<90%	55.976	372.32
Pheophorbide A methyl ester	-5.564	2	1	4.023	4	<90%	120.057	404.37
Ursolic acid	-7.617	1	1	6.492	4	≥90%	58.931	594.52
Beta-Sitosterol	-8.256	0	3	8.084	4	≥90%	20.815	606.71
Drug							
Orlistat	-6.299	1	3	8.333	4	≥95%	82.572	495.7

Figure 2: ADMET Description plot a) *D.ebenum* compounds b) *O.umbellata* compounds c) Drug Orlistat

properties profoundly impact the efficacy, safety, and pharmacokinetics of a drug, playing a crucial role in determining its clinical success. Selecting specific ADMET parameters and thresholds for compound evaluation requires careful consideration of several factors.

Absorption, the first consideration, predicts a drug's ability to enter systemic circulation post-administration. Parameters like human intestinal absorption (HIA), based on factors such as polar surface area and partition coefficient values, provide insights into a compound's ability to traverse biological membranes. Determining appropriate thresholds for HIA levels aids in identifying compounds with optimal

absorption potential, thus enhancing the likelihood of achieving therapeutic concentrations in systemic circulation.

Aqueous solubility, the second factor, is vital for drug formulation and bioavailability. A compound's solubility level, determined through regression models, dictates its dissolution behavior and suitability for oral administration. Setting thresholds for solubility levels ensures that chosen compounds possess adequate aqueous solubility for effective drug delivery.

The ability to penetrate the blood-brain barrier (BBB) is crucial in central nervous system (CNS) drug development. Predictions of BBB permeability, typically based on logBB values, assess a

compound's capability to penetrate the BBB and reach CNS targets. Establishing thresholds for logBB ranges assists in selecting compounds with desired CNS activity while minimizing the risk of adverse effects.

Protein binding (PPB) predictions estimate the fraction of a compound bound to plasma proteins, impacting its distribution and pharmacokinetics. Compounds with moderate PPB levels are preferred to ensure sufficient free drug concentrations for therapeutic effects.

Moreover, molecular properties such as polar surface area (PSA) and molecular weight also influence a compound's ADMET profile. PSA descriptors reflect a compound's potential for hydrogen bonding and membrane permeability, while molecular weight affects absorption, distribution, and metabolism. In conclusion, selecting specific ADMET parameters and thresholds requires balancing desirable pharmacokinetic properties with safety considerations. These criteria play a crucial role in prioritizing compounds with optimal ADMET profiles for further drug development and clinical evaluation(26,27).

Out of the 30 examined compounds from *D. ebenum* and *O. umbellata*, Notably, 1,4-naphthoquinone from *D. ebenum* and compounds such as Nicotinic acid, Alizarin,Alizarin 1-methyl ether, 1,3-Dimethoxy-2-hydroxy-9,10-anthraquinone, Anthraquinone, Dasycarpidan-1-methanol, acetate, Cedrelopsin, E-11-Methyl-12-tetradecen-1-ol acetate from *O. umbellata* exhibited satisfactory ADMET properties. Notably, the commonly used drug Orlistat demonstrated suboptimal ADMET characteristics. Consequently, only the nine bioactive compounds, along with Orlistat, were selected for toxicity evaluation. These compounds adhered to drug-likeness guidelines, underscoring their potential suitability for oral medication.

Evaluating TOPKAT profiling

The safety efficacy of the selected bioactive compounds was comprehensively examined in this study through various toxicity indicators, including Ames mutagenicity (AMES), rodent carcinogenicity (based on the Food and Drug Administration (FDA) dataset),biodegradability, skin sensitization and developmental toxicity potential properties, were assessed using the TOPKAT module of Discovery Studio. The TOPKAT carcinogenicity predictor estimated the probability of carcinogenicity in the range of 0.000 – 0.006. Particularly Cedrelopsin and Alizarin 1-methyl ether exhibited a lack of carcinogenicity, supported by negative discriminant scores and very low probabilities.

The TOPKAT mutagenicity predictor identified some compounds as mutagenic, with positive discriminant scores and probabilities ranging from 0.071 to 9.982 (28, 29). However, the Compounds Cedrelopsin and Alizarin 1-methyl demonstrated nonmutagenic properties. Furthermore, these compounds displayed Rat Oral LD50 values within the Optimum Prediction Space. Considering the collective findings (Table 2), Cedrelopsin and Alizarin 1-methyl ether emerged as ideal lead compounds, exhibiting lower Ames mutagenicity, rodent carcinogenicity, and developmental toxicity potential compared to the established drug Orlistat. This strongly suggests their promising application in drug development. In summary, Cedrelopsin and Alizarin 1-methyl ether were identified as safe drug candidates, and their selection for subsequent pharmacophore, docking, and simulation studies is supported by their favorable safety profiles.

This study identified two novel bioactive compounds - Cedrelopsin, a coumarin, and alizarin-1-methyl ether, an anthraquinone derivative. Previous *in silico* analyses suggested Cedrelopsin holds osteoporosis therapeutic properties, with favorable drug-like properties (30, 31). Moreover, coumarins from many edible plants demonstrate versatile bioactivities including antibacterial, antifungal, antiviral, anti-HIV, and anticancer effects (32). Alizarin-1-methyl ether also exhibited potent antifungal activity against human pathogens (33,34). Anthraquinones

likewise demonstrate diverse bioactivities encompassing anticancer, anti-inflammatory, antimicrobial, diuretic, vasorelaxant, and phytoestrogen effects, suggesting possible clinical utility for various diseases (35). In summary, these novel compounds have an array of biological properties spanning antibacterial to cytotoxic that warrant further probing to fully determine their therapeutic potential. Elucidating the mechanisms underlying their bioactivities could uncover new treatment approaches for treating obesity. This computational study provides a robust way to explore their pharmacological activity experimentally.

Pharmacophore findings

Toxicity screening revealed two phytochemicals, Cedrelopsin, and alizarin 1-methyl ether, as promising hit compounds for further evaluation as FAS inhibitors. This study leveraged pharmacophore modeling to identify compounds with molecular features conferring anti-obesity bioactivity through FAS binding. The pharmacophore features of a compound play a crucial role in predicting its interactions with the target. Heterocyclic compounds, integral in drug design, are found in over 90% of commercially available drugs, showcasing their broad therapeutic applications. The presence of specific

Table 2: The toxicological assessment of compounds using Discovery Studio									
Toxicity prediction									
Source of compounds	Compounds	Ames mutagenicity	FDA carcinogenicity (female mouse)	FDA carcinogenicity (male mouse)	Biodegradability	FDA carcinogenicity female rat	FDA carcinogenicity male rat)	Rat oral LD_{50}	Skin sensitization
D. ebenum	1,4-naphthoquinone	1	1	0.393	1	0.001	1	190 mg/kg	0.998
O. umbellata	Nicotinic acid	0	0	0	1	0	0	1.8g/kg	0
	Alizarin	1	0	1	0	0	1	2.1g/kg	1
	Alizarin 1-methyl ether	0.998	0.001	0.951	0	0.001	0.951	5.7 g/kg	0.005
	1,3-Dimethoxy-2-hydroxy-9,10-anthraquinone	1	0	0.645	0.022	0	0.645	7.9 g/kg	0.008
	Anthraquinone	0.001	1	1	0.982	1	1	3.5 g/kg	1
	Dasycarpidan-1-methanol, acetate	0	1	1	0	1	1	25.9mg/kg	1
	Cedrelopsin	0	0.152	0	0.976	0.152	0	5.7 g/kg	0
	E-11-Methyl-12-tetradecen-1-ol acetate	0.993	1	0.936	1	1	0.936	10 g/kg	0
Drug	Orlistat	1	1	0	0	1	0	3.5 g/kg	0

Diospyros ebenum and *Oldenlandia umbellata* Phytochemicals

functional groups or pharmacophores in a compound's structure often correlates with its toxicity (36).The geometric parameters within a 3D pharmacophore model delineate properties essential for target affinity. Calculated x, y, and z coordinates defining the spatial arrangement of key chemical features necessary for a molecule's interaction with a target protein (15,37). Moreover, distinguishing hydrophilic from hydrophobic points through the scrutiny of surrounding protein atoms, based on hydrogen-bond donating or accepting protein heavy atoms within a 3 Å radius, aligned with the typical distances observed in protein-ligand complexes where hydrogen bonds form between two heavy atoms (38). This approach provides valuable insights into the structural characteristics required for effective target interaction, laying the groundwork for the development of novel therapeutics in Obesity. In essence, the findings highlight the potential of Cedrelopsin and Alizarin 1-methyl ether to treat FAS-related medical conditions.

Table 3 and Figure 3 illustrate the pharmacophore features of the selected compounds, encompassing hydrogen bond acceptors (HBA), hydrogen bond donors (HBD), aromatic rings, and hydrophobic features. These features align with observations on Orlistat, a known FAS inhibitor. Ultimately, both hit compounds underwent docking studies against the FAS active site, setting the stage for further exploration of their potential as effective FAS inhibitors.

Exploration of Molecular Binding Sites

The study investigated the inhibitory efficacy of ligands by focusing on their interaction sites with FAS. A detailed examination identified the active site of FAS, and the nature of the interaction between Orlistat and FAS was determined using Discovery Studio 2D interaction analysis and literature review. The amino acid residues in the active site of FAS contain ARG 2482, SER 2308, TYR 2343, ALA 2419, HIS 2481, LEU 2222, SER 2308, GLU 2251, THR 2255, VAL 2256, THR 2307, SER 2221, PRO 2249, ASP 2338, PHE 2370, PHE 2371, LYS 2426, SER 2422, GLY 2339, TYR 2309, THR 2342, SER 2340, ILE 2250, GLN 2374, PHE 2423, PHE 2375 (20).Noteworthy findings revealed that Orlistat exhibited a substantial interaction with the active site, forming three hydrogen bonds with amino acids ARG 2482, SER 2308, and TYR 2343. Additionally, alkyl bond interactions were discerned with LEU 2222, HIS 2481, TYR 2343, and ALA 2419. These findings help to design novel FAS inhibitors that leverage similar residue interactions to effectively bind the activation site and reduce enzymatic activity for therapeutic effect Table 4.

Molecular docking for drug discovery and design

In the molecular docking study targeting FAS, the filtered compounds, Cedrelopsin and Alizarin 1-methyl ether, demonstrated notable binding affinity as indicated by LibDock scores. The docking results exhibited favorable interactions, including hydrogen bonds and hydrophobic contacts within the binding site of FAS, indicating the potential for stable complex formation (Figure 4). Notably, multiple configurations were observed during docking, each characterized by a combined score encompassing Vander Waals forces, H-bonds, pi interactions, and other parameters in the form of LibDockscores (16).

Comparison of the docking scores of Cedrelopsin and Alizarin 1-methyl ether with the control drug Orlistat revealed promising results, suggesting their potential as FAS inhibitors. These findings offer molecular insights into the interaction mechanisms of the bioactive compounds with the target, providing a foundation for understanding their mode of action. The presence of hydrogen bonds in the docked complexes implies a role in stabilizing the interactions, contributing to conformational stability and, consequently, significant inhibitory activity against FAS. In summary, the molecular docking results suggest that Cedrelopsin and Alizarin 1-methyl ether may serve as potential inhibitors of FAS, paving the way for further exploration in drug development.

Table 3: Pharmacophore features (Hydrogen donor, Hydrogen acceptor, Aromatics, and Hydrophobic) of the compounds

Compounds					
	Pharmacophore features	X	Y	Z	Radius
Cedrelopsin	HB_ACCEPTOR1	3.3	-4.56	2.72	2.2
	HB_ACCEPTOR2	5.08	-3.04	0.1	2.2
	HB_ACCEPTOR3	3.84	2	-0.06	2.2
	HB_ACCEPTOR4	-5.84	3.26	-0.16	2.2
	HB_ACCEPTOR5	-6.68	0.34	-0.08	2.2
	HB_DONOR1	5.08	-3.04	0.1	2.2
	HB_DONOR2	3.84	2	-0.06	2.2
	RING_AROMATIC1	0.307641	-1.46434	3.01502	2.2
	RING_AROMATIC2	0.355359	-1.62333	-2.98269	2.2
	Hydrophobic1	2.72	-4.04	-1.18	1.6
	Hydrophobic2	-1.08	3.36	0.9	1.6
	Hydrophobic3	0.44	-2	0.02	1.6
Alizarin 1-methyl ether	HB_ACCEPTOR1	2.92	-3.1	2.96	2.2
	HB_ACCEPTOR2	0.7	-5.26	0.48	2.2
	HB_ACCEPTOR3	-2.02	5.76	-0.42	2.2
	HB_ACCEPTOR4	6.62	2.26	0.06	2.2
	HB_ACCEPTOR5	5.26	-2.74	0.42	2.2
	HB_DONOR1	6.62	2.26	0.06	2.2
	HB_DONOR2	5.26	-2.74	0.42	2.2
	RING_AROMATIC1	1.88724	0.650384	-2.9348	2.2
	RING_AROMATIC2	-3.10253	-0.129466	2.99651	2.2
	RING_AROMATIC3	1.71709	1.08328	3.04714	2.2
	RING_AROMATIC4	-2.92913	-0.564534	-2.98518	2.2
	Hydrophobic1	2.76	-2.5	-0.96	1.6
	Hydrophobic2	-3.86	-0.58	0	1.6
	Hydrophobic3	2.56	1.58	0	1.6
Orlistat	HB_ACCEPTOR1	8.38	-1.34	2.22	2.2
	HB_ACCEPTOR2	8.92	4.5	2.46	2.2
	HB_ACCEPTOR3	3.18	-2.52	-0.92	2.2
	HB_ACCEPTOR4	5.98	-2.96	0.16	2.2
	HB_ACCEPTOR5	2.06	0.28	-1.08	2.2
	HB_ACCEPTOR6	13.16	1.26	-3.66	2.2
	HB_ACCEPTOR7	14.88	3.3	-2.26	2.2
	HB_ACCEPTOR8	18.96	3.82	-0.64	2.2
	HB_ACCEPTOR9	16.76	1.82	-0.92	2.2
					(*Contd.*)

Table 3: Pharmacophore features (Hydrogen donor, Hydrogen acceptor, Aromatics, and Hydrophobic) of the compounds (*Contd.*)

Compounds				
HB_ACCEPTOR10	18.36	6.66	0.24	2.2
HB_DONOR1	14.54	1.18	-0.76	2.2
Hydrophobic1	19.34	-8.42	0.06	1.6
Hydrophobic2	18.04	-6.3	-0.02	1.6
Hydrophobic3	14.92	-3.82	0.16	1.6
Hydrophobic4	11.96	-0.86	0.02	1.6
Hydrophobic5	-1.9	3.7	0.04	1.6
Hydrophobic6	2.26	3.22	0.26	1.6
Hydrophobic7	10.48	6.62	0.62	1.6

Table 4: Molecular docking of FAS with *D.ebenum,* and *O.umbellata* compounds

| Molecule	Absolute energy	Relative energy	Libdock score	No. of H-bond & interaction	Other bond interaction	No. of Carbon hydrogen bond & interaction
Cedrelopsin	42.6263	12.6795	69.5082	3 OH-HIS 2481, O-TYR 2343, O-ARG 2482	6 GLU 2251, ARG 2482, TYR 2307, VAL 2256	1 H-GLU 2251
Alizarin 1-methyl ether	48.3457	3.04866	52.8854	3 O-TYR 2343, O-SER 2308, O-TYR 2307	6 PRO 2249, HIS 2481, ILE 2250, GLU 2251	1 H-GLU 2251
Orlistat	67.4006	8.26036	144.714	3 O-ARG 2482, O-SER 2308, O-TYR2343	4 LEU 2222, HIS 2481, TYR 2343, ALA 2419	2 H-2308, H-2343
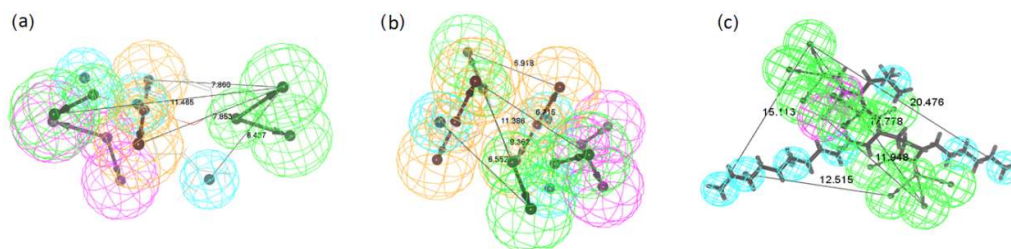
Figure 3: Pharmacophore model of FAS inhibitors (a) Cedrelopsin, (b) Alizarin 1-methyl ether, and (c) Orlistat mapping. Pharmacophoric features are represented as follows: hydrogen bond acceptor (green), hydrogen bond donor (magenta), hydrophobic (cyan), and ring aromatic (orange)
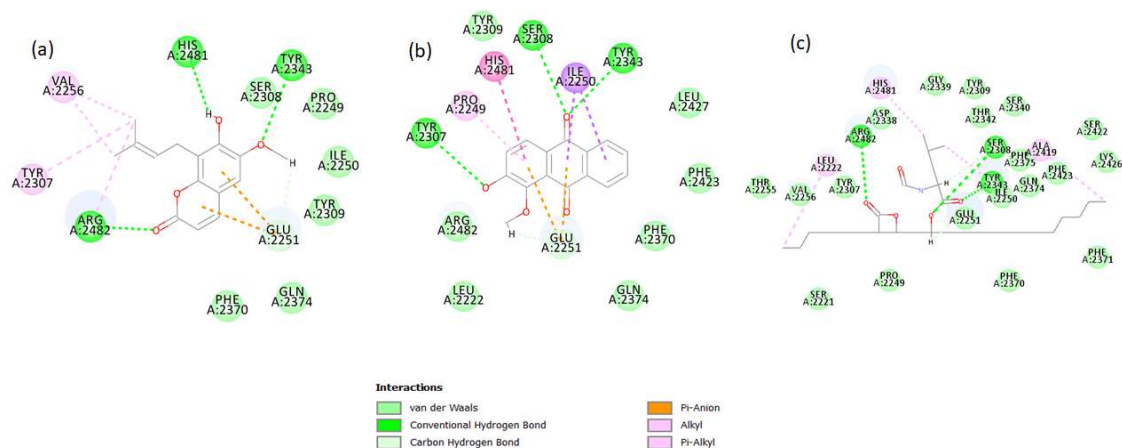
Figure 4: 2D interactions of enzyme FAS with a) Cedrelopsin b) Alizarin 1-methyl ether c) Orlistat
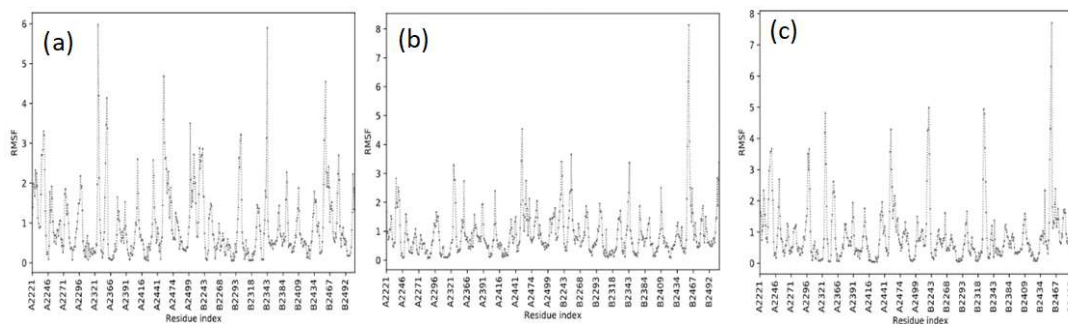

Figure 5: Value of the root mean square fluctuation (RMSF) plot of the compounds and FAS complex a) Cedrelopsin b) Alizarin 1-methyl ether c) Orlistat

Molecular dynamics analysis using cabs-flex 2.0

The conformational stability of FAS and its complexes with phytochemical ligands was assessed using CABS-flex. The dynamics of ligand-protein interactions were explored to identify key amino acid residues involved. Specifically, the analysis focused on a potent compound from previous docking studies, including Cedrelopsin, Alizarin 1-methyl ether, and the FDA-approved drug Orlistat. Results revealed that the Root Mean Square Fluctuation (RMSF) value of FAS, when bound to Alizarin 1-methyl ether and Orlistat, was notably high at 8 Å, decreasing to below 6 Å when bound to Cedrelopsin

(Figure 5). The reduced RMSF values suggest stable interactions in the latter complexes, indicating favorable conformational stability and highlighting the potential of Cedrelopsin as a stabilizing agent for FAS.

An examination of the RMSF values reveals that the amino acid residues at the termini of the protein demonstrated high flexibility with RMSF values above the average of 3.0 Å. In contrast, the majority of the interacting residues involved in binding displayed RMSF values under 2.0 Å, underscoring their comparative stability during the 10 nanosecond molecular dynamics simulation. Not with standing, a few

Diospyros ebenum and *Oldenlandia umbellata* Phytochemicals

critical binding residues near positions 2467, 2343, and 2321 showed some flexibility with RMSF values over 2.0 Å. Similarly, in its unbound state, the terminal residues exhibited higher RMSF values than the central region of the protein. Meanwhile, the changing RMSF values of the ligand signify ligand continuously altered its binding pose in an attempt to find a more stable configuration (39). The MD simulations affirmed the structural flexibility observed in the NS2B/NS3-taraxerol docking complex and NS5–apigenin complex, with RMSF values consistently 5 Å. This dynamic behavior aligns with findings from prior studies, highlighting the importance of considering structural flexibility in understanding protein-ligand interactions (40). The RMSF analysis uncovered significant fluctuations in the protein/peptide complexes, with SERPINI1 (serine proteinase inhibitor 1) exhibiting the most noteworthy fluctuation at 8.807 Å, observed at residue no. 353. These findings align with earlier studies that similarly emphasized the importance of understanding protein flexibility for elucidating functional implications. The observed diverse structural dynamics in the complexes contribute valuable insights into their flexibility, potentially influencing their biological functions (41).

The findings of this study align with previous research on FAS inhibitors and anti-obesity agents derived from natural sources. Specifically, the identification of organosulfur compounds in garlic, such as Allicin, Alliin, E-Ajoene, and Z-Ajoene, as potential FAS inhibitors resonates with the broader exploration of natural compounds for their anti-obesity properties. The similarity in binding sites between these compounds and statins underscores their potential as alternative therapeutic agents for managing lipid-related disorders (42). Additionally, the study is in line with previous research on FAS inhibitors like curcumin, resveratrol, and EGCG. Moreover, the discovery of citral's anticancer properties through lipogenesis inhibition further reinforces the multifaceted potential of natural compounds in combating

obesity and cancer (43). Furthermore, an earlier study introduces rosmarinic acid and its analogs, particularly ZINC85948835, as potential FAS inhibitors targeting the Thioesterase domain. Compared to previous studies, these compounds exhibit promising binding affinities and interactions with the FAS TE domain, suggesting their potential as novel therapeutic agents. In sum, this study expands the repertoire of natural compounds with anti-obesity and anticancer properties, offering new avenues for drug development and highlighting the potential of phytochemicals in combating metabolic and oncological diseases (44, 45).

Currently, no experimental validations have confirmed the predicted interactions between the lead compounds, Cedrelopsin, and Alizarin 1-methyl ether, and FAS. The study suggests further experimental validation to confirm these compounds' efficacy as anti-obesity agents. This typically involves in vitro assays to assess their inhibitory activity against FAS directly. While the earlier study proposed a novel mass spectrometry-based assay for monitoring FAS activity and product specificity, experimental validation of the lead compounds' interactions with FAS is crucial to confirm their inhibitory effects (46). Additionally, in vivo studies may be conducted to evaluate the efficacy of the lead compounds in animal models of obesity, further validating their potential as therapeutic agents.

The present study utilized several *in silico* prediction methods to analyze the oral bioavailability of compounds, which could facilitate the design of novel, safer drugs. Performing preliminary computational analyses enables the prediction of bioavailability before experimental testing, thus saving considerable time and money in drug development. In summary, *O. umbellata* phytochemicals, particularly Cedrelopsin and Alizarin 1-methyl ether, exhibit potent anti-obesity potential by targeting fatty acid synthase, offering non-toxic, efficacious alternatives for managing fatty acid accumulation and preventing obesity.

Current Trends in Biotechnology and Pharmacy
Vol. 18 (Supplementry Issue 4A) 121 - 137, November 2024, ISSN 0973-8916 (Print), 2230-7303 (Online)
10.5530/ctbp.2024.4s.10

134

Conclusion

In conclusion, the computational analyses into fatty acid synthase (FAS) inhibition highlighted the phytochemicals from *O.umbellata*, Cedrelopsin and Alizarin 1-methyl ether as promising lead compounds with favorable ADMET profiles, low toxicity, and significant binding affinity to FAS. Molecular docking and simulation studies underscored their potential as effective FAS inhibitors, offering insights into their mode of action and conformational stability. These initial *in silico* experiments highlight the potential of leveraging *O. umbellata* compoundsas potential candidates for further exploration in drug development to manage obesity, emphasizing their importance in advancing therapeutic strategies against lipogenesis.

Conflict of interest

The authors have declared that there are no existing conflicts of interest

References

1. Li, D., & Chen, F. (2023). The Perspectives of Plant Natural Products for Mitigation of Obesity. Nutrients, 15(5): 1150.

2. Park, S.H., Park, J., Lee, M., Kim, J., Eun, S., Jun, W., & Lee, J. (2023). Antiobesity effect of Kaempferia parviflora accompanied by inhibition of lipogenesis and stimulation of lipolysis. Food & Nutrition Research, 67.

3. Likitnukul, S., Thammacharoen, S., Sriwatananukulkit, O., Duangtha, C., Hemstapat, R., Sunrat, C., & Pinthong, D. (2023). Short-Term Growth Hormone Administration Mediates Hepatic Fatty Acid Uptake and De Novo Lipogenesis Gene Expression in Obese Rats. Biomedicines, 11(4), 1050.

4. Xu, G., Zhao, Z., Wysham, W.Z., Roque, D.R., Fang, Z., Sun, W., & Bae-Jump, V. (2023). Orlistat exerts anti-obesity and anti-tumorigenic effects in a transgenic mouse model of endometrial cancer. Frontiers in Oncology, 13.

5. Shaik Mohamed Sayed, U.F., Moshawih, S., Gupta, G., SINGH, S.K., CHELLAPPAN, D.K., Dua, K., & Goh, B.H. (2023). Natural Products as Novel Anti-Obesity Agents: Insights into Mechanisms of Action and Potential for Therapeutic Management. Frontiers in Pharmacology, 14: 1182937.

6. Athista, M., Harsiddhi, A., Nachiyar, C.V., &Sunkar, S. (2023). Therapeutic potential of natural compounds in the treatment of obesity: A review on computational and experimental studies. Medicinal Plants-International Journal of Phytomedicines and Related Industries, 15(1), 79-97.

7. Baravalia, Y., Kaneria, M., Vaghasiya, Y., Parekh, J., & Chanda, S. (2009). Antioxidant and antibacterial activity of Diospyros ebenum Roxb. leaf extracts. Turkish Journal of Biology, 33(2), 159-164.

8. Subramanian, P., Ravichandran, A., Manoharan, V., Muthukaruppan, R., Somasundaram, S., Pandi, B., & You, S. (2019). Synthesis of Oldenlandia umbellata stabilized silver nanoparticles and their antioxidant effect, antibacterial activity, and bio-compatibility using human lung fibroblast cell line WI-38. Process Biochemistry, 86, 196-204.

9. Sadybekov, A.V., &Katritch, V. (2023). Computational approaches streamlining drug discovery. Nature, 616(7958), 673-685.

10. Bassani, D., & Moro, S. (2023). Past, present, and future perspectives on computer-aided drug design methodologies. Molecules, 28(9), 3906.

11. Athista, M., Hariharan, V., Namratha, K., Pavankumar, G., &Sunkar, S. (2023). Computational identification of natural compounds as potential inhibitors for HMGCoA reductase: Natural inhibitors for HMGR. Current Trends in Biotechnology and Pharmacy, 17(4), 1457-1485.

12. Kim, S., Thiessen, P.A., Bolton, E.E., Chen, J., Fu, G., Gindulyte, A., & Bryant, S.H. (2016). PubChem substance and compound databases. Nucleic acids research, 44(D1): D1202-D1213.

Diospyros ebenum and *Oldenlandia umbellata* Phytochemicals

13. Subha, C., Pavithra, B., & Jophy Vincent, V. (2021). *In silico* molecular docking and admet toxicity studies of polyesters containing oxadiazole moiety. ijbpas, 10(11), 1497-1509.

14. Daoui, O., Elkhattabi, S., Chtita, S., Elkhalabi, R., Zgou, H., & Benjelloun, A.T. (2021). QSAR, molecular docking and ADMET properties *in silico* studies of novel 4, 5, 6, 7-tetrahydrobenzo [D]-thiazol-2-Yl derivatives derived from dimedone as potent anti-tumor agents through inhibition of C-Met receptor tyrosine kinase. Heliyon, 7(7).

15. Prasetiya, F.S., Destiarani, W., Prihastaningtyas, I.R.C., Agung, M.U.K., & Yusuf, M. (2023). Computational simulations of microalgae-derived bioactive compounds as a novel inhibitor against B-Raf V600E driven melanoma. Journal of Applied Pharmaceutical Science, 13(6): 068-086.

16. Önder, F.C. Discovery Of Donepezil-Like Compounds As Potential Acetylcholinesterase Inhibitors Determined By Pharmacophore Mapping-Based Virtual Screening And Molecular Docking. SdüTıpFakültesiDergisi, 30(2), 143-153.

17. Oduselu, G.O., Afolabi, R., Ademuwagun, I., Vaughan, A., & Adebiyi, E. (2023). Structure-based pharmacophore modeling, virtual screening, and molecular dynamics simulation studies for identification of Plasmodium falciparum 5-aminolevulinate synthase inhibitors. Frontiers in Medicine, 9, 1022429.

18. Alam, S., & Khan, F. (2018). Virtual screening, Docking, ADMET and System Pharmacology studies on Garcinia caged Xanthone derivatives for Anticancer activity. Scientific reports, 8(1), 5524.

19. Singh, J., Kumar, M., Mansuri, R., Sahoo, G.C., & Deep, A. (2016). Inhibitor designing, virtual screening, and docking studies for methyltransferase: a potential target against dengue virus. Journal of pharmacy &bioallied sciences, 8(3), 188.

20. Umar, A.K. (2021). Flavonoid compounds of buahmerah (Pandanus conoideus Lamk) as a potent SARS-CoV-2 main protease inhibitor: *in silico* approach.

Future Journal of Pharmaceutical Sciences, 7(1), 158.

21. Mandal, M., & Mandal, S. (2024). Discovery of multitarget-directed small molecule inhibitors from Andrographis paniculata for Nipah virus disease therapy: molecular docking, molecular dynamics simulation and ADME-Tox profiling. Chemical Physics Impact, 100493.

22. Pemble IV, C.W., Johnson, L.C., Kridel, S.J., & Lowther, W.T. (2007). Crystal structure of the thioesterase domain of human fatty acid synthase inhibited by Orlistat. Nature structural & molecular biology, 14(8), 704-709.

23. Rashed, K.N. (2013). Antioxidant activity from Diospyros Ebenum stems extracts and phytochemical profile. JAIS, 1: 70-72.

24. Reddy, B.M. (2021). Pharmacognostical and phytochemical evaluation of an important medicinal plant Oldenlandia umbellata L. Journal of Pharmacognosy and Phytochemistry, 10(6), 288-291.

25. Singh, S., & Srivastava, P. (2015). Molecular docking studies of myricetin and its analogues against human PDK-1 kinase as candidate drugs for cancer. Computational Molecular Bioscience, 5(02): 20.

26. Ponnan, P., Gupta, S., Chopra, M., Tandon, R., Baghel, A.S., Gupta, G., & Raj, H.G. (2013). 2D-QSAR, docking studies, and *in silico* ADMET prediction of polyphenolic acetates as substrates for protein acetyltransferase function of glutamine synthetase of *Mycobacterium tuberculosis*. International Scholarly Research Notices, 2013.

27. Alesawy, M.S., Elkaeed, E.B., Alsfouk, A.A., Metwaly, A.M., & Eissa, I.H. (2021). *In silico* screening of semi-synthesized compounds as potential inhibitors for SARS-CoV-2 papain-like protease: Pharmacophoric features, molecular docking, ADMET, toxicity and DFT studies. Molecules, 26(21): 6593.

28. Alesawy, M.S., Elkaeed, E.B., Alsfouk, A.A., Metwaly, A.M., & Eissa, I.H. (2021). *In silico* screening of semi-synthesized compounds as potential inhibitors for SARS-

CoV-2 papain-like protease: Pharmacophoric features, molecular docking, ADMET, toxicity and DFT studies. Molecules, 26(21), 6593.

29. Venkataramanaa, C.H.S., Sravania, K.R., Singha, S.S., &Madhavanb, V. (2011). In-silico ADME and toxcity studies of some novel indole derivatives. Journal of Applied Pharmaceutical Science, (Issue), 159-162.

30. Paramasivam, S., & Perumal, S.S. (2024). *In silico* Rationalization for Leads from Oldenlandia umbellata L. to Inhibit Multiple Molecular Targets Regulating Osteoporosis. Pharmacognosy Magazine, 09731296231196189.

31. Nascimento, L.P., Passos, M.D.S., Nogueira, T.S., Vieira, M.G., Moreira, A.S.N., Braz-Filho, R., &Vieiraa, I.J. (2021). Isolation and Identification of Prenylated Coumarins from the Species Flindersiabrayleyana F. Muell (Rutaceae). Revista Virtual de Química, 13(5), 1122-1129.

32. Hussain, M.I., Syed, Q.A., Khattak, M.N.K., Hafez, B., Reigosa, M.J., & El-Keblawy, A. (2019). Natural product coumarins: biological and pharmacological perspectives. Biologia, 74, 863-888.

33. Rath, G., Ndonzao, M., &Hostettmann, K. (1995). Antifungal anthraquinones from Morinda lucida. International journal of pharmacognosy, 33(2), 107-114.

34. Chien, S.C., Wu, Y.C., Chen, Z.W., & Yang, W.C. (2015). Naturally occurring anthraquinones: chemistry and therapeutic potential in autoimmune diabetes. Evidence-Based Complementary and Alternative Medicine, 2015.

35. Masi, M., & Evidente, A. (2020). Fungal bioactive anthraquinones and analogues. Toxins, 12(11): 714.

36. Oduselu, G.O., Afolabi, R., Ademuwagun, I., Vaughan, A., & Adebiyi, E. (2023). Structure-based pharmacophore modeling, virtual screening, and molecular dynamics simulation studies for identification of *Plasmodium falciparum* 5-aminolevulinate synthase inhibitors. Frontiers in Medicine, 9, 1022429.

37. Luo, L., Zhong, A., Wang, Q., & Zheng, T. (2021). Structure-based pharmacophore modeling, virtual screening, molecular docking, ADMET, and molecular dynamics (MD) simulation of potential inhibitors of PD-L1 from the library of marine natural products. Marine Drugs, 20(1), 29.

38. Mortier, J., Dhakal, P., &Volkamer, A. (2018). Truly target-focused pharmacophore modeling: a novel tool for mapping intermolecular surfaces. Molecules, 23(8), 1959.

39. Umar, A.K., Zothantluanga, J.H., Luckanagul, J.A., Limpikirati, P., &Sriwidodo, S. (2023). Structure-based computational screening of 470 natural quercetin derivatives for identification of SARS-CoV-2 Mpro inhibitor. PeerJ, 11, e14915.

40. Mukhtar, M., & Khan, H.A. (2023). Exploring the inhibitory potential of Nigella sativa against dengue virus NS2B/NS3 protease and NS5 polymerase using computational approaches. RSC advances, 13(27), 18306-18322.

41. Sumera, Anwer, F., Waseem, M., Fatima, A., Malik, N., Ali, A., & Zahid, S. (2022). Molecular docking and molecular dynamics studies reveal secretory proteins as novel targets of temozolomide in glioblastoma multiforme. Molecules, 27(21), 7198.

42. Bhadra, P. (2020). In-silico analysis of inhibitory action of garlic against hyperlipidemia by FAS enzyme. Indian Journal of Natural Sciences, 10(60): 20786-2079.

43. Balusamy, S.R., Perumalsamy, H., Veerappan, K., Huq, M.A., Rajeshkumar, S., Lakshmi, T., & Kim, Y.J. (2020). Citral induced apoptosis through modulation of key genes involved in fatty acid biosynthesis in human prostate cancer cells: *In silico* and in vitro study. BioMed research international, 2020.

44. Panman, W., Nutho, B., Chamni, S., Dokmaisrijan, S., Kungwan, N., & Rungrotmongkol, T. (2018). Computational screening of fatty acid synthase inhibitors

against thioesterase domain. J Biomol Struct Dyn, 36(15), 4114-4125.

45. Abhimanyu, Srivastava, P., & Jain, C. K. (2022). In-Silico Investigation of Plant-Derived Natural Allosteric Compounds Towards Enhanced Drug-Protein Interaction of MOA Protein Complex in Depression Based on Molecular Docking and Molecular Dynamic Simulation Approaches. Current Trends in Biotechnology and Pharmacy, 16(4), 529–539. https://doi.org/10.5530/ctbp.2022.4.86

46. Topolska, M., Martínez-Montañés, F., & Ejsing, C.S. (2020). A Simple and Direct Assay for Monitoring Fatty Acid Synthase Activity and Product-Specificity by High-Resolution Mass Spectrometry. Biomolecules, 10(1): 118.

A Study on Toxicity Mechanisms of Xenobiotics Using Network Pharmacology Approach

Shreenidhi K S, Vigneshwar R, Sai Rahul Sv, Jothi Murugan S, Maline M, Sujata Roy*, and Vijaya Geetha*

Department of Biotechnology, Rajalakshmi Engineering College (Autonomous), Thandalam, Chennai 602105, Tamil Nadu, India
*Corresponding author: sujataroy@rajalakshmi.edu.in

Abstract

In recent years, modern medicine has grown exponentially. Many drugs are being developed and reused for different diseases. Although these drugs help cure these diseases, there are some side effects on the human body. The most affected organ in the human body. Is the liver these side effects in the liver were studied using marine toxicity studies using several species of marine organisms. This study aimed to investigate the toxicity mechanisms of xenobiotics using a network pharmacological approach. Xenobiotics are chemicals that are foreign to an organism and exposure to them can cause adverse health effects. Network pharmacology is a systems-level approach that integrates information about interactions between drugs, proteins, and biological pathways. The study involved using publicly available data to construct a human xenobiotic-protein interaction network using sites such as PubChem, PharmMapper, the KEGG/PANTHER pathway, and the Cytoscape software. The network was analysed to identify key proteins and pathways involved in xenobiotic toxicity. The study also explores the potential for repurposing existing drugs to minimize xenobiotic toxicity. Study results reveal several key targets and pathways involved in xenobiotic toxicity, including oxidative stress, inflammation, and apoptosis. The study also identified several existing drugs that could potentially be repurposed to minimize xenobiotic toxicity. Taken together, this study provides insight into the mechanisms underlying xenobiotictoxicity and highlights the potential for using network pharmacological approaches toidentify novel therapies for the treatment of xenobiotic diseases.

Keywords: Xenobiotics, Network pharmacology, PubChem, PANTHER pathway, PharmMapper

Introduction

Xenobiotics are foreign chemical substances that the body doesn't naturally produce. The liver is the vital organ responsible for the metabolism and excretion of xenobiotics. Some xenobiotics can damage liver cells and become toxic (1-5),but others go through a process called biotransformation in the liver that makes them more readily excretable (6). The effects of xenobiotics are influenced by various factors, including dosage, duration of exposure, chemical properties of the xenobiotic, and individual variations in liver function (7-9). Hepatotoxicity, steatosis, inflammation, poor drug metabolism, and carcinogenicity are typical effects (10 - 11) hang. The effects of xenobiotics are very critical (12). It is true that knowledge of xenobiotic mechanisms is essential for remedial research. While many of the proteins impacted by xenobiotics are well-known, there might be some that are still unknown or poorly understood. Numerous enzymes, receptors, and transporters, including cytochrome P_{450} enzymes, nuclear receptors like PXR and CAR, and drug transporters like P-glycoprotein, have been found to be involved in the metabolism and response to xenobiotics (13-15). Ongoing research attempts to identify additional

proteins and pathways involved in xenobiotic-induced toxicity and therapeutic responses (16). Nevertheless, the complete scope of protein targets impacted by xenobiotics is still being clarified. This information is crucial for creating safer medications, focusing on treating specific diseases, and lessening the negative consequences of xenobiotic exposure (17-18).

Different studies have been reported on xenobiotics pathways (19). As CP450 is the main metabolising enzyme, it interacts with it. It also affects different detoxification pathways differently as the body eliminates it and its metabolites by these pathways. Many transporter pathways and signalling pathways are also affected by xenobiotics. Many xenobiotics may have harmful toxic effects that could be fatal if they are not completely removed and are not properly metabolized by xenobiotic metabolizing enzymes (20). That is why the spectrum of targets which get affected by xenobiotics should be studied. All xenobiotics are different, but as a foreign entity they have some similarity also (11). Here we have studied a few xenobiotics and their effects using bioinformatics tools (21). Also, their remedial methods were investigated. There are a number of xenobiotics present in the environment, but in this study, we have selected a few, these studies can be extended for other molecules using similar ways (20). The name of the compounds which we have chosen here are Acetaminophen, Amoxapine, Alfacalcidol, Atorvastatin, Bisphenol, Clomiphene, Dichlorvos, Diclofenac, Erythromycin and Lovastatin (22-25).

Artemisinin is an antimalarial drug derived from the sweet wormwood plant, *Artemisia annua*. Artemisinin-based combination therapies (ACT) are currently generally considered the best treatment for uncomplicated falciparum malaria (26-27). They are fast and reliably effective (28). The derivatives of artemisinin such as artemether, artesunate and dihydroartemisinic, have played a crucial role in the prevention and treatment of human schistosomiasis. They are also shown to be beneficial for many other conditions, against new viruses (e.g., HIV, Ebola virus, chikungunya virus, etc.) or classic infections caused by drug-resistant viral strains (e.g., human viruses, cytomegalovirus) (29). The fatal effects of diclofenac on marine life have been investigated. The hypothesis that the drug causes oxidative stress and metabolic disturbances in fish was supported by histopathological and cortisol studies. The toxic effects were reduced when *Artemisia pallens*, the remediator, was introduced, indicating the potential of the plant for natural regeneration and promoting environmental sustainability in fish models (30). Consequently, in order to prevent the long-term adverse effects, it is necessary to decrease the rate of use of painkillers like diclofenac (31). Here we have explored the possible remedial effects of xenobiotics and its mechanism through Bioinformatics lenses. First, we predicted the possible targets of these compounds and then studied and compared those using different bioinformatics tools (32-33).

Methodology

PubChem

PubChem is a large collection of freely accessible chemical information. The PubChem (pubchem.ncbi.nlm.nih.gov) is the world's largest collection of freely accessible chemical information. PubChem contains nucleotides, carbohydrates, lipids, peptides, chemically-modified macromolecules and other molecules. We collect information on chemical structures, identifiers, chemical and physical properties, biological activities, patents, health, safety, toxicity data, and many others. One of PubChem's key features is its ability to link chemicals to biological activity data. This allows researchers to explore the potential use of chemical compounds in drug discovery and other applications. This was accessed and the following drugs (Acetaminophen, Amoxapine, Alfacalcidol, Atorvastatin, Bisphenol, Clomiphene, Dichlorvos, Diclofenac,

Erythromycin and Lovastatin were searched for their structural information. These major drugs were chosen randomly for the study. Artemisinin also was searched and retrieved from the same website. The 3D conformers of the given xenobiotics were downloaded in .sdf format (34-37).

PharmMapper

The PharmMapper Server is a user-friendly online tool freely accessible designed to help find potential targets for specific small molecule probes using pharmacophore mapping. With its efficient mapping technique, PharmMapper can quickly identify potential target candidates from its database within hours(38). The server utilizes a comprehensive pharmacophore database that contains data on more than 7,000 protein structures and their related ligands (7). They have their own in-house repertoire of pharmacophore databases and annotations from different target databases like Binding DB, Target Bank. Drug Bank etc. This server is used for *in-silico* target identification using a pharmacophore model. The 3D conformer file was uploaded to the PharmMapper website (http://www.lilab-ecust.cn/pharmmapper/) and target count was set to 500. The default settings were used for other parameters. The results were downloaded in .csv file format (39).

PANTHER Pathway

PANTHER Pathway is a comprehensive online tool developed by the University of Pittsburgh to help students explore and plan their academic and career paths. This tool is available to current and prospective students, as well as alumni. There are over 177 pathways in the Panther pathway including metabolic and signalling pathways which can be explored. The targets from the PharmMapper results are used as input for the PANTHER pathway for pathway analysis. Various pathways for the involved targets and their molecular function can be accessed (40).The diagram can also be exported as SBGN Pathway and they are interactive and include tools for visualizing gene expression data.

Cytoscape

Cytoscape is an open source software platform for the visualization and analysis of complex networks. It is widely used in bioinformatics and systems biology, but can also be used in other fields that are related to network analysis, such as social network analysis, traffic network analysis, etc. (3).Cytoscape allows users to import network data from various sources, such as Excel spreadsheets, text files, or databases. Users can then manipulate the data, add properties to nodes and edges, and apply different algorithms to analyze and visualize the network. The PharmMapper results are used for drug interaction network analysis by cytoscape (41). The PDB ID is converted to Gene ID for accurate results (42). The drug name is given as source node and the target as target node. Using layout functions, the targets are displayed in a network (43). The intersection function is used to merge multiple networks and find all possible targets which are present in all xenobiotic drugs. All the networks of 10 xenobiotics were merged to get the common targets of all 10 compounds. The targets of artemisinin were compared with all the targets and found HSP90B1 is common (pdb 1d: 1tbw) with HSP90AA1 (1ihg) with diclofenac (44)

Homology Modelling, Docking and visualisation

From the PharmMapper and Cytoscape analysis we have come to know that HSP90 is the common target for all xenobiotics including diclofenac and artemisinin (45). Thus, we investigated the binding site and binding mode of diclofenac and Artemisinin with HSP90. As the experimental studies have been conducted with fish models, we have modelled the structure of HSP90 protein from "*Pangasianodon hypophthalmus*".

The protein sequence of 'heat shock protein 90, alpha (cytosolic), class A member 1, tandem duplicate 2' (Accession no.: XP_026779203) (46) of *Pangasianodon*

Current Trends in Biotechnology and Pharmacy
Vol. 18 (Supplementry Issue 4A) 138 - 151, November 2024, ISSN 0973-8916 (Print), 2230-7303 (Online)
10.5530/ctbp.2024.4s.11

141

hypophthalmus was obtained from NCBI GenBank. The template 'Chain A, HEAT SHOCK PROTEIN HSP 90 BETA' (PDB Id: 5FWK) (10) with 86.52% identity and 'Chain A, kDa heat shock protein, mitochondrial' (PDB Id: 4PJ1) (47) with 87.71% identity obtained from the PDB site was modelled using the template 'Chain A, HEAT SHOCK PROTEIN HSP 90 BETA' and 'Chain A, kDa heat shock protein, mitochondrial' respectively. The Modeller 10.1 tool was used in modelling to obtain the 3D structures of heat shock protein and then optimized. The protein model was validated using Ramachandran plot through PRO-CHECK analyses.

The ligands Artemisinin and Diclofenac were obtained from PubChem Artemisinin_Conformer3D_CID_68827 and Diclofenac_Conformer3D_CID_3033 (48) respectively. The 3D structures were docked into the docking grid of the 3D structures of heat shock protein: HSP90 by Autodock vina v1.2.0 (49). The identification of hydrogen and hydrophobic interactions in the protein-ligand complexes were analysed using BIOVIA Discovery Studio Visualizer (50). III. Visualization of Molecular Docking: The docking positions were validated through the best DOPE scores.

Results and Discussion

Cytoscape software was utilized to explore the xenobiotic and target interaction. Here we have shown only for AMOXAPINE (Figure 1) (51). Same procedure was followed for all 10 xenobiotics and then merged to get the common targets (Figure 2). (Other pictures can be provided as Supplementary materials)

Cytoscape Network of the targets obtained from the PharmMapper for the xenobiotic Amoxapine

Total 9 proteins are found to be the same in all the 10 xenobiotics. Beta-lactamase, Heat shock protein HSP90-alpha, Tyrosine-protein phosphatase non-receptor type I, CAMP –specific, 3,5 cyclic phosphodiesterase 4D, Stromelysin-1, CDK2, Glycogen phosphorylase, carbonic anhydrase 2, Mitogen-activated protein kinase 14.

Panther Pathway analysis

Panther pathway analysis of the gene list from the predicted targets of Acetaminophen shows that the most predominant path is unknown or uncharacterised. The second most predominant pathway is angiogenesis. Most of the other xenobiotics showed the same pattern (Figure 3).
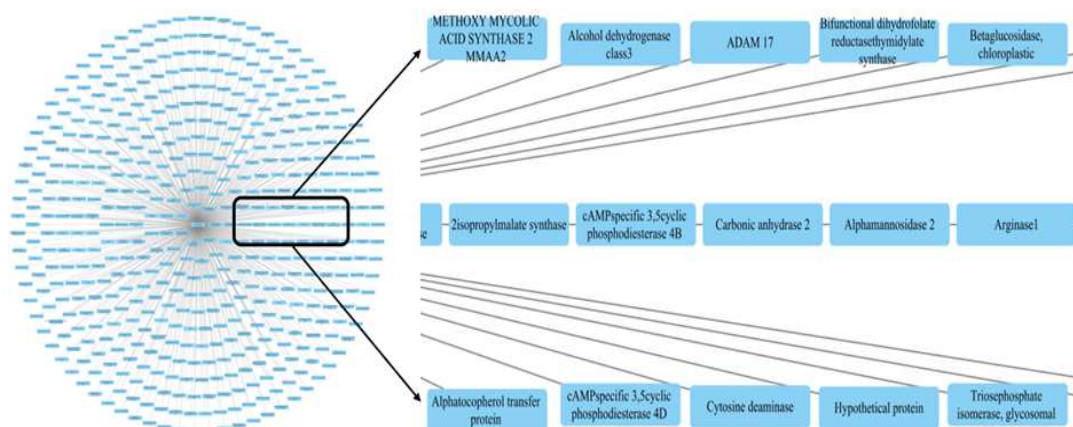

Figure 1: Cytoscape network for Amoxapine

Shreenidhi et al

Diclofenac and Artemisinin:

Our aim is to find the common pathways of these xenobiotics and whether artemisinin can act as a remedy (Figure 4) (52). To understand that we compared the targets of diclofenac (53) and targets of artemisinin using a Venn diagram. The uniport IDs of the targets from the output of PharmMapper of diclofenac and all the targets of artemisinin were taken and performed the Venn diagram analysis using (Draw Venn Diagram (ugent.be)). The common targets are listed below in Table 1. Most of the proteins are involved in enzymatic reaction, catalysis, metabolic process, cellular process and biological regulation. The network of genes which are affected by both diclofenac and artemisinin is shown in Figure 5. With these proteins Artemisinin and Diclofenac both may have competitive binding effects. ALB protein is a very crucial (high degree) protein in this network.

Comparison of data with Artemisinin

It has been observed that ALB gene, serum albumin binds with Artemisinin. Recent docked structure shows the atomic level interaction of Serum albumin and Artemisinin. Similarly, structural studies of the diclofenac, binding to human serum albumin has been resolved (54). In both the cases the residue R218 plays a crucial role. Both the compounds bind with the same cavity. The drug pharmacokinetics varies because of this competitive binding (55).

Detailed investigation of binding of artemisinin and diclofenac shows that artemisinin binds with HSP90B1 and Diclofenac binds with chaperon protein HSP90AA1 (not shown in the network). So, there must be a mechanistic role of HSP90 protein with both of these molecules so we did homology modelling studies of HSP90 protein using a fish model Figure 6.

The interaction of protein-ligand complexes indicates that the Artemisinin and Diclofenac binds to the same site and
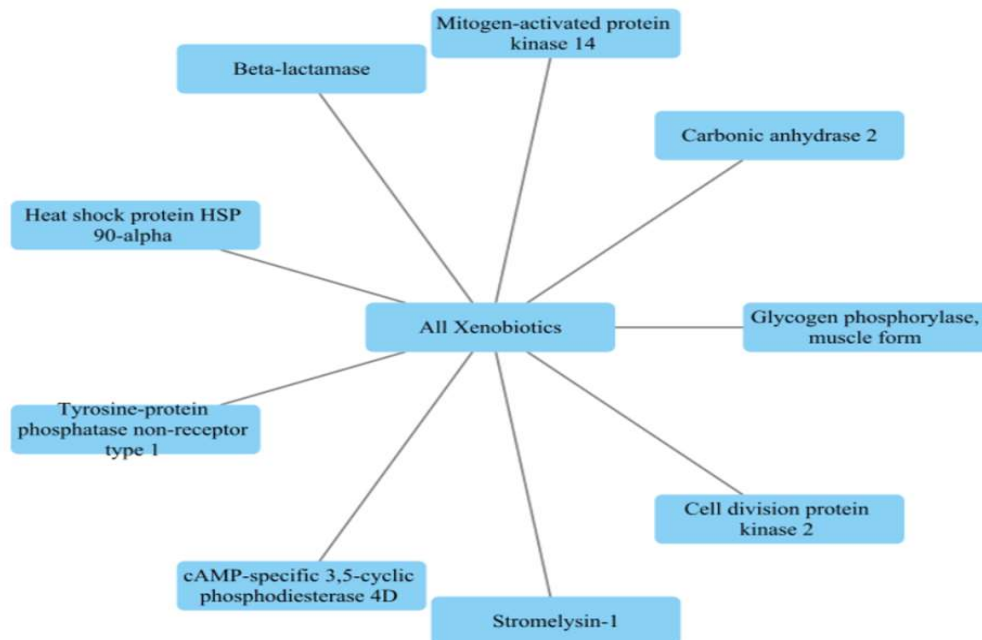

Figure 2: Cytoscape network of multiple xenobiotics

Toxicity Mechanisms of Xenobiotics

	No PANTHER category is assigned (UNCLASSIFIED)
	Angiogenesis (P00005)
	PDGF signaling pathway (P00047)
	Alzheimer disease-presenilin pathway (P00004)
	CCKR signaling map (P06959)

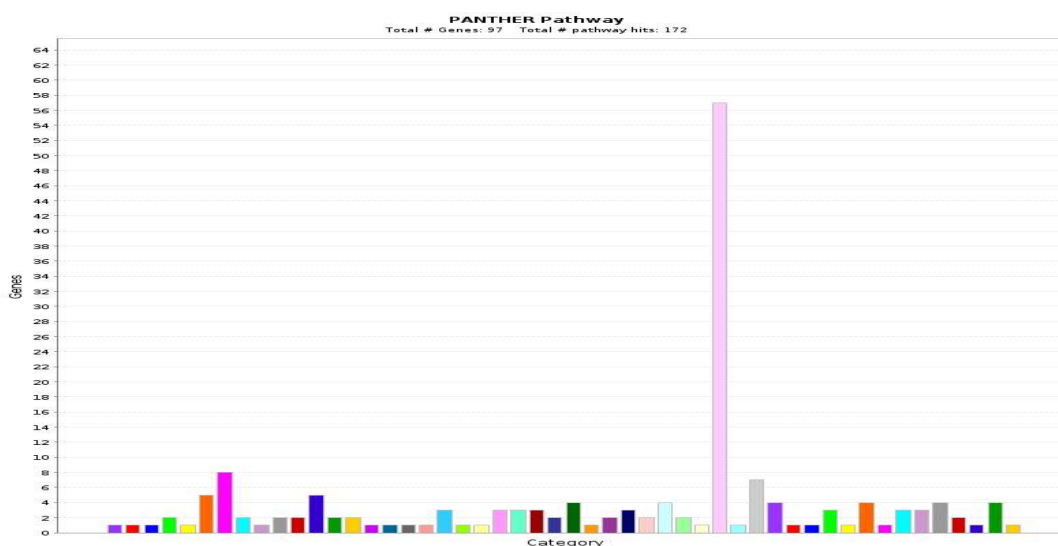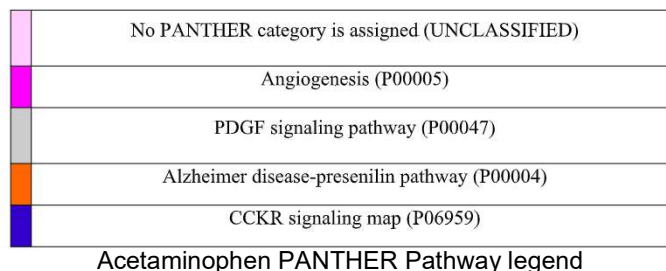Acetaminophen PANTHER Pathway legend

Figure 3: Panther pathway analysis of Acetaminophen

Artemisinin and the Diclofenac molecules tends to bind in different positions as the primary docking site is occupied. The amino acid associated with the interaction of HSP90 and Artemisinin are Phenylalanine (Phe134), Glycine (Gly133), and Serine (Ser109); HSP90 and Diclofenac are Glycine (Gly131 and Gly133), Phenylalanine (Phe134), Asparagine (Asn47); Diclofenac HSP90 complex and Artemisinin is Tyrosine (Tyr460); and Artemisinin HSP90 complex and Diclofenac are Threonine (Thr489), and Serine (Ser499).

The use of network pharmacology in investigating the toxicity mechanisms of xenobiotics offers a unique opportunity to explore the complex interactions between xenobiotics and the human body. The
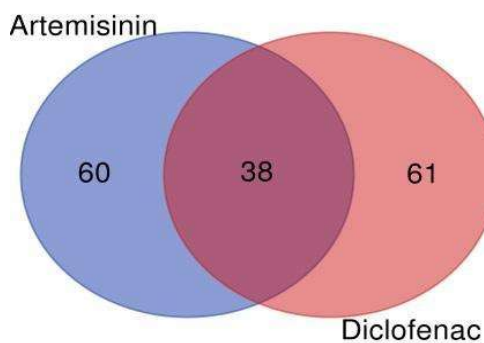

Figure 4: Common pathways between diclofenac and artemisinin

approach allows the recognition of key proteins and pathways involved in xenobiotic toxicity, which can inform the development of

S. No	Gene name	PANTHER Family/ Subfamily	PANTHER protein class
		Table 1: Common targets of diclofenac and artemisinin	
1.	Aldo-keto reductase	ALDO-KETO REDUCTASE FAMILY 1 MEMBER B1 (PTHR11732:SF294)	reductase
2.	Delta-aminolaevulinic acid dehydratase	DELTA-AMINOLEVULINIC ACID DEHYDRATASE (PTHR11458:SF0)	dehydratase
3.	Albumin	ALBUMIN (PTHR11385:SF15)	transfer/carrier protein
4.	Lysozyme	LYSOZYME C (PTHR11407:SF28)	glycosidase
5.	Kinesin-like protein	KINESIN-LIKE PROTEIN KIF11 (PTHR47970:SF26)	microtubule binding motor protein
6.	Serine threonine-protein kinase pim-1	SERINE_THREONINE-PROTEIN KINASE PIM-1 (PTHR22984:SF29)	non-receptor serine/threonine protein kinase
7.	Serine threonine-protein kinase Chk1	SERINE_THREONINE-PROTEIN KINASE CHK1 (PTHR24343:SF564)	non-receptor serine/threonine protein kinase
8.	Ribosyldihydronicotinamide dehydrogenase [quinone]	RIBOSYLDIHYDRONICOTINAMIDE DEHYDROGENASE [QUINONE] (PTHR10204:SF33)	oxidoreductase
9.	Mitogen-activated protein kinase 1	MITOGEN-ACTIVATED PROTEIN KINASE 1 (PTHR24055:SF599)	non-receptor serine/threonine protein kinase
10.	Nck-associated protein 1	NCK-ASSOCIATED PROTEIN 1 (PTHR12093:SF11)	-
11.	Fas-binding factor 1 FBF1	FAS-BINDING FACTOR 1 (PTHR33689:SF1)	-
12.	Protein farnesyltransferase_geranylgeranyltransferase type-1 subunit alpha	PROTEIN FARNESYLTRANSFERASE_GERANYLGERANYLTRANSFERASE TYPE-1 SUBUNIT ALPHA (PTHR11129:SF5)	acyltransferase
13.	Ephrin type-B receptor 4	EPHRIN TYPE-B RECEPTOR 4 (PTHR24416:SF296)	transmembrane signal receptor
14.	Glutathione S-transferase P	GLUTATHIONE S-TRANSFERASE P (PTHR11571:SF141)	transferase
15.	Caspase-7	CASPASE-7 (PTHR10454:SF31)	protease
			(Contd.)

Toxicity Mechanisms of Xenobiotics

Table 1: Common targets of diclofenac and artemisinin (*Contd.*)			
S. No	Gene name	PANTHER Family/ Subfamily	PANTHER protein class
16.	Cholinesterase	CHOLINESTERASE (PTHR43918:SF5)	esterase
17.	Carbonic anhydrase 2	CARBONIC ANHYDRASE 2 (PTHR18952:SF120)	dehydratase
18.	Caspase-3	CASPASE-3 (PTHR10454:SF198)	protease
19.	Peptidyl-prolyl cis-trans isomerase A	PEPTIDYL-PROLYL CIS-TRANS ISOMERASE A (PTHR11071:SF490)	chaperone
20.	Cyclin-dependent kinase 2	CYCLIN-DEPENDENT KINASE 2 (PTHR24056:SF521)	non-receptor serine/threonine protein kinase
21.	Oxysterols receptor LXR-beta	OXYSTEROLS RECEPTOR LXR-BETA (PTHR24082:SF316)	C4 zinc finger nuclear receptor
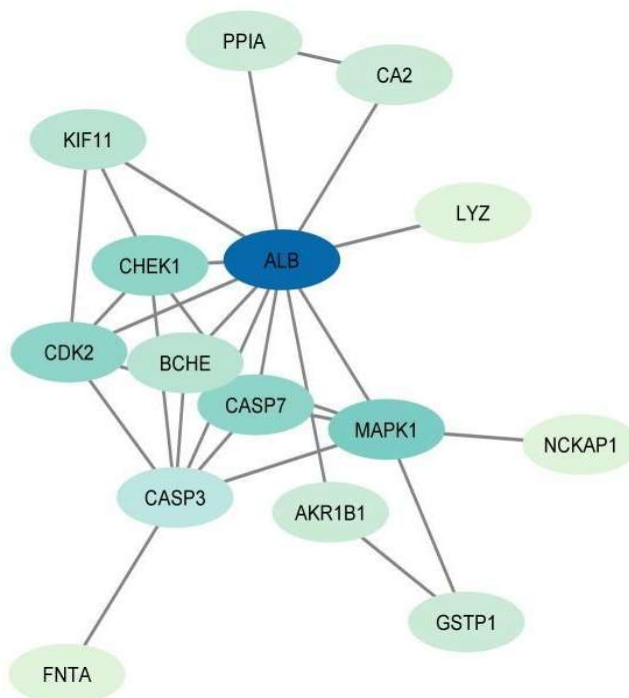
The colour of the nodes has been given according to the degree.
Dark colour denotes the high degree value.

Figure 5: Network of genes affected by both diclofenac and artemisinin using cytoscape

Shreenidhi et al

Current Trends in Biotechnology and Pharmacy
Vol. 18 (Supplementry Issue 4A) 138 - 151, November 2024, ISSN 0973-8916 (Print), 2230-7303 (Online)
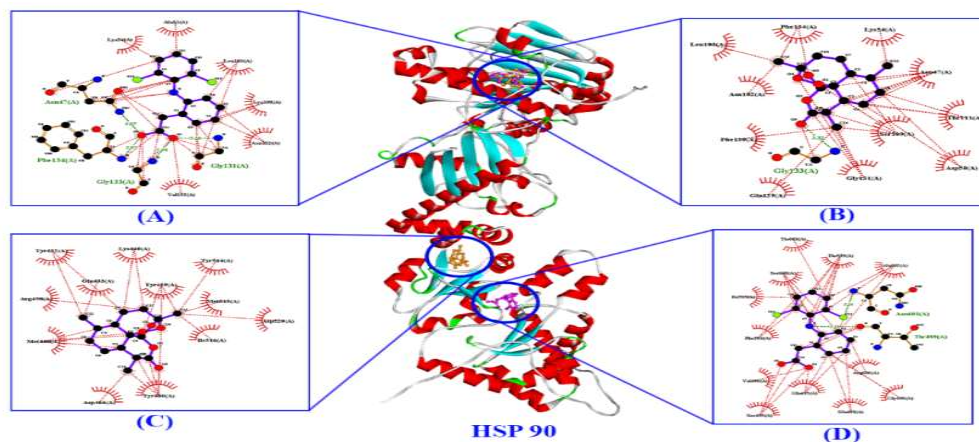10.5530/ctbp.2024.4s.11

146

Figure 6 The identification of hydrogen and hydrophobic interactions of HSP90. A and D: Artemisinin. B and C: Diclofenac

new remedial strategies for mitigating the adverse effects of xenobiotics.

By leveraging the power of network pharmacology, we can embark on an exciting journey touncover the mysteries of xenobiotic toxicity. This innovative approach enables us to map the intricate dance between xenobiotics and the human body, pinpointing the critical proteins and pathways that are implicated in harmful interactions. The knowledge gleaned from this endeavour has the potential to transform the approach with which we combat the adverse effects of xenobiotics, paving the way for the development of novel therapeutic strategies that promote human health and well-being.

The study identified several key pathways involved in xenobiotic toxicity, including oxidative stress, inflammation, and apoptosis. These pathways have been previously implicated in the pathogenesis for many diseases, including cancer, cardiovascular disease, and neurodegenerative disorders. Therefore, the identification of these pathways as being involved in xenobiotic toxicity suggests that the effects of xenobiotics on human health may cause many problems than previously thought. Beta-lactamase enzymes has a pivotal role in the detoxification of harmful substances in environment. They have the remarkable ability to break down certain beta-lactam-containing compounds found in drugs and chemicals, effectively rendering them harmless. Insome cases, beta-lactamase activity can even convert xenobiotics into less toxic forms,making them less harmful to living organisms.

While the effectiveness of beta-lactamases on xenobiotics may vary based on factors such as the specific enzyme, the type of xenobiotic, and the context in which it is encountered, the potential benefits of these enzymes cannot be ignored. By leveraging the power of beta-lactamases, we may be able to develop new strategies for neutralizing harmful pollutants and promoting environmental health.

Moreover, the versatility of beta-lactamases suggests that they could be used to address a range of environmental challenges. For example, they could be employed to clean up contaminated soil and water, or to break down harmful chemicals in industrial settings. The possibilities are vast, and the potential impact of beta-lactamases on our planet's ecosystems could be significant.

Tyrosine protein phosphatase non-receptor type 1 (PTPN1), also known as

protein tyrosine phosphatase 1B (PTP1B), is an enzyme involved in the regulation of many cellular processes, including xenobiotic metabolism. PTPN1 is primarily expressed in the liver and plays a crucial role in xenobiotic metabolism in this organ (56). Specifically, PTPN1 dephosphorylates and inactivates several key enzymes involved in drug metabolism, which includes cytochrome P_{450} enzymes, UDP-glucuronosyltransferase, and sulfotransferase. Although they can have both beneficial and adverse effects on drug efficacy and toxicity, they remain important targets for the development of new therapeutic strategies for various diseases.

MAPK14 is involved in a several cellular processes including inflammation, apoptosis (programmed cell death), and cell differentiation. Its activation is involved in regulating cell survival and death in response to various stimuli such as oxidative stress, cytokines and xenobiotics (57). In response to exposure to xenobiotics, MAPK14 may be activated, triggering cellular stress responses that ultimately lead to cell death. The activation of MAPK14 has been shown to promote survival of hepatocytes (hepatocytes) exposed to various xenobiotics such as alcohol and acetaminophen. On the other hand, activation of MAPK14 is also involved in the induction of cell death in response to certain xenobiotics such as arsenic and benzene. Carbonic anhydrase 2 (CA2) is a vital enzyme which plays a central role in maintaining the delicate balance of acid and base levels in our bodies. Found in diverse tissues such as the kidneys, lungs, and liver, CA2 facilitates the conversion of carbon dioxide into bicarbonate ions and protons, a process essential for proper respiration and ion transport (58). Moreover, recent research has revealed that CA2 also supports the growth and survival of certain cancer cells, making it an attractive target for the development of innovative cancer therapies. By inhibiting CA2, scientists have successfully reduced the viability and proliferation of cancer cells, raising hopes for a new generation of cancer treatments. Although the precise manner in which CA2 promotes cell survival remains unclear, researchers are making steady progress towards unravelling its mysteries. As we deepen our understanding of CA2's role in cellular processes, we may uncover novel opportunities to exploit its potential for the betterment of human health. Glycogen phosphorylase is a key enzyme in glycogen metabolism. This increase in glycogen phosphorylase activity may help provide an energy source to stressed cells and promote cell survival. Cell division protein kinase 2 (CDK2) is a key cell cycle regulator that controls the transition of cells from G1 to S phase. In addition to its role in cell cycle regulation, CDK2 has also been shown to play a role in DNA repair and apoptosis, processes critical in maintaining genomic stability and cell viability. The role of CDK2 in xenobiotic-induced cell survival is complex and context-dependent, and further studies are needed to fully understand the role of CDK2 in xenobiotic toxicity and carcinogenesis (59). Stromelysin 1 is a member of the matrix metalloproteinase (MMP) family and plays an important role in the degradation of extracellular matrix (ECM) proteins during tissue remodelling and repair processes. Overall, the precise role of stromelysin-1 in xenobiotic metabolism and cell viability are complex and context dependent. Further studies are needed to fully elucidate these functions and their potential impact on human health and disease. Cyclic AMP-specific 3',5'-cyclic phosphodiesterase 4D, also known as PDE4D, is an enzyme that catalyses the hydrolysis of cAMP (cyclic adenosine monophosphate) to inactive 5'-AMP. PDE4D has been found to play an important role in regulating the cAMP signalling pathway in various cellular processes including cell proliferation and differentiation.

Overall, PDE4Ds play an important role in regulating cellular responses to xenobiotic stress and cell survival (60). Modulation of PDE4D activity may be a promising target for the development of new therapeutic strategies for xenotoxicity and cancer therapy. HSP90 (Heat Shock Protein

90) is a powerful molecular chaperone that plays a vital role in safeguarding the integrity and functionality of numerous client proteins. These proteins are involved in a variety of cellular processes, including cell proliferation, differentiation, and survival. Remarkably, HSP90 has been shown to play a dual role in responding to xenobiotics, such as chemotherapy drugs, environmental toxins, and drugs of abuse. On one hand, it acts as a protective shield, preventing the denaturation and degradation of client proteins in the presence of these harmful compounds. On the other hand, it promotes cell survival by conferring resistance to chemotherapeutic agents and fostering cell resilience. The intricate mechanisms underlying HSP90-mediated regulation of xenobiotic responses are currently under intense scrutiny, with researchers eager to uncover new ways to leverage this knowledge for the development of innovative therapeutics. By understanding how HSP90 influences cellular responses to xenobiotics, scientists may be able to devise novel strategies to boost the effectiveness of cancer treatments while minimizing harmful side effects(61).

Additionally, this research may shed light on how to overcome chemoresistance, a major obstacle in the fight against cancer. It is important to note that this study has several limitations. Firstly, the study relied on publicly available data to construct the xenobiotic-protein interaction network, which may be incomplete or contain errors. Secondly, the study did not investigate the effects of specific xenobiotics on human health, instead focusing on the general mechanisms of xenobiotic toxicity. Therefore, further studies are necessary to determine the specific effects of different xenobiotics on human health and the mechanisms underlying these effects. In conclusion, the use of network pharmacology in investigating the toxicity mechanisms of xenobiotics are a promising approach that offers new insights into the complex interactions between xenobiotics and the human body. The findings of this study provide a basis for future research in this area, which has the potential to lead to the development of new therapeutic strategies for mitigating the adverse effects of xenobiotics on human health.

Conclusion

In summary, the application of network pharmacology in studying the toxicity mechanisms of xenobiotics has proven to be a game-changer. By illuminating the intricate connections between xenobiotics and the human body, this innovative approach has opened up new avenues for exploration and discovery. The insights gained from this research have laid the groundwork for future investigations that could lead to the creation of novel therapies designed to counteract the harmful effects of xenobiotics on human health. With the help of network pharmacology, we can now gain a deeper understanding of how xenobiotics interact with various biological pathways and networks within the body. This knowledge has the ability to transform the way we approach drug development and toxicity testing, ultimately leading to safer and more effective treatments for a wide range of diseases. As we continue to push the boundaries of possibilities with network pharmacology, we can look forward to a brighter future where the adverse effects of xenobiotics are minimized and human health is protected.

References

1. Cavalli, L., Cavalli, T., Marcucci, G., Falchetti, A., Masi, L., & Brandi, M.L. (2009). Biological effects of various regimes of 25-hydroxyvitamin D3 (calcidiol) administration on bone mineral metabolism in postmenopausal women. Clinical cases in mineral and bone metabolism: the official journal of the Italian Society of Osteoporosis, Mineral Metabolism, and Skeletal Diseases, 6(2), 169–173.
2. Berman, H.M., Westbrook, J., Feng, Z., Gilliland, G., Bhat, T.N., Weissig, H.,

Current Trends in Biotechnology and Pharmacy
Vol. 18 (Supplementry Issue 4A) 138 - 151, November 2024, ISSN 0973-8916 (Print), 2230-7303 (Online)
10.5530/ctbp.2024.4s.11

149

Shindyalov, I.N., & Bourne, P.E. (2000). The protein data bank. Nucleic Acids Research, 28, 235–242.

3. Abdel-Razzak, Z., Loyer, P., & Fautrel, A. (2018). Cytoscape: a software platform for visualizing molecular interaction networks in toxicology. Toxicology, 409, 142–156.

4. Sahu, B.D. (2016). Xenobiotic metabolism and toxicity in the liver. In Advances in Experimental Medicine and Biology, 905, 145–171.

5. Croom, E. (2012). Metabolism of xenobiotics of human environments. Progress in Molecular Biology and Translational Science, 112, 31–88.

6. Zhou, L., Chen, J., Li, J., et al. (2016). Artemisinin induced liver injury in patients with malaria: A systematic review. Expert Opinion on Drug Safety, 15(10), 1411–1421.

7. Zhang, Y., et al. (2020). Xenobiotics-induced hepatotoxicity: Mechanisms, identification and mitigation strategies. Frontiers in Pharmacology, 11, 690.

8. White, N.J. (2008). Qinghaosu (artemisinin): the price of success. Science, 320, 330–334.

9. Noman, E.A., Al-Gheethi, A.A.S., Talip, B.A., Radin Mohamed, R.M.S., Nagao, H., & Mohd Kassim, A.H. (2019). Xenobiotic organic compounds in greywater and environmental health impacts. In Management of Greywater in Developing Countries: Alternative Practices, Treatment and Potential for Reuse and Recycling, pp. 89–108.

10. Yapar, K., Kart, A., Karapehlivan, M., & Atakisi, E. (2009). Amoxapine-induced hepatotoxicity in rats and the protective effect of vitamins C and E. Exp Toxicol Pathol, 62(6), 639–644.

11. Navarro, V.J., & Senior, J.R. (2006). Drug-related hepatotoxicity. New England Journal of Medicine, 354(7), 731–739.

12. Yu, J., Chen, Y., & Huang, Y. (2019). Cytoscape 3.7.1-based network analysis of circRNA-associated ceRNA network and potential pathways in hepatic fibrosis. PeerJ, 7.

13. Zhao, X., Xiang, Q., & Shi, X. (2020). Toxicological Mechanism of Cytotoxicity Induced by Silver Nanoparticles in Liver Cells. Int J Mol Sci, 21(5).

14. Christian, T., Lopes, M., Franz, F., Sylva, L., Donaldson, Q., & Morris, G.D. (2010). Cytoscape Web: an interactive web-based network browser. Bioinformatics, 26(18), 2347–2348.

15. Rosenfeld, P.E., & Feng, L. (2011). Risks of hazardous wastes. William Andrew Publishing.

16. Thomas, P.D., Campbell, M.J., Kejariwal, A., Mi, H., Karlak, B., Daverman, R., Diemer, K., Muruganujan, A., & Narechania, A. (2003). PANTHER: a library of protein families and subfamilies indexed by function. Genome research, 13(9), 2129–2141.

17. Barradell, L.B., & Faulds, D. (1994). Cyproterone. A review of its pharmacology and therapeutic efficacy in prostate cancer. Drugs & aging, 5(1), 59–80.

18. Gerriets, V., Nappe, A.J., & Acetaminophen, T.M. (2022). Acetaminophen. StatPearls. StatPearls Publishing.

19. Scialli, A.R., Ang, R., Breitmeyer, J., & Royal, M.A. (2010). A review of the literature on the effects of acetaminophen on pregnancy outcome. Reprod Toxicol, 30(4), 495–507.

20. Rumack, B.H. (2002). Acetaminophen hepatotoxicity: the first 35 years. J Toxicol Clin Toxicol, 40(1), 3–20.

21. Nguyen Thanh Nguyen, Trung Hai Nguyen, T. Ngoc Han Pham, Nguyen Truong Huy, Mai Van Bay, Minh Quan Pham, Pham Cam Nam, Van V. Vu, & Son Tung Ngo (2020). Journal of Chemical Information and Modeling 60(1), 204-211.

22. García Rodríguez, L.A., & Hernández-Díaz, S. (2001). Relative risk of upper gastrointestinal complications among users of acetaminophen and nonsteroidal anti-inflammatory drugs. Epidemiology, 12(5), 570–576.

23. Dandachi, N., Choueiry, E., & Sinno, S. (2018). Erythromycin-induced liver injury: a rare adverse effect of a commonly used antibiotic. Am J Case Rep, 19, 1071–1075.

24. Ahmad, S., Hughes, M.A., Yeh, L.A., & Scott, J.E. (2012). Potential repurposing of known drugs as potent bacterial β-glucuronidase inhibitors. J Biomol Screen, 17(7), 957–965.

25. Gan T.J. (2010). Diclofenac: an update on its mechanism of action and safety profile. Current medical research and opinion, 26(7), 1715–1731.

26. Klonis, N. (2013). Altered temporal response of malaria parasites determines differential sensitivity to artemisinin. Proc. Natl. Acad. Sci. U S A, 110, 5157–5162.

27. Wang, H., Feng, X., Liu, M., & Hu, X. (2021). PubChem-based screening of potential liver injury-associated chemical components in medicinal herbs. Journal of Ethnopharmacology, 267, 113597.

28. Derry, S., Rabbie, R., & Moore, R.A. (2013). Diclofenac with or without an antiemetic for acute migraine headaches in adults. Cochrane Database Syst Rev, 4.

29. Sunghwan, E.E., & Bolton, S.H. (2013). PubChem3D: conformer ensemble accuracy. Journal of Cheminformatics, 5, 1–17.

30. Shreenidhi, K., & Bose, V.G. (2022). A Preliminary Investigation on the Antihepatotoxic Activity of Artemisia pallens Leaves in the Diclofenac-Treated – Pangasius Sps. Polish Journal of Environmental Studies, 31(5), 4837-4849.

31. Vijaya Geetha, Roy Sujata, K. Subramaniyan Shreenidhi, T.R. Sundararaman (2018). Histopathological and HPLC Analysis in the Hepatic Tissue of Pangasius sp. Exposed to Diclofenac. Polish Journal of Environmental Studies, 27(6).

32. Wang, X., Pan, C., Gong, J., Liu, X., & Li, H. (2016). Enhancing the enrichment of pharmacophore-based target prediction for the polypharmacological profiles of drugs. Journal of Chemical Information and Modeling, 56(6), 1175–1183.

33. Gehanno, P., Dreiser, R.L., Ionescu, E., Gold, M., & Liu, J.M. (2003). Lowest effective single dose of diclofenac for antipyretic and analgesic effects in acute febrile sore throat. Clin Drug Investig, 23(4), 263–271.

34. Souza, A.C.A., & Rocha, J.B.T. (2016). The effects of organophosphorus pesticides on the liver: The role of oxidative stress and metabolism. Journal of Toxicology and Environmental Health, Part B, 19(1), 1–15.

35. Kim, S., Thiessen, P.A., Bolton, E.E., Chen, J., Fu, G., & Gindulyte, A. (2016). PubChem substance and compound databases. Nucleic Acids Res, 44, 1202–1213.

36. Kim, S., Chen, J., Cheng, T., Gindulyte, A., He, J., He, S., Li, Q., Benjamin, A., Shoemaker, P.A., Thiessen, B., Yu, L., Zaslavsky, J., & Zhang, E.E. (2019). PubChem 2019 update: improved access to chemical data. Nucleic Acids Research, 47, 1102–1109.

37. Tu, Y. (2016). The discovery of artemisinin (qinghaosu) and gifts from Chinese medicine. Nature Medicine, 22(4), 411–413.

38. Unchorntavakul, C., & Reddy, K.R. (2013). Acetaminophen-related hepatotoxicity. Clin Liver Dis, 17(4), 587–607.

39. Liu, X., Ouyang, S., Yu, B., Liu, Y., Huang, K., Gong, J., Zheng, S., Li, Z., Li, H., & Jiang, H. (2010). PharmMapper server: a web server for potential drug target identification using pharmacophore mapping approach. Nucleic Acids Research, 38, 609–614.

40. Mi, H., Lazareva-Ulitsky, B., Loo, R., Kejariwal, A., Vandergriff, J., Rabkin, S., Guo, N., Muruganujan, A., Doremieux, O., Campbell, M.J., Kitano, H., & Thomas, P.D. (2005). The PANTHER database of protein families, subfamilies, functions and pathways. Nucleic Acids Research, 33.

41. Yu, J., Chen, Y., & Huang, Y. (2019). Cytoscape 3.7.1-based network analysis of circRNA-associated ceRNA network and potential pathways in hepatic fibrosis. PeerJ, 7.

42. Abbas, S., & Marwaha, R. (2022). Amoxapine. StatPearls. StatPearls Publishing.

43. Yang, X., Gong, Y., & Guo, Y. (2017). Network-based analysis of liver toxicity-related genes and pathways using Cytoscape. Toxicol Lett, 273, 17–25.

44. Chalasani, N., Fontana, R.J., Bonkovsky, H.L., Watkins, P.B., Davern, T., Serrano, J., Yang, H., & Rochon, J. (2008). Causes, clinical features, and outcomes from a prospective study of drug-induced liver injury in the United States. Gastroenterology, 135(6), 1924-1934.e4.

45. Kumar, A. (2006). Subject: diclofenac for veterinary use—regarding. Letter to "All State Drug Controllers" from the "Drug Controller General (India).

46. Aono, T., Kaneko, M., Numata, Y., Takahashi, Y., Yamamoto, T., & Kumashiro, H. (1981). Effects of amoxapine, a new antidepressant, on pseudoneurotic schizophrenia. Folia Psychiatr Neurol Jpn, 35(2), 115–121.

47. Björnsson, E.S., Gunnarsson, B.I., Gréttarsdóttir, H., et al. (2011). Risk of Elective Abdominal Surgery in Patients with Previous Idiosyncratic Drug-Induced Liver Injury. Gastroenterology, 140(5), 1417-1424.e1.

48. Björnsson, E., Jacobsen, E.I., & Kalaitzakis, E. (2012). Hepatotoxicity associated with statins: reports of idiosyncratic liver injury post-marketing. J Hepatol, 56(6), 374–380.

49. Björnsson, E.S., Bergmann, O.M., Björnsson, H.K., Kvaran, R.B., & Olafsson, S. (2013). Incidence, Presentation, and Outcomes in Patients with Drug-Induced Liver Injury in the General Population of Iceland. Gastroenterology, 144(7), 1419–1425.e3.

50. Bolton, E.E., Kim, S., & Bryant, S.H. (2011). PubChem3D: similar conformers. J Cheminform, 3.

51. Chen, X., Chen, M., & Xu, L. (2019). Cytoscape: a dynamic platform for visualizing molecular interaction networks and biological pathways in hepatocellular carcinoma. Oncol Lett, 17(3), 2861–2868.

52. Krishna, S., & Uhlemann, A.C. (2014). The mechanism of action of artemisinin, the active ingredient of Qinghaosu, the antimalarial herb. Parasitology Today, 10(9), 379-382.

53. Enserink, M. (2010). Malaria's drug miracle in danger. Science (New York, N.Y.), 328(5980), 844–846.

54. Derry, S., Rabbie, R., & Moore, R.A. (2013). Diclofenac with or without an antiemetic for acute migraine headaches in adults. Cochrane Database Syst Rev, 4.

55. Kohl, M., Wiese, S., & Warscheid, B. (2011). Cytoscape: software for visualization and analysis of biological networks. In Data mining in proteomics: from standards to applications, pp. 291–303.

56. Delibegovic, M., Zimmer, D., Kauffman, C., Rak, K., Hong, E.-G., Cho, Y.-R., Kim, J.K., Kahn, B.B., Neel, B.G., & Bence, K.K. (2009). Liver-Specific Deletion of Protein-Tyrosine Phosphatase 1B (PTP1B) Improves Metabolic Syndrome and Attenuates Diet-Induced Endoplasmic Reticulum Stress. American Diabetes Association, 590–599.

57. Austin, E.D., Newman, J.H., Loyd, J.E., & Phillips, J.A. (2020). Heritable and Idiopathic Forms of Pulmonary Arterial Hypertension. In Emery and Rimoin's Principles and Practice of Medical Genetics and Genomics (Seventh Edition), 439-464.

58. Jakubowski, M., Szahidewicz-Krupska, E., & Doroszko, A. (2018). The Human Carbonic Anhydrase II in Platelets: An Underestimated Field of Its Activity. Biomed Research International.

59. Łukasik, P., Załuski, M., & Gutowska, I. (2021). Cyclin-Dependent Kinases (CDK) and Their Role in Diseases Development–Review. International Journal of Molecular Science, 2935.

60. Beca, S., Helli, P.B., Simpson, J.A., Zhao, D., Farman, G.P., Jones, P., Tian, X., Wilson, L.S., Ahmad, F., Chen, S.R.W., Movsesian, M.A., Manganiello, V., Maurice, D.H., Conti, M., & Backx, P.H. (2014). Phosphodiesterase 4D (PDE4D) regulates baseline sarcoplasmic reticulum Ca2+ release and cardiac contractility, independently of L-type Ca2+ current. PubMed Central, 1024-1300.

61. Sumi, M.P., & Ghosh, A. (2022). Hsp90 in Human Diseases: Molecular Mechanisms to Therapeutic Approaches. Cells, 976.

Probiotic Characterization of Primate Origin
Lactiplantibacillus plantarum LG138

Reena Kumari, and Savitri*

Department of Biotechnology, Himachal Pradesh University, Shimla-171005, India
*Corresponding author: savvy2000in@gmail.com

Abstract

This study was aimed to characterize previously isolated lactic acid bacteria *Lactiplantibacillus plantarum* LG138 from primate feces for its probiotic potential. The ability of the isolate to withstand different *in vitro* gastrointestinal stresses was assessed over a period of time i.e. at pH 2.0 and 3.0, bile salts (0.5, 1.0 and 2.0 %) and lysozyme (50,100, 150 mg/ml). Further the *L. plantarum* LG138 was tested for hydrophobicity, auto-aggregation and co-aggregation abilities, coexistence, exopolysaccharide production and hemolytic activity. The isolate demonstrated significant growth in the presence of different types of artificialdigestive conditions (low pH, bile and lysozyme).Furthermore, oxbiledid not affect the viability of *L. plantarum* LG 138 cells compared to the control. The isolate *L. plantarum*LG138 exhibited 65.7 ± 0.32 % auto-aggregation after 24 h incubation. The hydrophobicity test found the culture moderately hydrophobic (35 to 69 %) forhexadecaneand highly hydrophobic (70 to 100 %) for toluene and xylene. Moreover, it was observed to co-aggregate (66.13 ± 0.18 %) with a pathogen, *Shigellaflexneri*, without antagonizing other probiotic bacteria. *L. plantarum*LG138 was found to be able to produce exopolysaccharide and found to be non-hemolytic. These findings highlight the potential of *L. plantarum* LG138 as a promising probiotic candidate, suitable for incorporation into pelleted orgranulated animal feed formulations.

Keywords: Lactic acid bacteria, primate, animal, probiotics, characterization

Introduction

Lactic acid bacteria (LAB) existing in the gut microbiota are vital for the wellbeing of both animals and humans. When utilized as probiotics, they show potential in boosting growth performance in livestock agriculture (1).LABasGram-positive microaerophilic organisms are extensively studied amongst the gastrointestinal (GIT) microbiota. Jin et al. (2) reported that the main LABs present in the milk from rhesus monkeys are belonging to the genera of *Streptococcus* and *Lactobacillus.* Out of these, many LAB species like *L. johnsonii, L. animalis*and *L. brevis* along with *Bacillus* species are notreported in human milk as revealed by different metagenomic studies. These bacteria due to their presence as indigenous species in the host gut are well acclimatized and mostly present as host-specific LAB populations (3).In extensive livestock farming operations, the circumstances often lead to heightened stress and health problems among the animals. The disruption in the microbiota balance can indeed be a significant factor contributing to disease development in such settings (4). These bacteria, commonly utilized as probiotics, contribute to maintaining the equilibrium of the microbiota in gut by engaging in competitive interactions with pathogens to ensure their survival, enhance growth performance, improve feed conversion efficiency, optimize nutrient utilization, modification of gut microbiome and promote gut health (5).The interest in the study of microbial heterogeneity of human and nonhuman animals correlating their importance in the functioning of GIT and wellness of host is becoming the new area of investigation. In primates, gut bacterial communities are known to be species specific, but they fluctuatemostly with stage of development, social organization and

nutrition with substantial loss of microbes in confinement(6).

The ideal probiotic microorganism should be able to withstand acidic conditions and tolerate bile without posing any risk of carcinogenicity or pathogenicity. Additionally, it should adhere to the host's epithelial tissue, enhance the gut microflora, decrease pathogen attachment, and produce secondary metabolites that combat pathogenic microorganisms (7-8). Modifying the microbial ecosystem can indeed result in improved livestock productivity. The introduction of live microbes as probiotics serves as a safe and effective substitute for antibiotics as growth supplements, as they carry no risk of toxicity in livestock products and leave behind no residues. In fact, the contact between LABs and gut microorganisms leads to an increase in propionate and total volatile fatty acids (VFAs) production. This beneficial interaction ultimately enhances feed utilization, improves growth performance, and reduces the diarrheal cases (9).

Despite the emergence of transgenic mice, nonhuman primates are still widely regarded as the premier laboratory animal due to their close evolutionary relationship to *Homo sapiens*. The rhesus monkey, in particular, is extensively used as a nonhuman primate model in medical research because of its close evolutionary proximity to humans (2). To ensure the most effective use of primates as models, it is essential for pathologists participating in study design and interpretation to have a thorough understanding of their histological anatomy, physiology, natural history, associated disease and place of primate origin (10). Kang et al. (11) suggested that lactobacillus strains derived from primates are more effective for intestinal health in primates compared to human-derived lactobacillus and other lactic acid strains.There is increasing support for the notion that gut microflora play a crucial role in regulating digestive health and the immune system. This presents a promising avenue for reducing idiopathic chronic diarrhea (ICD) and improving overall health and well-being

in nonhuman primates. Probiotics provide an alternative strategy for reducing the diarrheal incidences in captive nonhuman primates by bolstering the indigenous microflora in the gut.

Primates, in terms of anatomy, physiology, genetics, and immunology, closely resemble humans and are considered the preclinical animal species that most closely resemble us. They are extensively employed in various biotechnology research domains across the globe and kept in wild, semi-captive, and captive. Idiopathic chronic diarrhea, gastric dilatation, and rupture of unknown origin are the primary factors leading to spontaneous mortality in captive primates utilized primarily for experimental research.These conditions pose significant veterinary challenges, contributing to a multitude of health issues (12). Diverse factors have been considered as potential triggers for intestinal disorders, such as antibiotic consumption, stress, and *Clostridium perfringens* infection. However, a definitive mechanism has yet to be pinpointed. As a result, safeguarding the intestinal well-being of experimental primates, commonly utilized in studies related to brain and infectious diseases, holds significant importance not just in terms of veterinary care but also for ensuring experimental reproducibility (11).

Up to now, there has been a very few research studies focusing on primate probiotics. The aim of our research is to fill this gap in knowledge by presenting pertinent data. There is only one commercially available nonhuman primate–specific live probiotics named as Bio-Serv'sPrimiOtic and PrimiOtic Plus. The product contains *Lactobacillus reuteri*, a probiotic bacterium sourced from nonhuman primates which is a type of bacteria that naturally inhabits the digestive system of nonhuman primates. Its presence aids in establishing the bacteria in the primate gut, resulting in the beneficial impacts of probiotics on enhancing and maintaining gastrointestinal health (12). Primate facilities commonly depend on human lactic acid bacteria products to carry

Current Trends in Biotechnology and Pharmacy
Vol. 18 (Supplementry Issue 4A) 152 - 165, November 2024, ISSN 0973-8916 (Print), 2230-7303 (Online)
10.5530/ctbp.2024.4s.12

154

out indoor breeding experiments with primates. Hence, it is imperative to develop a probiotic strain exclusively tailored for primates to enhance their health and combat illnesses.

Currently, the ongoing practice involves the screening of new probiotics, particularly from underexplored species. The screening LAB strains from wild primates, inhabiting their natural unexplored gut environments, presents a promising opportunity for isolating novel species with excellent characteristics and developing potent probiotics to enhance production in animal-related industries. Besides, isolating and identifying lactic acid bacteria (LAB) strains with favorable probiotic traits from wild primates holds significant potential for their practical utilization as starter, adjunct, and protective cultures in improving animal food and feed products. Moreover, performing technological characterization of these strains can enhance their efficacy in diverse applications. The study was aimed to assess the probiotic characteristics of the isolated LAB strain. This involved conducting a series of tests to evaluate their acid tolerance, bile tolerance, lysozyme resistance, non-hemolytic activity, auto-aggregation, co-aggregation capability, coexistence compatibility, and antibiotic susceptibility etc.

Materials and Methods

The organism and storage conditions

The organism was previously isolated by Kumari et al. (13) from feces of primates of Shimla region in Himachal Pradesh.

Growth in low pH

The survival of the isolate acidic conditions was analyzedfollowing the procedure of Maragkoudakis et al. (14). The isolatewastreatedwithdifferentlow pH conditions (pH 2, pH 3 and pH 7).Then the isolate was kept at 37 ºC for 3 h and its survival was calculated and expressed as log cfu/ml.

Tolerance to bile salts

The bile tolerance ability of the given isolate was performed as per previously given methodbyGilliland et al. (15). The isolate was put into sterile MRS broth (9 ml) containing different Ox-bile concentrations (0.5 %, 1 % and 2 %). Then the isolate was kept at 37 ºC for 3 h and its survival expressed as log cfu/ml.

Lysozyme resistance test

The lysozyme tolerance was evaluated according to method of Zago et al. (16). 100 μl of freshly prepared LAB cultures was inoculated into the 10ml of MRS broth supplemented with different lysozyme concentration (50,100,150 mg/ml) and kept at 37ºC for 24 h. The survival of the isolate was recordedas of log cfu/ml.

Surface properties

The cell surface hydrophobicity of the isolatewasdeterminedaccording to the previously reported modified method of Rosenberg et al. (17). The cells of the freshly grown isolate were harvested (10,000 rpm, 10 min at 4ºC) by centrifugation.Then suspended in sterile normal saline after three washing with saline and optical density (O.D.$_{600}$) was adjusted at 1.0. The bacterialcell suspension and different solvents (n-hexadecane, xylene and toluene) were taken in equal amounts and incubated at room temperature for 1 h.

The adherence of the isolate to hydrocarbons was calculated as:
Hydrophobicity (%) = $[(A_1-A_2)/A_1] \times 100$

Whereas, A_1 and A_2 are absorbance before and after mixing with solvents at 600 nm.

Auto-aggregation Test

Auto-aggregation ability was assessedfollowing the method described by Colladoet al (18) withsome modifications. The cell suspension was prepared similarly to cell surface hydrophobicity test.The cells were incubated at 37ºC for 24 h and O.D.$_{600}$ was measured at 1,3,24 h using a UV-Vis

spectrophotometer. Auto-aggregation % was measured as:

Auto-aggregation % = 1- (A_x/A_y) ×100,

Where A_x represents the absorbance at time t=1,3, 24 h and A_y the absorbance at t=0h (i.e.1.0).

Co-aggregation Test

This assay was performed by according to Handley et al. (19). The isolate and the indicator organism *Shigellaflexneri*were grown inMRS and nutrient broth at 35 ºC for 24 h. The cell suspension of both was prepared similarly to cell surface hydrophobicity test. The % co-aggregation wascalculated using Handley's equation as:

$$Coaggregation (\%) = \frac{[A_{Path} + A_{LAB} 2]-A_{Mix}}{A_{Path} - A_{LAB}/2]} \times 100$$

Where A_{path}represents the absorbance of the pathogen, $A_{LAB}$is the absorbance of theisolate and $A_{mix}$is the absorbance of the mixture.

Coexistence Test

The selected isolate was checked for its compatibility with other LAB isolates using 'cross streak method' as given by Guoet al. (20). The freshly grown cultures of all the isolates were streaked perpendicular to each other on MRS agar plates. The plates were observed for presence or absence of antagonism after incubation at 37 ºCfor 24 h.

Antibiotic sensitivity test

The test was conducted following the guidelines given by Clinical and Laboratory Standards Institute (21).The 100 µl of freshly grown culture was swabbed on the Mueller Hinton Agar plates and allowed to dry. Then antibiotic discs were placed on the agar surface and incubated at 35ºC for 24 h. After incubation, the plates were observed for formation of zones of inhibition and their diameters were recorded.

Antagonistic activity

The antimicrobial activity was evaluated using agar well diffusion method as given by Mishra and Prasad (22). The CFS (cell free supernatants) was prepared by centrifuging (1000 rpm for 10 min) the culture grown overnight in MRS medium and then screened against eight food spoilage causing bacteria (*S. aureus* MTCC 96, *L. monocytogenes* MTCC 657, *S. flexneri, B. cereus* MTCC 1272, *P. aeruginosa* MTCC 424, *E. coli* MTCC 118, *A.hydrophilla*and*S. typhi*).The fresh cultures of indicators were swabbed on agar surface and 100 µl of CFS was poured into the wells prepared in the agar plates.The zones of inhibition were observed and recorded after 24 h incubation at optimum temperature.

Exopoysaccharide (EPS) production

The qualitative evaluation for EPS production was done following the method given by Kersaniet al.(23). The 24 h old LAB culture was streaked on the plates of ruthenium red milk agar plates.The plates were observed for the formation of white color colonies against pink background. Overnight grown LAB cultures were streaked on the surface of plates containing ruthenium red milk agar medium. After incubation at 37 ºC for 24 h, exopolysaccharide producers appeared as white colonies and were selected for further studies.

Hemolytic activity

Hemolytic activity of the isolate wasassessed according to the method of Lombardi et al. (24).The 24 h old bacterial culture was streaked on blood agar plate and observed for presence of hemolysis after overnight incubation at 37 ºC.

Statistical Analysis

Each experimental trial was conducted three times, and the results were presented as mean ± standard deviation (SD). Statistical analysis was conducted using SPSS version 27.0.1 (SPSS Inc.111., USA). The significance level (p < 0.05) was determined through analysis of variance (ANOVA).

Results and Discussion

Survival rate at low pH

To examine the survival rate of probiotic strains based on their ability to withstand low pH levels is an important probiotic characteristic.Probiotic bacteria need to endure the stomach environment (highly low pH), tolerating pH values as low as 2.0 and become colonized to show beneficial effects on the host (25).Based on our results, the isolate survived under different acidic conditions and shown ability to survivewhich was not unexpected because these bacteria are well known to be an indigenous flora of the gastrointestinal tract of animals.In our study, with a small amount of viability loss (1.04 log cycles at pH 2.0 and 0.4 log cycles at pH3.0), (Table1). In a study carried out by Zielinska et al. (26), it was discovered that *Lactobacillus* probiotic strains demonstrated a survival rate varying from 30% to 100% upon exposure to gastric juice with a pH of 3.*L. plantarum* uses several strategies to withstand the stress of acid and bile salt. Huang et al. (27) illustrated that *L. plantarum* ZDY2013 possesses the ability to remove protons from the intracellular environment, contributing to the maintenance of pH homeostasis.

Bile tolerance

Another critical attribute of probiotics is their ability to tolerate bile salts, as these substances can break down lipids of membranes leading to cell death due to leakage of its contents. In this study, the log value of the population after incubation for 3 h without 0.3% oxbile was 9.5, but it was 7.46 at 0.5% oxbile, followed by 7.45 and 7.40 1and 2 % oxbileconcentration respectively.This shows a better survival at different bile salt concentration owing to previously conditioning in primate intestinal tract.Another study has demonstrated that *Lactobacillus plantarum* and *L. paracasei*exhibit acceptable survival(6.19 and 6.0 log cfu/ml) in a bile salt environment even in a high concentration (0.3%) (28). Choi et al. (29) reported that bile salt concentration was increased from 0.3 to 1%, population of *L. plantarum* GBL16 was reduced by 0.7–2.1 log cfu/ml while that of GBL17 was reduced by 0.7–1.4 log cfu/ml, similar to the reduction in population of commercial *L. plantarum* (KCCM40399) which was decreased by 1.3–2.4 log cfu/ml with increasing of bile salt concentrations. The resistance to bile salt of the strains might be induced by potential presence of some proteins.The differing levels of bile tolerance observed lactic acid strains were linked to six proteins (GshR1, Bsh1, Cfa2, GshR4, AtpH and OpuA). These proteins are believed to be pivotal in the response to /and adaptation to bile salts in *L. plantarum.*

Lysozyme resistance test

The initial prerequisite for potential probiotic bacteria is to possess resistance against lysozyme found in the saliva. This is crucial because the lysozyme present in the

Table1: Effect of pH (2.0, 3.0 and 7.0) and bile salt concentrations (0.5, 1.0 and 2.0%) on viable count of LAB isolates

Isolates	Acid tolerance (log cfu/ml)			Bile tolerance (log cfu/ml)			
	pH 2.0	pH 3.0	pH 7.0	Control	0.5 %	1 %	2 %
L. plantarum LG 138	8.53 ± 0.15	9.17 ± 0.25	9.57 ± 0.09	9.50±0.10	7.46±0.02	7.45±0.02	7.40±0.04
L. rhamnosus LGG	7.47 ± 0.12	7.97 ± 0.21	8.67 ± 0.09	8.7±0.20	7.33 ± 0.09	7.10 ± 0.21	6.83 ± 0.2
(Note: Values represented as mean ± standard deviation (SD) of triplicate analysis)							

*LactiplantibacillusPlantarum*LG138

oral cavity has the ability to lyse Gram-positive bacterial cells.Our results as shown in the Figure 1indicated thatdue to their gut origin the isolate showed good lysozyme resistance (8.63, 8.40 and 8.20 log cfu/ml at concentration of 50,100 and 150mg/ml respectively) as compared to initial 8.83 log cfu/ml in control after 3 h incubation.Nandha and Shukla (30) studied the growth of LAB isolates in the presence of 100 mg/ml of lysozyme which reveals that the decline in LAB growth in the presence of lysozyme ranged from 0.23 to 3.80 logarithmic units after the 60-min incubation period. This outcome agrees with the results obtained for isolates from vegetables, camel milk, and fermented foods(31).

Surface hydrophobicity

Following the hydrophobicity criteria given by Tyfa et al. (56)i.e.strongly hydrophobic (>50%), moderately hydrophobic (20–50%) and hydrophilic (<20%), the strain was found to be strongly hydrophobic for xylene (75.87 ± 0.22 %) followed by n-hexadecane (65.10 ± 0.17 %) and toluene (70.30 ± 0.12 %), demonstrating more hydrophobic than hydrophilic cell surface of isolate (Figure 2).The results of LAB hydrophobicity in this investigation were higher than LAB isolates as reported by El-Deeb et al. (32)from dromedary camels showing 49.6 ± 0.6% hydrophobicity for hexadecane, followed by xylene (44.3 ± 0.5%) and toluene (41.6 ± 0.6%).Isolates with a substantial presence of surface proteins and lipoteichoic acids generally display higher hydrophobicity compared to isolates containing a significant amount of hydrophilic polysaccharides.Cell surface hydrophobicity plays a critical role in indicating a bacterium ability to adhere to human intestinal cells, which is essential for probiotic effectiveness. This hydrophobic property is believed to facilitate bacterial adhesion to epithelial tissue, thereby aiding in their colonization and survival within the gastrointestinal tract(33).

Auto-aggregation ability

The interaction of cellular surface components like soluble proteins, lipoteichoicacidand carbohydrates result in cell aggregation.Following 24 h incubation at 37ºC, *L.plantarum* LG138 exhibited a co-aggregation ability of 65.7 ± 0.32%, as shown in Table 2 reflecting its higher potential of colonization in the gut epithelium. Auto-aggregation is an essential probiotic trait that contributes to the formation
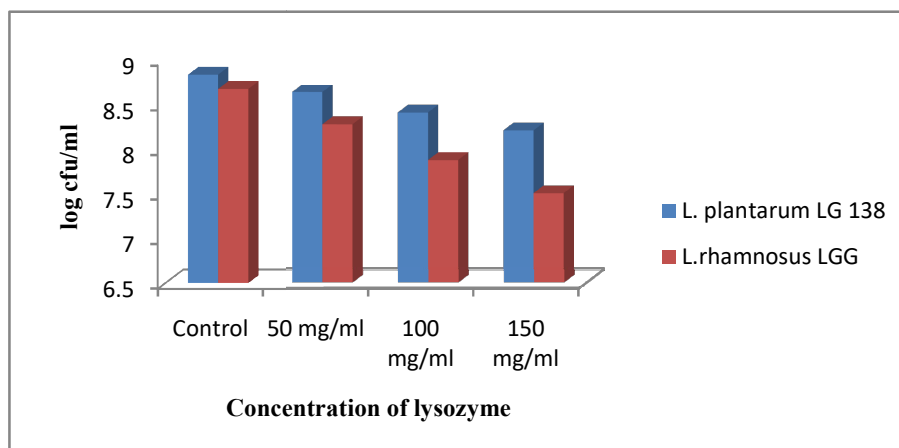

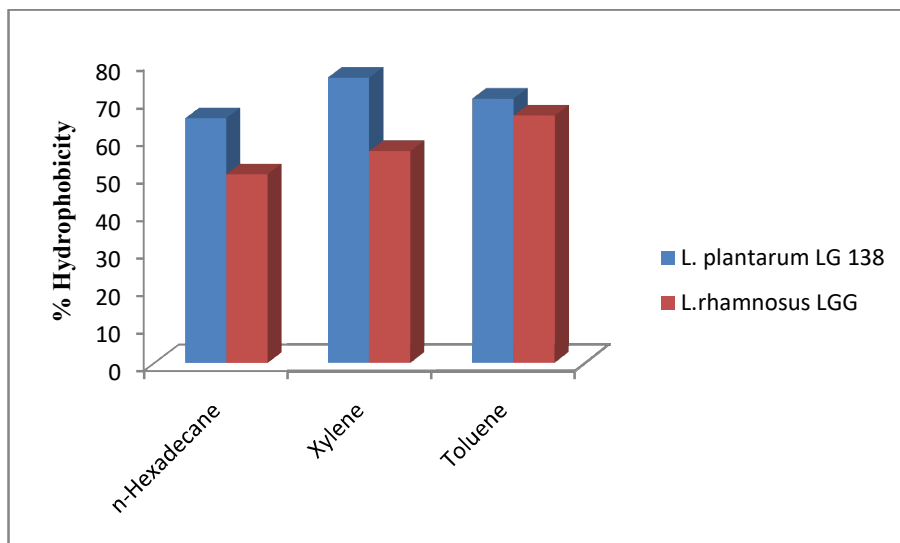**Fig.1:** Lysozyme tolerance of LAB isolates in different concentrations (50,100,150 mg/ml) of lysozyme

Current Trends in Biotechnology and Pharmacy
Vol. 18 (Supplementry Issue 4A) 152 - 165, November 2024, ISSN 0973-8916 (Print), 2230-7303 (Online)
10.5530/ctbp.2024.4s.12

158

Fig.2: Hydrophobicity of LAB isolates towards various hydrocarbons (n-hexadecane, xylene and toluene)

Table 2: Auto-aggregation (%) and co-aggregation (%) of the LAB isolates at time interval of 1 h, 3 h and 24 h

Isolates	Auto-aggregation ability (%)			Co-aggregation ability (%)		
	1 h	3 h	24 h	1 h	3 h	24 h
L. plantarum LG 138	20.9 ± 0.26	30.3 ± 0.25	65.7 ± 0.32	20.3 ± 0.26	24.87 ± 0.18	66.13 ± 0.18
Lactobacillus rhamnosus LGG	18.7 ± 0.31	28.17 ± 0.2	69.97 ± 0.24	19.9 ± 0.25	22.67 ± 0.3	61.53 ± 0.18
(Note: Values represented as mean ± standard deviation (SD) of triplicate analysis)						

of biological niches, particularly within the gut of the organism. The clustering of bacteria relies on the auto-aggregation ability and hydrophobicity of the microbe. Similarly Jang et al. (34) described that *L. brevis* KU15153 and LGG showed 21.44% and 22.68% auto-aggregation abilities, respectively after 4 h incubation. After 24 h incubation, auto-aggregation of *L. brevis* KU15153 (52.55%) was higher than that of LGG (44.70%). *Lactobacillus plantarum strain GCC_19M1 exhibited 29.60% auto-aggregation,*

suggesting a reduced capacity to colonize and attach to the intestinal epithelium(35).The test results suggest that the combined influence of auto-aggregation and hydrophobicity could potentially boost the adherence capability of probiotic strains.

Co-aggregation Ability

Co-aggregation assesses the level of bacterial adherence between the test strain and the enteric fever pathogen. The % co-aggregation (66.13 ± 0.18%) as depicted in

the Table 2 demonstrates that *Lactobacillus plantarum* LG138 effectively prevented the growth of *Shigellaflexneri* within 24 hours of incubation in the pathogen exclusion study.Liu et al. (36) reported the results of co-aggregation of *Lactobacillus* isolates in the presence of target pathogens. The highest co-aggregation rates to *S. flexneri*, *S. paratyphi* B, and *E. coli* were obtained for isolate 115-4 (37.19, 45.93, and 28.19%, respectively). In the co-aggregation process, LABs release antimicrobial substances which effectively protect the surrounding environment from foodborne infections and this serves as an essential defense mechanism for the host (37). This co-aggregation ability of LAB isolates with pathogens is likely due to the presence of proteinaceous components on the cell surface and interactions between carbohydrates and lectins.
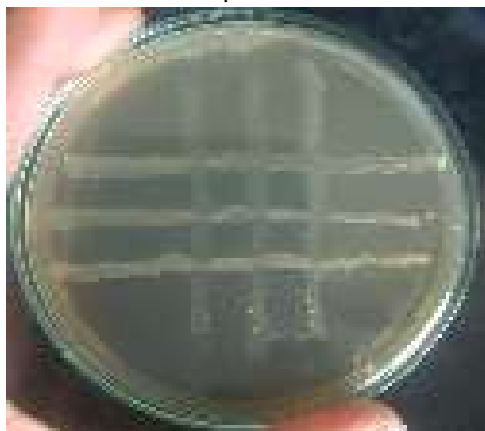
Fig.3: Cross streak test observed no antagonism among LAB isolates

Co-existence Test

The compatibility of the studied *Lactobacillus* strain with other lactic acid bacteria is ascertained to guarantee their co-existence with other probiotic bacteria in the products and subsequently in the intestinal environment of the host.The lactobacilli have been reported as antimicrobial-producing strains, and thus, antagonism amongst them they may potentially inhibit other strains and result in diminished efficacy in multispecies probiotic formulations(38).The examination of compatibility between isolated bacteria was conducted using the "cross-streak" method (Figure 3). Through this method, it was determined that there is no antagonistic effect among the selected bacterial strains. These findings align with the research conducted by Mahmoudi et al. (39), which reported that strains of *Bifidobacterium* and *Lactobacillus*, having anti-inflammatory and anti-obesity properties, were able to grow symbiotically. A contradictory result was revealed by Sabo et al. (40)the isolate *L. lactis* subsp. *lactis* C173 and *L. lactis* subsp. *lactis* C195 revealed their antagonistic effect against *E. faecium* C43.

Antibiotic sensitivity

The isolate showed the relatively high susceptibility to cotrimoxazole (22 mm), co-trimazine (20 mm) and oxacillin (20 mm), as clear from Figure 4. In addition, the
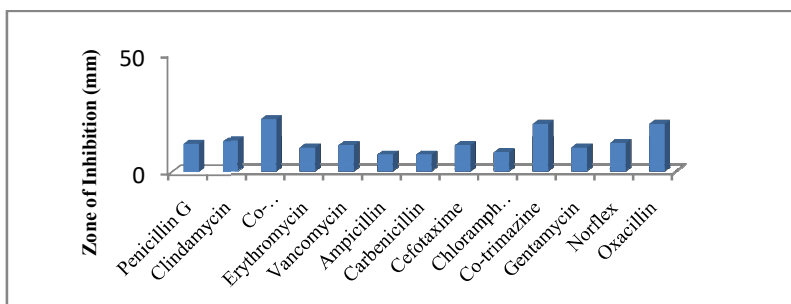

Fig.4: Antibiotic resistance profile of lactic acid bacteria

Kumariet al

absence of transferable resistance genes is an imperative requirement for approval of probiotics.The inherent resilience of probiotic strains enhances the therapeutic and preventive advantages when combined with antibiotics, facilitating the restoration of intestinal microbiota.Furthermore, it has been reported that *Lactobacillus* lacks the transfer of streptomycin, kanamycin, and ciprofloxacin resistance (16). Several strains displayed resistances to tetracycline, ampicillin, and cefotaxime, in line with earlier studies (41) and in agreement with the majority of commercially available probiotics.Probiotic varieties might encounter antibiotics within the digestive system of animals when antibiotics are employed to maintain animal health. Therefore to show their effect as probiotics, the strains need to have nontransferable antibiotic resistance ensuring their safety and survival in the host (42).

Antagonistic activity

The examined isolate displayed inhibitory effects (15.97 ± 0.18 to24.60 ± 0.15 mm diameter) against specific Gram-positive and Gram-negative pathogenic bacteria (Figure 5). Lactobacilli can counteract pathogens through various mechanisms, including the production of antimicrobial substances like lactic acid, acetic acid, hydrogen peroxide, and bacteriocins. Additionally, they compete for resources andco-aggregate with pathogens (43).The

antagonistic activity was of *Lactobacillus plantarum* LG138 was found higher than *Lactobacillus plantarum* isolated from Raw cow milk which exhibited weak antibacterial activity (range of 0- 5mm diameter) against *Staphylococcus aureus, Staphylococcus* epidermidis, *Pseudomonas aeruginosa* and *E. coli.* (44). Contrary, The filtered supernatant of *L. plantarum*was found to be strongly inhibiting the growth of*E. coli* and *B. subtilis* ,*P. aeruginosa* and *S. hominis* having mm 29 and 27 ,38 ,36 ,zones of inhibition respectively as reported byQasim and Jafta 45 .(In addition to the findings of Kos et al. (46), probiotic strains have also been found to exhibit antagonistic activity against prevalent pathogens such as *S. aureus*, *P. aeruginosa*, *E. coli*, *Y. enterocolitica*, and *L. monocytogenes*. Kang et al. (11) investigated the antibacterial activity of monkey and human origin LABs against monkey origin enteric bacteria by the agar disc diffusion test and broth culture inhibition assay and found the higher antimicrobial properties of monkey origin LABs against homogenous enteric bacteria although humans and monkeys were phylogenetically similar species.

Exopoysaccharide Production

The screening of the isolatefor EPS production is greatly sought after because of the numerous health advantages it provides, including immunomodulation, pathogen inhibition, and the capacity to reduce
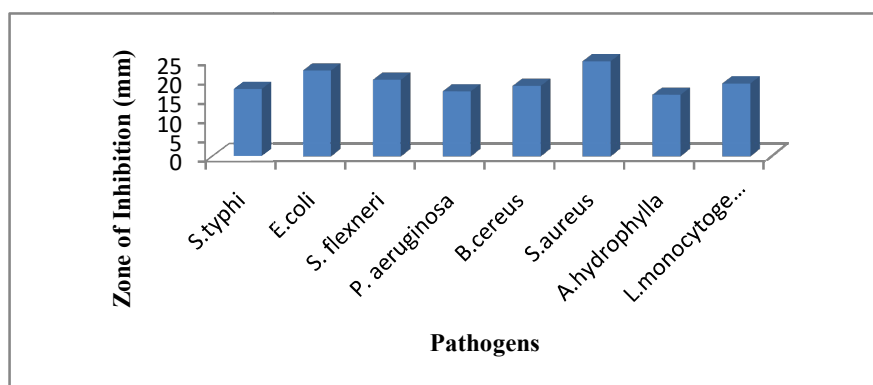

Fig.5: Antimicrobial activity of LAB isolates against food pathogens

*LactiplantibacillusPlantarum*LG138

Current Trends in Biotechnology and Pharmacy
Vol. 18 (Supplementry Issue 4A) 152 - 165, November 2024, ISSN 0973-8916 (Print), 2230-7303 (Online)
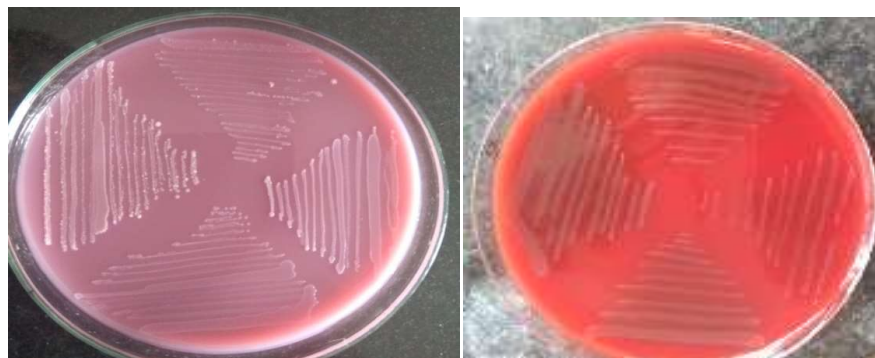10.5530/ctbp.2024.4s.12

161

Fig.6: a) Exopolysaccharide production b) Hemolytic activity shown by the isolate

cholesterol levels.The white colony growth against pink background was observed when the isolate was streaked onto ruthenium red skim milk agar during the study indicates its ability to produce EPS. This is because the generation of either capsular EPS or secreted EPS would preventbacterial cell getting stained by the dye present in the medium(47). The isolate producing exopolysaccharide on skimmed milk-ruthenium red plates are shown in Figure 6a.The production of EPS using this medium was also previously investigated by NandhaandShukla (30) and our result are in line with them.

The estimation of hemolysis activity serves as a crucial probiotic assay, ensuring the safety of food products produced using these organisms. The non-toxic nature of *L. plantarum* LG 138 is demonstrated by its ability to induce γ-hemolysis, safeguarding both the environment and individuals (Figure 6b). Islam et al. (25) reported gamma-hemolytic potentiality of *Lactobacillus plantarum* DMR14 from oats indicated that it is not toxic to the environment or to individuals. Similar observations have been reported byMaragkoudakis et al. [11] in which *Lactobacillus* species isolated from dairy products have been shown to be non-hemolytic. On the contrary, another study reported LAB isolateswhich have shown hemolytic activity (48).

Conclusion

Primates have been extensively employed in worldwide research as preclinical models for various severe conditions, such as infectious, neurological, and metabolic disorders. The demand for primate research has significantly increased, particularly in infectious disease studies like COVID-19, leading to a global scarcity of primate resources. Indeed, preventing intestinal diseases in primates is crucial in veterinary medicine to safeguard and sustain resources for indoor breeding research of these animals. In the present investigation, the probiotic characteristics of LAB derived from primates were thoroughly investigated. The results are deemed valuable research data that could facilitate the development of new lactic acid strains beneficial for primates. The study reveal potential probiotic of primate origin *Lactiplantibacillus plantarum* LG138, due to survival in artificial conditions of the GI tract, γ-hemolytisis, antibiotic resistance, and strong inhibitory activity against food pathogens.The tested isolate of *L. plantarum* LG138 appeared to endowed with features similar to a probiotic organism.This isolate may be further subjected to*in vivo* studies with lab animals andtheassessment of their health benefits will encourage the utilization of the strain in bothfeed and pharmaceutical industry.

Competing Interests

The authors have no relevant financial or non-financial interests to disclose.

References

1. Kereszteny, T., Libisch, B., Orbe, S. C., Nagy, T., Kerenyi, Z., Kocsis, R., Posta, K., Papp, P. P., Olasz, F. (2023). Isolation and Characterization of Lactic Acid Bacteria With Probiotic Attributes From Different Parts of the Gastrointestinal Tract of Free-living Wild Boars in Hungary. Probiotics and Antimicrobial Proteins. https://doi.org/ 10.1007/s12602-023-10113-2.

2. Jin, L., Hinde, K., Tao, L. (2011). Species diversity and relative abundance of lactic acid bacteria in the milk of rhesus monkeys (Macacamulatta). Journal of medical primatology. 40(1):52–58. https://doi.org/10.1111/j.1600-0684.2010.00450.x.

3. Suzuki-Hashido, N.,Tsuchida, S., Azumano, A., Goossens,B., Saldivar, D.A.R., Stark, D.J.,Tuuga, A., Ushida, K., Matsuda, I.(2023). Isolation of bacteria from freeze-dried samples and the functional characterization of species-specific lactic acid bacteria with a comparison of wild and captive proboscis monkeys. Microorganisms. 11: 1458. https://doi.org/10.3390/ microorganisms11061458.

4. European Parliament and the Council of the European Union (2008) Commission Regulation (EC) No 429/2008 of 25 April 2008 on detailed rules for the implementation of Regulation (EC) No 1831/2003 of the European Parliament and of the Council as regards the preparation and the presentation of applications and the assessment and the authorization of feed additives. Official Journal of European Union. L133:1-653. http://data.europa.eu/eli/reg/2008/429/oj.

5. Gioia, D. D., Biavati, B. (2018). Probiotics and Prebiotics in Animal Health and Food Safety.Springer International Publishing AG. https://doi.org/10.1007/978-3-319-71950-4

6. Adli, D.N., Sjofjan, O., Sholikin, M. M., Hidayat, C., Utama, D.T., Jayanegara, A., Natsir, M.H., Nuningtyas,Y.F., Pramujo, M., Puspita, P.S. (2023). The effects of lactic acid bacteria and yeast as probiotics on the performance, blood parameters, nutrient digestibility, and carcase quality of rabbits: a meta-analysis, Italian Journal of Animal Science. 22:1: 157-168.https://doi.org/ 10.1080/1828051X.2023.2172467.

7. Barelli, C., Albanese, D., Stumpf, R.M., Asangba, A., Donati, C., Rovero, F., Hauffe, H.C. (2020). The gut microbiota communities of wild arboreal and ground-feeding tropical primates are affected differently by habitat disturbance. mSystems 5:e00061-20. https://doi.org/10 1128/ mSystems.00061-20.

8. Prabhurajeshwar C., Chandrakanth R.K. (2017). Probiotic potential of Lactobacilli with antagonistic activity against pathogenic strains: an in vitro validation for the production of inhibitory substances. Biomedical Journal. 40:270–283. https://doi.org/10.1016/j.bj.2017.06.008.

9. Jiang, X., Xu, H.J., Cui, Z.Q. and Zhang, Y.G. (2020). Effects of supplementation with *Lactobacillus plantarum*299v on the performance, blood metabolites, rumen fermentation and bacterial communities of preweaning calves. Livestock Science. 239: 104120.

10. Lowenstine , L.J. (2003). A Primer of Primate Pathology: Lesions and nonlesions. Toxicologic Pathology. 31(Suppl.), 92–102.

11. Kang, P.Y., Do, K.H.,Koo,B.S., Wan-KyuLee,W.K. (2022). Comparative antimicrobial activity of human and monkey origin lactic acid bacteria on simian enteric bacteria.Journal of Biomedical and translational Research. 23(3):55-65.https://doi.org/10.12729/jbtr.2022.23.3.55.

12. Koo, B. S., Baek, S. H., Kim, G., Hwang, E. H., Oh, H., Son, Y., Lim, K. S., Kang, P., Lee, H. Y., Jeong, K. J., Kim, Y. H., Villinger, F., Hong, J. J. (2020). Idiopathic chronic diarrhea associated with dysbiosis in a captive Cynomolgus macaque (*Macacafascicularis*). Journal of Medical primatology. 49(1): 56–59. https://doi.org/10.1111/jmp.12447Anver, M.

R. (1982). Acute gastric dilatation in nonhuman primates: review and case studies. Veterinary Pathology. Supplement19 (Suppl 7):126–133. https://doi.org/ 10.1177/030098588201907s09.

13. Kumari, R., Lata, P.,Sharma, K.B., Rangra, S., Savitri (2023).Statistical optimization of fermentation media for postbiotic metabolite production from *Lactobacillus plantarum*LG 138 of primate origin. Mapana Journal of Sciences. 22:41–68.

14. Maragkoudakis, P.A., Zoumpopoulor, G., Miaris, C., Kalantzopoulos, G., Pot, B.,Tsakalidou, E. (2006). Probiotic potential of *Lactobacillus* strains isolated from dairy products. International Dairy Journal16: 189-99.https://doi.org/10.1016/j.idairyj.2005. 02.009

15. Gilliland, S. E., Staley, T. E., & Bush, L. J. (1984). Importance of bile tolerance of *Lactobacillus acidophilus* used as a dietary adjunct. Journal of Dairy Science. 67(12): 3045-3051. https://doi.org/ 10.3168/jds.S0022-0302(84)81670-7

16. Zago, M., Fornasari, M.E., Carminati, D., Burns, P., Suarez, V.B., Vinderola, G., Reinheimer, J.A., Giraffa, G. (2011).Characterization and probiotic potential of *Lactobacillus plantarum* strains isolated from cheeses. *Food Microbiology.28(5):* 1033–40.

17. Rosenberg, M., Gutnick, D., Rosenberg, E. (1980). Adherence of bacteria to hydrocarbons: a simple method for measuring cell surface hydrophobicity. FEMS Microbiology Letters. 9(1):29-33.

18. Collado, MC, Grzeskowiak L, Salminen S. (2007).Probiotic strains and their combination inhibit *in vitro* adhesion of pathogens to pig intestinal mucosa. Current Microbiology.55:260–265.

19. Handley, P. S., Harty, D. W., Wyatt, J. E., Brown, C. R., Doran, J. P., & Gibbs, A. C. (1987). A comparison of the adhesion, co-aggregation and cell-surface hydrophobicity properties of fibrillar and fimbriate strains of *Streptococcus salivarius*. Journal of General Microbiology. 133(11):3207–3217. https://doi.org/10.1099/ 00221287-133-11-3207.

20. Guo, Z., Wang, J., Yan, L., Chen, W., Liu, X. M., Zhang, H. P. (2009). *In vitro* comparison of probiotic properties of *Lactobacillus casei* Zhang, a potential new probiotic, with selected probiotic strains. LWT-Food Science and Technology. 42 (10):1640-1646.

21. Clinical and Laboratory Standards Institute (CLSI).(2012). Performance standards for antimicrobial susceptibility testing. Twenty-Second Informational Supplement. CLSI Document M100-MS19.Wayne, PA: CLSI.

22. Mishra, B. K., Hati, S., Brahma, J., Patel, M., & Das, S. (2018). Identification and characterization of yeast strains associated with the fermented rice beverages of GaroHills, Meghalaya, India. International Journal of Current Microbiology and Applied Sciences. 7(2); 3079-90.https://doi.org/ 10.20546/ijcmas.2018.702.371

23. Kersani, I., Zadi-Karam, H., Karam, N.E. (2017). Screening of exopolysaccharide-producing coccal lactic acid bacteria isolated from camel milk and red meat of Algeria. African journal of Biotechnology.16(18): 1078-1084.

24. Lombardi, A., Dal Maistro, L., De Dea, P., Gatti, M., Giraffa, G., Neviani, E. (2002). A polyphasic approach to highlight genotypic and phenotypic diversities of *Lactobacillus helveticus* strains isolated from dairy starter cultures and cheeses. Journal of Dairy Research. 69(1):139-149.https://doi.org/ 10.1017/s0022029901005349

25. Islam, S., Biswas, S., Jabin, T., Moniruzzaman, M., Biswas, J., Uddin, M. S., Akhtar-E- Ekram, M., Elgorban, A. M., Ghodake, G., Syed, A., Saleh, M. A., &Zaman, S. (2023). Probiotic potential of *Lactobacillus plantarum* DMR14 for preserving and extending shelf life of fruits and fruit juice. Heliyon. 9(6): e17382. https://doi.org/10.1016/j.heliyon.2023.e17382

26. Mbye, M., Baig, M. A., AbuQamar, S. F., El-Tarabily, K. A., Obaid, R. S., Osaili, T. M., Al-Nabulsi, A. A., Turner, M. S., Shah, N. P., &Ayyash, M. M. (2020). Updates on understanding of probiotic lactic acid bacteria responses to environmental stresses and

highlights on proteomic analyses. Comprehensive Reviews in Food Science and Food Safety. 19(3):1110–1124. https://doi.org/10.1111/1541-4337.12554

27. Zielinska, D., Rzepkowska, A., Radawska, A., Zielinski, K. (2015). In vitro screening of selected probiotic properties of Lactobacillus strains isolated from traditional fermented cabbage and cucumber. Current Microbiology. 70:183-194.

28. Huang, R., Pan, M., Wan, C., Shah, N. P., Tao, X., & Wei, H. (2016). Physiological and transcriptional responses and cross protection of *Lactobacillus plantarum* ZDY2013 under acid stress. Journal of Dairy Science. 99(2): 1002-1010.

29. Choi, H. R., Chung, Y. H., Yuk, H. G., Lee, H., Jang, H. S., Kim, Y., & Shin, D. (2018). Characterization of *Lactobacillus plantarum* strains isolated from black raspberry and their effect on BALB/c mice gut microbiota. Food Science and Biotechnology. 27(6): 1747–1754. https://doi.org/10.1007/s10068-018-0420-3

30. Nandha, M. C., &Shukla, R. M. (2023). Exploration of probiotic attributes in lactic acid bacteria isolated from fermented *Theobroma cacao L.* fruit using *in vitro* techniques. Frontiers in Microbiology. 14:1274636. https://doi.org/10.3389/fmicb.2023.1274636

31. Alameri, F., Tarique, M., Osaili, T., Obaid, R., Abdalla, A., Masad, R., Al-Sbiei, A., Fernandez-Cabezudo, M., Liu, S.-Q., Al-Ramadi, B., Ayyash, M.(2022). Lactic acid bacteria isolated from fresh vegetable products: potential probiotic and postbiotic characteristics including immunomodulatory effects. *Microorganisms.10*: 389.https://doi.org/10.3390/microorganisms10020389

32. El-Deeb W.M., Fayez, M., Elsohaby, I., Ghoneim, I., Al-Marri, T., Kandeel, M., ElGioushy M. 2020. Isolation and characterization of vaginal Lactobacillus spp. in dromedary camels (*Camelusdromedarius*): *in vitro* evaluation of probiotic potential of selected isolates. PeerJ 8:e8500 DOI 10.7717/peerj.8500

33. Garcia, A., Navarro, K., Sanhueza, E., Pineda, S., Pastene, E., Quezada, M., Henriquez, K., Karlyshev, A.,Villena, J., Gonzalez, C. (2017). Characterization of Lactobacillus fermentum UCO-979C, a probiotic strain with a potent anti-Helicobacter pylori activity. Electronic Journal of Biotechnology. 25: 75-83.

34. Jang, H.J., Lee, NK. & Paik, HD. (2019). Probiotic characterization of *Lactobacillus brevis* KU15153 showing antimicrobial and antioxidant effect isolated from kimchi. Food Science and Biotechnology.28: 1521–1528. https://doi.org/10.1007/s10068-019-00576-x

35. SoumitraNath, JibalokSikidar, Monisha Roy, Bibhas Deb. (2020). *In vitro* screening of probiotic properties of *Lactobacillus plantarum* isolated from fermented milk product. *Food Quality and Safety*. 4(4):213–223.https://doi.org/10.1093/fqsafe/fyaa026

36. Liu, C., Xue, W-j, Ding, H., An, C., Ma, S-j., Liu, Y. (2022) Probiotic Potential of Lactobacillus Strains Isolated From Fermented Vegetables in Shaanxi, China. Frontiers in Microbiology. 12:774903. doi: 10.3389/fmicb.2021.774903

37. Reid, G., McGroarty, J.A., Angotti, R., Cook, R.L. (1988). *Lactobacillus* inhibitor production against *Escherichia coli* and co-aggregation ability with uropathogens. Canadian Journal of Microbiology. 34: 344–351.

38. Timmerman, H.M., Koning, C.J., Mulder, L., Rombouts, F.M., Beynen, A.C., 2004. Monostrain, multi-strain and multispecies probiotics—a comparison of functionality and efficacy. International Journal of Food Microbiology. 96: 219–233.

39. Mahmoudi, I., Telmoudi, A., Hassouna, M. (2018)."Beneficial Effects of Probiotic Lactobacillus plantarum Isolated from Cow, Goat and Sheep Raw Milks". Acta Scientific Microbiology. 1.2:17-20.

40. Sabo, S. D. S., Mendes, M. A., Araujo, E. D. S., Muradian, L. B. A., Makiyama, E. N., LeBlanc, J. G., Borelli, P., Fock, R. A., Knobl, T., & Oliveira, R. P. S. (2020). Bioprospecting

Current Trends in Biotechnology and Pharmacy
Vol. 18 (Supplementry Issue 4A) 152 - 165, November 2024, ISSN 0973-8916 (Print), 2230-7303 (Online)
10.5530/ctbp.2024.4s.12

165

of probiotics with antimicrobial activities against Salmonella Heidelberg and that produce B-complex vitamins as potential supplements in poultry nutrition. Scientific Reports. 10(1):7235. https://doi.org/10.1038/s41598-020-64038-9

41. Somashekaraiah, R., Shruthi, B., Deepthi, B. V., and Sreenivasa, M. Y. (2019). Probiotic properties of lactic acid bacteria isolated from neera: a naturally fermenting coconut palm nectar. Frontiers in Microbiology. 10:1382. https://doi.org/10.3389/fmicb.2019.01382.

42. Jose, N. M., Bunt, C. R.,Hussain, M. A. (2015). Comparison of microbiological and probiotic characteristics of lactobacilli isolates from dairy food products and animal rumen contents. Microorganisms. 3(2): 198-212.

43. Vieco-Saiz, N., Belguesmia, Y., Raspoet, R., Auclair, E., Gancel, F., Kempf, I., Drider, D. (2019).Benefits and inputs from lactic acid bacteria and their bacteriocins as alternatives to antibiotic growth promoters during food-animal production. Frontiers in Microbiology.10:57.https://doi.org/10.3389/fmicb.2019.00057

44. Fahem,W.D., Alabden, S.S.Z., Tawfeeq, A.A. (2021). Molecular investigation of Lactobacillus plantarum isolated from raw cow milk in Kirkuk/Iraq. Natural Volatiles and Essential Oils. 8(5): 9162-9172.

45. Qasim, D.A., Jafta, I.J.(2023). Antibacterial activity of Lactiplantibacillus plantarum from dairy products Against some food borne bacteria. The Iraqi Journal of Veterinary Medicine. 47(1): 44-51. https://doi.org/10.30539/ijvm.v47i1.1500

46. Kos, B., Suskovi, J., Beganovi, J., Gjurai, K., Frece, J., Iannaccone, C., Canganella, F. (2008). Characterization of the three selected probiotic strains for the application in food industry.World Journal of Microbiology and Biotechnology. 24: 699–707. https://doi.org/10.1007/s11274-007-9528-y.

47. Mora, D., Fortina,M.G.,Parini,C.,Ricci, G.,Gatti, M.,Giraffa,G.,Manachini,P.L. (2002). Genetic diversity and technological properties of Streptococcus thermophilus strains isolated from dairy products. Journal of Applied Microbiology. 93(2): 278–287.

48. Sieladie, D.V., Zambou, N.F., Kaktcham, P.M., Cresci, A., Fonteh, F. (2011) Probiotic properties of Lactobacilli strains isolated from raw cow milk in the Western Highlands of Cameroon. Innovative Roman Food Biotechnology. 9:12–28.

Bioprofiling of Polyherbal Mixture Towards Plant-Derived Pharmaceuticals

E Jancy Mary [1], and L Inbathamizh[2*]

[1]Faculty of Life Sciences, Sathyabama Institute of Science and Technology, Chennai-600119, India
[2]Department of Biotechnology, Sathyabama Institute of Science and Technology, Chennai-600119, India
*Corresponding author: inbathamizh.bte@sathyabama.ac.in

Abstract

Herbs are the major sources that protect us from the attack of free radicals. The methanolic extract of polyherbal mixture comprising the leaves of *Ocimumtenuiflorum, Mentha piperita, Trigonella foenum-graecum, Plectranthusamboinicus* and *Acalypha indica* was taken for the study. The research was designed to evaluate phytonutrients, antioxidant and antimicrobial activities of polyphenolic compounds extracted from the polyherbal mixture. The results of the investigation indicated a high phenol content of 10.452± 0.010 mg/g along with flavonoids 6.976± 0.014mg/g and tannins 9.08± 0.012mg/g which are also polyphenols as compared to saponins0.250± 0.006mg/g, glycosides 0.058± 0.009mg/g and alkaloids 0.051± 0.005 mg/g in the polyherbal extract. The polyherbal formulation showed maximum yield of polyphenolic compounds in maceration extract which was 476.63µg GAE/mL compared to that of soxhlet method of 403.95µg GAE/mL. The phenolic Thin Layer Chromatography (TLC) profile of methanol:hexane exhibited 7 to 8 spots (3:1). The polyphenolic compounds exhibited higher antioxidant activity with EC50 values of 61.67±0.07 µg/mL and 33.95±0.10 µg/mL through ferric reducing antioxidant power (FRAP) assay and phosphomolybdenum analysis respectively and IC50 values of 73.34±0.12 µg/mL and 26.76±0.10 µg/mL through superoxide scavenging radical analysis and 2, 2 azino bis 3 ethylbenzothiazoline 6 sulfonic acid (ABTS) radical scavenging analysis respectively. Disk diffusion method revealed that they exhibited antimicrobial activities against oral pathogens such as *Streptococcus mutans, Candida albicans, Actnimyces viscosus* and *Staphylococcus aureus* with inhibition zones of 14.20±1.15 mm, 15.00±1.00 mm, 21.07±0.57 mm and 22.00±0.51 mm respectively. Finally, the research concluded that the polyherbal extract had antimicrobial and antioxidant properties, and that it could be a significant source of bioactive compounds with potential biological benefits.

Keywords: Polyherbal mixture, Polyphenols, Maceration and Soxhlet Extraction, TLC, Antioxidant Activity and Antimicrobial Activity.

Introduction

The role of plants as a significant source of drugs and therapeutic agents has been passed down through the generations and playsa crucial part in health care. India is the huge manufacturer of medicinal plants and is thus capably known as the agricultural garden of the globe (1). Polyherbal mixture has been utilized throughout the world due to its wide range of therapeutic properties and for reducing toxicity. Due to synergistic effect, polyherbal formulations confer more effectiveness in many diseases compared to single plant (2). These plants can thrive in temperatures between 20°C to 30°C, as they are very adaptable to a variety of conditions. These can be cultivated in farms, gardens, pots, or other containers, based on the resources and space that are available. Based on the similarity between environmentalconditions and the ease of cultivation process, these plants were selected for this study (3).

Mentha piperita (family- Lamiaceae) commonly known as Peppermint is a strongly aromatic herb and most widely used in

medicinal preparations. Traditionally, the peppermint plant has many pharmacological effects such as anticarcinogenic, antitumorigenic, dental protective, antioxidant, antimicrobial, antinociceptive, antiallergic, anti-inflammatory and antiviral activities with high phenol, tannin and flavonoid content (4).

Ocimum tenuiflorum (family-Lamiaceae) commonly known as Holy basil is a traditional plant used in Ayurvedic medicine. The scientific studies indicated tulsi has antiviral, antistress, antifungal, antioxidant, hepatoprotective, antibacterial, immunomodulating, antipyretic, anti-inflammatory, antimalarial, antidiuretic, hypolipidemic and antidiabetic properties. Holy basil is being used in combination with other plants to show good healing properties with high polyphenolic content (5).

Acalypha indica (family-Euphorbiaceae) commonly known as Indian acalypha is an ethnomedicinal herb used in many other countries. Indian acalypha has various therapeutic uses such as anticancer, antiulcer, anti-inflammatory, antifungal, anthelmintic, antibacterial, antihyperlipidemic, antidiabetic, antiobesity, hepatoprotective, wound healing and antivenom properties with high polyphenol and flavonoid content (6).

Trigonella foenum- graecum (family-Fabaceae) commonly known as Fenugreek is used as a dietary supplement. Fenugreek is beneficial for the control of different complications through its antioxidant, antitumor, anti-inflammatory, anticancer, cardioprotective, hepatoprotective, neuroprotective, nephroprotective, antimicrobial and immunomodulatory activities with high polyphenol and flavonoid content with high polyphenol, tannin and flavonoid content (7).

Plectranthus amboinicus (family-Lamiaceae) commonly known as Indian borage is an herbal medicine used in the traditional system. Indian borage shows many biological properties such as antidiabetic, antimicrobial, anxiolytic, antifungal, analgesic, anti-inflammatory, antiplatelet aggregation, diuretic, skincare, antimalarial, antibiofilm, wound healing, and antineoplastic activities. *P. amboinicus* possesses increased effect if given in combination with different herbs (8).

In the latest periods, the quantitative analysis evaluates the total content of secondary metabolites such as phenols, flavonoids, tannins and alkaloids show the therapeutic importance of plant. This technique is active in a crucial role to analyze the secondary phytonutrients that provide health-promoting and disease-curing properties (9). The maceration and soxhlet extraction have the most important effect on phenolic compounds which act as antioxidant sources useful in the pharmaceutical and food industry (10). The thin layer chromatography (TLC) separates the bands in different solvent system to analyze the bioactive constituents (11).Ferric reducing power assay (FRAP), phosphomolybdenum assay, superoxide scavenging radical analysis and 2, 2 azino bis 3 ethylbenzothiazoline 6 sulfonic acid (ABTS) radical scavenging analysis are employed to assay the free radical eliminating activity in the prevention of numerous illness and promotion of health in plant species (12).Many disorders are treated using herbal combinations because of their pharmacological qualities. The majority of polyherbal mixtures are used in microbial therapy (13).

A detailed literature review for the individual plants of *M. piperita, O. tenuiflorum, A. indica, T. foenum-graecum* and *P. amboinicus*is available (3). But no published papers are available so far explaining the synergistic effect imposed by the combination of these herbs and the details regarding the quantitative analysis, free radical scavenging property and antimicrobial activity. Hence, the present work was framed to determine quantitative analysis, antioxidant activity and antimicrobial activity of the polyherbal mixture. The synergistic effect is so effective to emphasize that polyherbal mixture has significant applications. This further helps in the therapeutics against diseases such as dental caries, inflammatory diseases and cancer.

Materials and Methods

Assemblage and Certification of Herbal Plants

Herbs such as *M. piperita, O.tenuiflorum, A. indica, T. foenum- graecum* and *P. samboinicus* were collected from Chennai, Tamilnadu and were authenticated by Dr. P. Sathiyarajeswaran, Assistant Director in charge and Dr. K. N. Sunil Kumar, Researcher and Pharmacognosy, Department Head, Central Council for Research in Siddha (CCRS), Madras (Authentication number: 252-06082101-05).

Extraction

Dried plant materials of 500 g each in the ratio 1:1:1:1:1 were mixed and extracted with methanol by using an orbital shaker for 72 hours. The polyherbal combinations were filtered by grade one chromatography sheet. An extract was subjected for evaporation in front of a stream of air at 37° C which yielded a polyherbal semisolid mass of 9.18 g of methanol extract and then the polyherbal mixture was stored in an airtight container for further analysis. Applying the formula, the percentage (%) yield was determined by calculating the dry weight of polyherbal mixture (14).

Percentage yield = Amount of the wet polyherbal methanolic extract/ Amount of the wet polyherbal mixture material * 100

Quantitative Analysis of Phytonutrients

Quantitative Assessment of Alkaloid Content

About 5 ml of phosphate buffer solution, equal volume of bromocresol green reagent and small amount of test substance were mixed. The resultant combination was thoroughly dissolved in 4 ml of chloroform. Chloroform was utilized to dilute the polyherbal mixture. At 470 nm, the complex's absorbance in chloroform was evaluated in comparison to a control that was made identically but without polyherbal extract. Atropine equivalents in mg/g were used to report the results, with atropine acting as the reference.(15, 16).

Quantitative Assessment of Flavonoid Content

Quercetin was used as a standard in the aluminum chloride procedure to calculate the total flavonoid concentration. To a 10 mL volumetric flask, 1 mL of the polyherbal test solution and 4 mL of water were mixed. Aluminum trichloride and sodium nitrate were mixed shortly after 5 min. The resulting mixture was mixed with 2 ml of 1M sodium hydroxide after it had been kept at appropriate temperature for the experiment. The final volume was quickly increased to using water. Using a blank spectrometer, the absorbing capacity of the resultant was determined at 510 nm. The findings were given as mg QE/g dry weight, or quercetin equivalents (15,17).

Quantitative Assessment of Saponin Content

After diluting the polyherbal test sample in 80% methanol, 2 ml of vanilin in ethanol was mixed. Next, 2 ml of a mixture of 72% sulfuric acid was thoroughly mixed before being heated on a water bath for 10 min at 60°C. At 544 nm, the absorbance was measured in relation to a reagent blank. The data was represented as mg/g equivalent of diosgenin, which acts as a standard (18, 19).

Quantitative Assessment of Phenol Content

Using Folin-Ciocalteu's reagent, the polyherbal test sample's total phenolic content was measured with minor modification. In short, 0.4 ml of diluted folin's solution was mixed to polyherbal test solution. 4 mL of sodium carbonate reagent was mixed after 5 min. Add 10 mL distilled water to the tubes to reach a final capacity; they were left to remain at ambient temperature for 90 minutes. Using a spectrophotometer, the absorbing capacity of the polyphenolic extract was determined at 750 nm compared to the blank. Gallic acid serves as the standard in the construction of a calibration curve, and the extract's total amount of polyherbal phenolic compounds was reported in gallic acid (mg) per gram of wet mass (15, 18).

Quantitative Assessment of Tannin Content

By combining equal amount of polyherbal extract and distilled water and agitating for 20 min, the entire tannin quantity of the polyherbal formulation was measured with slight modification. About 0.5 mL of 0.008M potassium ferrocyanide solution and 1 mL of 0.1M ferric chloride in HCL solution was added. At normal room temperature, the tubes were mixed for 5 min. Using a spectrophotometer, the formulation's absorbing capacity was calculated at 120 nm. Using tannic acid as a reference, a curve for calibration was created. In mg of tannic acid per gram of dehydrated extracts, total tannins were determined (17, 20).

Quantitative Assessment of Glycosides Content

The modified method to calculate the total amount of glycosides in the polyherbal extract, the polyherbal extract was mixed with distilled water, then agitated for 10 min. To the above polyherbal mixture, 1 mL of acetic acid and 0.1 mL of 5% ferric chloride was mixed and let undisturbed for 90 min. In comparison to the blank reagent, the absorbance was determined at 568 nm. The standard utilized to generate the curve for calibration was digoxin. Digoxin mg/g of dried polyherbal extracts was used for calculating total glycoside content (21, 22). All the quantitative assays were carried out in triplicates, and the mean ± SD was used to represent the results.

Extraction Methods

Maceration Method

A conical flask containing about 25 g of polyherbal substance was mixed with 75 mL of methyl alcohol and left for 72 hours. Polyherbal extracts were obtained by filtering and collecting the supernatant. A modified method of using 70% instead of 80% methyl alcohol was followed to obtain maximum yield. The optimal solvent concentration had an impact based on the solubility, selectivity, density, interactions and mass transfer of the target compounds (23, 24).

Soxhlet Method

The modified method of the polyherbal substance was ground up with a mechanical blender, around 20 g of polyherbal fine powder was poured into a 12 x 3 cm thimble made of sturdy filter paper, which was then put within the Soxhlet extractor's thimble chamber. 300 mL of 70% methyl alcohol solvent were placed in a round-bottomed flask and connected to a Soxhlet extractor; the extractor was then used when combined with the condenser. The water circulation device was attached to the condenser's input and outflow knobs for water movement (cooling). In this configuration a round-bottomed flask was put on the heating mantle. Upon heated through the heating mantle, the solvent that was used started to evaporate and passed through both the Soxhlet chamber and condenser. The compounds disintegrated and emerged from the substance when the condensate then dropped down into the thimble container. The process was restarted after the solvent level achieved its maximum level and was taken off *via* the siphon arm and emptied into the round-bottom flask. For the production of gummy extract, the polyherbal supernatant in the round-bottomed flask was then condensed at 50°C (23, 25).

Thin layer chromatography

The modified method using a capillary tube, the polyherbal phenolic sample was spotted on the TLC paper approximately 0.5 cm above the bottom. The developing phenolic solvent was poured into the chromatographic beaker and left to run until it reached three quarters of the TLC sheet (the spot shouldn't come into contact with the solvent). After the plates being removed, the solvent front was marked by a pencil and let to evaporate. Next, the TLC plate was seen in the presence of ultraviolet (UV) light. Iodine pellets were put into the plates in order to see the distinct bands (26).

Mary et al

Current Trends in Biotechnology and Pharmacy
Vol. 18 (Supplementry Issue 4A) 166 - 185, November 2024, ISSN 0973-8916 (Print), 2230-7303 (Online)
10.5530/ctbp.2024.4s.13

170

R_f value = Solute's travel distance/ Solvent's travel distance

Free Radical Scavenging Assays

Ferric ion reducing antioxidant power test

The modified ferric ion reducing antioxidant power method employs a redox-linked colorimetric procedure with antioxidants serving as reductants (27). The varying doses of 20-120μg/mL polyherbal extracts were mixed with 1 mL of a 0.2M buffered phosphate solution at pH 6.6 and 1 mL of 1% potassium ferricyanide solution. To the resulting mixture, 1 mL of 10% trichloroacetic acid and iron chloride (0.1%) was mixed and incubated at room temperature. The resultant solution's measured at 700 nm was estimated. The positive control used was ascorbic acid. The assays were conducted in triplicates, and the mean ± SD was used to represent the results.

Phosphomolybdenum assay

The reduction test method, which is predicated on the creation of green phosphomolybdenum complex, was used to assess the antioxidant capacity with small modifications (27). 1 mL of phosphomolybdenum solution was mixed with extracts at different concentrations of 20–120 μg/mL. After being sealed, the tubes were left to incubate for 30 minutes at 95°C in a water bath. After bringing the sample down to a normal room temperature, the antioxidant activity of the polyphenolic extracts was measured at 695 nm using the positive control ascorbic acid. The assays were conducted in triplicates, and the mean ± SD was used to represent the results. The percentage of polyphenolic extract reduction for both the assays was calculated by

% of reduction = [(Abs (sample) – Abs (control)/Abs (sample)] x 100

Superoxide radical scavenging activity

This method was used to scavenge radicals containing superoxide with minor modifications (28). Different amounts of methanol extract, 50 mM phosphate buffer solution at pH 7.8, 1.5 mM the B vitamin riboflavin, 12 mM edetic acid and 50 mM Nitrotetrazolium Blue chloride were added to the resulting mixture in that sequence. The process was initiated by subjecting the resultant mixture to UV light for 90 sec. The absorbing capacity at 590 nm was calculated shortly after illumination, and the IC50 was determined. Every test was carried out in triplicates, and the outcomes were reported as mean ± SD. The positive control used was ascorbic acid.

ABTS$^+$ Radical cation scavenging assay

The ABTS free radical cation scavenging capability was analyzed to determine the antioxidant properties with small modifications (29). The reaction mixture of persulfate of potassium with ABTS reagent and allowed to stand at room temperature in a dark place for 12–16 hours prior being utilized. After being stable for two days, the ABTS solution was diluted to an absorbance of 730 nm using 5 mM phosphate-buffered saline solution at pH 7.4. The absorbance was determined 10 minutes by adding 10–60 μg/mL various doses of polyphenolic solution to diluted ABTS solution and incubated at 25°C. The positive control was ascorbic acid. Every test was carried out in triplicates, and the outcomes were reported as mean ± SD.

The percentage of polyphenolic extract inhibition for both the assays was calculated by:

$$\% \text{ of inhibition} = \frac{\text{Absorbance}_{Control} - \text{Absorbance}_{Sample}}{\text{Absorbance}_{Control}} \times 100$$

Evaluation of Antimicrobial Activity

Bactericidal Assay

Using the agar disc diffusion method, the polyphenolic extract of bacteriostatic capability of *S. mutans*, *S.aureus* and *A.viscosus* was investigated. After being cascaded into an aseptic cell culture dish, Mueller-Hinton agar was densified. Mueller-Hinton agar was inoculated with thick peptidoglycan gram-positive *S. aureus, S.*

Current Trends in Biotechnology and Pharmacy
Vol. 18 (Supplementry Issue 4A) 166 - 185, November 2024, ISSN 0973-8916 (Print), 2230-7303 (Online)
10.5530/ctbp.2024.4s.13

171

mutans, and A. viscosus using aseptic cotton buds and nutritional liquid broth medium. A cork auger that was aseptic was used to make pentaholes in agar for the samples, standard, and control (0.8cm width). Each individual hole was filled with various concentration of polyphenolic extract against a positive control tetracycline. The cell culture dish was then kept at 98.6°F for the duration of the night. The outcomes were shown as mean ± SD, with each assay carried out in triplicate. The zone of inhibition in mm surrounding the hole was used to measure the antibacterial activity (30,31).

Fungicidal Assay

Densification was achieved by cascading potato dextrose agar into an aseptic cell culture dish. C. albicans fungus swabbed and left in a cell culture dish for 48 hours. Next, using a cork auger, the sample of polyphenolic extract was poured into the wells in various amounts. After filling each individual hole with various concentrations against a positive control fluconazole, the cell culture dish was kept at 98.6°F for 48 hours. The outcomes were shown as mean ± SD, with each assay carried out in triplicates. The zone of inhibition in mm surrounding the hole was used to assess the fungicidal capability (32, 33). Elevated humidity has the ability to modify the agar medium's diffusion characteristics and hydration level, which

could impact the antibacterial agents' rates of diffusion. The size and form of inhibitory zones may vary as a result of this. When handling and preparing agar plates, weather factors like heat or high humidity might raise the risk of contamination. This may result in lower antibacterial agent concentrations in the agar, which could compromise the assay's accuracy. The assays were repeated to overcome this problem.

Results and Discussion

Polyherbal Methanolic Fractionation

Polyherbal mixture upon extraction with methanol solvent resulted in the extract with the yield of 1.836%. Some of the key elements influencing extract yields and the plant materials' subsequent antioxidant activity are the type of extracting solvent used. The activity varies depending on the different chemical properties and polarity of the phytoconstituents.

Quantitative Analysis of Phytonutrients

Quantitative Assessment of Alkaloid Content

The total alkaloid content in the polyherbal methanol extract were found to be 0.051 ± 0.005 mg/g of polyherbal extract ($y=0.2292\,x+0.1658$, $R^2 =0.9931$) (Figure 1). Earlier studies have indicated the total
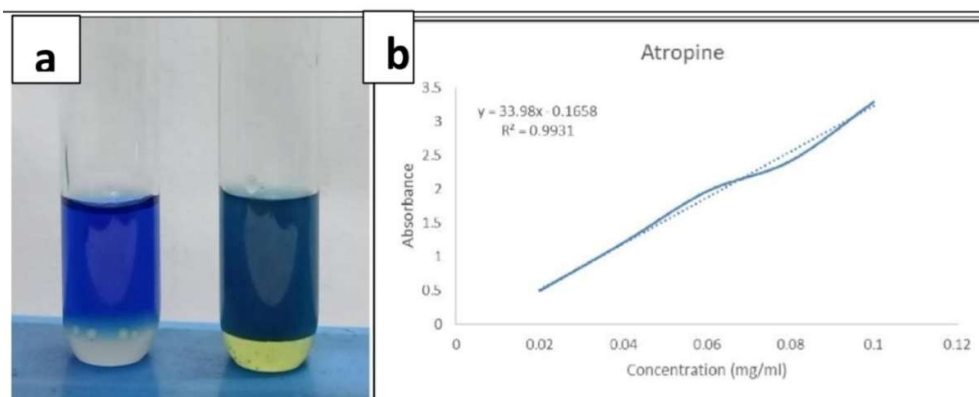

Figure 1: Quantitative Assessment of Alkaloid Content (a) Alkaloid formation at 20mg/ml (b) Standard graph and estimation of alkaloid in the sample

Current Trends in Biotechnology and Pharmacy
Vol. 18 (Supplementry Issue 4A) 166 - 185, November 2024, ISSN 0973-8916 (Print), 2230-7303 (Online)
10.5530/ctbp.2024.4s.13

172

alkaloid content was found to be 0.00313mg/g in ocimum leaf and 5.92% in *Moringa concanensis.*Alkaloids are employed for their antimicrobial and hypoglycemic qualities. Due to the presence of numerous components that are essential for maintaining good health, the phytochemical constituents appeared to have the potential to both improve their health and serve as a source of helpful pharmaceuticals (34, 35).

Quantitative Assessment of Flavonoid Content

The total flavonoid content in the polyherbal methanol extract was found to be 6.976± 0.014mg/g (y=0.2292x+0.2441, R^2 =0.9989) which was more significant than earlier work of polyherbal extract (Figure 2). In a study, the total flavanoid content of calotropis leaf was found to be 2.285mg/g (36). Earlier work on polyherbal formulations such as DBC (34 multiple herbs) and DMV (22 multiple herbs) showed total flavanoid content of 2.30 and 1.78mg/g respectively (37). The nature of these chemical components, which are in charge of the intended therapeutic characteristics and specific physiological consequences, dictated the pharmacological activity of the polyherbal extract of the herbal formulation. Strong positive linear correlation (r), which is near to +1, was displayed in all of the calibration graphs. According to the graphs, absorbance values rise in tandem with concentration levels. The polarity of the solvents utilized in the extraction process affects the quantity of flavonoids present in plant extracts. With the aid of several calibration curves, the sample values were examined, and various graphs were used to produce the various concentration values. The highest concentration of flavonoids is produced by a polyherbal mixture of *Cassia alata, Wedeliatrilobata, and Hugonia syntactic.* (38).

Quantitative Assessment of Saponin content

The total saponin contents in the polyherbal methanol extract was found to be 0.250 ± 0.006mg/g of polyherbal extract (y=3.3753 x+0.0179, R^2 =0.9971) (Figure 3). Earlier studies have indicated total saponin content of ocimum leaf as 0.016mg/g (34). In intracellular histochemistry labeling, saponins act as mild detergents and are utilized to enable antibodies to interact with proteins within the cell. Saponins are involved in weight loss, hyperglycemia and hypercholesterolemia with antioxidant, anticancer and anti-inflammatory properties (35). As a natural defense mechanism, saponins bitter flavor has assisted in keeping plants safe from soil microbes, insects, and mammalian herbivores. Numerous studies
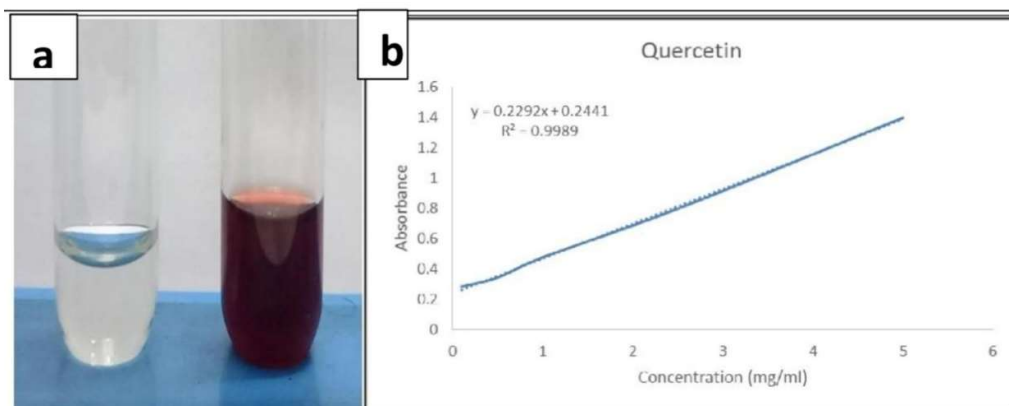

Figure 2: Quantitative Assessment of Flavonoid Content (a) Flavonoid formation at 20mg/ml (b) Standard graph and estimation of flavonoid in the sample

Bioprofiling of Polyherbal Mixture

Current Trends in Biotechnology and Pharmacy
Vol. 18 (Supplementry Issue 4A) 166 - 185, November 2024, ISSN 0973-8916 (Print), 2230-7303 (Online)
10.5530/ctbp.2024.4s.13

173

have documented a broad spectrum of pharmaceutical and therapeutic properties of saponins, including minimal oral toxicity in humans. *Crinum zeylanicums* total saponin content was found to be 37% through quantitative research. The findings showed that the medicinal plant is beneficial to health and is thought to be a versatile herb that can treat a wide range of ailments (39).

Quantitative Assessment of Phenol content

The total phenol contents in the polyherbal methanol extract were found to be 10.452 ± 0.010mg/g of polyherbal extract (y=0.2107 x+0.1887, R2 =0.8608) which was more significant than that found in earlier works of polyherbal extracts (Figure 4). In a study, the total phenol content of mentha leaf was found to be 7.96 mg/g (34). Earlier work on polyherbal formulations such as DBC (34 multiple herbs) and DMV (22 multiple herbs) showed total phenol content of 4.503 and 5.21mg/g respectively (37). The highest standard by which other bactericides that is evaluated is still phenols and phenolic compounds, which are widely employed in disinfections (33). The leaves of *Psidium*
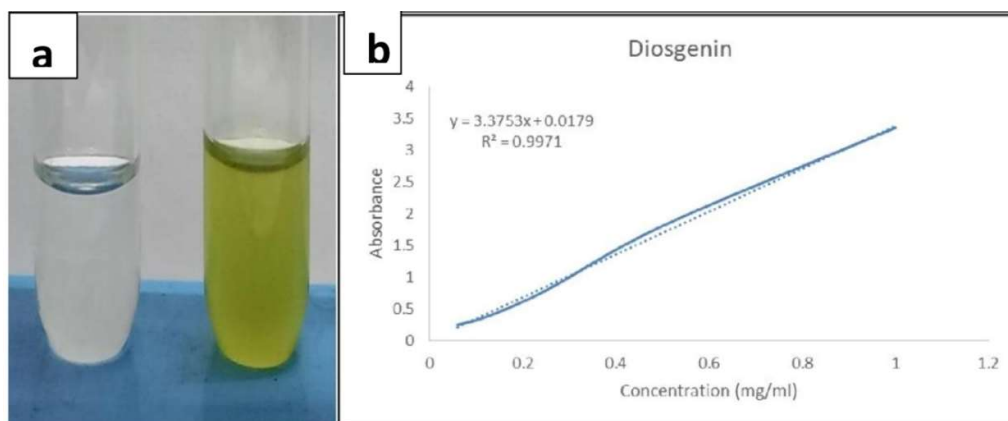

Figure 3: Quantitative Assessment of Saponin Content (a) Saponin formation at 20mg/ml (b) Standard graph and estimation of saponin in the sample
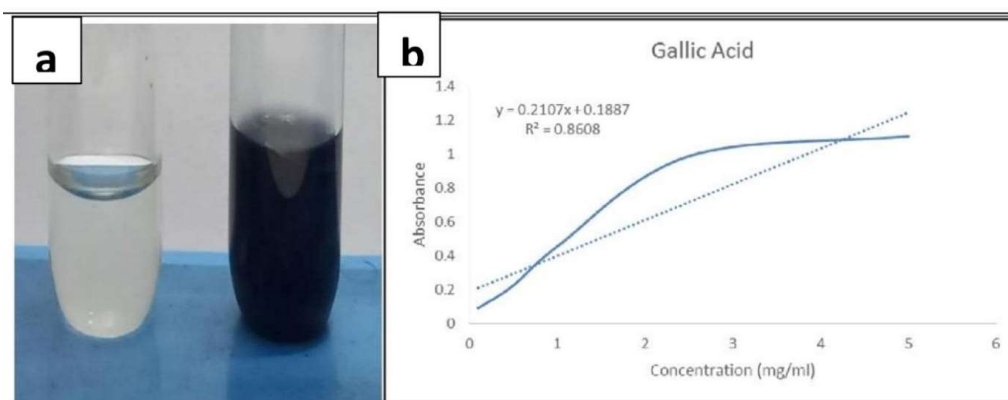

Figure 4: Quantitative Assessment of Phenol Content (a) Phenol formation at 20mg/ml (b) Standard graph and estimation of phenol in the sample

Current Trends in Biotechnology and Pharmacy
Vol. 18 (Supplementry Issue 4A) 166 - 185, November 2024, ISSN 0973-8916 (Print), 2230-7303 (Online)
10.5530/ctbp.2024.4s.13

174

guajava methanol extract showed 2.6% total phenol content. Polyphenolic substances have a well-established antibacterial action in addition to their substantial antiphlogistic, free radical-scavenging and carcinoma-preventive effects. Phenolic substances exhibit many bactericidal modes of action; including preventing the synthesis of nucleic acid and neutralizing the outer layer of cells. Research also revealed that polyphenols may have anti-fungal properties through blocking glucosamine, a development signal found only in the cells of fungi of specific genera, and ergosterol, an essential component of the microbial cell wall (41).

Quantitative Assessment of Tannin content

The total tannin contents in the polyherbal methanol extract were found to be 9.08 ± 0.012mg/g of polyherbal extract (y=0.1069 x+0.0555, R^2 =0.9934) which was more significant than that in earlier works of polyherbal extracts (Figure 5). In a study, the total tannin content of mentha leaf was found to be 2.15 mg/g (40). Earlier work on MAT20 polyherbal formulations of total tannin content showed 0.3453mg/g (41). The total tannin content of the methanol extract of *Psidium guajava* leaves in a study was 3.1%. Strong antibacterial properties are exhibited by tannins, which are soluble in water, chemical substances that are extensively distributed in the kingdom of plants. Tannins prevent the development of microbes through a variety of

mechanisms, such as iron chelation process, deprivation of vital compounds that drive microbial development, disruption of microbe activity in metabolism through inhibition of oxidative phosphorylation, and inhibition of enzymes that necessary for the outside of cell membrane. Through processes like the blocking of enzymes outside the cell, deprivation of substrate, and suppression of the process of oxidative phosphorylation, tannins function as antibacterial agents. The polyphenolic molecule is a bio preservative that finds application in both the food and medicinal industries. (32).

Quantitative Assessment of Glycosides content

The total glycosides contents in the polyherbal methanol extract were found to be 0.058 ± 0.009mg/gof polyherbal extract (y=0.0174 x+0.0319, R^2 =0.9881) (Figure 6). In a study, the total glycosides content of different Nigerian samples was found to be 3 to 7.3 mg/ g. Congestive heart failure has been treated with cardiac glycosides because of their direct action, which increases the contraction of the myocardium. Cardiac glycosides directly affect smooth muscles within the circulatory system. They have an indirect impact on cardiac electrical activity, vascular resistance, and capacitive in addition to their impact on brain tissues. he glycosides found in *Cordia millenii, Tetrapleura tetraptera, Afzeliabipindensis, Moringa species* and *Combretodendron macrocarpum* were
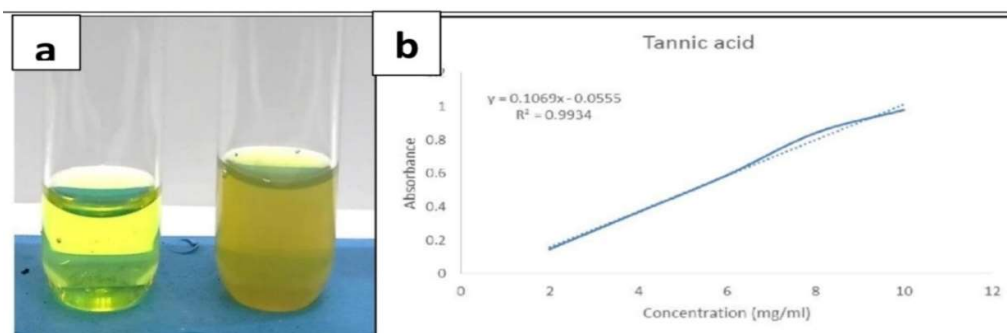

Figure 5: Quantitative Assessment of Tannin Content (a) Tannin formation at 20mg/ml (b) Standard graph and estimation of tannin in the sample

Bioprofiling of Polyherbal Mixture

found to have potential medical uses. According to the findings, these softwood grains from Nigeria may be a source for the phytonutrients that are useful to the complementary and alternative healthcare sectors (43).

The high phenol content along with flavonoids and tannins which are also polyphenols were indicative of application of the polyherbal mixture in the treatment of inflammation and cancer (44-46).

Maceration and Soxhlet Extraction method

The average of polyherbal polyphenolic compound yields of the maceration and Soxhlet extraction method is presented in Figure 7. The result showed that the phenol content yield of maceration extraction method is 476.63µg GAE/mL. The tannin content yield of maceration extraction method is 623.86µg GAE/mL. The flavonoid content yield of maceration extraction method is 27.21µg GAE/mL. The result showed that the phenol content yield of Soxhlet extraction method is 403.95µg GAE/mL. The tannin content yield of Soxhlet extraction method is 565.70µg GAE/mL. The flavonoid content yield of Soxhlet extraction method is 26.85µg GAE/mL

On the whole, maceration extraction method has maximum yield of extraction compared to soxhlet extraction method. Methanol extracted more phytochemicals than chloroform and hexane, according to research on five distinct Sudanese medicinal plants that are rich in phytochemicals, particularly phenolic compounds. In comparison to soxhlet extraction, the maceration extract has a higher percent yield. The methanolic maceration technique has better antioxidant activity against standard propyl gallate (47).

The maceration extraction of wali seeds has more total phenolic content about 4.9mgGAE/100g sample compared to soxhlet extraction with about 3.8mg GAE/100g sample and has higher antioxidant activity reported in maceration extraction (48).

The macerated southern bugle subspecies Pseudoiva extracts was rich in polyphenols with about 25.26 µg gallic acid equivalents per mg of extract, flavonoids about 821.43 µg quercetin per mg of phenolic solution, and tannins about 95.58 µg catechin equivalents per mg of phenolic solution. The macerated methanol extract has the ability to scavenge free radicals (49).

Thin layer chromatography (TLC)

The results of methanolic polyphenol TLC profile are shown in Fig 8. In the solvent system, methanol and hexane taken in the ratio 3:1 respectively exhibited the presence
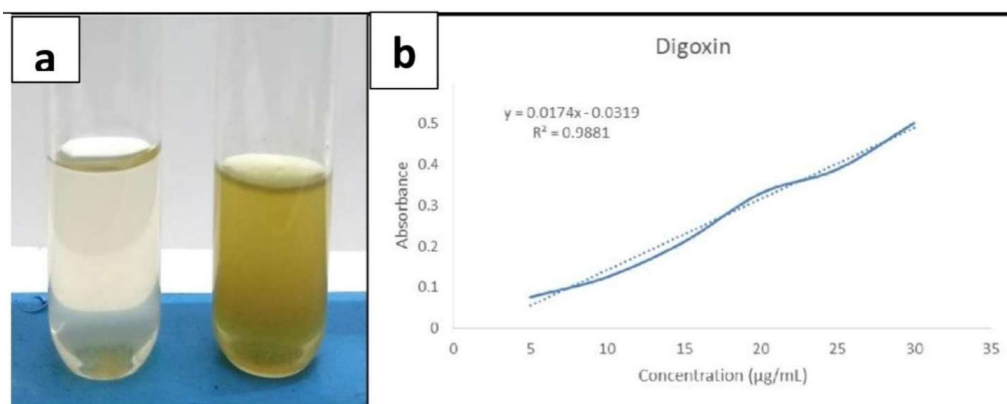

Figure 6: Quantitative Assessment of Glycoside Content (a) Glycosides formation at 20mg/ml (b) Standard graph and estimation of glycosides in the sample

Current Trends in Biotechnology and Pharmacy
Vol. 18 (Supplementry Issue 4A) 166 - 185, November 2024, ISSN 0973-8916 (Print), 2230-7303 (Online)
10.5530/ctbp.2024.4s.13

176

of phenol (Rf 0.56). Flavonoid was present in 3:1 ratio of toluene and chloroform solvent system respectively (Rf 0.34). In the solvent system, methanol and hexane taken in the ratio 3:1 respectively exhibited the presence of tannin (Rf 0.45).

Using TLC to screen out *Cyperus rotundus*, the Rf values were ascertained. TLC is a separation method used to determine many bioactive components. Excellent pharmacological qualities and great selectivity, efficacy, and peak parameters are all provided by the chromatographic condition (50).

A high concentration of flavonoids and tannins, which are phenolic components, was found in the methanol extract of Armenian herbs. As mobile phases in TLC study, various solvent systems were employed to draw conclusions about the characteristics of active antibacterial agents. The development of TLC plates using the solvent systems glacial acetic acid, methanol, butanol, and water demonstrated the presence of polyphenolic compounds as separated bands (51).

Antioxidant Assays

FRAP Test

The method is frequently employed to assess the antioxidant potential of polyphenols. The polyherbal mixture exhibited a stronger reducing property, as
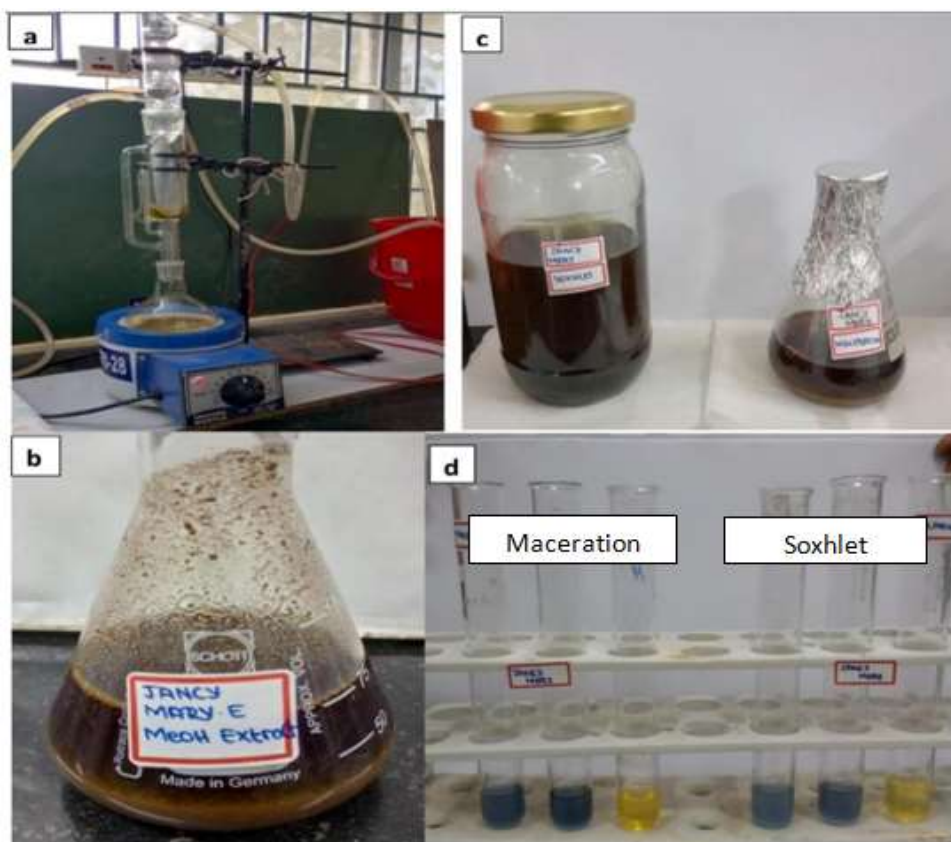

Figure 7: Maceration and Soxhlet Extraction Methods (a) Soxhlet Extraction (b) Maceration Extraction (c) Polyphenolic Extract (d) Phyto polyphenol
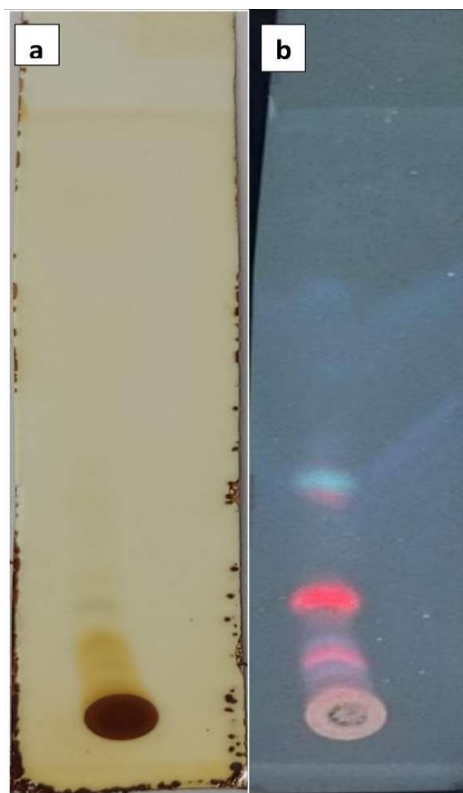
Bioprofiling of Polyherbal Mixture

Figure 8: Thin Layer Chromatography (a) TLC Profile (b) TLC with UV light

evidenced by the percentage inhibition of the polyphenolic extracts. Results as in Figure 9 depicted that the polyphenolic extracts were stronger in the FRAP analysis with a concentration at 50% of reduction (EC50) value as 61.67±0.07 µg/mL. The reducing property improved with an increase in polyphenol concentration and was dosage dependent. An earlier study indicated concentration at 50% of inhibition (IC50) value of 79.92mg/mL by the polyherbal extract of Dasamoolarishtam through FRAP analysis (52).

Using the FRAP assay to measure maximum antioxidant activity, a strong synergism was demonstrated when *Syzygium aromaticum* and *Rosmarinus officinalis* (methanol extracts) were combined. Excellent free radical scavenging activities are demonstrated by the combination of *Mentha piperita* and *Thymus vulgaris* methanol extracts by FRAP tests. Because of their synergistic interactions, using extracts in different combinations produced an optimal antioxidant effect even at lower doses than when using the extracts alone (53).

Phosphomolybdenum Assay

The method is employed to determine the antioxidant potential of plant extracts. The polyherbal mixture showed a significant reducing effect, as evidenced by the percentage inhibition of the polyphenolic extracts. Results as in Figure 10 depicted that the polyphenolic methanol extracts have greater potency in the phosphomolybdenum test with a concentration at 50% of reduction (EC50) value is33.95±0.10 µg/mL. The reducing property improved with an increase indosage dependent and polyphenolic concentration. An earlier study indicated EC50 value of 80mg/mL by the polyherbal extract of Dasamoolarishtam through phosphomolybdenum activity (52)

The phosphomolybdenum complex was used to test the polyherbal DhanwantaramKashayam decoction, and the results showed that it had a significant impact on the antioxidant properties, with an inhibitory concentration (IC50) of 50.4µg/ml. The phytochemicals in the polyherbal kashayam indicate its potent antioxidant properties, and it reduces molybdenum radicals to treat gynecological illness. The potent antioxidant polyherbal decoction activity may be the cause for its positive effects in body's system as reported in Ayurvedic medical system. (54).

Superoxide Radical Scavenging Activity

The method is used to scavenge superoxide radicals and enhance the nutritional value of food. This method of antioxidants is the most important inhibition mechanism. Results as in Figure 11 depicted that the polyphenolic extracts have good effect in the superoxide radical scavenging activity with a concentration at 50% of
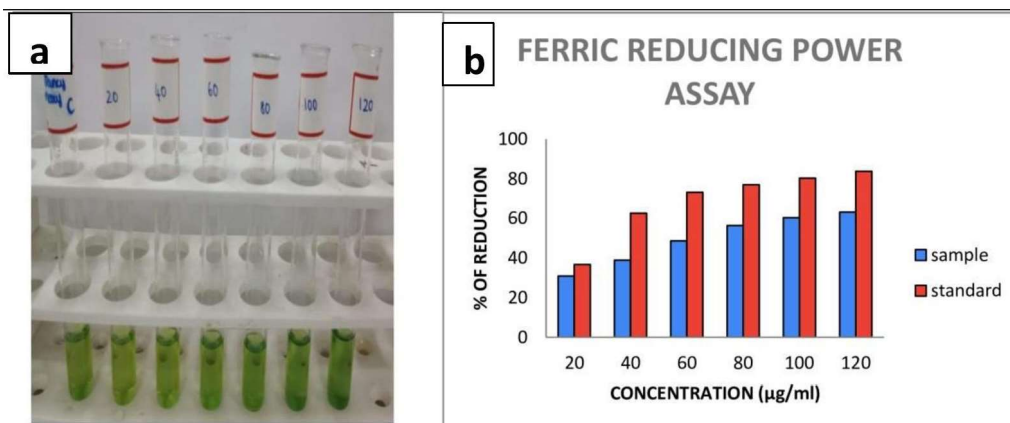
Fig 9: Ferric Ion Reducing Antioxidant Power Test (a) Experimental analysis (b) Graphical representation of reducing power
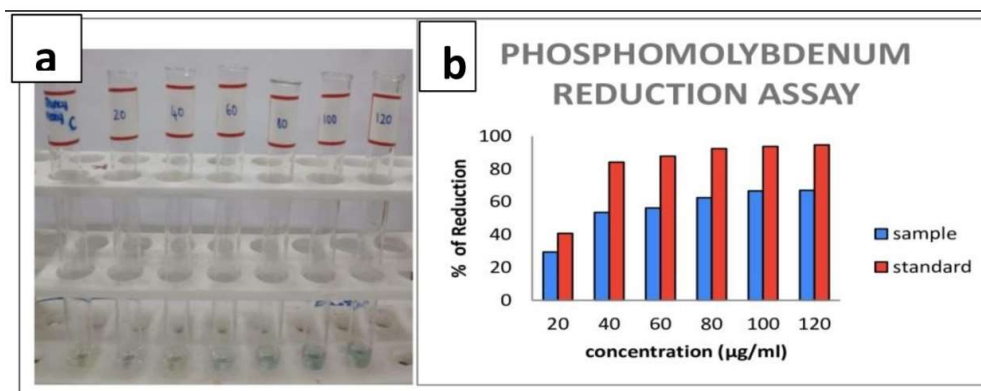

Fig 10: Phosphomolybdenum Assay (a) Experimental analysis (b) Graphical representation of reducing power

inhibition (IC_{50}) value as 73.34±0.12 µg/mL.The ability to scavenge radicals was dose-dependent and had polyphenolic concentration. An earlier study indicated the IC50 value of 0.22mg/mL by the polyherbal extract of Dasamoolarishtam through superoxide radical scavenging activity (52).

The polyherbal methanolic extract of thirikaduguchooranam from zingiber and piper species showed good strong effect with IC50 concentration of 2230 µg/ml. The methanolic extract of polyherbal parangipattaichooranam from smilax and ocimum species exhibited notable radical elimination action with IC50 concentration of 2860 µg/ml. The strong antioxidant qualities of the polyherbal mixture may be attributed to phenols and their derivatives. The removal of fungus and bacteria in polyherbal formulations may be due to the presence of several secondary phytoconstituents (55).

ABTS+Radical Cation Scavenging Assay

The procedure is technically simple and has been frequently used for screening and routine measurement of natural extracts. Results as in Figure 12 depicted that the polyphenolic methanol extracts
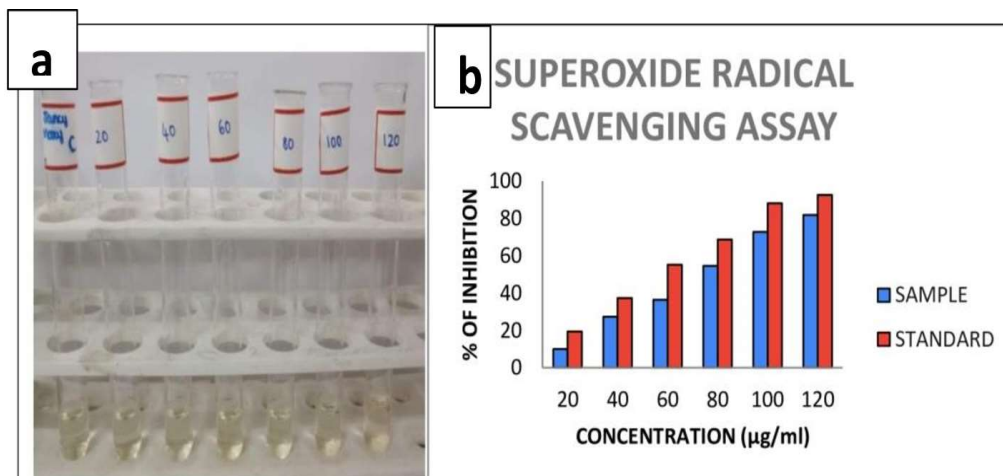
Current Trends in Biotechnology and Pharmacy
Vol. 18 (Supplementry Issue 4A) 166 - 185, November 2024, ISSN 0973-8916 (Print), 2230-7303 (Online)
10.5530/ctbp.2024.4s.13

179

Figure11: Superoxide Radical Scavenging Activity (a) Experimental analysis (b) Graphical representation of radical scavenging activity
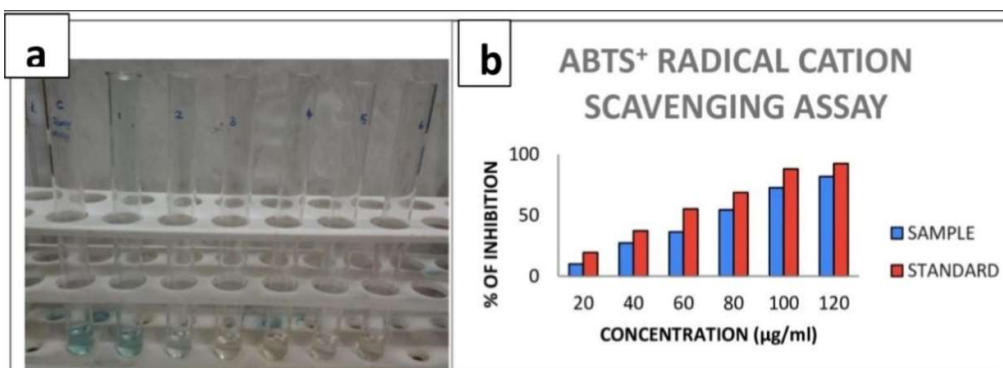

Figure 12: ABTS$^+$ Radical Cation Scavenging Assay (a) Experimental analysis (b) Graphical representation of radical scavenging activity

exhibited ABTS$^+$ radical scavenging activity with a concentration at 50% of inhibition (IC$_{50}$) value of 26.76±0.10 μg/mL.The capacity to scavenge radical cation was based on the polyphenolic concentration. This could have explained the extract's potent antioxidant action against free radicals as well as its numerous pharmacological qualities. An earlier study indicated the IC50 value of 0.0278μg/mL by the polyherbal extract of Dasamoolarishtam through ABTS$^+$ radical scavenging activity (52)

The polyherbal combination of vati from Withania, Cucurma, Zingiber, Boswellia, Commiphora, Aloe, Hemidesmus and Berberis species showed highest ABTS scavenging activity (96%) and demonstrated potential as a source of anti-inflammatory agents that could be useful in treating a variety of human ailments. The study also demonstrated the significance of OH group location and number in phenolics for antioxidant action. The synergistic interaction between the herbs may aid to increase the antioxidant activity. (56).

The polyphenolic methanol extract showing excellent scavenging activity implied its antioxidant potential towards inhibition of inflammation and carcinogen activation (45, 46).

The results of all the antioxidant assays indicated significant antioxidant

Figure 13: Antimicrobial Activity of Polyphenolic extract against a-*S. mutans,* b- *C. albicans,* c- *S. aureus and* d-*A. viscosus and* standard- Tetracycline (a, c, and d), Fluconazole (b)

activity of the polyherbal extract under study over the earlier works.

Evaluation of Antimicrobial Activity

By assessing the zone of inhibition, the methanol extract of the polyphenols had the highest inhibitory property against oral cavity-producing organisms like *S. mutans, C. albicans, A. viscosus* and *S. aureus.* The polyphenolic extract exhibited the largest zone of inhibition and maximum antibacterial activity against *S. aureus* at a dose of 500 µg/mL and *S. mutans* activity appeared to be the lowest. The outcomes were contrasted with the typical tetracycline. When compared to the other bacteria under investigation, *S. aureus* was the target of more activity at all concentrations. There is an increase in both the concentration and the zone of inhibition. Comparing the fungicidal action with fluconazole, the highest effect was observed against *C. albicans. S. aureus > A. viscosus> C. albicans > S. mutans* was the overall order of the polyherbal extract's antibacterial effectiveness against the germs (Figure 13 and Table 1). The results showed that the extracts' arithmetic average ± standard deviation was statistically significant at **$p<0.01$ when compared to different concentrations. This approach may
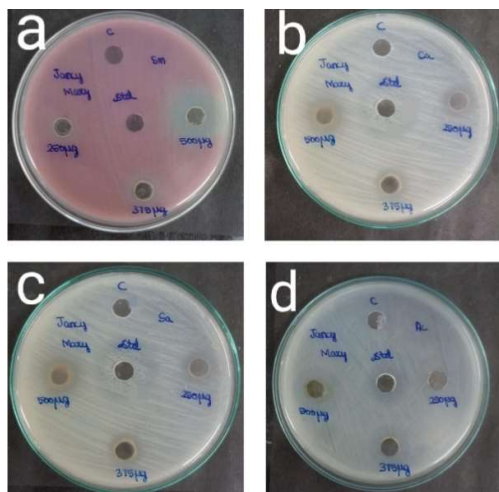
Table 1: Zone of inhibition against dental pathogens		
Organisms	Extract Concentrations (µg/mL)	Polyphenolic Extract
S. mutans	250	11.53± 0.57**
	375	12.00± 1.00**
	500	14.20± 1.15**
	Standard (500)	16.35 ± 1.50**
S. aureus	250	18.30± 1.00**
	375	20.10± 1.00**
	500	22.00± 0.57**
	Standard (500)	20.50 ± 0.57**
A. viscosus	250	18.00± 1.00**
	375	19.50± 1.00**
	500	21.07± 0.57**
	Standard (500)	20.63 ± 0.57**
C. albicans	250	10.37± 1.52**
	375	12. 07± 1.52**
	500	15. 00± 1.00**
	Standard (500)	12.83 ± 0.57**

Bioprofiling of Polyherbal Mixture

frequently produce more beneficial results in the rainy season than it does during the summer season because of the ideal environmental conditions and decreased danger of contamination (57).

When examined against the standard vitamin C by DPPH levels evaluation, the polyherbal mixture extract from *Phyllanthus* species, *Camellia sinensis*, *Khaya senegalensis*, *Nauclealati folia* and *Zingiber officinale* displayed a substantial antioxidant capacity than to its component extracts (58).In comparison to cavity germs, the polyherbal mixture of *Salvia officinalis, Thymus serpyllum, Mentha arvensis, Cinnamomum zeylanicum* and *Rosemaryinus officinalis* demonstrated important microbicidal properties that inhibited the development of oral pathogens, reduced symptoms of gum infection and periodontal disorders, prevented bacteria from sticking to surfaces, and strengthened the gingivae in the dental cavity (59). *Streptococcus mutans*, *Lactobacillus* and *Actinomyces viscosus* as a polyherbal mixture of kantahkari and mastic shown strong microbicidal activities, suppressed the cariogenic microbial flora and might be utilized for decay inhibition in the form of dentifrices and buccal region cleanses (60). The amount of phenolic and flavonoid compounds demonstrated antioxidant and antimicrobial activities that might be of significance in novel therapeutic and pharmaceutical applications (61). The potential mechanism of polyherbal formulation through synergistic interactions between various compounds, such as phenols and flavonoids, which have the dual abilities of scavenging free radicals and inhibiting microbial growth, may be responsible for the antioxidant and antimicrobial effects of the polyherbal methanol extract. Polyherbal formulation should be further analysed for cytotoxic effect to check the toxicity. The manifestation of a large number of diseases may be due to variations and defects in antioxidant and antimicrobial mechanisms. Compounds with antioxidant and antimicrobial properties may provide solutions to such diseases. Due to

their wide range of health benefits, phytonutrients such as polyphenols are used in many different areas of healthcare including cardiovascular protection, brain support, gut health promotion and anti-inflammatory responses.

Conclusion

The appearance of distinct polyphenolic nutrientsin methanolic extract of polyherbal formulation containing leaves of *M. piperita, O. tenuiflorum, A. indica, T. foenum- graecum* and *P. amboinicus* showed higher phenolic concentration than other constituents, including flavonoids and tannin. When compared to soxhlet extraction techniques, the macerated methanolic phenol compound exhibited an excellent extraction rate. Referential data from the investigation would be used to accurately identify the bioactive chemicals and select the best solvent system for separating them from the phenolic TLC profile. The results of the research indicated that the polyphenolic extract had a higher radical scavenging, metal ion reducing potential and microbicidal effect. Polyherbal phytonutrients, antioxidant and antimicrobial are related to their applications in traditional medicine. The study concluded that the polyherbal mixture's numerous phytonutrients with strong antibacterial and antioxidant properties make it useful for its cytoprotective role against number of diseases. Because of thesynergistic interactions of potential bioactive compounds prevailing in the polyherbal mixture, the research helps to develop safe, effective, and evidence-based herbal treatments for the prevention of a variety of health issues through the discovery of novel herbal drugs.

Conflict of Interest

The authors declare no conflict of interest.

References

1. Kanthal, L.K., Dey, A., Satyavathi, K. and Bhojaraju, P. (2014). GC-MS analysis of bioactive compounds in methanolic extract of

Lactucaruncinata DC. *Pharmacognosy Research*, 6, 58-61.

2. Karole, S., Shrivastava, S., Thomas, S., Soni, B., Khan, S., Dubey, J., Dubey, S.P., Khan, N. and Jain, D.K. (2019). Polyherbal formulation concept for synergic action: a review. *Journal of Drug Delivery and Therapeutics*, 9, 453-66.

3. Jancy Mary, E. and Inbathamizh, L. (2022) Phytochemistry and Pharmacology of Five Traditionally Valuable Herbal Plants: A Review. *Research Journal of Biotechnology,* 17(3), 141-172.

4. Trevisan, S. C. C., Menezes, A. P. P., Barbalho, S. M. and Guiguer, É. L. (2017). Properties of mentha piperita: a brief review. *World Journal of Pharmaceutical and Medical Research*, 3, 309-13.

5. Joshi, R. K., Setzer, W. N. and Da Silva, J. K. (2017). Phytoconstituents, traditional medicinal uses and bioactivities of Tulsi (Ocimum sanctum Linn.): a review. *American Journal of Essential Oils and Natural Products*, 5, 18-21.

6. Chekuri, S., Lingfa, L., Panjala, S., Sai Bindu, K. C. and Anupali, R. R. (2020). Acalypha indica L.-an important medicinal plant: a brief review of its pharmacological properties and restorative potential. *European Journal of Medicinal Plants*, 31, 1-10.

7. Almatroodi, S.A., Almatroudi, A., Alsahli, M.A. and Rahmani, A.H., (2021). Fenugreek (Trigonella foenum-Graecum) and its active compounds: A review of its effects on human health through modulating biological activities. *Pharmacognosy Journal*, 13, 813-821.

8. Punet Kumar, S. and Kumar, N. (2020). Plectranthusamboinicus: a review on its pharmacological and pharmacognostical studies. *American Journal of Physiology*, 10, 55-62.

9. Lahare, R. P., Yadav, H. S., Bisen Y. K. and Dashahre, A. K. (2021) Estimation of total phenol, flavonoid, tannin and alkaloid content in different extracts of Catharanthus roseus from Durg district, Chhattisgarh, India. *Schizophrenia bulletin*, 7, 1-6.

10. Savic Gajic, I., Savic, I., Boskov, I., Zerajic, S., Markovic, I. and Gajic, D. (2019). Optimization of ultrasound-assisted extraction of phenolic compounds from black locust (Robinia epseudoacaciae) flowers and comparison with conventional methods. *Antioxidants*, 8(8), 248.

11. Ginovyan, M., Ayvazyan, A., Nikoyan, A., Tumanyan L. and Trchounian, A. (2020). Phytochemical screening and detection of antibacterial components from crude extracts of some Armenian herbs using TLC-bioautographic technique. *Current Microbiology*, 77, 1223-32.

12. Anugraha, S., Vennila, L., Asaikumar, L., Vijayakumar, N., Panbilnathan, A., Krishnan, A. and Arya, R. (2019) In-vitro antioxidant activity of methanolic leaf and root extracts of Elephantopusscaber. *Journal of Pharmacognosy and Phytochemistry*, 8(3), 404-12.

13. Aslam, MS., Ahmad, MS., Mamat, AS., Ahmad, MZ. and Salam, F. (2016). An update review on polyherbal formulation: A global perspective. *Systematic Reviews in Pharmacy*, 7(1), 35.

14. Basit, A., Ahmad, S., Sherif, A. E., Aati, H. Y., Ovatlarnporn, C., Khan, M. A., Rao, H., Ahmad, I., Shahzad, M. N., Ghalloo, B. A. and Shah, H. (2022). New mechanistic insights on Justiciavahlii Roth: UPLC-Q-TOF-MS and GC–MS based metabolomics, in-vivo, in-silico toxicological, antioxidant based anti-inflammatory and enzyme inhibition evaluation. *Arabian Journal of Chemistry*, 15, 104135.

15. Rana, R. and Ashawat, M. S. (2023). Quantitative Analysis of Phytoconstituents of Hydroalcoholic Extract of Carica Papaya Leaf. *Journal of Advanced Zoology*, 44(S5), 1545-50.

16. Sapkal, P.R., Tatiya, A.U., Firke, S.D., Redasani, V.K., Gurav, S.S., Ayyanar, M., Jamkhande, P.G., Surana, S.J., Mutha, R.E. and Kalaskar, M.G. (2023). Phytochemical profile, antioxidant, cytotoxic and anti-inflammatory activities of stem bark extract and fractions of Ailanthus excelsaRoxb.: *In vitro*, *in vivo* and *in silico* approaches. *Heliyon*, 9(5),1.

17. Kapewangolo, P., Tawha, T., Nawinda, T., Knott, M. and Hans, R. (2016). Sceletiumtortuosum demonstrates *in vitro* anti-HIV and free radical scavenging activity. *South African Journal of Botany*, 106, 140-3.

18. Boopathy, U., Chandrasekar, S. and Durairaj, R. (2023). Qualitative and Quantitative Analysis of Cinnamomum Tamala Leaf Extract. *Journal of Advanced Zoology*, 44(S5), 3071-81.

19. Snehalatha, V.R. and Rasmi, A.R., 2021. Phytochemical evaluation and pharmacognostic standardization of Syzygium palghatense endemic to Western Ghats. *Future Journal of Pharmaceutical Sciences*, 7, pp.1-13.

20. Sajid Ansari., Subham Kumar Lohani., Ayush Kumar., Makhmur Hayat. and Arnab Roy. (2024). Evaluation of Phytochemicals in crude extracts derived from the Aerial parts of Lantana camara, International Journal of Pharmaceutical Sciences, 2(3), 1279-1289.

21. Akintola, O. O., Aderounmu, A. F., Abiola, I. O., Abodurin, K. E., Adeniran, T., Agboola, F. and Olokeogun, O. S. (2020). Quantitative Analysis of Phytochemical Compounds in Barks and Leaves of OkoubakaAubrevillei Collected from Iwo, Southwestern Nigeria. *Journal of Bioresource Management*, 7(3), 11.

22. Nalado, Y.A. and Tijjani, A. (2023). Qualitative and Quantitative Phytochemical Analysis of Aloe barbadensis Miller Leaf Extracts. *UMYU Scientifica*, 2(1), 24-30.

23. Ihedioha, T. E., Asuzu, I. U., Anaga, A. O. and Ihedioha, J. I. (2021). Comparative evaluation of the hepatoprotective activity of methanol leaf extracts of Pterocarpus santalinoides DC obtained by cold maceration and Soxhlet extraction techniques. *The Thai Journal of Pharmaceutical Sciences*, 45(6), 442-50.

24. Amalia, T., Saputri, F.C. and Surini, S. (2019). Total phenolic contents, quercetin determination and anti elastase activity of Melastomamalabathricum L. leaves extract from different method of extractions. *Pharmacognosy Journal*, 11(1).

25. Tambun, R., Alexander, V., and Ginting, Y. (2021). Performance comparison of maceration method, soxhletation method, and microwave-assisted extraction in extracting active compounds from soursop leaves (Annona muricata): A review. In IOP Conference Series: Materials Science and Engineering, IOP Publishing, 1122(1), 012095.

26. Illuri, R., Eyini, M., Kumar, M., Prema, P., Nguyen, V. H., Bukhari, N. A., Hatamleh, A. A., and Balaji, P. (2022). Bio-prospective potential of Pleurotus djamor and Pleurotus florida mycelial extracts towards Gram positive and Gram-negative microbial pathogens causing infectious disease. *Journal of Infection and Public Health*, 15(2), 297-306.

27. Nibir, Y. M., Sumit, A. F., Akhand, A. A., Ahsan, N. and Hossain, M. S. (2017). Comparative assessment of total polyphenols, antioxidant and antimicrobial activity of different tea varieties of Bangladesh. *Asian Pacific Journal of Tropical Biomedicine*, 7(4), 352-7.

28. Jayakumari, L., Sivaraj, C. and Manimaran, A. (2023). Methanol leaf extract of Syzygium samarangense: Antioxidant, Antibacterial Activities and GC-MS analysis. *Research Journal of Pharmacy and Technology*, 16(5), 2154-60.

29. Bale, A. T., Salar, U., Khan, K. M., Chigurupati, S., Fasina, T., Ali, F., Ali, M., Nanda, S. S., Taha, M., and Perveen, S. (2021). Chalcones and bis-chalcones analogs as DPPH and ABTS radical scavengers. *Letters in Drug Design and Discovery*, 18(3), 249-57.

30. Hussein, H., Al-Khafaji, N. M. S., Al-Mamoori, A. H. and Al-Marzoqi, A. H. (2018). Evaluation of *in vitro* antibacterial properties of the crude Phenolic, Alkaloid and Terpenoid extracts of Cassia senna L. against Human gram-negative Pathogenic Bacteria. *Plant Archives* 18(1): 354-356.

31. Tiwari G, Patil S, Bondarde P, Khadke S, and Gakhare R (2018) Antimicrobial efficacy of commercially available plant essential oils with calcium hydroxide as intracanal medicaments against *enterococcus faecalis*: An *in-vitro* study. *IOSR Journal of Dental and Medical Sciences*, 17(6): 19-24.

32. Sivareddy, B., Reginald, B. A., Sireesha, D., Samatha, M., Reddy K.H, and

Current Trends in Biotechnology and Pharmacy
Vol. 18 (Supplementry Issue 4A) 166 - 185, November 2024, ISSN 0973-8916 (Print), 2230-7303 (Online)
10.5530/ctbp.2024.4s.13

184

Subrahamanyam G (2019) Antifungal activity of solvent extracts of *Piper betle* and *Ocimum sanctum* Linn on *Candida albicans*: An *in vitro* comparative study. *Journal of Oral and maxillofacial pathology* 23(3): 333.

33.   Ghosh, S., Subudhi, E. and Nayak S (2008) Antimicrobial assay of Stevia rebaudianaBertoni leaf extracts against 10 pathogens. *International Journal of Integrative Biology* 2(1): 27-31.

34.   Airaodion, A.I., Ibrahim, A.H., Ogbuagu, U., Ogbuagu, E.O., Awosanya, O.O., Akinmolayan, J.D., Njoku, O.C., Obajimi, O.O., Adeniji, A.R. and Adekale, O.A. (2019). Evaluation of phytochemical content and antioxidant potential of Ocimumgratissimum and Telfairia occidentalis leaves. *Asian Journal of Research in Medical and Pharmaceutical Sciences*, 7(1), 1-11.

35.   Santhi, K. and Sengottuvel, R. (2016). Qualitative and quantitative phytochemical analysis of Moringa concanensis Nimmo. *International Journal of Current Microbiology and Applied Sciences*. 5(1), 633-40.

36.   Akinnusotu, A., Dada, I.B.O. and Abulude, F.O. (2021). Comparative Analysis of Phytochemical Screening of Some Selected Plant Leaves from Western Nigeria. *International Journal of Traditional and Natural Medicines*, *11*(1), 1-15.

37.   Dinakaran, S.K., Chelle, S. and Avasarala, H. (2019). Profiling and determination of phenolic compounds in poly herbal formulations and their comparative evaluation. *Journal of traditional and complementary medicine*, *9*(4), 319-327.

38.   Kumar, S. S., Kumar, U.M., Prashanth, A., Sarkar, B., and Sindhuja, J. (2017). Quantitative Analysis of Phytoconstituents of Chloroform Extract of Poly Herbal Formulation. *International Journal of Pharmaceutical Sciences Review and Research*, 46, 157-60.

39.   Daben, J. M., Dashak, D. A. and Lohdip, A. M., (2021). Quantitative evaluation of alkaloids, flavonoids, saponins, steroids and tannins contents from the successive solvent extracts of crinum zeylanicum bulb. *Journal of Chemical Society of Nigeria*, 46(5), 1.

40.   Murtala, M., Abdulmumin, T.M., Abdulmumin, Y., Ismail, S.Y., Maimuna, M.D., Amina, L.A., Shahida, S.I., Sadiya, A.B., Abdullahi, N.A., Sadeeq, M.S. and Shehu, A.M. (2022). Evaluation of Phytochemical Contents and Antioxidant Activity of Mentha spicata (Spearmint) Grown in Kano, Nigeria. *Asian Journal of Biochemistry, Genetics and Molecular Biology*, *11*(1), 18-25.

41.   Prajapati, S.K., Malaiya, A., Mishra, G., Jain, D., Kesharwani, P., Mody, N., Ahmadi, A., Paliwal, R. and Jain, A. (2022). An exhaustive comprehension of the role of herbal medicines in Pre-and Post-COVID manifestations. *Journal of Ethnopharmacology*, *296*, 115420.

42.   Das, M. and Goswami, S. (2019). Antifungal and antibacterial property of guava (Psidium guajava) leaf extract: Role of phytochemicals. *International Journal of Health Sciences and Research*, 9(2), 39-45.

43.   Ezeonu, C.S. and Ejikeme, C.M. (2016). Qualitative and quantitative determination of phytochemical contents of indigenous Nigerian softwoods. *New journal of Science*, *2016*, 1-9.

44.   Li, G., Ding, K., Qiao, Y., Zhang, L., Zheng, L., Pan, T. and Zhang, L. (2020). Flavonoids regulate inflammation and oxidative stress in cancer. *Molecules*, *25*(23), 5628.

45.   Rahman, M. M., Rahaman, M. S., Islam, M. R., Rahman, F., Mithi, F. M., Alqahtani, T. and Uddin, M. S. (2021). Role of phenolic compounds in human disease: current knowledge and future prospects. *Molecules*, *27*(1), 233.

46.   Baer-Dubowska, W., Szaefer, H., Majchrzak-Celińska, A. and Krajka-Kuźniak, V. (2020). Tannic acid: specific form of tannins in cancer chemoprevention and therapy-old and new applications. *Current Pharmacology Reports*, *6*, 28-37.

47.   Adam, O. A., Abadi, R. S. and Ayoub, S. M. (2019). The effect of extraction method and solvents on yield and antioxidant activity of certain sudanese medicinal plant extracts. *The Journal of Phytopharmacology*, 8(5), 248-52.

Current Trends in Biotechnology and Pharmacy
Vol. 18 (Supplementry Issue 4A) 166 - 185, November 2024, ISSN 0973-8916 (Print), 2230-7303 (Online)
10.5530/ctbp.2024.4s.13

185

48. Risnadewi, W. N., Muliasari, H., Hamdin, C. D. and Andayani, Y. (2019). Comparative antioxidant activity of Bruceajavanica (L) Merr seed extract derived from maceration and soxhletation method. InAIP Conference Proceedings, AIP Publishing, 2199, 1.

49. Senhaji, S., Lamchouri, F., Bouabid, K., Assem, N., El Haouari, M., Bargach, K. and Toufik, H. (2020). Phenolic contents and antioxidant properties of aqueous and organic extracts of a Moroccan Ajugaiva subsp. *Pseudoiva. Journal of Herbs, Spices and Medicinal Plants*, 26(3), 248-66.

50. Jain, D., Upadhyay, R., Jain, S., Prakash, A., and Janmeda, P. (2022). TLC and HPTLC finger printing analysis of Cyperusrotundus (Linn.). *Letters in Applied Nano Bioscience*, 11(3), 3861-70.

51. Ginovyan, M., Ayvazyan, A., Nikoyan, A., Tumanyan, L. and Trchounian, A. (2020). Phytochemical screening and detection of antibacterial components from crude extracts of some Armenian herbs using TLC-bioautographic technique. *Current Microbiology*, 77, 1223-32.

52. Narayanasamy, A. and Mohammed, M.S (2022). Evaluation of phytochemical profile and antioxidant status of laboratory mode Dasamoolarishtam health tonic and a marketed product. *Asian pacific journal health sciences*, 3(1), 16-22.

53. Mapeka, T. M., Sandasi, M., Viljoe., A. M. and van Vuuren, S. F. (2022). Optimization of Antioxidant Synergy in a Polyherbal Combination by Experimental Design. *Molecules*, 27(13), 4196.

54. Renganathan, S. and Pillai, R. G. (2021). Preliminary analysis of phytochemicals and *in vitro* free radical scavenging activity of Dhanwantaram Kashayam. *Journal of Advanced Biotechnology and Experimental Therapeutics*, 4(1), 95-105.

55. Sethumathi, P. P., Manjuparkavi, K., Lalitha, V., Sivakumar, T., Menaka, M., Jayanthi, A. and Kumar, B. A. (2021). Evaluation of *in vitro* antioxidant and antimicrobial activity of polyherbal formulation of Thirikaduguchooranam and Parangipattaichooranam. *Annals of Phytomedicine*, 10(2), 169-74.

56. Joshi, P., Yadaw, G. S., Joshi, S., Semwal, R. B. and Semwal, D. K. (2020). Antioxidant and anti-inflammatory activities of selected medicinal herbs and their polyherbal formulation. *South African Journal of Botany*. 130, 440-7.

57. Furtado, F.B., De Aquino, F.J., Nascimento, E.A., Martins, C.D.M., De Morais, S.A., Chang, R., Cunha, L.C., Leandro, L.F., Martins, C.H., Martins, M.M. and da Silva, C.V. (2014). Seasonal variation of the chemical composition and antimicrobial and cytotoxic activities of the essential oils from Inga laurina (Sw.) Willd. *Molecules*, 19(4), 4560-4577.

58. Hussein, H., Al-Khafaji, N. M. S., Al-Mamoori, A. H. and Al-Marzoqi, A. H. (2018). Evaluation of *in vitro* antibacterial properties of the crude Phenolic, Alkaloid and Terpenoid extracts of Cassia senna L. against Human gram-negative Pathogenic Bacteria. *Plant Archives,* 18(1), 354-356.

59. Tiwari, G., Patil, S., Bondarde, P., Khadke, S., and Gakhare, R. (2018). Antimicrobial efficacy of commercially available plant essential oils with calcium hydroxide as intracanal medicaments against enterococcus faecalis: An *in-vitro* study. *IOSR Journal of Dental and Medical Sciences*, 17(6), 19-24.

60. Sivareddy, B., Reginald, BA., Sireesha, D., Samatha, M., Reddy, K. H. and Subrahamanyam, G. (2019). Antifungal activity of solvent extracts of Piper betle and Ocimum sanctum Linn on Candida albicans: An *in vitro* comparative study. *Journal of Oral maxillofacial pathology,* 23(3), 333.

61. Elansary, H. O., Szopa, A., Kubica, P., O. El-Ansary, D., Ekiert, H. and A. Al-Mana, F. (2020). Malus baccata var. gracilis and Malus toringoides bark polyphenol studies and antioxidant, antimicrobial and anticancer activities. *Processes*, 8(3), 283.